

AFIT/GAE/ENY/91D-29

1

AD-A243 875



DTIC
ELECTE
JAN 03 1992
S D D

**Robust Grasp Design Using
Grasp Force Focus Positioning**

THESIS

**Freddie D. Zayas
Capt USAF**

AFIT/GAE/ENY/91D-29

92-00051



Approved for public release; distribution unlimited

92 1 2 059

REPORT DOCUMENTATION PAGE

Form Approved
OMB No. 0704-0188

Public reporting burden for this collection of information is estimated to average 1 hour per response, including the time for reviewing instructions, searching existing data sources, gathering and maintaining the data needed, and completing and reviewing the collection of information. Send comments regarding this burden estimate or any other aspect of this collection of information, including suggestions for reducing this burden, to Washington Headquarters Services, Directorate for Information Operations and Reports, 1215 Jefferson Davis Highway, Suite 1204, Arlington, VA 22202-4302, and to the Office of Management and Budget, Paperwork Reduction Project (0704-0188), Washington, DC 20503

1. AGENCY USE ONLY (Leave blank)		2. REPORT DATE 2 Dec 91	3. REPORT TYPE AND DATES COVERED Master's Thesis	
4. TITLE AND SUBTITLE Robust Grasp Design Using Grasp Force Focus Positioning			5. FUNDING NUMBERS	
6. AUTHOR(S) Freddie D. Zayas, Captain, USAF				
7. PERFORMING ORGANIZATION NAME(S) AND ADDRESS(ES) AFIT/ENY Air Force Institute of Technology (AU) Wright-Patterson AFB, Ohio, 45324-6583			8. PERFORMING ORGANIZATION REPORT NUMBER AFIT/GAE/ENY/91D-29	
9. SPONSORING / MONITORING AGENCY NAME(S) AND ADDRESS(ES)			10. SPONSORING / MONITORING AGENCY REPORT NUMBER	
11. SUPPLEMENTARY NOTES				
12a. DISTRIBUTION / AVAILABILITY STATEMENT Approved for public release, distribution unlimited			12b. DISTRIBUTION CODE	
13. ABSTRACT (Maximum 200 words) A three-finger precision grasp is used to rotate a cylindrical object about a threaded post. Three fingered grasps are unique in that the homogeneous solution for the contact forces produces a grasp force focus. Mapping of focus points which meet grasp stability and joint torque criteria results in a usable focus region. The effects of applied torque, contact location, and object position and orientation on usable regions are presented. Stability behavior about the region is also examined. Results are used to demonstrate a technique for robust grasp design.				
14. SUBJECT TERMS Robotics, Grasping, Internal contact forces, Grasp force focus			15. NUMBER OF PAGES 213	
			16. PRICE CODE	
17. SECURITY CLASSIFICATION OF REPORT Unclassified	18. SECURITY CLASSIFICATION OF THIS PAGE Unclassified	19. SECURITY CLASSIFICATION OF ABSTRACT Unclassified	20. LIMITATION OF ABSTRACT UL	

GENERAL INSTRUCTIONS FOR COMPLETING SF 298

The Report Documentation Page (RDP) is used in announcing and cataloging reports. It is important that this information be consistent with the rest of the report, particularly the cover and title page. Instructions for filling in each block of the form follow. It is important to *stay within the lines* to meet optical scanning requirements.

Block 1. Agency Use Only (Leave blank).

Block 2. Report Date. Full publication date including day, month, and year, if available (e.g. 1 Jan 88). Must cite at least the year.

Block 3. Type of Report and Dates Covered. State whether report is interim, final, etc. If applicable, enter inclusive report dates (e.g. 10 Jun 87 - 30 Jun 88).

Block 4. Title and Subtitle A title is taken from the part of the report that provides the most meaningful and complete information. When a report is prepared in more than one volume, repeat the primary title, add volume number, and include subtitle for the specific volume. On classified documents enter the title classification in parentheses.

Block 5. Funding Numbers. To include contract and grant numbers; may include program element number(s), project number(s), task number(s), and work unit number(s). Use the following labels:

C - Contract	PR - Project
G - Grant	TA - Task
PE - Program Element	WU - Work Unit Accession No.

Block 6. Author(s). Name(s) of person(s) responsible for writing the report, performing the research, or credited with the content of the report. If editor or compiler, this should follow the name(s).

Block 7. Performing Organization Name(s) and Address(es). Self-explanatory.

Block 8. Performing Organization Report Number. Enter the unique alphanumeric report number(s) assigned by the organization performing the report.

Block 9. Sponsoring/Monitoring Agency Name(s) and Address(es). Self-explanatory.

Block 10. Sponsoring/Monitoring Agency Report Number. (If known)

Block 11. Supplementary Notes. Enter information not included elsewhere such as: Prepared in cooperation with...; Trans. of...; To be published in... When a report is revised, include a statement whether the new report supersedes or supplements the older report

Block 12a. Distribution/Availability Statement. Denotes public availability or limitations. Cite any availability to the public. Enter additional limitations or special markings in all capitals (e.g. NOFORN, REL, ITAR).

DOD - See DoDD 5230.24, "Distribution Statements on Technical Documents."

DOE - See authorities.

NASA - See Handbook NHB 2200.2.

NTIS - Leave blank.

Block 12b. Distribution Code.

DOD - Leave blank.

DOE - Enter DOE distribution categories from the Standard Distribution for Unclassified Scientific and Technical Reports.

NASA - Leave blank.

NTIS - Leave blank.

Block 13. Abstract. Include a brief (Maximum 200 words) factual summary of the most significant information contained in the report.

Block 14. Subject Terms. Keywords or phrases identifying major subjects in the report.

Block 15. Number of Pages. Enter the total number of pages.

Block 16. Price Code. Enter appropriate price code (NTIS only).

Blocks 17. - 19. Security Classifications. Self-explanatory. Enter U.S. Security Classification in accordance with U.S. Security Regulations (i.e., UNCLASSIFIED). If form contains classified information, stamp classification on the top and bottom of the page.

Block 20. Limitation of Abstract. This block must be completed to assign a limitation to the abstract. Enter either UL (unlimited) or SAR (same as report). An entry in this block is necessary if the abstract is to be limited. If blank, the abstract is assumed to be unlimited.

Robust Grasp Design Using Grasp Force Focus Positioning

THESIS

Presented to the Faculty of the School of Engineering
of the Air Force Institute of Technology

Air University

In Partial Fulfillment of the

Requirements for the Degree of

Master of Science in Aeronautical Engineering

Freddie D. Zayas, B.S. in Mechanical Engineering

Capt USAF

December 12, 1991



Accession For	
NTIS	CRAed
DTIC	TAB
Unannounced	
Justification	
By	
Distribution	
Availability Codes	
Dist	Avail and/or Special
A-1	

Preface

This thesis could not have become a reality without the help of several people. First and foremost is my advisor, Dr. Curtis Spenny, who took the time and effort to guide me safely towards the light at the end of the tunnel. Thanks for your patience and inspiration during those late night consultations. I'd also like to thank Capt. Ron Eddy for helping me out with my many computer and software headaches. In addition, I'd like to thank my committee members, Dr. William Wiesel and Dr. Brad Liebst, for their inputs and assistance.

Special thanks to all my volleyball/racquetball buddies for those much-needed breaks away from AFIT life, and to my good friends Tim and Tracy Morris for feeding me and giving me a place to sleep during my last few weeks at AFIT. Finally, I'd like to thank my wife Janie. Thanks for bearing with me through all those late night escapades at school, and for forgiving me for all those trips and outings we missed because I was too far behind in my thesis work.

Freddie D. Zayas

Table of Contents

	Page
Preface	ii
Table of Contents	iii
List of Figures	viii
List of Tables	xii
Abstract	xiii
I. Introduction	1-1
1.1 Motivation	1-1
1.2 Objective	1-3
1.3 Background	1-4
1.4 Problem Statement	1-8
1.5 Method of Approach	1-9
1.6 Contributions	1-12
1.7 Organization	1-13
II. Model Kinematics	2-1
2.1 Description of Hand Model	2-1
2.2 Hand Model Coordinate Frames	2-1

2.2.1	Palm Frame	2-3
2.2.2	Finger 0 Coordinate Frames	2-4
2.2.3	Finger 1 and Finger 2 Coordinate Frames	2-7
2.3	Cylinder Coordinate Frames	2-10
2.4	Inverse Kinematic Relationships	2-15
2.5	Model Application	2-20
III.	Grasp Analysis	3-1
3.1	Grasping Forces	3-1
3.2	The Contact Force Particular Solution	3-2
3.3	The Internal Grasp Force Focus	3-4
3.4	The Homogeneous Solution	3-5
3.5	Constraints on Total Contact Forces	3-8
3.6	The Constraint Map	3-9
3.7	Determining Joint Torques for Hand Model	3-10
3.7.1	Manipulator Jacobian	3-11
3.7.2	Equivalent Maximum Joint Torques	3-13
3.8	Joint Torque Constraint Maps	3-14
IV.	Computer Generation of Constraint Maps	4-1
4.1	Grasp Simulation Setup	4-1
4.1.1	Kinematic Parameters	4-1
4.1.1.1	Contact Location	4-2
4.1.1.2	Grasp Configuration	4-3

4.1.1.3 Artificial Constraints	4-3
4.1.2 Grasp Parameters	4-6
4.2 Computer Programs	4-9
 V. Results and Discussion	 5-1
5.1 Overview	5-1
5.1.1 Desirable Grasp Characteristics	5-1
5.1.2 Ideal Grip	5-2
5.1.3 Comparing Grips	5-2
5.2 Effects of Cylinder Rotation on SAS Region	5-4
5.3 Effects of Grasp Configuration on SAS region	5-11
5.3.1 Retracted Grasp	5-12
5.3.2 Extended Grasp	5-12
5.3.3 Intermediate Thumb-Bias Grasp	5-13
5.3.4 Intermediate Finger-Bias Grasp	5-13
5.3.5 Intermediate Finger-Bias (Maximum) Grasp	5-14
5.3.6 Advantages/Disadvantages of Finger-Bias Grasps	5-14
5.4 Increasing Torquing Capability	5-15
5.4.1 Single Point Grasp Focus	5-15
5.4.2 Designing a Robust Grasp for High Torque Applications	5-16
5.5 Effects of Contact Location on SAS Region	5-19
5.5.1 Retracted Finger-Bias Grasp with Symmetric Contacts	5-23

5.5.2 Retracted Thumb-Bias Grasp with Symmetric Contacts	5-26
5.6 Locating the Grasp Focus	5-30
5.7 Summary	5-39
 VI. Conclusions	 6-1
 VII. Recommendations	 7-1
7.1 Real-Time Implementation	7-1
7.2 Model Optimization	7-1
7.3 Incorporating Rolling Contacts	7-1
 Appendix A. Constraint Map Set #2	 A-1
 Appendix B. Constraint Map Set #3	 B-1
 Appendix C. Constraint Map Set #4	 C-1
 Appendix D. Constraint Map Set #5	 D-1
 Appendix E. Constraint Map Set #6	 E-1
 Appendix F. Inverse Kinematics Computer Program	 F-1
 Appendix G. Grasp Analysis Computer Program	 G-1

Appendix H. Manipulator Jacobian	H-1
Bibliography	BIB-1
Vita	VITA-1

List of Figures

Figure	Page
2.1 Schematic of Three-Fingered Hand Model	2-2
2-2 Joint 1 & 2 Layout for Three-Fingered Hand Model	2-2
2-3 Finger Coordinate Frame Layout	2-3
2-4 Cylinder Frame Assignments with respect to Palm Frame	2-12
2-5 Position & Orientation of Contact Frames	2-13
2-6 Cylinder Orientation Angle α_b	2-23
3-1 Balancing the External Moment	3-3
3-2 Prescribing the Grasp Force Focus Location	3-6
4-1 Neutral-Bias Retracted Grasp Configuration	4-4
4-2 Neutral-Bias Extended Grasp Configuration	4-4
4-3 Thumb-Bias Intermediate Grasp Configuration	4-5
4-4 Finger-Bias Intermediate Grasp Configuration	4-5
4-5 Locating the Error Region within the Net SAS Region	4-8
5-1 Intermediate Neutral-Bias Grasp, $\phi_b = 50^\circ$	5-6
5-2 Intermediate Neutral-Bias Grasp, $\phi_b = 30^\circ$	5-6
5-3 Intermediate Neutral-Bias Grasp, $\phi_b = 15^\circ$	5-7
5-4 Intermediate Neutral-Bias Grasp, $\phi_b = 0^\circ$	5-7
5-5 Intermediate Neutral-Bias Grasp, $\phi_b = -15^\circ$	5-8
5-6 Intermediate Neutral-Bias Grasp, $\phi_b = -30^\circ$	5-8
5-7 Intermediate Neutral-Bias Grasp, $\phi_b = -40^\circ$	5-9
5-8 Intermediate Neutral-Bias Grasp, $\phi_b = -50^\circ$	5-9
5-9 Net SAS region for Intermediate Neutral-Bias Grasp	5-10

5-10 Retracted Finger-Bias Grasp, $\phi_b = 50^\circ$; Max. Torque, 100° Rotation	5-17
5-11 Retracted Finger-Bias Grasp, $\phi_b = -20^\circ$; Max. Torque, 100° Rotation	5-17
5-12 Retracted Finger-Bias Grasp, $\phi_b = -30^\circ$; Max. Torque, 100° Rotation	5-18
5-13 Retracted Finger-Bias Grasp, $\phi_b = -50^\circ$; Max. Torque, 100° Rotation	5-18
5-14 Retracted Finger-Bias Grasp, $\phi_b = 50^\circ$; Max. Torque, 50° Rotation	5-20
5-15 Retracted Finger-Bias Grasp, $\phi_b = 30^\circ$; Max. Torque, 50° Rotation	5-20
5-16 Retracted Finger-Bias Grasp, $\phi_b = 20^\circ$; Max. Torque, 50° Rotation	5-21
5-17 Retracted Finger-Bias Grasp, $\phi_b = 5^\circ$; Max. Torque, 50° Rotation	5-21
5-18 Retracted Finger-Bias Grasp, $\phi_b = 0^\circ$; Max. Torque, 50° Rotation	5-22
5-19 Net SAS Region for Retracted Finger-Bias Grasp, ; Maximum Torque, 50° Rotation	5-22
5-20 Retracted Finger-Bias Grasp, Symmetric Contacts; $\phi_b = 30^\circ$	5-24
5-21 Retracted Finger-Bias Grasp, Symmetric Contacts; $\phi_b = 20^\circ$	5-24
5-22 Retracted Finger-Bias Grasp, Symmetric Contacts; $\phi_b = -20^\circ$	5-25
5-23 Retracted Finger-Bias Grasp, Symmetric Contacts; $\phi_b = -30^\circ$	5-25
5-24 Retracted Thumb-Bias Grasp, Symmetric Contacts; $\phi_b = 30^\circ$	5-27
5-25 Retracted Thumb-Bias Grasp, Symmetric Contacts; $\phi_b = -30^\circ$	5-27
5-26 RTB Grasp; Symmetric Contacts; $\phi_b = 30^\circ$, High Torque	5-28
5-27 RTB Grasp; Symmetric Contacts; $\phi_b = -30^\circ$, High Torque	5-28
5-28 Net SAS Region for Retracted Thumb-Bias Grasp w/Symmetric Contacts	5-29

5-29	Stable Region Grid for Retracted Finger-Bias Grasp with Semi-Symmetric Contacts	5-31
5-30	Stable Region Grid for Retracted Thumb-Bias Grasp with Symmetric Contacts	5-31
A-1	Retracted Neutral-Bias Grasp, $\phi_b = 50^\circ$	A-2
A-2	Retracted Neutral-Bias Grasp, $\phi_b = 0^\circ$	A-2
A-3	Retracted Neutral-Bias Grasp, $\phi_b = -50^\circ$	A-3
B-1	Extended Neutral-Bias Grasp, $\phi_b = 50^\circ$	B-2
B-2	Extended Neutral-Bias Grasp, $\phi_b = 30^\circ$	B-2
B-3	Extended Neutral-Bias Grasp, $\phi_b = 15^\circ$	B-3
B-4	Extended Neutral-Bias Grasp, $\phi_b = 0^\circ$	B-3
B-5	Extended Neutral-Bias Grasp, $\phi_b = -15^\circ$	B-4
B-6	Extended Neutral-Bias Grasp, $\phi_b = -20^\circ$	B-4
C-1	Intermediate Thumb-Bias Grasp, $\phi_b = 50^\circ$	C-2
C-2	Intermediate Thumb-Bias Grasp, $\phi_b = 30^\circ$	C-2
C-3	Intermediate Thumb-Bias Grasp, $\phi_b = 15^\circ$	C-3
C-4	Intermediate Thumb-Bias Grasp, $\phi_b = 0^\circ$	C-3
C-5	Intermediate Thumb-Bias Grasp, $\phi_b = -15^\circ$	C-4
C-6	Intermediate Thumb-Bias Grasp, $\phi_b = -30^\circ$	C-4
C-7	Intermediate Thumb-Bias Grasp, $\phi_b = -40^\circ$	C-5
C-8	Intermediate Thumb-Bias Grasp, $\phi_b = -50^\circ$	C-5
D-1	Intermediate Finger-Bias Grasp, $\phi_b = 50^\circ$	D-2
D-2	Intermediate Finger-Bias Grasp, $\phi_b = 30^\circ$	D-2
D-3	Intermediate Finger-Bias Grasp, $\phi_b = 15^\circ$	D-3
D-4	Intermediate Finger-Bias Grasp, $\phi_b = 0^\circ$	D-3

D-5	Intermediate Finger-Bias Grasp, $\phi_b = -15^\circ$	D-4
D-6	Intermediate Finger-Bias Grasp, $\phi_b = -30^\circ$	D-4
D-7	Intermediate Finger-Bias Grasp, $\phi_b = -40^\circ$	D-5
D-8	Intermediate Finger-Bias Grasp, $\phi_b = -50^\circ$	D-5
D-9	Net SAS Region for Intermediate Finger-Bias Grasp	D-6
E-1	Intermediate Finger-Bias Grasp, $\phi_b = 50^\circ$; Maximum Bias	E-2
E-2	Intermediate Finger-Bias Grasp, $\phi_b = 30^\circ$; Maximum Bias	E-2
E-3	Intermediate Finger-Bias Grasp, $\phi_b = 15^\circ$; Maximum Bias	E-3
E-4	Intermediate Finger-Bias Grasp, $\phi_b = 0^\circ$; Maximum Bias	E-3
E-5	Intermediate Finger-Bias Grasp, $\phi_b = -15^\circ$; Maximum Bias	E-4
E-6	Intermediate Finger-Bias Grasp, $\phi_b = -30^\circ$; Maximum Bias	E-4
E-7	Intermediate Finger-Bias Grasp, $\phi_b = -40^\circ$; Maximum Bias	E-5
E-8	Intermediate Finger-Bias Grasp, $\phi_b = -50^\circ$; Maximum Bias	E-5

List of Tables

Table	Page
2-1 D-H Parameters for Finger 0	2-8
2-2 D-H Parameters for Finger 1 and Finger 2	2-12
2-3 D-H Parameters for Cylindrical Object	2-13
2-4 Joint Angle Limits	2-18
3-1 Contact Type Designations	3-10
4-1 Kinematic Parameters	4-7
5-1 Contact Forces for Grid Points 1 through 5; Semi-Symmetric Contacts	5-32
5-2 Contact Forces for Grid Points 6 through 9; Semi-Symmetric Contacts	5-33
5-3 Contact Forces for Grid Points 1 through 5; Symmetric Contact	5-34
5-4 Contact Forces for Grid Points 6 through 9; Symmetric Contact	5-35
6-1 Threading Task Characteristics VS Grasp Parameters	6-5

Abstract

A three-finger precision grasp is used to rotate a cylindrical object about a threaded post. Three fingered grasps are unique in that the homogeneous solution for the contact forces produces a grasp force focus. Mapping of focus points which meet grasp stability and joint torque criteria results in a usable focus region. The effects of applied torque, contact location, and object position and rotation on usable regions are presented. Stability behavior about the region is also examined. Results are used to demonstrate a technique for robust grasp design.

Robust Grasp Design Using Grasp Force Focus Positioning

1. Introduction

1.1 Motivation

→ The versatility of robotic hands permit fine motion manipulation on a wide variety of objects. This distinct advantage of manipulating an assortment of objects eliminates the need for multiple custom end effectors. Today's economy demands that new technology advancements lead to operational systems which are efficient, robust, and low cost. Perhaps the most desirable characteristic for current technology is the ability to perform a wide variety of tasks with a single system configuration. Robotic systems configured with articulated hands have the potential to satisfy each of these attributes and more.

↖ With the advent of articulated hands, such as the JPL/Stanford hand and the Utah/MIT Dexterous Manipulator, much attention has been focused on addressing the problems related to the grasping and the manipulation of objects. Programming or "teaching" a robotic hand to perform even the simplest of tasks is a challenge and requires that each complex problem be broken down into solvable portions. A basic requirement for performing many tasks is knowing how to correctly grasp an object so that it can be manipulated in a safe and efficient manner.

A type of grasp used to rotate a cylindrical object about a threaded post is called a three-finger precision or "tripod" grip [1:p1534]. This type of grasp configuration uses the tips of the thumb, index, and middle fingers to hold the object for fine manipulation tasks. After establishing a secure grasp, the coordinated joint-action of each finger imparts the rotational motion of the object about the post.

Typically the task described above also requires the hand to apply torque to the object to overcome external forces acting on it such as friction. Developing an analytical technique to successfully perform this or similar tasks with a robotic manipulator is complex. The solution to this problem requires the determination of the correct combination of kinematic parameters and contact forces to accomplish the task.

One basic requirement is that the robotic hand must securely grasp the object. This implies that there is no loss of contact or contact slip. In addition, the grasp employed must be within the capabilities of the hand; that is, the resulting contact forces must not exceed the joint torque limits for each of the fingers. Ultimately, a single grasp configuration must be determined to complete the task successfully. A single grasp solution is desirable since it avoids the implementation complexities of regrasping or adjusting contact forces.

Specifying a three-finger precision grasp presents a multitude of ways in which the object can be positioned and oriented with respect to the hand. For example, the object can be held in close or extended away from the hand, or it can be biased to one side or the other. Simply stated, there are various ways to hold or "grip" an object for manipulation tasks. The fundamental problem in choosing a single grasp solution is determining which grip provides the best solution.

How to grasp the object relative to the hand requires an in-depth understanding of how the position and orientation of the object effects the hands ability to maintain a secure grasp. The resulting spacial relationships are important since the joint torquing capability of each finger is limited. If the external forces acting on the object are significant in magnitude, then one must also determine the best way to hold the object so that the hand can oppose these forces. This overall planning process is referred to as *grasp planning*.

Real-time implementation problems also become evident during the planning phase due to differences between the system model and the actual robot hand. Errors due to sensor limitations, modelling assumptions, control schemes, and external disturbances can have a significant effect on the successful completion of the task. If the expected error can be specified, then it too can be incorporated into the grasp planning solution. Doing so results in a grasp which is inherently conservative or *robust*, and represents a planned approach for using the grasp to absorb errors.

This thesis focuses on the fundamental problem of grasp planning using multi-fingered robotic hands. A three-finger precision grasp model is used to simulate the task of rotating a cylinder about a threaded post while opposing an external moment.

The problem of grasp planning was chosen because the result will contribute to the solution of a larger scale task currently being studied at AFIT; a task which demonstrates intelligent part mating skills. The specific task involves the use of a multi-fingered robotic hand to affix an oil filter to a threaded post. This study focuses on obtaining a grasp planning solution to the combined problem of rotating the filter about the threaded post while applying continuous torque.

1.2 Objective

Using a three-finger precision grasp, the contact points on an object determine a plane. This type of three-point contact layout presents a special geometrical property for analytical use. If a line is extended in both directions along the internal force vector at each contact point, the three lines will meet at a unique point. This point is termed the grasp force focus [2:3].

This study examines the combined effects of three facets of grasp planning: 1) contact stability, 2) joint torque limitations, and 3) grasp robustness. Contact stability is defined as the ability of the end-effectors to maintain contact with an object without slipping [4:p191]. Grasp robustness, as defined here, is the ability of the initial grasp configuration to maintain stability in the presence of errors. That is, the design of the grasp configuration (object position, orientation, and contact locations) is such that the sensitivity to external disturbances is minimized. This results in a conservatively designed grasp for the specific task application; thus, the grasping and manipulating ability of the grasp is sub-optimized to achieve a specified level of robustness.

The study objective is to develop a grasp planning procedure for grasping and manipulating a cylinder using a three-finger precision grasp. The manipulation task simulates rotating a cylinder about a threaded post while opposing an external moment. Using the procedure, the user can determine a single grip which guarantees grasp stability, robustness, and high torquing capability for performing the manipulation task. A generalized model of an existing robotic hand, including joint torque limitations, will form the basis of the analysis. To achieve this objective, the analysis utilizes the method of grasp force focus positioning.

1.3 Background

In a recent publication [5] it is stated that "The majority of the literature to date on multi-fingered hands examines kinematic design, generation of stable grasp configurations, and the use of task requirement as a criterion for choosing grasps [6]; [7]; [8]; [9]; [10]; [11]". These studies demonstrated various techniques to analyze the complexities of multi-fingered hands using simplified planner models. In addition, several concentrated efforts

have also developed control algorithms to address the difficult subject of rolling and sliding contacts [2]; [12]; [13]; [14]; [15]. The combined results represent significant progress towards proper grasp planning.

Three recent works have developed techniques for grasp planning which incorporate grasp force focus positioning. Unlike other methods, this one uses the direct technique of positioning the grasp focus at specific locations to obtain a desired result. In contrast to early grasp stability studies, focus positioning permits the in-depth analysis and thorough understanding of the effects of variables required for grasp analysis. This, in turn, allows the study of broader task applications and general solutions using existing manipulators.

The method of grasp force focus positioning was first introduced by Brock [2], who used grasp force positioning to initiate controlled slipping in robotic grasps. The goal was to enhance the object manipulation capabilities of a robotic hand. The method was demonstrated using the Salisbury robot hand. The three-fingered hand spun a cylindrical object about one of its transverse axes by altering the grasp in a controlled manner. The grasp allows the object to spin by using gravity as the inducing force.

The concept of using the grasp force focus for grasp analysis can also be found in a 1991 publication by Yoshikawa and Nagai [16]. The purpose of this paper was to propose a new definition of grasping and manipulating forces for multi-fingered robot hands. The motivation was to define grasping and manipulating forces in a physically meaningful way. The paper defines the grasping force for three fingered hands as an internal force that satisfies the static friction constraint. The manipulating force is defined as a fingertip force that satisfies three conditions: 1) it produces the specified resultant force, 2) it is not in the inverse direction of the grasping force, and 3) it is orthogonal to

the grasping force component. The results of the study are used to develop and present an algorithm for decomposing a given fingertip force into manipulating and grasping forces.

The application of Brock's method was extended to include the joint torque limitations of the fingers by Edwards in 1990 [3]. The focus placement method was explored theoretically, with the primary effort dedicated to single-finger power grasps with one contact point at each of the three links. Edwards modelled the power grasp using a single-finger of the Utah/MIT Dexterous Hand (UMDH). The fundamental difference between Brock's and Edwards' work is where the grasp focus is placed. Brock places the focus in an area which produces the desired type of slipping. The intent of Edwards' work was to constrain the placement of the grasp focus to the stable region, and thus avoid contact slip.

Edwards graphically developed and compared constraint maps for various contact locations based upon predefined joint-torque limitations. Each constraint map represents a usable region for force placement which allows a stable grasp without violating joint-torque limits. Such regions were defined by Edwards as "Safe and Stable" regions. The goal was to determine the optimum focus location for a three-point power grasp of a cylindrical object which provides the manipulator with the greatest ability to exert torque on the object. Edwards also examined the effects of contact location, external moment magnitude, coefficient of friction, and cylinder radius on the safe and stable region. The results demonstrated that optimal focus location is dependent upon contact location, joint-torque limitations, and external torque direction.

There are two key findings from Edwards' research which are incorporated into this study. First, Edwards demonstrated that for an enveloping three point grasp, the optimum focus location is at the center of the cylinder [3:p4-13]. In addition he

demonstrated that the size of the stable region will remain constant if the ratio of external torque to grasp force magnitude remains constant [3:p4-8].

Application of Edwards' constraint mapping technique to the goals of this thesis requires some modifications. The primary difference lies in the modeling of the robotic hand. The requirements call for a general hand model comprised of three independently controlled fingers, as opposed to one. This adds a significant level of added complexity. For a single-finger power grasp, the finger joint angles are fixed and the object does not move relative to the hand. Therefore, the safe and stable region remains constant since the finger joint torques are constant. Given a constant cylinder radius and coefficient of friction, the safe and stable region is only a function of contact location, contact forces, and joint torque limitations.

This study models a three-finger precision grasp of the cylinder and the cylinder is rotated about its' longitudinal axis. Like Edwards' model, the grasp must also oppose an external torque. However, with a precision grasp the joint angles vary as the cylinder is rotated. As the joint angles change, so do the joint torques. This has a direct effect on the safe and stable region. In addition to cylinder rotation, the joint angles are also dependent on how the cylinder is positioned with respect to the hand. Therefore, using a precision grasp the safe and stable region also becomes a function of cylinder position and orientation.

Unlike Edwards' thesis, the intent of this study is not to determine the optimal grasp focus location. Instead it is to understand grasp stability behavior in the neighborhood of a given focus point in the safe and stable region as the object is manipulated. In Edwards' study, the safe and stable region is reduced to a single point. This point corresponds to the optimal grasp focus location, and thus the maximum torquing

capability for a single-finger power grasp. In this study, it is assumed that the actual position of the desired grasp focus may vary due to controller errors. Thus, the torquing capability of the grasp is sub-optimized to achieve a specified level of grasp robustness.

The combination of object manipulation, joint-torque limits, and constraint mapping is in itself the "new" area of study. To develop a grasp planning procedure, the study uses the method of grasp force focus positioning and constraint mapping. This method is used to examine various grasp configurations by varying cylinder position and orientation. The different grasp configurations are then compared to develop general relationships for cylinder position and orientation with respect to the hand.

1.4 Problem Statement

Develop a planning procedure for grasping and manipulating a cylinder using a three-finger precision grasp. Examine a manipulation task which simulates rotating a cylinder about a threaded post while opposing an external moment. The solution must satisfy the following grasp requirements:

- a) Use a single grasp configuration.
- b) Insure grasp stability and robustness over a specified cylinder rotation range.
- c) Take into account joint torque limitations of each finger.
- d) Provide the greatest capability to oppose external moments acting on the cylinder.

The resulting grasp planning procedure must allow the user to design a three-finger precision grasp based on stability criteria, torquing capability, and grasp robustness.

1.5 Method of Approach

This study examines grasp planning through the development of a three-fingered model of an existing manipulator. The grasp configuration models a three finger precision grasp of a cylindrical object. Point-contacts are assumed for each finger to avoid the complexities of rolling contacts, an unnecessary complication for this initial study of precision grasps. The study consists of two sections: 1) Inverse Kinematic Relationships and 2) Grasp Analysis. The final step is to incorporate the analytical results into a computer program to generate the appropriate data for graphical analysis.

The robotic hand model used in this study is based on the Utah/MIT Dexterous Manipulator (UMDH). This hand was chosen from a practical standpoint since two of them are used at AFIT for ongoing research. The design and function of the UMDH closely resemble that of the human hand. This convenient aspect allows direct comparison of analysis results to ones own hand to confirm or question study findings.

The kinematic data for the UMDH is documented in two sources, [17] and [18]. The key information for computing inverse kinematic relationships is the coordinate-frame layout of each finger joint. Of the two cited sources, the report generated by MIT contains the most complete documentation of coordinate frames; therefore, this data will be utilized in the ensuing analysis.

The Denavit-Hartenburg convention is applied to develop homogeneous transformation matrices to relate fingertip position with respect to the "inertial" or palm frame. The fingertip position is a function of four joint variables. The base joint of each finger permits side-to-side rotational motion, and the remaining three contribute to the curling motion of the finger. For a point contact, there are only three unknowns; however, each finger has four degrees of freedom. The fourth degree of freedom is

eliminated by setting the rotation angle of the two most distal joints equal to each other. This results in a curling motion similar to that of human fingers.

In a similar manner, the transformation matrix which relates object position and orientation with respect to the palm frame is determined. The object variables for study are proximity to the hand and rotation angle. The transformation matrices for each finger and the object are combined to form the three finger precision grasp model for finger-joint angle determination.

The method of grasp analysis used by Edwards [3] is applicable to this study since a planar grasp is employed. Summarizing the method, the solution for the contact forces can be broken into two parts: 1) the particular solution, and 2) the homogeneous solution. For this project, the particular solution represents the contact forces at each contact point required to balance the applied or external moment. The homogeneous solution represents the set of contact forces that exert no net force or moment on the grasped object. The set of homogeneous or internal contact forces has an infinite number of possible solutions.

The different internal grasp force solutions can be resolved through the use of grasp force focus positioning. The focus position will uniquely determine the solution if the grasp force magnitude is predetermined. Mapping of all focus points which meet grasp stability and joint-torque criteria will result in a usable region for focus positioning. If joint-torque limitations are ignored, the focus or "constraint" map will be made up of focus points which meet the stable no-contact-slip criteria. If the grasp force magnitude is sufficiently large, this region is reduced in size once joint-torque limitations are reintroduced.

The main effort will involve developing set of computer programs to determine how the safe and stable region changes as the object is rotated about its transverse axis. In

addition, it will also examine how this region changes as a function of object position with respect to the hand. One program will calculate the joint angles for each finger, using inverse kinematic relationships, for a given object orientation and position. The second program will use this data as input and calculate the data required for constraint mapping using the grasp analysis results. The constraint maps for each run are generated using a commercially available graphics package.

In examining the change in the safe and stable region, it is also important to know which finger-joint violates the stable area. Therefore, the focus mapping program will also generate joint-torque boundary lines within the stable region for each joint in violation. With this feature it is possible to determine which finger joints contribute to the violation and their corresponding relationship to object position and orientation.

To examine grasp robustness it is necessary to generate constraint maps at selected intervals of the object rotation range. The intersection of all constraint maps represents the net useful safe and stable region for object manipulation. Contact location is also examined to determine its effects on the net region. Stability behavior is analyzed by selecting a focus point within the net region and determining how contact forces and joint torques are effected as the focus deviates from the location.

The final step is to determine how to position the object for increased torquing capability and grasp robustness. This can only be accomplished after establishing the general relationships from the graphical analysis. Torquing capabilities are examined for full and partial rotations by setting the stable grasp region to a predetermined size. The size of the region directly relates to a constant external torque-to-grasp force ratio. Maintaining a constant ratio, the external torque is increased until the point at the cylinder center no longer resides in the net region.

In summary, the approach is to use the method of grasp force focus positioning to complete three basic steps. The first step is to examine various grasp configurations by varying the position and orientation of the cylinder with respect to the hand. The second is to develop relationships which compare the different grasp configurations. The final step is to use these relationships to design a robust grasp for high torque applications.

1.6 Contributions

The grasp force focus positioning method permits the thorough examination of grasp variables and their effects on grasp stability and robustness. The in-depth understanding gained by using this method provides the user with key information for grasp planning. This project successfully demonstrates a planning procedure for robust grasp design using a three finger precision grasp of a cylindrical object; the results of which complete another milestone towards demonstrating intelligent part mating skills by the AFIT Robotics Laboratory.

By using a generalized system model, the study findings are applicable to similar grasping tasks currently under research. The model can be easily adjusted to represent other existing or new hand designs by simply changing hand dimensions and joint torque limitations. The effectiveness of various hand designs can then be examined for specific task applications using the presented planning procedure. The versatility of the procedure and techniques presented provides a grasp planning tool for use within the robotics community.

1.7 Organization

Chapter II will discuss the development of the system model and the determination of the inverse kinematic relationships. Chapter III summarizes the grasp analysis and grasp force focus positioning method developed by Edwards [3]. Modifications to the analysis for application to this study are also included. A description of the two computer programs written for graphical analysis is given in Chapter IV. Chapter V examines the results from the graphical analysis and presents examples of the analysis procedure used. Study conclusions are discussed in Chapter VI. Finally, Chapter VII gives recommendations for use of these results and suggestions for future study efforts.

II. Model Kinematics

2.1 Description of Hand Model

The robotic hand model configuration presented in this chapter is based on the Utah/MIT Dexterous Hand (UMDH). The UMDH is a right-handed, four-fingered (three fingers and one thumb) dexterous hand. Each finger of the hand has four degrees of freedom from which to specify fingertip position in 3-space. The hand kinematic data presented herein is cited from a report generated by Narasimhan [17]. In general, the extracted information concerns coordinate frame layouts and dimensions for the UMDH.

The grasp force positioning method can only be applied to three-point-contact grasps since the solution is only unique for this particular application. Therefore, the grasp analysis requires the development of a three fingered hand model. A schematic of the three-fingered hand model under study is shown in Figure 2-1. The numbering scheme for each finger is: a) Thumb - Finger 0, b) Index finger - Finger 1, c) Middle finger - Finger 2. The label J_{ij} represents the numbering scheme for joint i on finger j . This type of subscript notation also denotes specific hand coordinate frame axes and joint angles references within this study.

2.2 Hand Model Coordinate Frames

The ease of determining kinematic relationships for a robotic hand is entirely dependent on proper selection of coordinate frames. The Denavit-Hartenburg (D-H) notation method is used to denote the joint coordinate frames for each finger. The labeling of each joint frame is depicted in Figure 2-2 and Figure 2-3, and is done so in a manner which is consistent with [17:p117].

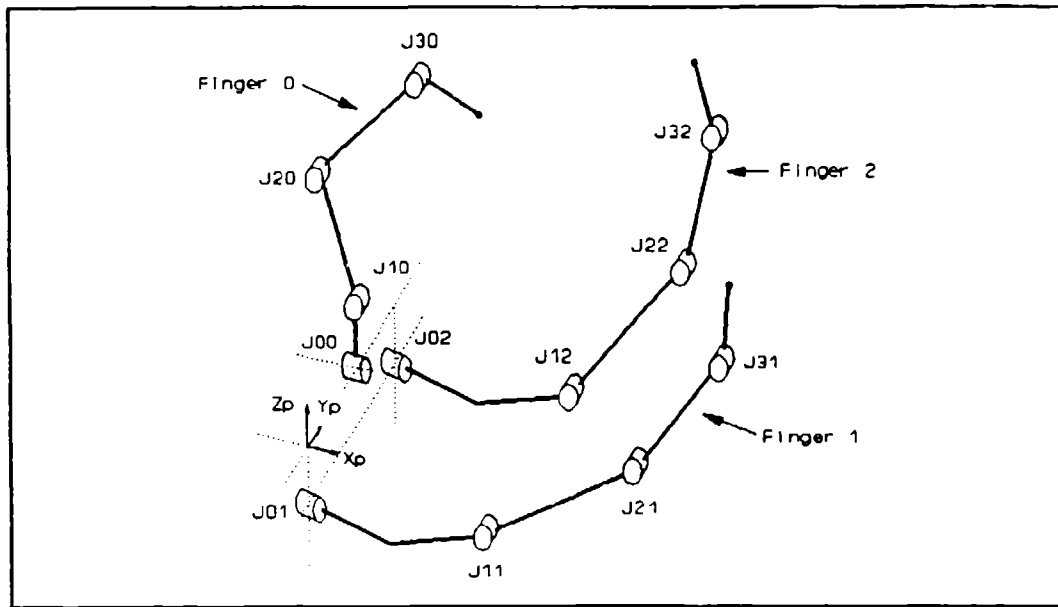


Figure 2-1. Schematic of Three-Fingered Hand Model

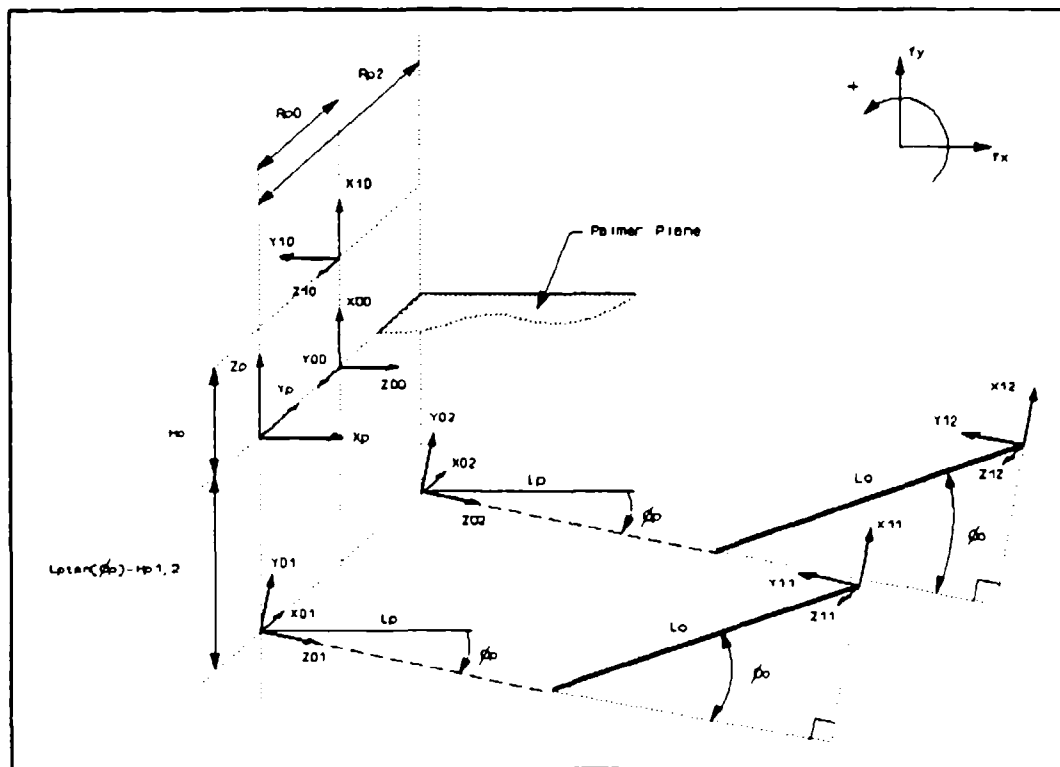


Figure 2-2. Joint 1 & 2 Layout for Three Fingered Hand Model

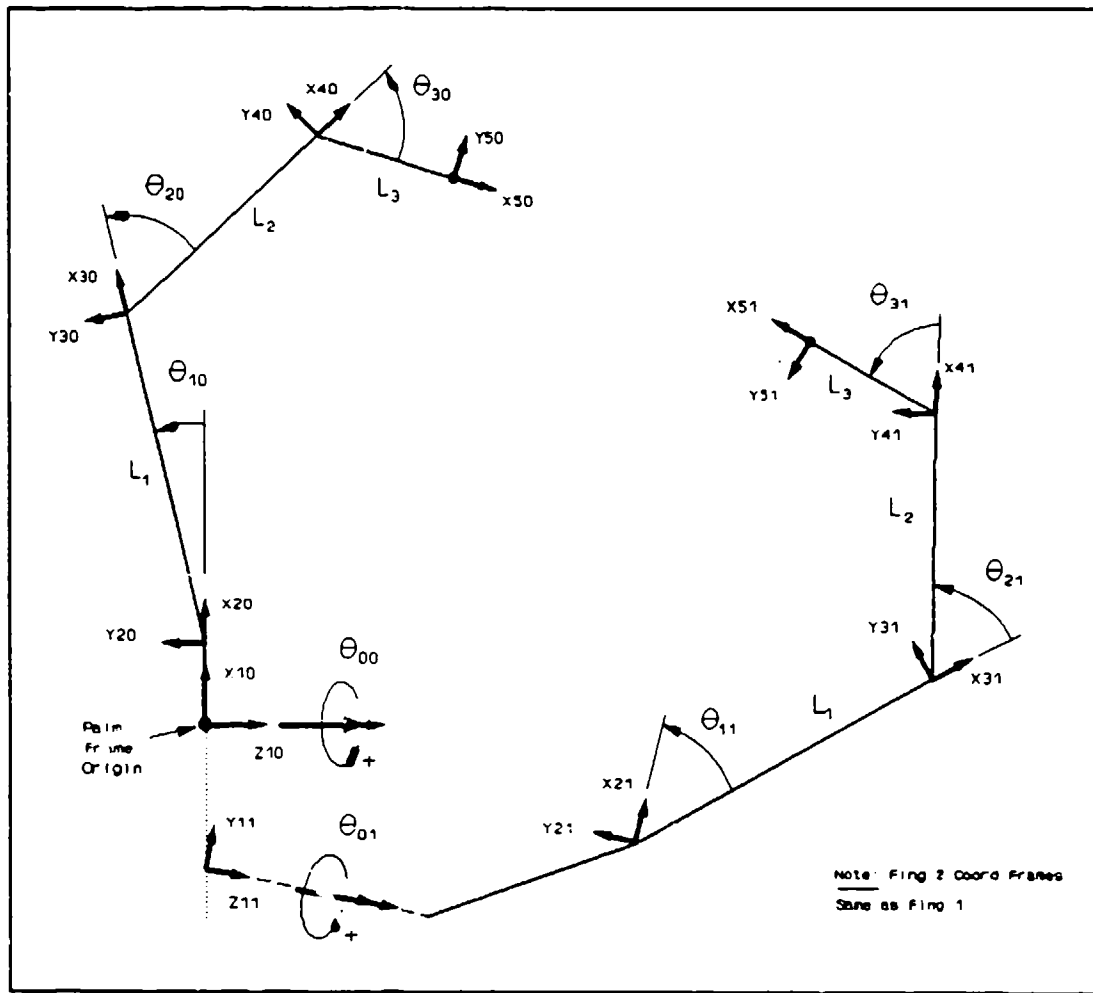


Figure 2-3. Finger Coordinate Frame Layout: x_p - z_p planar view, positive y_p -axis direction

2.2.1 Palm Frame. The palm frame $\{x_p, y_p, z_p\}$ is the frame to which all other frame positions and orientations are referenced. The palm frame is located directly above J_{01} and in the plane containing the base frame origin $\{x_{0j}, y_{0j}, z_{0j}\}$ ($j=0,1,2$) for each finger. The palm frame is aligned with the hand such that the x_p - and y_p -axes lie in the palmer plane, and the positive z_p -axis is perpendicular to it and pointing out.

The coordinate frame assignments for Finger 0 differs from those for Finger 1 and Finger 2 in two areas; 1) the location and orientation of the base or zero joints (J_{0j}) with

respect to the palm frame, and 2) the position of Joint 1 (J_{1j}) with respect to the base joint. For these reasons the frame assignments for Finger 0 are addressed separately from those for Finger 1 and Finger 2.

2.2.2 Finger 0 Coordinate Frames. The base joint of Finger 0 is located a distance R_{p0} from the palm frame origin as measured along the positive Y_p -axis. The base joint rotates about the z_{00} -axis, which is parallel to the palmer plane and aligned with the x_p -axis. The base joint frame assignment does not follow the conventional D-H method and is treated as an intermediate coordinate frame. The relation between the base joint for Finger 0 and the palm frame is expressed as [17:p122]:

$$Trans(Y_p, R_{p0}) \cdot Rot(Y_p, \pi/2) \cdot Rot(z', \pi)$$

where R_{p0} for Finger 0 is 0.695 inches, and z' denotes the z_p -axis after the rotation about the y_p -axis. The homogeneous transformation or A matrix relating the position and orientation of the base joint frame to the palm frame is:

$${}^pA_1 = \begin{vmatrix} 0 & 0 & 1 & 0 \\ 0 & -1 & 0 & R_{p0} \\ 1 & 0 & 0 & 0 \\ 0 & 0 & 0 & 1 \end{vmatrix} \quad (2.1)$$

Joint 1 (J_{10}) is positioned a distance H_0 above the base joint as measured along the positive x_{00} -axis. The value of H_0 in the analytical model is equal to 0.4 inches. Joint 1 of Finger 0 rotates about the z_{10} -axis, which is parallel to the palmer plane and in the

direction of the negative y_p -axis. This joint and the remaining joints on Finger 0 follow the D-H frame assignment convention from which the A matrices can be derived from the standard D-H matrix:

$${}^iA_{i+1} = \begin{bmatrix} C_{\theta_{i0}} & -S_{\theta_{i0}}C_{\alpha_i} & S_{\theta_{i0}}S_{\alpha_i} & a_iC_{\theta_{i0}} \\ S_{\theta_{i0}} & C_{\theta_{i0}}C_{\alpha_i} & -C_{\theta_{i0}}S_{\alpha_i} & a_iS_{\theta_{i0}} \\ 0 & S_{\alpha_i} & C_{\alpha_i} & d_i \\ 0 & 0 & 0 & 1 \end{bmatrix} \quad (2.2)$$

where $C_{\theta_{i0}}$ denotes $\cos(\theta_{i0})$, $S_{\theta_{i0}}$ denotes $\sin(\theta_{i0})$, and i designates the joint number.

The A matrix relating the position and orientation of the Joint 1 frame of Finger 0 to its' base joint frame is:

$${}^1A_2 = \begin{bmatrix} \cos\theta_{00} & 0 & -\sin\theta_{00} & H_0\cos\theta_{00} \\ \sin\theta_{00} & 0 & \cos\theta_{00} & H_0\sin\theta_{00} \\ 0 & -1 & 0 & 0 \\ 0 & 0 & 0 & 1 \end{bmatrix} \quad (2.3)$$

where θ_{00} is the variable joint rotation angle for Joint 1.

The frame assignments for the remaining three joints on Finger 0 correspond to simple revolute axes. All three joint rotation axes are parallel and are perpendicular to the plane of finger movement termed the *operational plane* [17:p120]. Each joint rotates about its' z-axis which is perpendicular to the z_{10} -axis of the base joint. The corresponding A matrices for each joint are:

$${}^2A_3 = \begin{vmatrix} \cos\theta_{10} & -\sin\theta_{10} & 0 & l_1\cos\theta_{10} \\ \sin\theta_{10} & \cos\theta_{10} & 0 & l_1\sin\theta_{10} \\ 0 & 0 & 1 & 0 \\ 0 & 0 & 0 & 1 \end{vmatrix} \quad (2.4)$$

$${}^3A_4 = \begin{vmatrix} \cos\theta_{20} & -\sin\theta_{20} & 0 & l_2\cos\theta_{20} \\ \sin\theta_{20} & \cos\theta_{20} & 0 & l_2\sin\theta_{20} \\ 0 & 0 & 1 & 0 \\ 0 & 0 & 0 & 1 \end{vmatrix} \quad (2.5)$$

$${}^4A_5 = \begin{vmatrix} \cos\theta_{30} & -\sin\theta_{30} & 0 & l_3\cos\theta_{30} \\ \sin\theta_{30} & \cos\theta_{30} & 0 & l_3\sin\theta_{30} \\ 0 & 0 & 1 & 0 \\ 0 & 0 & 0 & 1 \end{vmatrix} \quad (2.6)$$

where θ_{i0} is the variable joint rotation angle for Joint i on Finger 0. For the hand model l_1 is 1.7 inches and l_2 is 1.3 inches, where l is the length of each finger appendage. The term l_3 represents the distance from Joint 3 to the fingertip, and is set to a value of 0.735 inches for the hand model.

Since the model assumes point-contacts, l_3 is also the constant distance to the contact point on the object. In a more general application, the contact point would be represented by an additional coordinate frame and separated from the fingertip frame by a variable length l_c and variable angle β . The D-H parameters for Finger 0 are summarized in Table 2-1.

Given the A matrices for each joint, the transformation matrix relating the position and orientation of the fingertip frame $\{x_{50}, y_{50}, z_{50}\}$ on Finger 0 with respect to frame n at J_{n0} (where $n < 5$) is given by:

$${}^nT_5 = {}^nA_{n+1} {}^{n+1}A_{n+2} \cdot \cdot \cdot {}^4A_5 \quad (2.7)$$

Using Equation 2.7, the transformation matrix relating the position and orientation of the fingertip frame on Finger 0 to $\{x_{10}, y_{10}, z_{10}\}$ is:

$${}^1T_5 = \begin{vmatrix} C_{00}C_{123,0} & -C_{00}S_{123,0} & -S_{00} & C_{00}(H_o + l_3C_{123,0} + l_2C_{12,0} + l_1C_{10}) \\ S_{00}C_{123,0} & -S_{00}S_{123,0} & C_{00} & S_{00}(H_o + l_3S_{123,0} + l_2S_{12,0} + l_1S_{10}) \\ -S_{123,0} & -C_{123,0} & 0 & l_3S_{123,0} + l_2S_{12,0} + l_1S_{10} \\ 0 & 0 & 0 & 1 \end{vmatrix} \quad (2.8)$$

and the transformation matrix relating the position and orientation of the fingertip frame on Finger 0 to its' base joint frame $\{x_{20}, y_{20}, z_{20}\}$ is :

$${}^2T_5 = \begin{vmatrix} C_{123,0} & -S_{123,0} & 0 & l_3C_{123,0} + l_2C_{12,0} + l_1C_{10} \\ S_{123,0} & C_{123,0} & 0 & l_3S_{123,0} + l_2S_{12,0} + l_1S_{10} \\ 0 & 0 & 1 & 0 \\ 0 & 0 & 0 & 1 \end{vmatrix} \quad (2.9)$$

2.2.3 Finger 1 and Finger 2 Coordinate Frames. The origins of the base joint frames on Finger 1 and Finger 2 are equally positioned below the palmer plane and in the y_P - z_P plane of the palm frame. The coordinate frames of both joints are aligned such that

Table 2-1. D-H Parameters for Finger 0

Joint + 1	d_i	a_i	α_i	θ_{i0}
1	0	H_{P0}	$-\pi/2$	θ_{00}^*
2	0	l_1	0	θ_{10}^*
3	0	l_2	0	θ_{20}^*
4	0	l_3	0	θ_{30}^*

* variable joint angle i for Finger 0

their x -axes are parallel to the palmer plane and in the direction of the positive y_p -axis. In addition, both frames are rotated counterclockwise about their respective x -axes by a fixed angle φ_p . The base joint of Finger 1 resides along the negative z_p -axis and the base joint of Finger 2 is separated from it by a fixed distance R_{P2} , as measured along the positive x_{11} -axis. The base joint of Finger 1 and Finger 2 rotates about the z_{11} -axis and z_{12} -axis, respectively. Like the base joint for Finger 0, both of these base joint frame assignments do not follow the conventional D-H method and are treated as intermediate coordinate frames. The relation between the base joint for Finger k ($k=1,2$) and the palm frame is expressed as [17:p118]:

$$Trans(y_p, R_{Pk}) \cdot Trans(z_p, l_p \tan \varphi_p - H_p) \cdot Rot(y_p, \pi/2 + \varphi_p) \cdot Rot(z', \pi/2)$$

where z' denotes the z_p -axis after the rotation about the y_p -axis, and:

$$\begin{aligned} R_{P1} &= 0 \text{ inches} & H_{\hat{r}} &= 0.95 \text{ inches} \\ R_{P2} &= 1.39 \text{ inches} & \varphi_p &= 12 \text{ degrees} \\ l_p &= 1.05 \text{ inches} \end{aligned}$$

It should be noted that the value chosen for R_{P2} is different than that in [17]. The actual value of R_{P2} in [17:p119] is equal to 1.42 inches. For this study R_{P2} is set equal to twice that of R_{P0} so that the positioning of base joint J_{01} and J_{02} is symmetric about the base joint for Finger 0. The intent is to minimize asymmetrical properties in the forthcoming analysis.

The A matrix for Finger 1 or Finger 2 relating the position and orientation of base joint frame $\{x_{2k}, y_{2k}, z_{2k}\}$ to the palm frame is:

$${}^P A_1 = \begin{vmatrix} 0 & \sin \varphi_P & \cos \varphi_P & 0 \\ 1 & 0 & 0 & R_{Pk} \\ 0 & \cos \varphi_P & -\sin \varphi_P & l_P \tan \varphi_P - H_P \\ 0 & 0 & 0 & 1 \end{vmatrix} \quad (2.10)$$

where $k = 1, 2$

The first link (l_0) of Finger 1 or Finger 2 makes a fixed angle φ_0 with the z -axis of rotation at the base joint. For the hand model, φ_0 equals 30 degrees and l_0 equals 1.2 inches. The A matrix for Finger 1 or Finger 2 relating the position and orientation of the Joint 1 frame to its base frame is:

$${}^1 A_2 = \begin{vmatrix} \cos \theta_{0k} & 0 & -\sin \theta_{0k} & l_0 \sin \varphi_0 \cos \theta_{0k} \\ \sin \theta_{0k} & 0 & \cos \theta_{0k} & l_0 \sin \varphi_0 \sin \theta_{0k} \\ 0 & -1 & 0 & \frac{l_F}{\cos \varphi_P} + l_0 \cos \varphi_0 \\ 0 & 0 & 0 & 1 \end{vmatrix} \quad (2.11)$$

where $k = 1, 2$ and θ_{1k} is the variable joint angle for Joint 1 on finger k

Since the remaining frame assignments for both Finger 1 and Finger 2 are identical to those for Finger 0, the form of the corresponding A matrices is also the same. Therefore, the A matrices represented by Equations 2-4, 2-5, 2-6 and 2-9 apply to Finger 1 and Finger 2 with the appropriate change of joint angle subscripts. The D-H parameters for Finger 1 or Finger 2 are summarized in Table 2-2.

Using Equation 2.7 the transformation matrix relating the position and orientation the fingertip frame on Finger k to coordinate frame $\{x_{1k}, y_{1k}, z_{1k}\}$ is:

$${}^1T_5 = \begin{vmatrix} C_{0k}C_{123,k} & -C_{0k}S_{123,k} & -S_{0k} & C_{0k}(l_o \sin \varphi_o + l_3 C_{123,k} + l_2 C_{12,k} + l_1 C_{1k}) \\ S_{0k}C_{123,k} & -S_{0k}S_{123,k} & C_{0k} & S_{0k}(l_o \sin \varphi_o + l_3 S_{123,k} + l_2 S_{12,k} + l_1 S_{1k}) \\ -S_{123,k} & -C_{123,k} & 0 & l_o \cos \varphi_o + \frac{l_p}{\cos \varphi_p} - l_3 S_{123,k} - l_2 S_{12,k} - l_1 S_{1k} \\ 0 & 0 & 0 & 1 \end{vmatrix} \quad (2.12)$$

where $k = 1, 2$, and subscripts $123,k$ and $12,k$ denotes $(\theta_{1k} + \theta_{2k} + \theta_{3k})$ and $(\theta_{1k} + \theta_{2k})$, respectively.

2.3 Cylinder Coordinate Frames

The final step in the system modeling task is the frame assignments for the cylinder. The goal is to select a framework configuration which permits variations of cylinder proximity and orientation with respect to the hand. As before, the palm frame is the frame of reference. The frame assignments for cylinder position with respect to the palm frame are shown in Figure 2-4. These frame assignments allow the body to be moved towards

or away from Finger 0, and held in close to or extended away from the palm. The frame assignments also allow for the rotation of the cylinder centerline about the y_p -axis.

The first frame is positioned a distance R_b from the palm frame origin, as measured along the positive y_p -axis. The value of R_b is set to 0.695 inches, which is equal to R_{p0} . This particular value provides for model symmetry about the x - z plane of base joint on Finger 0. That is, the cylinder centerline resides in the x - z plane of $J00$, and $J10$ and $J20$ are symmetrically positioned about this plane (reference Section 2.2.2 and Figure 2-1). The origin of Frame 2b is coincident with the Frame 1b and the x_{2b} -axis is aligned with the y_{1b} -axis. The frame is rotated clockwise about the x_{2b} -axis by an angle α_b such that the z_{2b} -axis is pointing towards Finger 1 and 2. The third frame is displaced from Frame 2b by a variable distance d_3 , and Frame 4b is positioned a variable distance d_4 from Frame 3b. The cylinder is aligned with Frame 4b such that its centerline is along the z_{4b} -axis and the cylinder contact plane is coincident with the x_{4b} - y_{4b} plane.

The frame assignments for cylinder orientation and contact position are shown in Figure 2-5. The body frame, *Frame B*, is fixed to the cylinder center and rotates about Frame 4b by a variable angle ϕ_b . The contact frame origins are located at the cylinder surface, and are rotated from the B_y -axis by a fixed angle ψ_j ($j=0,1,2$). The subscript for contact frame C_0 , C_1 , and C_2 corresponds to the contact made by Finger 0, Finger 1, and Finger 2, respectively. The cylinder radius r_c is set to 1.0812 inches for the study model.

The D-H parameters for the cylinder are summarized in Table 2-3. The A matrices for each of the cylinder coordinate frames are:

$${}^pA_1 = \begin{vmatrix} 0 & 0 & 1 & 0 \\ 0 & -1 & 0 & R_b \\ 1 & 0 & 0 & 0 \\ 0 & 0 & 0 & 1 \end{vmatrix} \quad (2.13)$$

Table 2-2. D-H Parameters for Finger 1 and Finger 2

Joint+1	d_i	a_i	α_i	θ_{ij}
1	$\frac{l_p}{\cos(\varphi_p)} + l_o \cos(\varphi_o)$	$l_o \sin(\varphi_o)$	$-\pi/2$	θ_{0j}^*
2	0	l_1	0	θ_{1j}^*
3	0	l_2	0	θ_{2j}^*
4	0	l_3	0	θ_{3j}^*

* variable joint angle i for Finger k , $k = 1, 2$

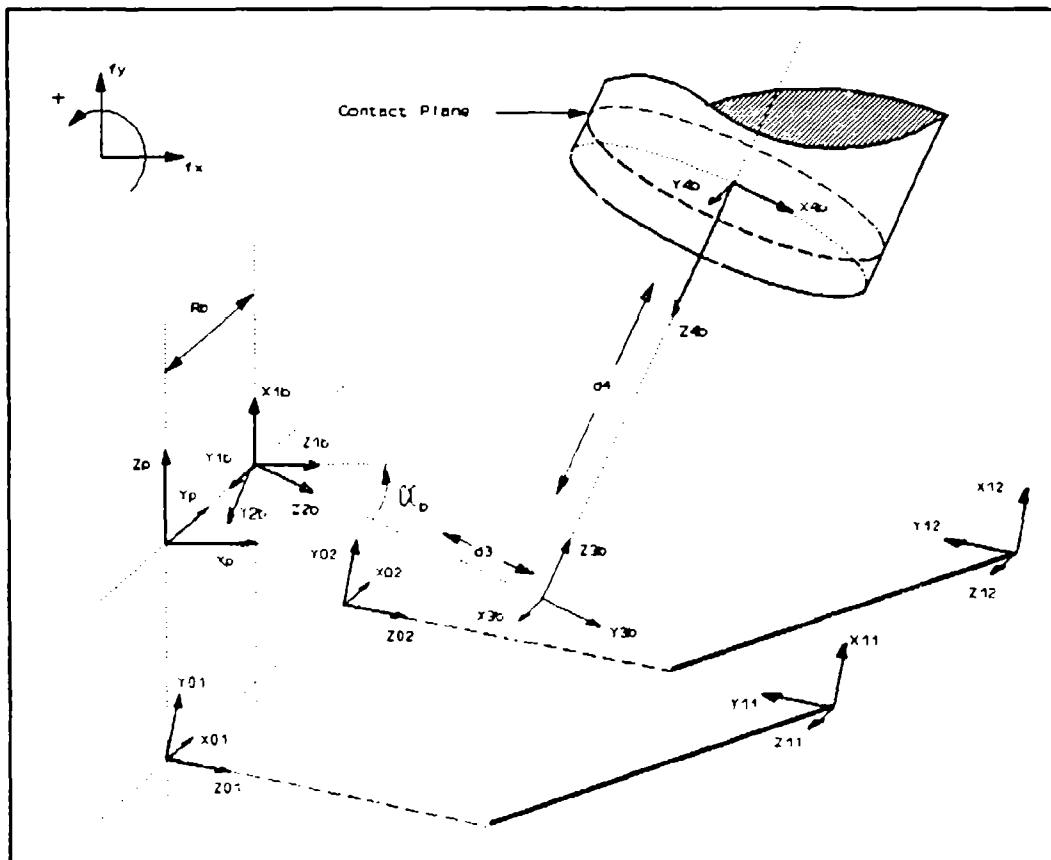


Figure 2-4. Cylinder Frame Assignments with respect to Palm Frame

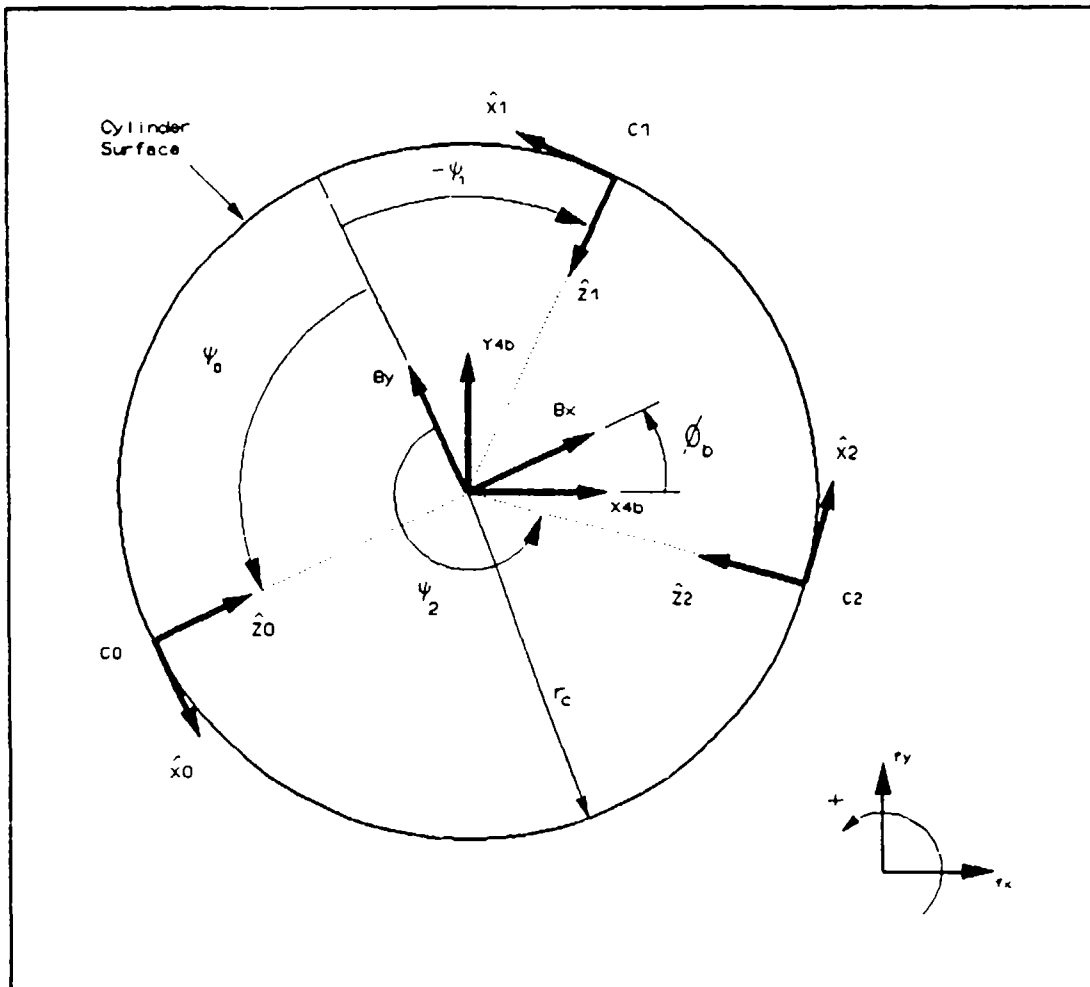


Figure 2-5. Position & Orientation of Contact Frames

Table 2-3. D-H Parameters for Cylindrical Object

Frame +1	d_i	a_i	α_i	θ_i
2	0	0	α_b	$\pi/2$
3	d_3^*	0	$\pi/2$	0
4	d_4^*	0	π	$\pi/2$
B	0	0	0	φ_b^*
$C_j^{\#}$	0	0	0	$\psi_j^{\#}$

* variable

$\#$ for contact j , $j=0,1,2$

$${}^1A_2 = \begin{vmatrix} 0 & -\cos\alpha_b & \sin\alpha_b & 0 \\ 1 & 0 & 0 & 0 \\ 0 & \sin\alpha_b & \cos\alpha_b & 0 \\ 0 & 0 & 0 & 1 \end{vmatrix} \quad (2.14)$$

$${}^2A_3 = \begin{vmatrix} 1 & 0 & 0 & 0 \\ 0 & 0 & -1 & 0 \\ 0 & 1 & 0 & d_j \\ 0 & 0 & 0 & 1 \end{vmatrix} \quad (2.15)$$

$${}^3A_4 = \begin{vmatrix} 0 & 1 & 0 & 0 \\ 1 & 0 & 0 & 0 \\ 0 & 0 & -1 & d_4 \\ 0 & 0 & 0 & 1 \end{vmatrix} \quad (2.16)$$

$${}^3A_4 = \begin{vmatrix} \cos\phi_b & -\sin\phi_b & 0 & 0 \\ \sin\phi_b & \cos\phi_b & 0 & 0 \\ 0 & 0 & 1 & 0 \\ 0 & 0 & 0 & 1 \end{vmatrix} \quad (2.17)$$

$${}^B A_{Cj} = \begin{vmatrix} -\cos\psi_j & 0 & \sin\psi_j & -r_c \sin\psi_j \\ \sin\psi_j & 0 & -\cos\psi_j & r_c \cos\psi_j \\ 0 & -1 & 0 & 0 \\ 0 & 0 & 0 & 1 \end{vmatrix} \quad (2.18)$$

where Cj denotes contact j , $j = 0, 1, 2$

Using Equation 2.7, the homogeneous transformation matrix relating the position and orientation of each contact with respect to the palm frame is given by:

$${}^P T_{Cj} = \begin{vmatrix} -C_{a_b} C(\varphi_b + \psi_j) & -S_{a_b} & C_{a_b} S(\varphi_b + \psi_j) & -d_4 S_{a_b} + C_{a_b} (d_3 - r_c S(\varphi_b + \psi_j)) \\ S(\varphi_b + \psi_j) & 0 & -C(\varphi_b + \psi_j) & R_b - r_c C(\varphi_b + \psi_j) \\ -S_{a_b} C(\varphi_b + \psi_j) & C_{a_b} & S_{a_b} S(\varphi_b + \psi_j) & d_4 C_{a_b} + S_{a_b} (d_3 - r_c S(\varphi_b + \psi_j)) \\ 0 & 0 & 0 & 1 \end{vmatrix} \quad (2.19)$$

where subscript Cj denotes contact j , $j = 0, 1, 2$

2.4 Inverse Kinematic Relationships

The inverse kinematic relationships for the system model are easily determined from the A matrices for the hand and cylinder. The first step is to determine the 3-space coordinates of each contact location in terms of the palm frame coordinates. Note that this assumes that the cylinder position and orientation with respect to the palm frame is known in advance. From Equation 2.19 the scalar 3-space contact positions written in palm frame coordinates is given by:

$$\begin{aligned} {}^P X_{Cj} &= -d_4 S_{a_b} + C_{a_b} (d_3 - r_c S(\varphi_b + \psi_j)) \\ {}^P Y_{Cj} &= R_b - r_c C(\varphi_b + \psi_j) \\ {}^P Z_{Cj} &= d_4 C_{a_b} + S_{a_b} (d_3 - r_c S(\varphi_b + \psi_j)) \end{aligned} \quad (2.20)$$

where Cj denotes contact j , $j = 0, 1, 2$

To solve for the inverse kinematic equations, it is necessary to convert the x, y, z contact positions as expressed in the palm frame to the appropriate joint frame. The general equation to convert the 3-space position of *Contact j* , as written in palm frame coordinates, to the local cartesian coordinates at *Joint n* ($n=1,2$) on *Finger j* ($j=0,1,2$) is given by:

$$\begin{pmatrix} {}^nX_{C_j} \\ {}^nY_{C_j} \\ {}^nZ_{C_j} \\ 1 \end{pmatrix} = [{}^PA_n]^{-1} \begin{pmatrix} {}^PX_{C_j} \\ {}^PY_{C_j} \\ {}^PZ_{C_j} \\ 1 \end{pmatrix} \quad (2.21)$$

where C_j denotes contact frame j , and n denotes frame n on Finger j .

Using Equation 2.21 the cartesian coordinates of Contact 0 written in coordinate frame $\{x_{10}, y_{10}, z_{10}\}$ located on Finger 0 is:

$$\begin{aligned} {}^{10}X_{C0} &= {}^PZ_{C0} \\ {}^{10}Y_{C0} &= R_{P0} - {}^PY_{C0} \\ {}^{10}Z_{C0} &= {}^PX_{C0} \end{aligned} \quad (2.22)$$

An issue to resolve before proceeding with the solution for each joint angle is the possibility of multiple joint angle solutions. Multiple joint angle solutions are possible for each finger of the hand model by positioning any two adjacent finger links in an elbow-up or elbow-down configuration. Proper selection of artificial constraints on the last three joints of each finger will avoid this problem entirely. Since the design of the UMDH naturally restricts adjacent links to only one possible configuration, similar constraints can

be applied to the hand model. Joint rotation limits for each finger in the hand model in presented in Table 2-4. The joint limits imposed are based on actual measurements of corresponding joints on the UMDH.

With the contact position written in the base joint of Finger 0, the joint angle θ_{00} from the geometric relation:

$$\theta_{00} = \arctan\left(\frac{{}^{00}y_{co}}{{}^{00}x_{co}}\right) \quad (2.23)$$

The final step is to solve for the three remaining joint angles for Finger 0 (θ_{10} , θ_{20} , θ_{30}) in terms of contact position and θ_{00} . However, locating the fingertip at the contact location is a 3 degree of freedom task; therefore one of the remaining finger joint angles is redundant. This problem exists for all three fingers, since each one has four joints. One method to resolve this redundancy for each finger is to specify a general equation of constraint on the last two distal joints:

$$\theta_{3j} = K \times \theta_{2j} \quad (2.24)$$

where K is a proportionality constant, and θ_{ij} is the joint angle i for Finger j , $j = 0, 1, 2$.

The result of this approach is similar to the joint angle rotation of the last two distal joints on a human finger [17:p29]. To solve for the remaining joint angles on Finger 0 it is first necessary to transfer the cartesian coordinates of Contact 0 to the local coordinate frame $\{x_{20}, y_{20}, z_{20}\}$:

Table 2-4. Joint Angle Limits

Joint	Joint Rotation Limit (degrees)		
	Finger 0	Finger 1	Finger 2
0	-45 to 45	115 to 65	115 to 65
1	-60 to 15	-60 to 11	-60 to 11
2	-90 to 6.5	6.5 to 90	6.5 to 90
3	-90 to 0	0 to 90	0 to 90

$$\begin{aligned}
 {}^2X_{C0} &= -H_o + {}^1X_{C0}\cos\theta_{00} + {}^1Y_{C0}\sin\theta_{00} \\
 {}^2Y_{C0} &= -{}^1Z_{C0} \\
 {}^2Z_{C0} &= {}^1Y_{C0}\cos\theta_{00} - {}^1X_{C0}\sin\theta_{00}
 \end{aligned} \tag{2.25}$$

Given the 3-space position of the contact and noting that the three remaining joint axes are parallel to one another, the solution for three joint angles is a simple geometry problem. From Equation 2.8, the X and Y position components of Contact 0 written in the $\{x_{20}, y_{20}, z_{20}\}$ frame can also be expressed as:

$$\begin{aligned}
 {}^2X_{C0} &= l_1\cos\theta_{10} + l_2\cos(\theta_{10} + \theta_{20}) + l_3\cos(\theta_{10} + \theta_{20} + \theta_{30}) \\
 {}^2Y_{C0} &= l_1\sin\theta_{10} + l_2\sin(\theta_{10} + \theta_{20}) + l_3\sin(\theta_{10} + \theta_{20} + \theta_{30})
 \end{aligned} \tag{2.26}$$

The value of K in Equation 2.24 is set to 1, such that $\theta_{30} = \theta_{20}$, to simplify the solution. Squaring Equation 2.26 and using the cosine double angle identity, the equation reduces to a quadratic form in terms of θ_{20} .

$$4l_1l_3(\cos\theta_{20})^2 + 2(l_1l_2 + l_2l_3)\cos\theta_{20} - ({}^2X_{C0}^2 + {}^2Y_{C0}^2 - l_1^2 - l_2^2 - l_3^2 + 2l_1l_3) \quad (2.27)$$

The solution of which is:

$$\theta_{20} = \arctan\left(\frac{-\sqrt{1-D^2}}{D}\right) \quad (2.28)$$

where

$$D = \frac{-\frac{2l_2(l_1+l_3)}{l_1l_3} + \sqrt{\frac{4l_2^2(l_1+l_3)^2}{l_1^2l_2^2} - \frac{16(l_1^2+l_2^2-2l_1l_3+l_3^2-{}^2X_{C0}^2-{}^2Y_{C0}^2)}{l_1l_3}}}{8}$$

Note the minus sign before the radical in Equation 2.29 corresponds to the elbow-up configuration for Finger 0 (reference Figure 2-3).

Finally the solution for the last joint angle on Finger 0 is given by:

$$\theta_{10} = \arctan\left(\frac{{}^2Y_{C0}}{{}^2X_{C0}}\right) - \arctan\left(\frac{l_2\sin\theta_{20} + l_3\sin(2\theta_{20})}{l_1 + l_2\cos(\theta_{20}) + l_3\cos(2\theta_{20})}\right) \quad (2.29)$$

Applying the same joint angle solution method to Finger 1 and Finger 2 only requires a change to the coordinate transformations from the palm frame to the appropriate finger joint and a change of subscripts. Since the kinematic structure of both fingers are identical, the ensuing equations apply to both. Using Equation 2.21 the cartesian coordinates of Contact k written in base joint coordinate frame $\{x_{1k}, y_{1k}, z_{1k}\}$ for Finger k ($k=1,2$) is:

$$\begin{aligned}
{}^1X_{Ck} &= -R_{Pk} + {}^PY_{Ck} \\
{}^1Y_{Ck} &= H_P \cos \varphi_P + {}^PX_{Ck} \sin \varphi_P + {}^PZ_{Ck} \cos \varphi_P - l_P \cos \varphi_P \tan \varphi_P \\
{}^1Z_{Ck} &= {}^PX_{Ck} \cos \varphi_P - {}^PZ_{Ck} \sin \varphi_P - H_P \sin \varphi_P + l_P \sin \varphi_P \tan \varphi_P
\end{aligned} \tag{2.30}$$

and the cartesian coordinates of Contact k written in coordinate frame $\{x_{2k}, y_{2k}, z_{2k}\}$ for Finger k is:

$$\begin{aligned}
{}^2X_{Ck} &= {}^1X_{Ck} \cos \theta_{0k} + {}^1Y_{Ck} \sin \theta_{0k} - l_o \sin \varphi_o \\
{}^2Y_{Ck} &= l_o \cos \varphi_o + \frac{l_P}{\cos \varphi_P} - {}^1Z_{Ck} \\
{}^2Z_{Ck} &= - {}^1X_{Ck} \sin \theta_{0k} + {}^1Y_{Ck} \cos \theta_{0k}
\end{aligned} \tag{2.31}$$

Using Equation 2.30, the solution for θ_{0k} is given by (2.23) with the appropriate subscript changes. Similarly, the solution for θ_{1k} is given by Equation 2.29 using Equation 2.31. The solution for θ_{2k} is similar in form to Equation 2.28. By changing the sign before the radical to a positive to account for the elbow down configuration of Finger k , Equation 2.28 can be used to solve for θ_{2k} . The equation for D in Equation 2.28 is still valid using Equation 2.31.

2.5 Model Application

The inverse kinematic equations from Section 2.4 form the basis to determine finger joint angles as a function of cylinder position and orientation. The inverse kinematic analysis for this project consists of using a Sun computer workstation to run a Fortran program which incorporates the model equations. The input to the program consists of specific values for contact location, cylinder position and orientation, and cylinder rotation

increment. With this data the program will output the resulting joint angles for each specified rotation increment and determine the allowable maximum rotation range of the cylinder. The definition of the allowable rotation range is simply the resulting rotation range which does not violate any of the joint angle limits.

There are two additional features which the program provides as output. The first is the specification of the angle which the last finger link (l_3) makes with the cylinder contact plane. The program output provides this data, termed *fingertip grasp angles* or simply "*grasp angles*", for each of the three fingers. This data is useful since it indicates where the contact point is relative to the fingertip. A negative grasp angle corresponds to a contact location on the topside or "fingernail" portion of the fingertip. A positive grasp angle corresponds to a contact location on the underside of the fingertip. This is a desirable contact location since on actual robotic hands, this area is typically covered with a slip-resistant coating and may also house contact sensors.

The second feature of the program is the output of joint angle data for each finger, corresponding to a specific cylinder rotation angle. This discrete rotation angle is specified as an input parameter and the resulting data is sent to an external data file. The next chapter develops grasp and torque equations for inclusion in a grasp force focus mapping program which uses the joint angle data file as one of its inputs.

The inverse kinematics program utilizes five input parameters to specify cylinder position and orientation: 1) contact location (ψ_0, ψ_1, ψ_2), 2) discrete cylinder rotation angle (ϕ_0), 3) cylinder proximity (d_4), 4) cylinder bias (d_3), and 5) cylinder tilt angle (α_b). A sixth input parameter specifies the cylinder rotation increment. The cylinder bias parameter refers to positioning or biasing the cylinder towards Finger 0 or towards Fingers 1 and 2.

Of the six input parameters, the only parameter which is not variable is the cylinder tilt angle (α_b). One of the objectives of this project is to determine the effects of joint torque limits on the grasp focus as a function of cylinder position and orientation. In doing this, it is desirable to maximize the range of the cylinder position parameters d_3 and d_4 . These two parameters have the greatest effect on the size of the torque "moment arm" for each joint. There are two items which bound the range of d_3 and d_4 , joint angle limits and finger length.

Although not intuitively obvious, there is a specific value for α_b which maximizes the range of d_3 and d_4 . The determination of this value is simple since each of the fingers in the hand model are of the same length and have identical joint rotation ranges for the two most distal joints. The joint rotation ranges can be derived from the corresponding joint angle limits (Table 2-4). In addition, the base joint and Joint 1 locations for Fingers 1 and 2 are equally positioned from the corresponding joints on Finger 0. In short, the value of α_b is equal to the angle formed by a plane parallel to the palm and the plane formed by Joint 1 of each finger (Figure 2-6). The resulting value of α_b is 24.0777 degrees.

With the cylinder oriented at this particular value, the distance from Joint 1 to the contact plane is equal for each of the fingers. In addition there is a unique value for d_3 over the range of d_4 at which the contact angles for each of the fingers are equal. At this setting the absolute value of the two distal joints of each finger are equal and the cylinder position is "neutrally" bias. With the cylinder in a neutrally bias position, the range of d_4 is at a maximum. Changing the value α_b reduces the ranges of d_3 and d_4 since one of the fingers will bind before the others due to the joint angle limits.

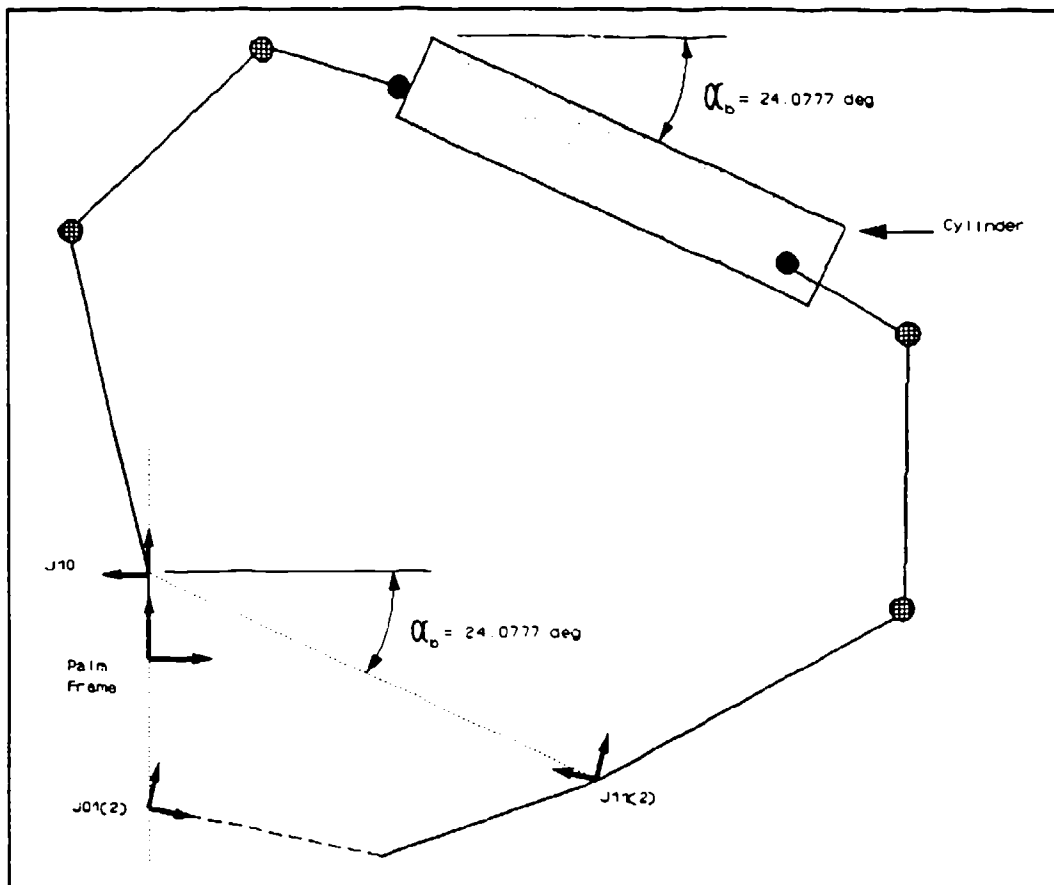


Figure 2-6. Cylinder Tilt Angle α_b

In summary, the inverse kinematics program can be used to calculate finger joint angles for various cylinder positions and orientations. Different combinations of the five variable model parameters can be used to analyze the effects of joint-torque limits on the grasp focus region, once the grasp analysis is complete. The selection of specific values for each variable will be discussed in Chapter IV.

III. Grasp Analysis

3.1 Grasping Forces

A three fingered precision grasp presents a special case for grasp analysis since all three contacts lie in a plane. Constraining the external forces to this plane further simplifies the analysis. This is the case for this project since the only external force for inclusion in the analysis is an applied moment acting about the cylinder centerline. The grasping analysis presented by Edwards [3:p2-1 to 2-11] is applicable to this study and is summarized in the following sections for completeness.

The grasp analysis begins by first examining the general relationship between the contact forces and moments exerted on the object by the fingers, and the external forces and moments applied to the object by the environment. If the contact forces and moments (represented by \vec{c}) cause a static balance with the external forces and moments (represented by \vec{F}), then the grasp matrix W relates the two vectors.

$$\vec{F} = W \vec{c} \quad (3.1)$$

where W depends on the grasp configuration.

Given \vec{F} and W it is possible to find a solution for \vec{c} by using the pseudo-inverse of W ($W^\#$). If the general solution is not unique, the solution of \vec{c} is the sum of a particular solution and a homogeneous solution.

$$\vec{c} = \vec{c}_p + \vec{c}_h \quad (3.2)$$

where

$$\vec{c}_p = W^* \vec{F} \quad (3.3)$$

$$\vec{c}_h = N \lambda \quad (3.4)$$

The term N in Equation 3.4 is a matrix whose columns are orthonormal vectors that span the null space of W , and λ is a vector of arbitrary magnitudes. The homogeneous solution (Equation 3.3) represents the internal grasping forces. The particular solution (Equation 3.4) represents the additional force to balance the external forces acting on the object.

3.2 The Contact Force Particular Solution

For this project \vec{c}_p is a vector composed of the tangential forces at each contact which, as a whole, balance the external moment about the cylinder centerline (B_z -axis) as shown in Figure 3-1. This constrains the solution such that $\sum M_{Bz} = 0$. Since all of the forces are constrained to the contact plane, all forces perpendicular to it equal zero. Specifying that the solution to \vec{c}_p must also balance external forces in the B_x - and B_y -directions implies that $\sum F_{Bx} = 0$ and $\sum F_{By} = 0$. Applying the three constraints ($\sum M_{Bz} = 0$, $\sum F_{Bx} = 0$, and $\sum F_{By} = 0$) in matrix form results in an equation in terms of the tangential forces at each contact and their respective contact angles ψ .

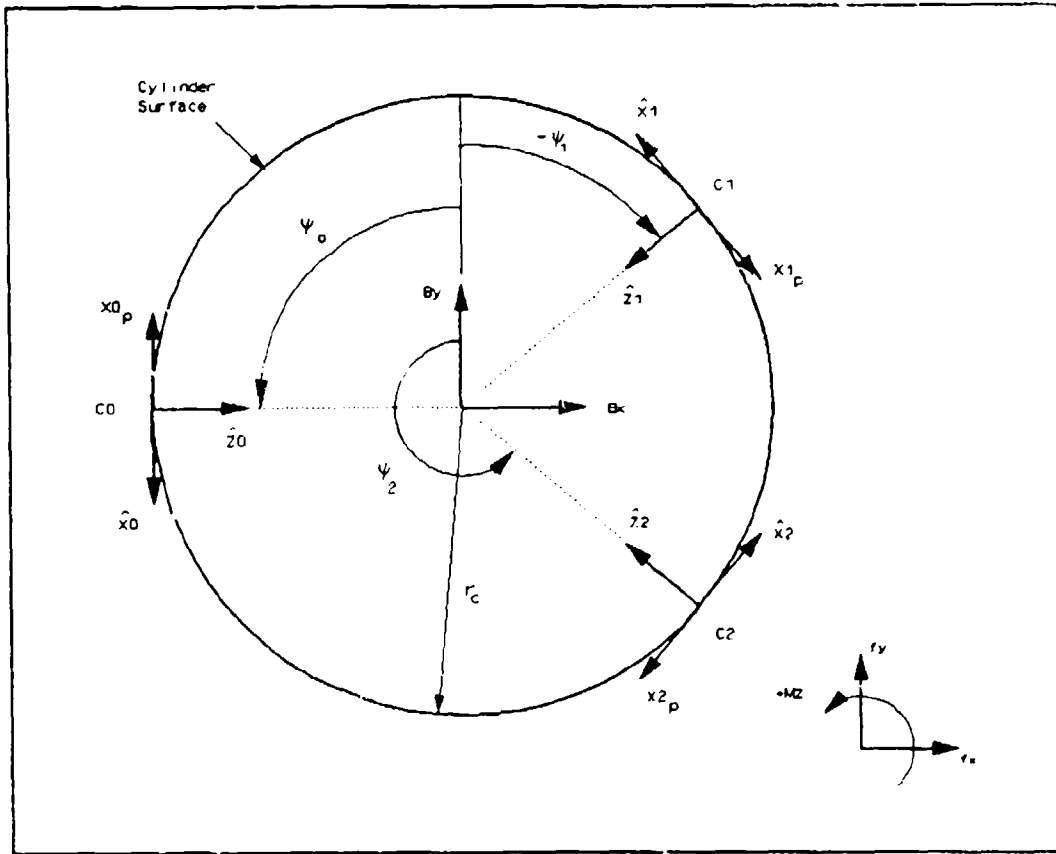


Figure 3-1. Balancing the External Moment [3:p2-2]

$$\begin{pmatrix} f_{B_x} \\ f_{B_y} \\ m_{B_z} \end{pmatrix} = \begin{bmatrix} \cos \psi_0 & \cos \psi_1 & \cos \psi_2 \\ \sin \psi_0 & \sin \psi_1 & \sin \psi_2 \\ -r_c & -r_c & -r_c \end{bmatrix} \begin{pmatrix} X_{0,r} \\ X_{1,r} \\ X_{2,r} \end{pmatrix} \quad (3.5)$$

The objective of this project only concerns how to balance an external moment on the cylinder; thus, the external forces f_{B_x} , and f_{B_y} are zero. Since the matrix in Equation 3.5 is square, Gaussian elimination yields the solution;

$$\begin{aligned}
X_{0r} &= \frac{B_4 B_5 - B_2 B_7}{B_1 B_4} \\
X_{1r} &= \frac{B_4 B_6 - B_3 B_7}{B_1 B_4} \\
X_{2r} &= \frac{B_7}{B_4}
\end{aligned} \tag{3.6}$$

where

$$\begin{aligned}
B_1 &= \cos \psi_1 - \cos \psi_0 \\
B_2 &= \cos \psi_1 - \cos \psi_2 \\
B_3 &= \cos \psi_2 - \cos \psi_0 \\
B_4 &= \sin(\psi_2 - \psi_1) + \sin(\psi_1 - \psi_0) + (\psi_0 - \psi_2) \\
B_5 &= -\frac{m_{Bz}}{r_c} \cos \psi_1 \\
B_6 &= \frac{m_{Bz}}{r_c} \cos \psi_0 \\
B_7 &= \frac{m_{Bz}}{r_c} \sin(\psi_0 - \psi_1)
\end{aligned} \tag{3.7}$$

Therefore given a moment m_{Bz} on a cylinder of radius r_c , the solution for the contact forces required to balance the moment can be determined if the contact angles are known.

3.3 The Internal Grasp Force Focus

The internal grasp forces exert no net forces or moments on the cylinder. If a line is extended in both directions along the internal force vector at each contact point, the three lines will meet at a unique point; assuming the contact points are not collinear. This

point is termed the grasp force focus [2][3]. Although the internal force vectors define the grasp focus, a unique homogeneous solution cannot exist until the magnitudes of the internal grasp forces are specified. Using Brock's and Edwards' definition, the internal grasp force magnitude is given by:

$$m_g = \sqrt{X_{0,i}^2 + Z_{0,i}^2} + \sqrt{X_{1,i}^2 + Z_{1,i}^2} + \sqrt{X_{2,i}^2 + Z_{2,i}^2} \quad (3.8)$$

where the subscript i denotes internal forces.

3.4 The Homogeneous Solution

For a three point planar grasp there are six internal force components; thus, six independent constraint equations are required to uniquely determine the homogeneous solution. The first three constraints are inherent in the definition of the internal grasp forces ($\sum M_{Bz} = 0$, $\sum F_{Bx} = 0$, and $\sum F_{By} = 0$). Specifying the grasp force magnitude in Equation 3.8 provides a fourth constraint.

Three more constraints are derived from the condition that the internal force vector at each contact must lie along a line through the corresponding contact point and the prescribed grasp focus. The grasp plane coordinates (x_g, y_g) define the position of the grasp focus within the contact plane, as shown in Figure 3-2. Translating the components to local contact frame coordinates yields the three constraint equations:

$$(x_g \sin \psi_j - y_g \cos \psi_j + r_c) X_{j,i} + (x_g \cos \psi_j + y_g \sin \psi_j) Z_{j,i} = 0 \quad j=0,1,2 \quad (3.9)$$

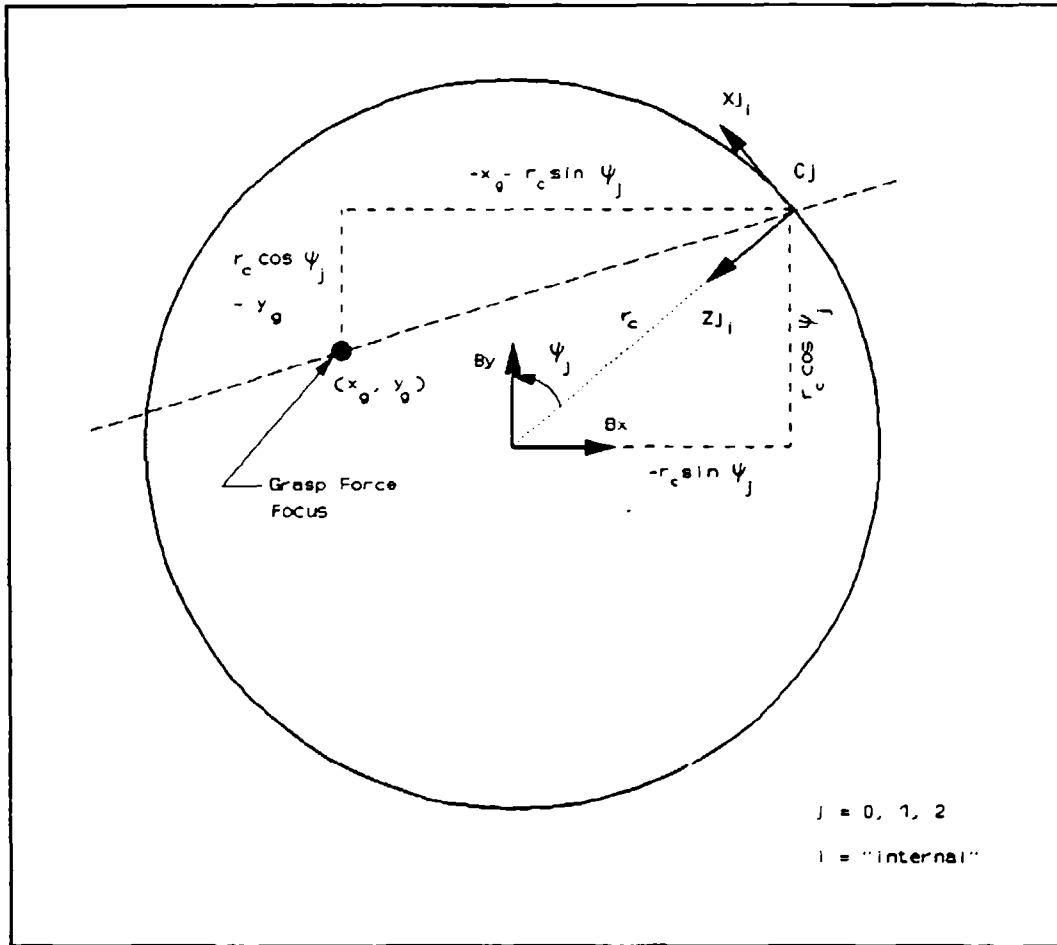


Figure 3-2. Prescribing the Grasp Force Focus Location [3:p2-6]

Combining Equations 3.6 and 3.9 in matrix form reveals that only five of the six equations are independent. The remaining five equations are sufficient to solve for five of the force components in terms of Z_{2i} . The resulting five expressions are substituted into Equation 3.8 to solve for Z_{2i} . Equation 3.10 shows how back substitution is then used to obtain solutions for the other five force components.

$$\begin{aligned}
Z_{2_i} &= \frac{m_g}{\sqrt{W_1^2 + W_2^2} + \sqrt{W_3^2 + W_4^2} + \sqrt{W_5^2 + 1}} \\
X_{0_i} &= W_1 Z_{2_i} \\
Z_{0_i} &= W_2 Z_{2_i} \\
X_{1_i} &= W_3 Z_{2_i} \\
Z_{1_i} &= W_4 Z_{2_i} \\
X_{2_i} &= W_5 Z_{2_i}
\end{aligned} \tag{3.10}$$

where

$$\begin{aligned}
W_1 &= \frac{V_1}{P_9 Q_3 R_4} & W_4 &= \frac{V_4}{P_9 R_4} \\
W_2 &= \frac{V_2}{P_2 P_9 Q_3 R_4} & W_5 &= -\frac{P_{10}}{P_9} \\
W_3 &= \frac{V_3}{P_9 Q_3 R_4}
\end{aligned}$$

where

$$\begin{aligned}
V_1 &= U_2 P_9 - U_1 P_{10} & V_3 &= U_6 P_9 - U_5 P_{10} \\
V_2 &= U_4 P_9 - U_3 P_{10} & V_4 &= R_6 P_9 - R_5 P_{10}
\end{aligned}$$

where

$$\begin{aligned}
U_1 &= Q_3 R_4 - Q_5 R_4 + Q_4 R_5 & U_4 &= R_3 R_4 - R_1 R_6 \\
U_2 &= Q_4 R_6 - Q_6 R_4 & U_5 &= Q_5 R_4 - Q_4 R_5 \\
U_3 &= R_2 R_4 - R_1 R_5 & U_6 &= Q_6 R_4 - Q_4 R_6
\end{aligned}$$

where

$$\begin{aligned}
 Q_1 &= P_3 - P_1 & Q_4 &= P_4 P_1 - P_3 P_2 \\
 Q_2 &= P_5 - P_1 & Q_5 &= P_6 P_2 + P_1 P_5 - P_2^2 - P_1^2 \\
 Q_3 &= P_4 P_2 + P_1 P_3 - P_2^2 - P_1^2 & Q_6 &= P_1 P_6 - P_5 P_2
 \end{aligned}$$

where

$$\begin{aligned}
 P_1 &= -\cos \psi_0 & P_6 &= \sin \psi_2 \\
 P_2 &= \sin \psi_0 & P_7 &= x_g \sin \psi_1 - y_g \cos \psi_1 + r_c \\
 P_3 &= -\cos \psi_1 & P_8 &= x_g \cos \psi_2 + y_g \sin \psi_2 \\
 P_4 &= \sin \psi_1 & P_9 &= x_g \sin \psi_2 - y_g \cos \psi_2 + r_c \\
 P_5 &= -\cos \psi_2 & P_{10} &= x_g \cos \psi_2 + y_g \sin \psi_2
 \end{aligned}$$

Substituting for all of the parameters will yield expressions for the six internal contact force components in terms of: r_c , ψ_0 , ψ_1 , ψ_2 , x_g , y_g , and m_g . Given the cylinder radius, contact locations, and grasp force focus location and magnitude, a unique solution for the internal grasp forces can be determined using Equation 3.10.

3.5 Constraints on Total Contact Forces

The complete solution for the contact forces is the vector sum of the particular and homogeneous contact forces. The general equation for the six components of force expressed in local contact coordinates is:

$$\begin{aligned}
 X_{j,r} &= X_{j,p} + X_{j,h} & j &= 0, 1, 2 \\
 Z_{j,r} &= Z_{j,h}
 \end{aligned} \tag{3.11}$$

where the subscript T denotes the total contact force component.

There are two criteria to impose for maintaining grasp stability. The first is that the fingertip cannot break contact with the cylinder; this implies that the normal contact forces must be positive. The second criteria is that the tangential force at each contact must be less than the maximum forces sustainable by static friction.

Table 3-1 lists the three types of contacts which result from the two contact criteria. Of the three, only contact type 1 meets both requirements. Thus the desirable solution for contact forces will result in contact type "1" at each of the three contacts. The contact types for the three contacts can be arranged sequentially, starting with Contact 0, in a three-digit code such as "312".

3.6 The Constraint Map

Each focus point within the contact plane has a corresponding contact code. Examining each point in the plane will result in discrete regions of identical codes with defined boundaries between adjacent regions. Edwards defines the map which graphically depicts these regions and boundaries as the *Constraint Map* [3:p2-10]. For this project the region of interest is the one which satisfies the grasp stability criteria in Section 3.5; that is, the "111" contact code region. Edwards appropriately defines this particular region as the *Stable Area* [3:p3-5] or for use herein, the *Stable Region*.

The grasp analysis equations imply that if the contact locations, cylinder radius, friction coefficient, and external moment are constant, the only way to change the contact force solution is to vary m_g or the focus location (x_g, y_g) . However, the maximum value of m_g is bounded by the joint torque limits of the hand. Beyond this maximum value,

Table 3-1. Contact Type Designations [1]

<i>Criteria</i>	<i>Contact Type</i>
$Z_{jT} \leq 0$	3
$Z_{jT} > 0, X_{jT} \geq \mu Z_{jT}$	2
$Z_{jT} > 0, X_{jT} < \mu Z_{jT}$	1

adjusting the focus location is the only remaining method to effect the contact force solution.

For a given constraint map, the only variable parameter is the location of the grasp focus. All of the other grasp parameters ($r_c, \psi_0, \psi_1, \psi_2, \mu, M_{Bz}, m_g$) remain constant. Changing any one of the other parameters will result in a different constraint map. Edwards demonstrated however, that if the ratio of $m_g r_c$ to M_{Bz} is constant then the constraint map will also remain constant. Edwards defines this ratio as c_{map} [3:p4-8]. This a useful property for comparing different constraint maps, as will become evident in the next chapter.

3.7 Determining Joint Torques for Hand Model

Changing the location of the grasp focus directly effects the commanded contact forces which the hand must provide. If the hand grasping the cylinder has limited joint torquing capabilities, then there may be areas within the stable region which are

unacceptable for focus placement. The net region for positioning the grasp focus which satisfies both stability and joint torque criteria is defined as the *Safe and Stable Region* [3:p4-22].

The joint torques are not only a function of the commanded contact forces, but also a function of cylinder position and orientation. Using the kinematic equations from Chapter II, the final issue to resolve is the relationship between contact forces and joint torques.

3.7.1 Manipulator Jacobian. The endpoint or end-effector forces are related to the joint torques by the transpose of the manipulator Jacobian [19:p243].

$$\vec{\tau} = J^T {}^0\vec{F} \quad (3.12)$$

where $\vec{\tau}$ is a vector of the joint torques for a given finger, and ${}^0\vec{F}$ is a vector of the endpoint force components expressed in the base joint frame. Since the hand model assumes point contacts and each finger has four joints, the Jacobian (J) is a 3 X 4 matrix.

There are two details to consider before applying Equation 3-12 to the hand model. First, the kinematic structure of Finger 0 is different than that for Fingers 1 and 2. Therefore, the corresponding Jacobian matrices are different since the A -matrices form the basis for J . The Jacobian matrix for each finger is fairly large in size, and therefore are listed in Appendix H. The second issue is that the contact force components (Equation 3-11) are expressed in contact frame coordinates. These components must first be translated into finger base frame coordinates before using Equation 3-12. The contact forces can be assembled into the following vectors:

$$\bar{F}_{C0} = \begin{pmatrix} X_{0r} \\ 0 \\ Z_{0r} \end{pmatrix} \quad \bar{F}_{C1} = \begin{pmatrix} X_{1r} \\ 0 \\ Z_{1r} \end{pmatrix} \quad \bar{F}_{C2} = \begin{pmatrix} X_{2r} \\ 0 \\ Z_{2r} \end{pmatrix} \quad (3.13)$$

These forces can then be translated to the appropriate finger base frame with rotation matrices.

$${}^0\bar{F}_{C0} = R_0 \bar{F}_{C0} \quad {}^1\bar{F}_{C1} = R_1 \bar{F}_{C1} \quad {}^2\bar{F}_{C2} = R_2 \bar{F}_{C2} \quad (3.14)$$

Substituting Equations 3-13 and 3-14 into Equation 3-12, the joint torques on Finger j ($j=0,1,2$) is given by:

$$\begin{pmatrix} \tau_{0j} \\ \tau_{1j} \\ \tau_{2j} \\ \tau_{3j} \end{pmatrix} = J_j^T R_j \begin{pmatrix} X_{jr} \\ 0 \\ Z_{jr} \end{pmatrix} \quad (3.15)$$

where J_0, J_1, J_2 are the Jacobian matrices for Fingers 0, 1, and 2 respectively (see Appendix H), and the rotation matrices R_j are given by:

$$R_0 = \begin{bmatrix} -S_{a_b} C(\varphi_b + \psi_{C0}) & C_{a_b} & S_{a_b} S(\varphi_b + \psi_{C0}) \\ S(\varphi_b + \psi_{C0}) & 0 & -C(\varphi_b + \psi_{C0}) \\ -C_{a_b} C(\varphi_b + \psi_{C0}) & -S_{a_b} & C_{a_b} S(\varphi_b + \psi_{C0}) \end{bmatrix} \quad (3.16)$$

$$R_k = \begin{bmatrix} S(\varphi_b + \psi_{ck}) & 0 & C(\varphi_b + \psi_{ck}) \\ -S(\alpha_b + \varphi_p) C(\varphi_b + \psi_{ck}) & C(\alpha_b + \varphi_p) & S(\alpha_b + \varphi_p) S(\varphi_b + \psi_{ck}) \\ -C(\alpha_b + \varphi_p) C(\varphi_b + \psi_{ck}) & -S(\alpha_b + \varphi_p) & C(\alpha_b + \varphi_p) S(\varphi_b + \psi_{ck}) \end{bmatrix} \quad (3.17)$$

where $k = 1, 2$

3.7.2 Equivalent Maximum Joint Torques. Each link of a UMDH finger is actuated by flexor and extensor tendons. These tendons can be adjusted to obtain a desired co-contraction level, such that they work against each other to provide finger stiffness. If the co-contraction level is set to zero, only the flexor tendons are in tension when grasping an object. Using this as an assumption maximizes the flexional torque capabilities of each finger, and simplifies the determination of equivalent maximum joint torques.

Using technical data for the UMDH from [17] and [20] Edwards goes into detail on how to determine the equivalent maximum joint torques for a given finger [3:p2-16 to 2-18]. If the pulley radii at each joint and the maximum flexor tendon tension are known values, the equivalent maximum torques for a UMDH finger are:

$$\begin{pmatrix} \tau_0 \\ \tau_1 \\ \tau_2 \\ \tau_3 \end{pmatrix}_{\max} = \begin{bmatrix} r_0 & 0 & 0 & 0 \\ 0 & r_1 & r_1 & r_1 \\ 0 & 0 & r_2 & r_2 \\ 0 & 0 & 0 & r_3 \end{bmatrix} \begin{pmatrix} T_0 \\ T_1 \\ T_2 \\ T_3 \end{pmatrix} \quad (3.18)$$

where r_0, r_1, r_2, r_3 are the pulley radii at joints zero, one, two, and three respectively.

Equation 3-18 can be applied to each of the fingers since each of the corresponding joints

are identical. Therefore, the maximum joint torques derived by Edwards can be used in this project. The only difference is the addition of the base or zero joint. For simplicity, it will be assumed that the maximum joint torque for the base joint is the same as that for joint one. This approximation is valid since the flexor tendon tensions for the two joints are the same [20:p1.13]. The only real assumption is that the pulley radii are equal. Given this, the equivalent maximum joint torques for each finger in the hand model are:

$$\begin{pmatrix} \tau_0 \\ \tau_1 \\ \tau_2 \\ \tau_3 \end{pmatrix}_{\max} = \begin{pmatrix} 2.958 \text{ Nm} \\ 2.958 \text{ Nm} \\ 1.139 \text{ Nm} \\ 0.427 \text{ Nm} \end{pmatrix} \quad (3.19)$$

For a particular grasp, the joint torques are calculated using Equation 3-15 and compared to the maximum joint torque limits in Equation 3-19. If anyone of the calculated joint torques exceed the specified limit, then one of two grasp parameters must be readjusted. Either the grasp force magnitude must be reduced or the grasp focus must be repositioned to an area within the stable region where the limits are not exceeded. Repositioning the grasp focus is reasonably easy but knowing where to reposition it to is not always intuitively obvious.

3.8 Joint Torque Constraint Maps

The joint torque constraint map is similar to the constraint maps discussed earlier in this chapter. Instead of mapping contact code regions, the joint torque constraint map identifies two distinct regions within the grasp plane for each finger joint; the region where the joint torque limit is exceeded for a specific joint, and the region where it is not. Since

there are only two regions, mapping only the boundary between the two is all that is necessary. Mapping only the boundary infers that one can still identify which side of the boundary is the "good" side.

As mentioned in Section 3.7, the SAS region meets both grasp stability criteria and joint torque criteria. The SAS region can be thought of as a subset of the parent stable region. If no joint torque limits are exceeded for a specified stable grasp, then the SAS and Stable regions are the same. Stated another way, if the joint torque boundary lines never cross over the stable region, the SAS region is the entire stable region. The SAS region is reduced only when the joint torque boundary lines cross over the stable region. When this occurs, the SAS region becomes a subset of the stable region.

This finally brings us to the main point of this project. The size of the SAS region is dependent on the imposed joint torque limits. If the grasped object is manipulated, the size of the SAS region will change from one object position and orientation to the next since the joint torques for each finger are changing. It is feasible that positioning the grasp focus at one point may be acceptable for only a small portion of the manipulation task. Therefore it is necessary to gain an understanding of how the SAS region changes as an object is manipulated.

A grasp analysis computer program was developed to generate the data for mapping joint torque boundary lines, and stable and SAS regions for a given grasp configuration. Joint angle data from the inverse kinematics program discussed in Chapter II is used as input data to establish the specific cylinder position, orientation, and contact location. The evolution of the SAS region is examined as a function of cylinder rotation by generating maps at discrete rotation increments. These "snapshot" map sets are also generated as a function of cylinder proximity to the hand.

IV. Computer Generation of Constraint Maps

4.1 Grasp Simulation Setup

With the kinematic and grasp analysis complete, we are now able to analyze the grasping and manipulation of the cylinder. To reiterate, the project goal is to develop a planning procedure for grasping a cylinder and rotating it about its longitudinal axis while opposing an external moment. The procedure must be able to examine various grasp configurations by varying cylinder position and orientation. One of the study objectives is to develop relationships which compare the stability, robustness, and torquing capability of the different grasp configurations. To do this we must first establish the simulation parameters. These parameters are divided into two sets: 1) Kinematic Parameters ($\psi_0, \psi_1, \psi_2, r_c, \phi_b, d_4, d_3, \alpha_b$), and 2) Grasp Parameters (M_{Bz}, m_g, μ). It should be noted that the contact angles (ψ_0, ψ_1, ψ_2), and cylinder radius (r_c) are considered both Kinematic and Grasp parameters.

4.1.1 Kinematic Parameters. The kinematic parameters establish the contact locations on the cylinder (ψ_0, ψ_1, ψ_2), and the cylinders' position (d_4, d_3, α_b) and orientation (ϕ_b) with respect to the hand. In determining the contact locations, one must keep in mind that the cylinder is going to be rotated about its' transverse axis. One approach is to select the contact locations such that the cylinder rotation is symmetric about some "neutral" position.

4.1.1.1 Contact Location. The coordinate frame origins for the cylinder are all located in the x - z plane of the base joint on Finger 0 (reference Section 2.3). This is also the plane of symmetry for the locations of the base joint and joint one for Fingers 1 and 2 (reference Section 2.2.2). Therefore, the contact location scheme should take advantage of this plane of symmetry.

The neutral position of the cylinder occurs when its' rotation angle (ϕ_b) equals zero. By setting the contact angle $\psi_0 = 90^\circ$ and $\psi_1 = \psi_2 \pm 90^\circ$ ("+" for $+\psi_2$, "-" for $-\psi_2$) the contact locations will be symmetric about the x - z plane of the base joint on Finger 0 when $\phi_b = 0^\circ$. With this contact scheme, the maximum clockwise rotation of the cylinder is equal to the maximum counter-clockwise rotation. This is only true if the joint rotation limits and link lengths for Fingers 1 and 2 are identical, which is true for the hand model.

In Section 2.3 the cylinder radius r_c was set to 1.0812 inches. This particular radius value was selected with the semi-symmetric contact configuration set in mind. With the cylinder in the neutral position ($\phi_b = 0^\circ$) and the contact angles set to $\{\psi_0 = 90^\circ, \psi_1 = -50^\circ, \psi_2 = -130^\circ\}$, each of the fingers are parallel to the x - z plane of the palm frame; i.e., their respective base joints are also in a neutral position $\{\theta_{00} = 0^\circ, \theta_{01} = 90^\circ, \theta_{02} = 90^\circ\}$. This implies a maximum cylinder rotation angle without violating joint rotation limits.

The computer simulation examines two different configurations of contact locations. The first will be with the contact angles set to $\{\psi_0 = 90^\circ, \psi_1 = -50^\circ, \psi_2 = -130^\circ\}$. This contact configuration will be termed *semi-symmetric*, since two of the three angles separating the contacts are equal ($140^\circ, 140^\circ, 80^\circ$). The second contact configuration is set to $\{\psi_0 = 90^\circ, \psi_1 = -30^\circ, \psi_2 = -150^\circ\}$. This contact configuration will be termed *symmetric*, since all three angles separating the contacts are equal ($120^\circ, 120^\circ, 120^\circ$).

4.1.1.2 Grasp Configuration. The parameters d_4 , d_3 , and α_b establish how the hand "holds" the cylinder. In Section 2.5 the desired cylinder tilt angle, α_b , was calculated as -24.0777° . At this angle, the range of d_4 and d_3 is maximized. The cylinder proximity parameter (d_4) determines how close or far away the cylinder is from the palm frame origin. The cylinder bias parameter determines whether the cylinder is bias towards Finger 0 (thumb-bias) or towards Fingers 1 and 2 (finger-bias).

For the simulation a *retracted* grasp configuration refers to a minimal value for d_4 , and an *extended* grasp configuration refers to a maximal value for d_4 . An *intermediate* grasp configuration refers to a mid-range value for d_4 . There are three "types" of values for d_3 for each value of d_4 : *thumb-bias*, *neutral* (equal fingertip angles) and *finger-bias*. Figures 4-1 through 4-4 show examples of the different types of grasp configurations for the simulation. Note that different grasp configuration combinations can be examined (i.e. thumb-bias neutral grasp, finger-bias neutral grasp, etc.)

4.1.1.3 Artificial Constraints. As discussed in Section 2.5, the range of the cylinder bias parameter (d_3) and the cylinder proximity parameter (d_4) is bounded. The maximum value of d_4 is limited by finger lengths and its' minimum value is limited by fingertip grasp angles. For this study, the grasp angles must be positive so that the contact location resides on the bottom-side of the fingertip.

The range of d_3 is bounded by either joint angle limits (reference Table 2-4) or by the constraint of positive grasp angles. In a retracted grasp configuration (minimum value of d_4), the range of d_3 is limited by grasp angles. As the value of d_4 increases, the range of d_3 may be bounded by either joint angle limits or by the positive grasp angle constraint.

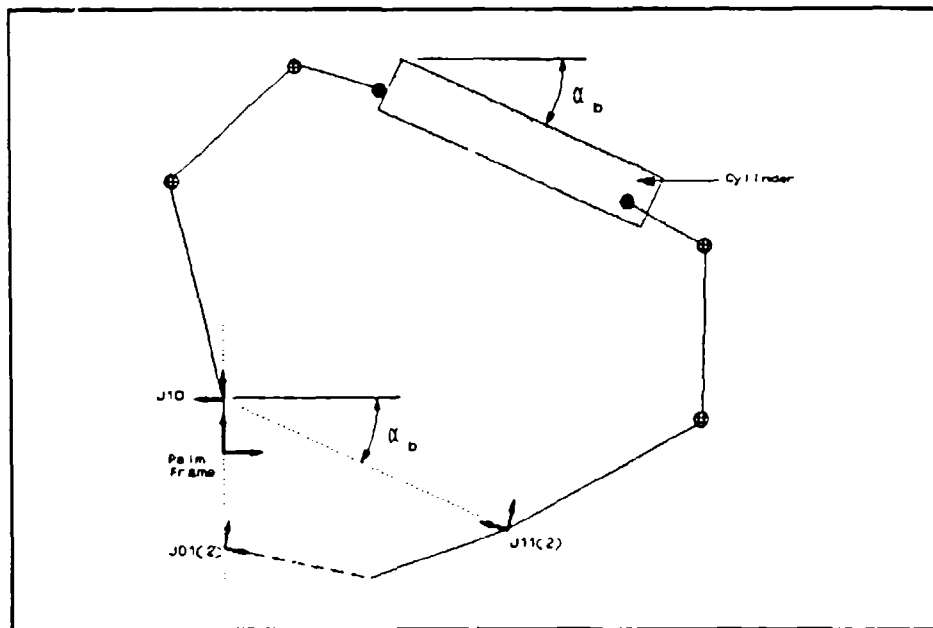


Figure 4-1. Retracted Neutral-Bias Grasp Configuration

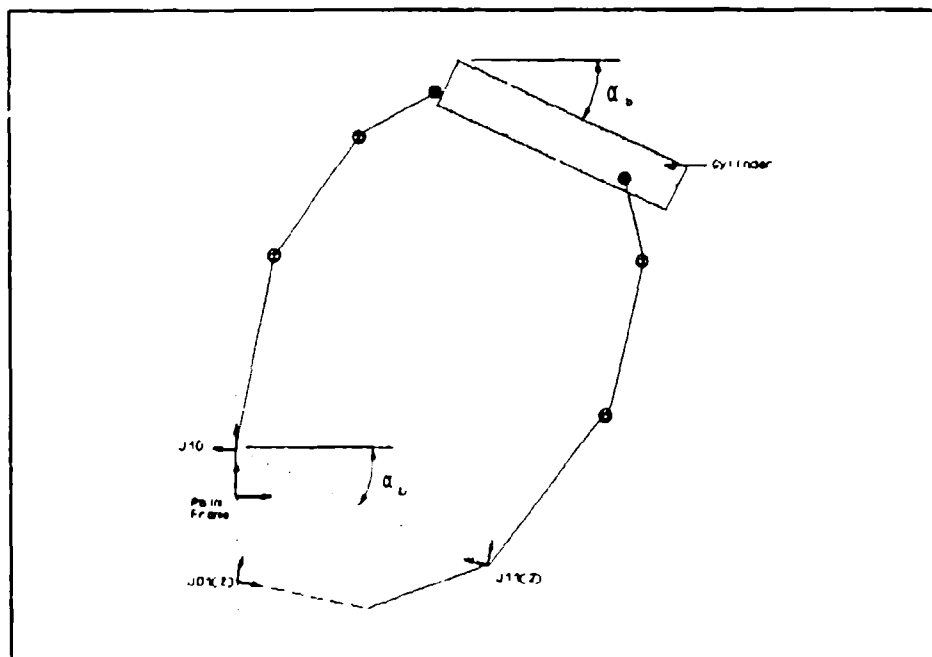


Figure 4-2. Extended Neutral-Bias Grasp Configuration

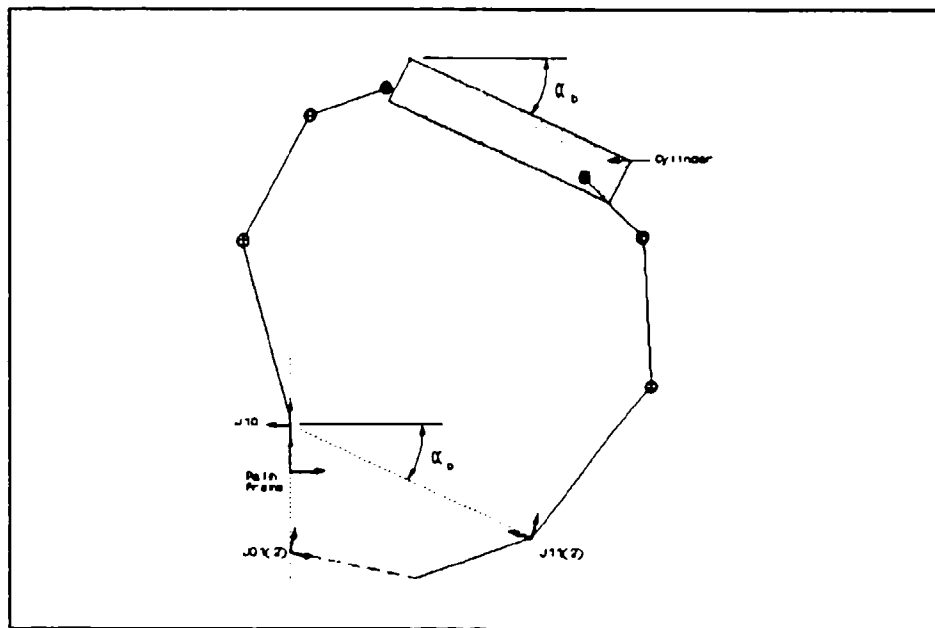


Figure 4-3. Intermediate Thumb-Bias Grasp Configuration

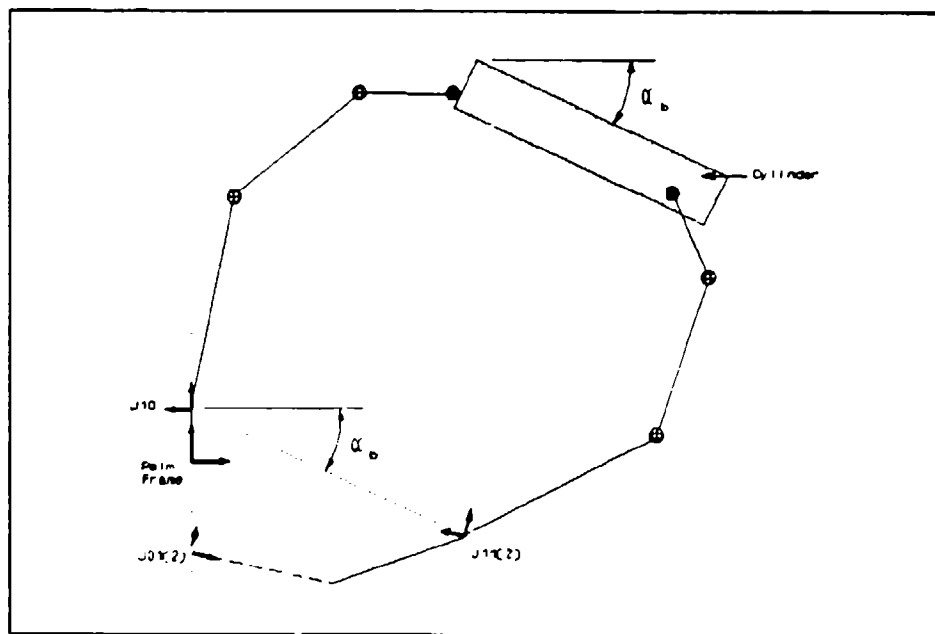


Figure 4-4. Intermediate Finger-Bias Grasp Configuration

An artificial constraint is imposed on the cylinder rotation angle to avoid positioning the contact on the "fingernail" portion of the fingertip (positive grasp angle). For the first contact configuration, ϕ_b is limited to $\pm 50^\circ$; for the second, ϕ_b is limited to $\pm 30^\circ$.

Table 4-1 provides a summary of the corresponding values for ψ_0 , ψ_1 , ψ_2 , r_c , ϕ_b , d_4 , d_3 , and α_b . Select combinations of the kinematic parameters will be utilized as input to the inverse kinematics program.

4.1.2 Grasp Parameters. The grasp parameters establish how "hard" the cylinder is grasped (grasp force magnitude), the magnitude and direction of the applied torque, and the static friction coefficient for each contact location. As mentioned earlier, if c_{map} (ratio of $m_g r_c$ to M_{Bz}) is constant then the constraint map will also remain constant. This in-turn means that the size and shape of the stable region will remain constant. Mathematically c_{map} is improper since a zero value for M_{Bz} makes c_{map} go to infinity. With r_c as a constant, the variable ratio will be redefined as:

$$c_{map} \triangleq \frac{M_{Bz}}{m_g r_c} \quad \text{for } m_g > 0 \quad (4.1)$$

Equation 4.1 is a useful property for comparing different constraint maps. For this project, one of the task objectives is to apply the greatest amount of torque over a specified cylinder rotation range. All the kinematic and grasp parameters are predetermined, except m_g and M_{Bz} . Assume that the grasp focus positioning accuracy for the hand is known. That is, given the limitations of the hand controller, sensors, etc., the grasp focus can be positioned at a specific point within the grasp plane $\{x_g, y_g; \pm XX \text{ mm}\}$.

Table 4-1. Kinematic Parameters

<i>Input</i>	<i>Nominal Value</i>	<i>Input</i>	<i>Nominal Value</i>
α_b	-24.0777°	r_c	1.0812 in. (27.5 mm)
d_3	0.52 in. (13.2 mm) Thumb-bias	d_4	3.01969 in. (76.7 mm) Retracted
	1.16335 in. (29.5 mm) Neutral-Bias		3.46 in. (87.9 mm) Intermediate
	1.8067 in. (45.9 mm) Finger-Bias		3.9055 in. (99.2 mm) Extended
ψ_0, ψ_1, ψ_2	{90°, -50°, -130°}	ϕ_b	Variable Maximum $\pm 50^\circ$
	{90°, -30°, -150°}		Variable Maximum $\pm 30^\circ$

The focus positioning error ($\pm XX$ mm) corresponds to the desired region for grasp focus positioning. Therefore, c_{map} can be adjusted (by varying m_g and M_{Bz} separately) until the resulting stable region encompasses an area equivalent to the size of the error region. This is a coarse setting for c_{map} since the desired error region may be partially or totally eliminated by torque limit lines as the cylinder is rotated. The preferred goal is to enclose the error region within the net SAS region (See Figure 4-5). The net SAS region is the intersection of all the SAS regions sampled at discrete rotation increments.

The coarse setting of c_{map} serves a purpose, it "freezes" the size of the Stable region. Since the SAS region is a subset of the stable region, further adjustments are made by only changing the c_{map} ratio. Reducing the ratio will increase the size of the net SAS region, because of the joint torque reduction due to a smaller value for m_g .

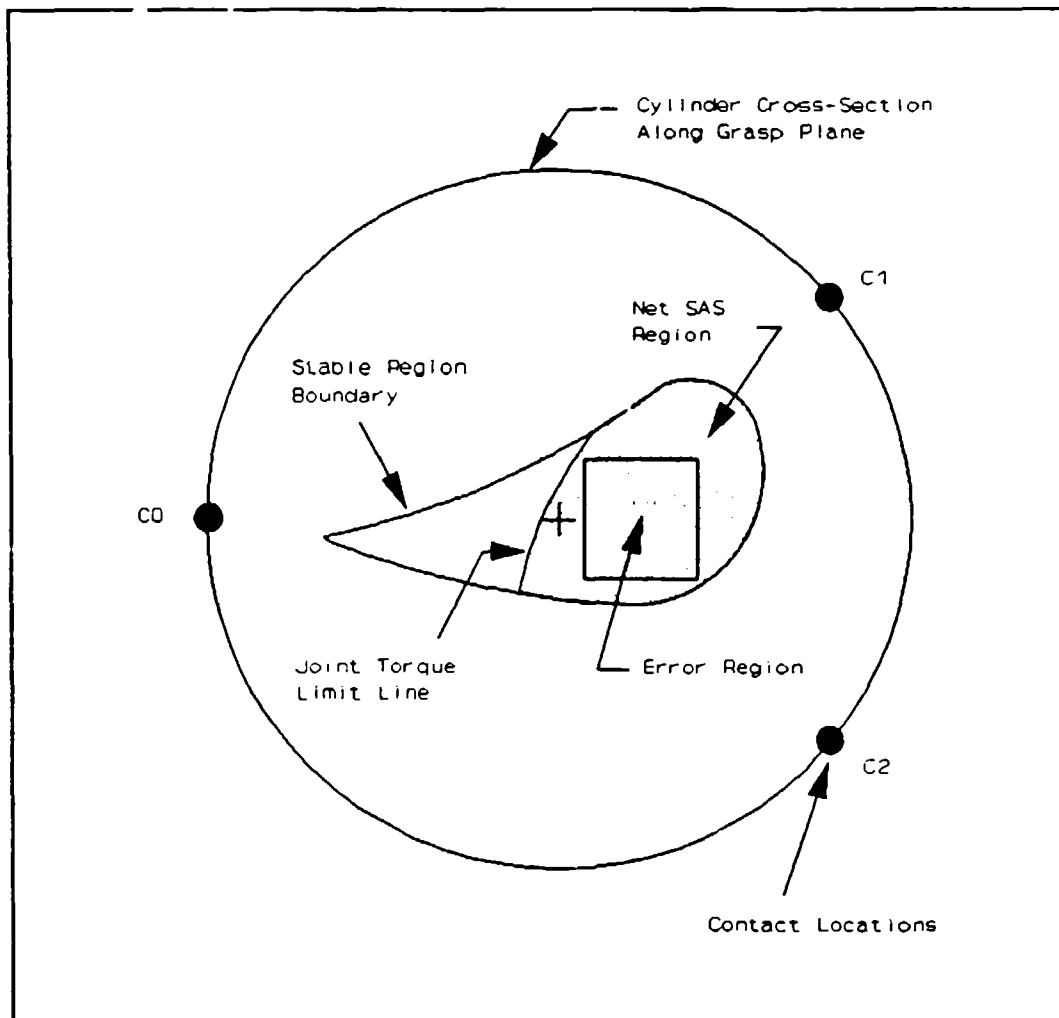


Figure 4-5. Locating the Error Region within the Net SAS Region

However, reducing the c_{map} ratio also corresponds to a reduction in applied torque. When the solution is close at hand, fine adjustments are made to c_{map} by increasing or decreasing M_{Bz} only.

Once the final value of c_{map} is established, the same ratio is used for different grasp configurations (i.e. extended finger-bias, etc). The different grasp configurations are compared to determine which configuration provides the maximum torquing capability over a specified cylinder rotation range.

4.2 Computer Programs

The inverse kinematics and grasp analysis programs are used in combination to generate the necessary data for a single constraint map. Each constraint map represents a specific grasp configuration and cylinder rotation angle. For example, one map may represent a retracted neutral-bias grasp of the cylinder, with the cylinder oriented at a rotation angle (ϕ_0) equal to -15° . Generating several of these maps at different cylinder rotation angles, comprises a *constraint map set* for a specific grasp configuration.

A map set can be thought of as representing a "quasi-static" rotation of the cylinder. Granted this approach to simulating cylinder rotation ignores dynamic effects, but it does allow the examination of how the SAS region changes as the cylinder is rotated. If one assumes that the inertial properties of the fingers and the cylinder are small in magnitude and/or the rotational movement is slow, the approach is valid.

By specifying ϕ_0 as an input parameter, the inverse kinematics program will calculate and output the corresponding finger joint angles and specified kinematic parameters to an external data file called "Hand.dat". The grasp analysis program will use this data file as input. The grasp analysis program will prompt the user for five primary inputs. The first two are M_{Bz} and m_g . The third input is the value for the static friction coefficient μ .

The remaining two inputs relate to sampling points for locating the grasp focus. One of these inputs requests the user to specify the map scale. The map scale is the number of cylinder radii from the center of the map to its edge; where map center corresponds to the cylinder center. This results in a square map over which to sample for grasp focus locations. The last parameter is the resolution of the map, where the

resolution is measured from the map center in the x and y directions. The map resolution parameters divide the map into a N by M equally spaced grid.

The grasp program samples each grid point to determine if it is an acceptable location for the grasp focus. To become an acceptable focus location, the particular sample point must satisfy stability and joint torque limit criteria. The combination of all acceptable points form the SAS region. The program also generates the data for mapping the joint torque and stable region boundary lines. A plot of the resulting data is then made using commercially available software. This plot is superimposed over an image of the cylinder cross-section and contact locations for visual reference (similar to Figure 4-5).

V. Results and Discussion

5.1 Overview

5.1.1 Desirable Grasp Characteristics. With the analysis complete, we can now use the computer programs to examine various grasp configurations by varying cylinder position and orientation. From this, general relationships can be developed which compare the stability, robustness, and torquing capability of the different grasp configurations.

There are three desirable grasp characteristics for the cylinder manipulation task. The first is that the grasp must satisfy stability and joint torque criteria over a specified cylinder rotation range (50° to 100° for this study). This is the basic requirement; if not satisfied, the task cannot be successfully completed. The second requirement is that the grasp must satisfy robustness criteria. The third requirement is that the grasp must provide the greatest torquing capability to oppose external moments. Both of these last two requirements are considered user specified requirements, and are therefore optional. If desired, the two requirements must be satisfied over the specified cylinder rotation range. For this study it is assumed that all three requirements are imposed.

Each of the desirable grasp characteristics are directly related to the net SAS region. All points within the net SAS region satisfy stability and joint torque criteria. As mentioned in the introduction, Edwards demonstrated that for an enveloping three-point grasp (which is the case herein) the cylinder center point is the optimum location for applying the maximum amount of torque [3:p4-13] (this statement will be proven in

Section 5.6). Therefore, from a cylinder torque perspective, the best point for locating the grasp focus is at the center of the cylinder.

To satisfy robustness criteria, the net SAS region must enclose the error region (reference Section 4.1.2). From a robustness perspective, the geometric center of the net SAS region is the optimum location for the grasp focus. From this point, the focus can achieve the largest planar deviation from its' nominal position.

If the net SAS region is larger than the error region, this implies that the grasp has the potential to apply more torque to the cylinder. This is due to the fact that the size of the net region is directly related to the external moment magnitude; as the external moment magnitude is increased, the size of the net SAS region decreases.

5.1.2 Ideal Grip. Combining all this information, the conditions for an "ideal" grip can be assembled. For an ideal grip, the net SAS region is equal in size and shape to that for the error region. With this condition, the two regions can be centered directly over the center of the cylinder to achieve the maximum combination of grasp torquing capability and robustness. As will be demonstrated in the ensuing sections, the ideal grip cannot be achieved with the hand model employed. However, with proper planning an acceptable grasp configuration can always be achieved.

5.1.3 Comparing Grips. The issue to address first is how the SAS region evolves as the cylinder is rotated. This will provide the basic understanding of which joint or joints on each finger effect the size and shape of the SAS region. The effects of grasp configuration on the net SAS region is then examined by developing constraint maps for

each of the different grasp combinations (reference Section 4.1.1.2). An equal comparison can be made by setting the external moment and grasp force magnitude to a constant value. Given this, the net SAS region becomes a function of: a) cylinder orientation (cylinder rotation angle), b) cylinder position (cylinder bias and proximity), and c) contact location.

The results examine the effects of cylinder proximity, cylinder bias, and contact location on the size and shape of the net SAS region for the following cases:

Case 1. Varying Cylinder Proximity

- Retracted Grasp
- Intermediate Grasp
- Extended Grasp

Case 2. Varying Cylinder Bias

- Thumb-Bias
- Neutral Bias
- Finger-Bias

Case 3. Changing Contact Locations

- Semi-Symmetric Contacts
- Symmetric Contacts

The goal is to develop relationships which compare the stability, robustness, and torquing capability of the different grasp configurations. With these relationships we can

determine which grasp configuration corresponds to the highest torquing capability over a specified cylinder rotation range. This will be demonstrated by combining the relationships to design a robust grasp for high torque applications.

Finally, the net SAS region is examined in detail to determine stability behavior within the neighborhood of grasp focus point. The objective is three-fold. The first is to gain some insight as to the advantages and disadvantages of locating the grasp focus at different points within the net SAS region. The second is to prove that the cylinder center point is the optimal focus location for increased torquing capability. The third is to discuss what determines the shape of the stable region.

The grasp planning procedure presented herein is a generalized approach for grasp design. It is not intended to represent an optimization scheme; although the different constraint maps can be compared to determine relative "maximum" graphical solutions.

5.2 Effects of Cylinder Rotation on SAS Region

The grasp initial configuration will consist of an intermediate neutral grasp (refer to Table 4-1) using a semi-symmetric contact location layout $\{\psi_0 = 90^\circ, \psi_1 = -50^\circ, \psi_2 = -130^\circ\}$. This configuration combination will also serve as the baseline configuration for later comparisons to different grasp types. Metric units will be used for convenience since generating specific types of constraint maps can require small parameter changes.

The external moment (M_{B_z}) is set to 0.6 N-m (counter-clockwise) and the internal grasp force magnitude is set to 67 N. Using Equation 4-1, this corresponds to a c_{map} value of 0.3261 (where $r_c = 27.46$ mm). The starting value for the cylinder rotation angle (ϕ_b or "Phi Body") is 50 degrees. This angle represents the maximum counter-clockwise

rotation angle. The resulting constraint map is shown in Figure 5-1, which includes the joint angles for each of the three fingers. The joint angle term, T_{ij} , at the bottom of the figure denotes joint angle θ at joint i on finger j (where $i=0,1,2,3$ and $j=0,1,2$).

The circle represents the cylinder cross-section within the contact plane. The terms $C0$, $C1$, and $C2$ denote the contact locations for Fingers 0, 1, and 2 respectively. The shaded area within the circle represents the SAS region. The curve surrounding the SAS region denotes the stable region boundary. The SAS region and the stable region are synonymous for this rotation increment; i.e., the joint torque limits have no effect on the SAS region. Note that the geometric center of the SAS region is bias towards the first contact point, even though the contact locations are symmetric about the horizontal center axis. This phenomena will be examined further in Section 5-6.

Clockwise rotation samples are then taken at seven successive values for ϕ_b $\{30^\circ, 15^\circ, 0^\circ, -15^\circ, -30^\circ, -40^\circ, -50^\circ\}$. The maximum clockwise cylinder rotation occurs when $\phi_b = -50$ degrees; therefore the total *potential* rotation angle for this grasp and contact configuration is 100 degrees. Potential is stressed since the actual total rotation angle can be less than 100 degrees if the SAS region is eliminated prior to the end of rotation. The constraint maps for each of the rotation samples are shown in Figures 5-2 through 5-8. The new term, J_{ij} , represents a specific joint torque limit line due to a joint torque violation at joint i on finger j (where $i=0,1,2,3$ and $j=0,1,2$).

Comparing the series of figures, it is evident that joint torque limits progressively reduce the size of the SAS region as the cylinder is rotated in a clockwise direction. Keep in mind that this is true for a counter-clockwise external moment. Although not demonstrated, the opposite is true for an opposing clockwise external moment; that is, the

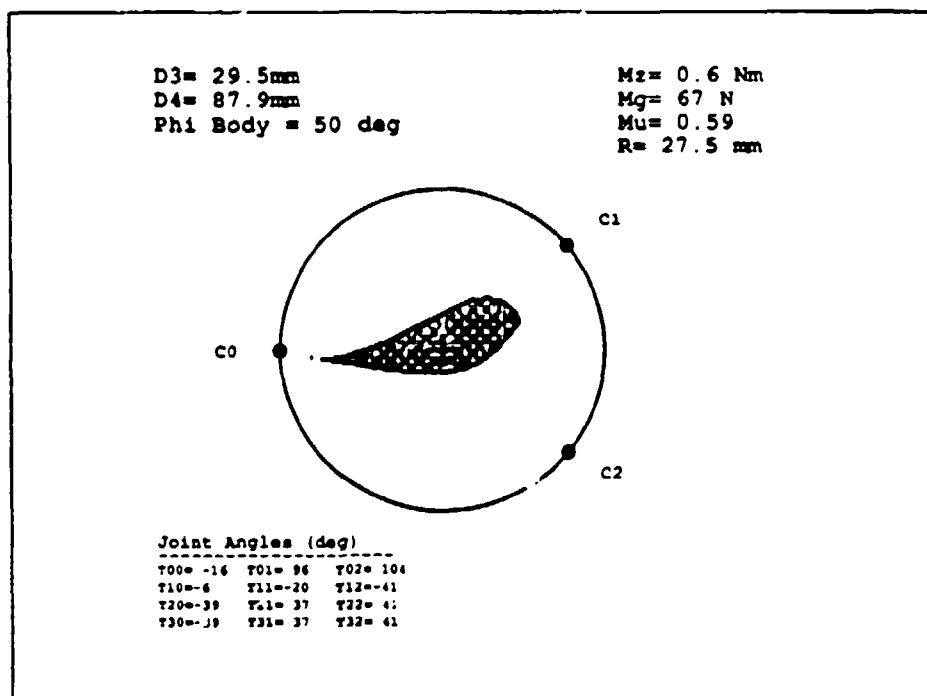


Figure 5-1. Intermediate Neutral-Bias Grasp, $\phi_b = 50^\circ$

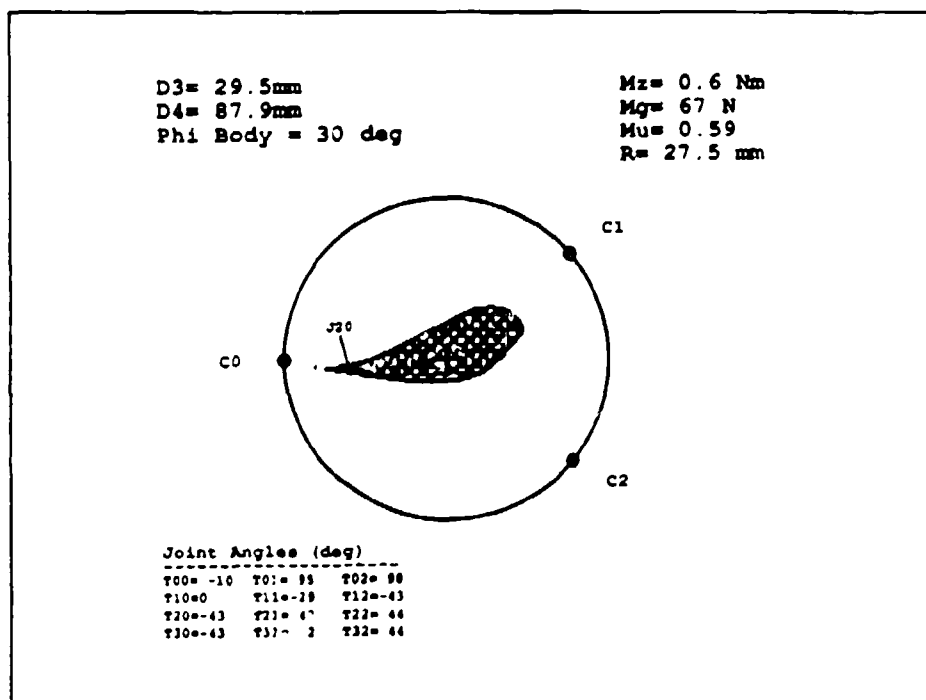


Figure 5-2. Intermediate Neutral-Bias Grasp, $\phi_b = 30^\circ$

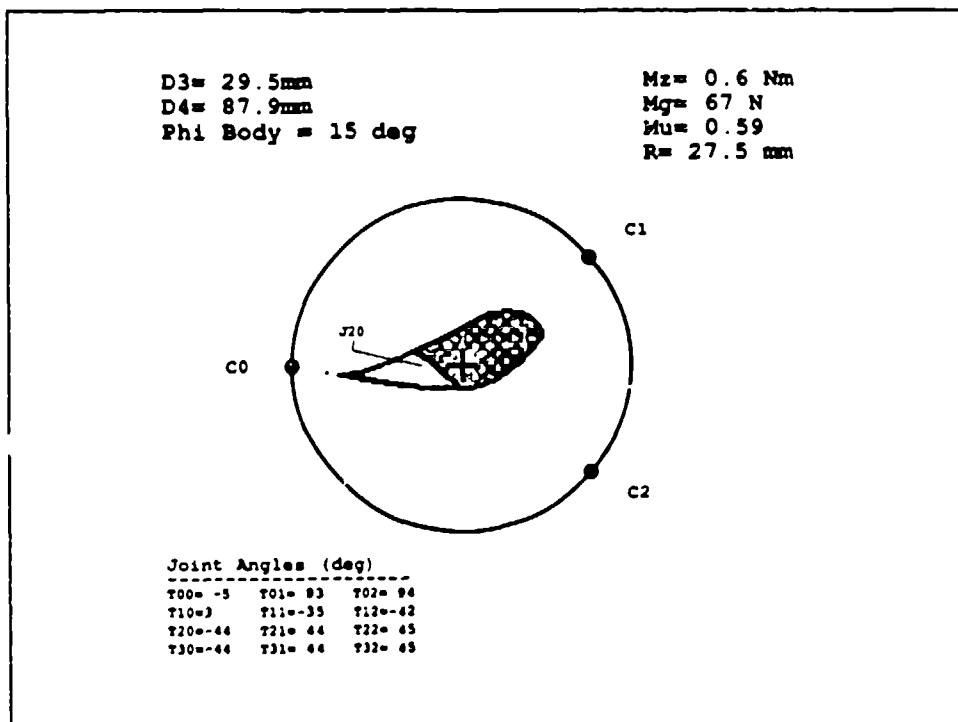


Figure 5-3. Intermediate Neutral-Bias Grasp, $\phi_b = 15^\circ$

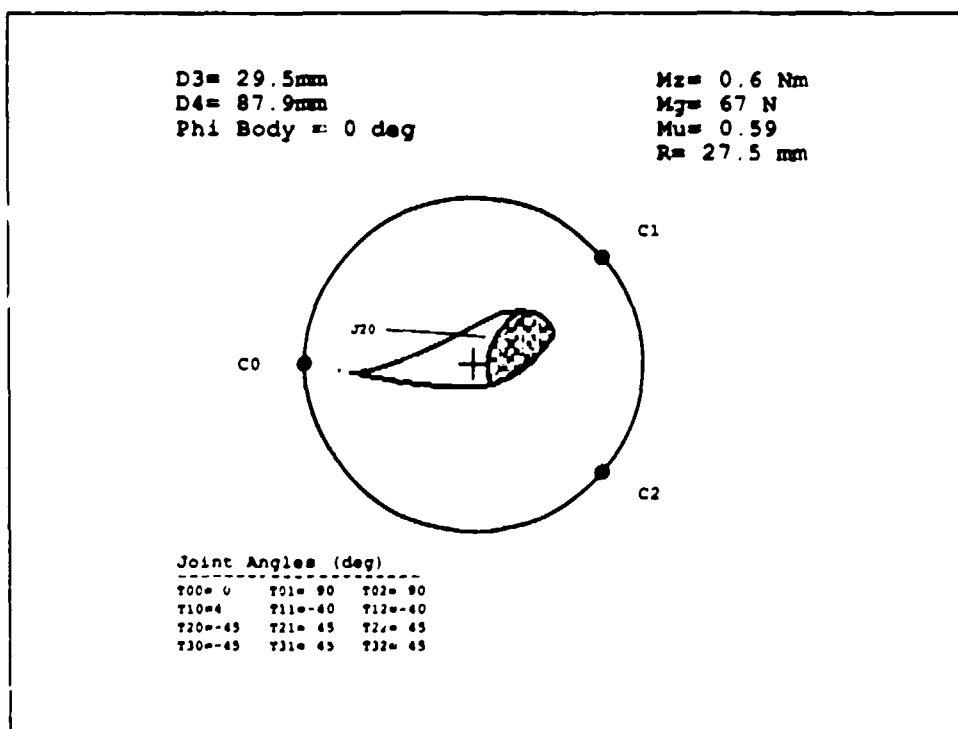


Figure 5-4. Intermediate Neutral-Bias Grasp, $\phi_b = 0^\circ$

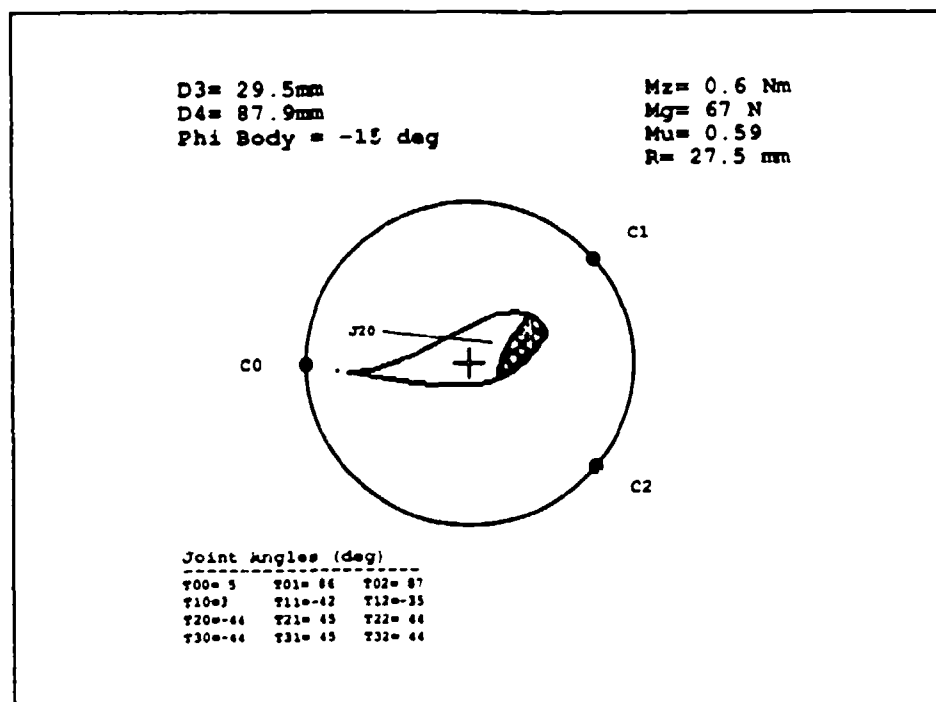


Figure 5-5. Intermediate Neutral-Bias Grasp. $\phi_b = -15^\circ$

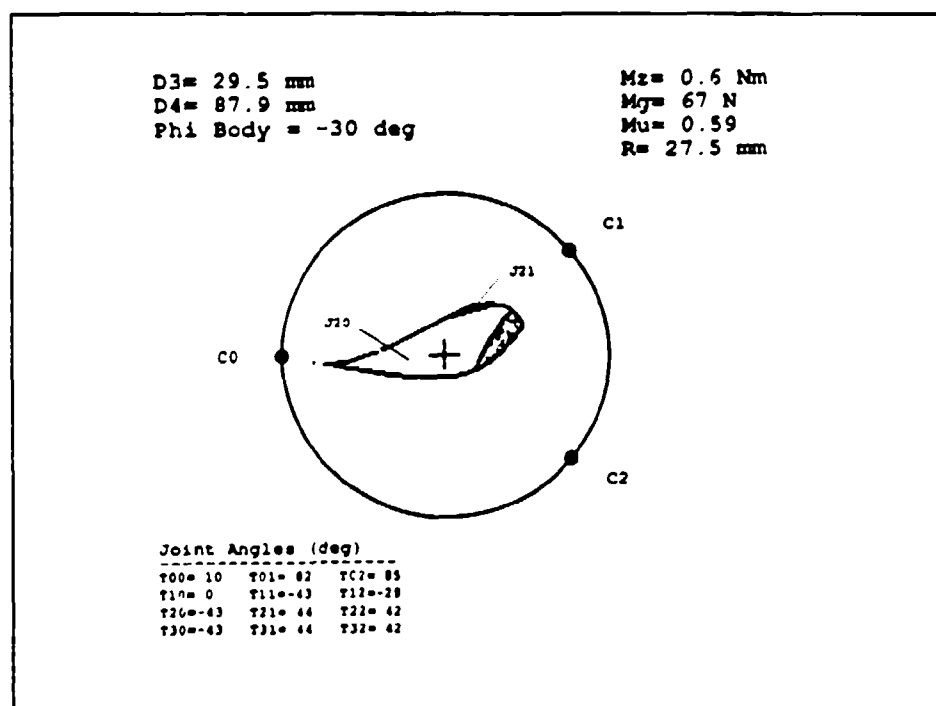


Figure 5-6. Intermediate Neutral-Bias Grasp. $\phi_b = -30^\circ$

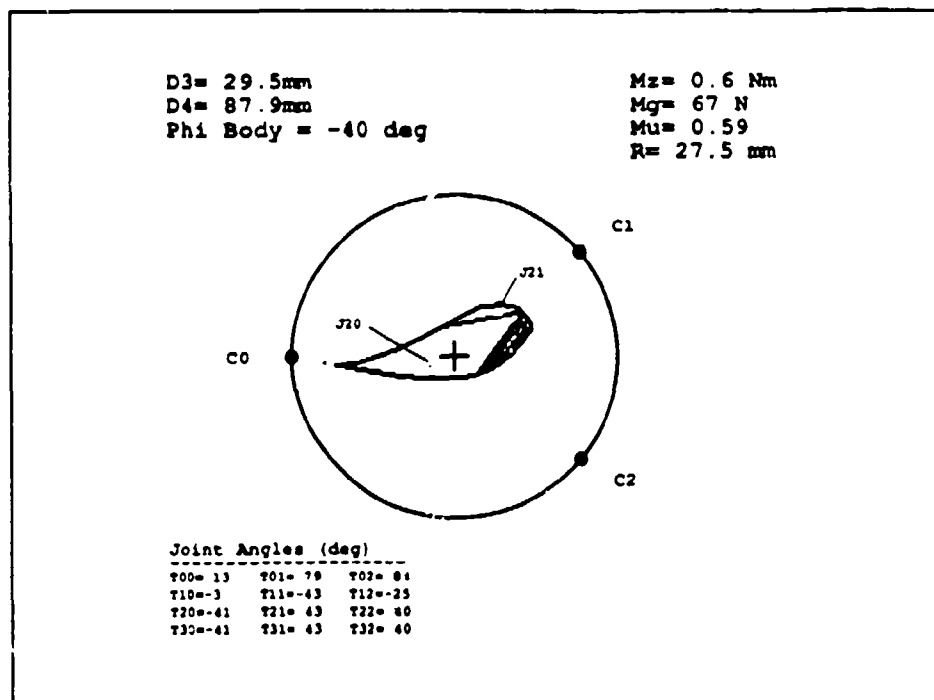


Figure 5-7. Intermediate Neutral-Bias Grasp, $\phi_b = -40^\circ$

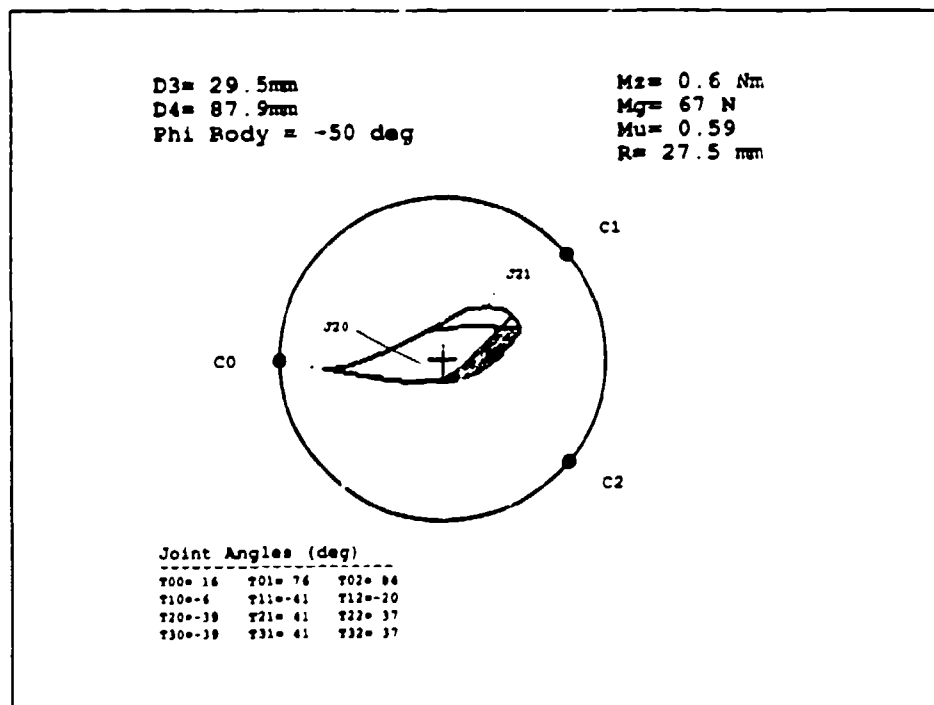


Figure 5-8. Intermediate Neutral-Bias Grasp, $\phi_b = -50^\circ$

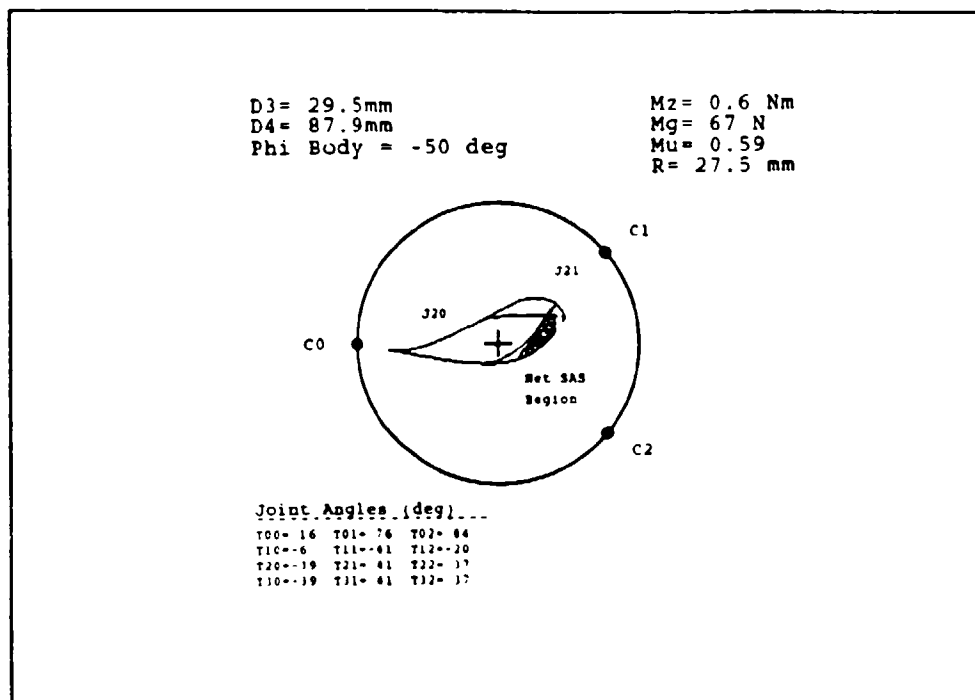


Figure 5-9. Net SAS Region for Intermediate Neutral-Bias Grasp

joint torque limits progressively reduce the size of the SAS region as the cylinder is rotated in a *counter-clockwise* direction. Note that the cylinder center is no longer a valid point for locating the grasp focus after the first half of rotation. The net SAS region (intersection of all SAS regions) is shown in Figure 5-9.

After the cylinder is rotated past $\phi_b = 30^\circ$, the size and shape of the SAS region is primarily determined by J_{20} . This is not surprising since Finger 0 opposes Fingers 1 and 2. A valid question is, why joint two and not joint one? Referring back to Figure 4-3, the moment arm for joint two is approximately half that for joint one. However, the joint torque limit for joint two (2.958 N-m) is less than 40% of the limit for joint one (1.139 N-m). Therefore, in general J_{10} may or may not cross over into the stable region; in either case it always "follows" J_{20} and does not effect the SAS region. This in fact does occur,

but the line is not depicted in the figures for clarity. This is a hand design dependent phenomena. If different hand dimension or joint torque limits are used, then different results can be expected.

The joint torque limit for joint zero is the same as that for joint one, and its moment arm is slightly longer than that for joint one. Like *J10*, the figures indicate that the limit lines for joint zero also lag behind and do not effect the SAS region.

At the final phase of rotation (-30° to -50°), *J21* approaches and eventually violates the top portion of the SAS region. Although not shown for clarity reasons, the limit line for joint two on Finger 2 also crosses into the stable region in the same manner. However, it lags behind the limit line for joint two on Finger 1. A more appropriate example of this type of behavior will presented in Section 5.3.2.

The last item to point out is the general movement of *J20*. At the beginning phase of rotation, the line forms at the lower left portion of the stable region. As the cylinder rotation progresses, the line rotates about the bottom mid-point area of the stable region and "sweeps" across towards contacts one and two. This sweeping motion is very pronounced between $\phi_i = 15^\circ$ and $\phi_b = -15^\circ$. During the final phase of rotation, the sweeping movement of the line slows and the rotation point slides back towards the center area along the bottom edge of the Stable region.

5.3 Effects of Grasp Configuration on SAS region

The evolution of the SAS region is now examined for different grasp configurations using the same c_{map} value and contact configuration as before. The resulting net SAS region is then compared to the net SAS region for the baseline configuration (intermediate neutral-bias grasp).

5.3.1 Retracted Neutral-Bias Grasp. The cylinder rotation is sampled at three discrete rotation angles $\{50^\circ, 0^\circ, -50^\circ\}$. Figures A-1 through A-3 (see Appendix A) show the constraint map for each value of ϕ_b . Only three rotation increments are necessary since the SAS region does not change until ϕ_b equals -50 degrees. This is a significant improvement over the intermediate grasp since the net SAS region is approximately the same as the stable region. This is in effect due to the short moment arm for each finger joint. Note that the first joint torque limit line to enter the stable region is $J20$. The net SAS region is identical to the SAS region in Figure A-3.

5.3.2 Extended Neutral-Bias Grasp. The cylinder rotation is sampled at six discrete rotation angles $\{50^\circ, 30^\circ, 15^\circ, 0^\circ, -15^\circ, -20^\circ\}$. Figures B-1 through B-6 (reference Appendix B) show the resulting constraint map for each value of ϕ_b . After $\phi_b = -15^\circ$ the SAS region fails to exist; therefore, the net SAS region does not exist, assuming a full rotation is desired. At best a partial cylinder rotation from 50° to -15° is possible if the grasp focus can be located in a small region just below the far left hand side of the stable region. In this case the net SAS region would be approximately equal to the intersection of the SAS regions shown in Figure B-2 and Figure B-5. This grasp configuration is overpowered by the c_{map} combination of commanded grasp force magnitude and external moment; that is, the resulting contact forces are beyond the joint torquing capability of the hand during the final phase of cylinder rotation. This in effect reduces the total cylinder rotation angle by 35 degrees.

For this grasp configuration, there are more joint torque limit lines which influence the SAS region since the joint moment arms are at a maximum. Again it is apparent that in the end, the net SAS region is primarily determined by $J20$. Note that the cylinder

center point is eliminated for grasp focus location after $\phi_b = 30^\circ$ (one-third of the cylinder rotation).

As mentioned in Section 5.2, joint torque limit lines may enter the stable region, but have no effect on the SAS region. In general these "lagging" lines are not shown in the figures for clarity reasons. The only limit lines shown are the ones which do effect the SAS region at some point during the cylinder rotation. For demonstration purposes, Figure B-5 retains all joint torque limit lines entering the stable region.

5.3.3 Intermediate Thumb-Bias Grasp. The cylinder rotation is sampled at eight discrete rotation angles $\{50^\circ, 30^\circ, 15^\circ, 0^\circ, -15^\circ, -30^\circ, -40^\circ, -50^\circ\}$. Figures C-1 through C-8 (reference Appendix C) show the resulting constraint map for each value of ϕ_b . During the first part of rotation (50° to 30°), the SAS regions are slightly larger than corresponding regions for the baseline grasp (intermediate neutral-bias grasp). However, the SAS region degrades rapidly compared to the baseline grasp of Figure 5-8 as the rotation progresses to the final orientation angle. This results in a smaller net SAS region. The net SAS region is equivalent to the SAS region shown in Figure C-6.

5.3.4 Intermediate Finger-Bias Grasp. The cylinder rotation is sampled at six discrete rotation angles $\{50^\circ, 30^\circ, 15^\circ, 0^\circ, -15^\circ, -30^\circ, -40^\circ, -50^\circ\}$. Figures D-1 through D-8 (reference Appendix D) show the resulting constraint map for each value of ϕ_b . The first half of rotation is a significant improvement over the baseline configuration. After a 50° rotation the cylinder center point is still well within the SAS region. In fact, the center point is a valid focus point until the rotation angle approaches -30 degrees.

Note that $J20$ is again the primary influence for the SAS region; although $J21$ and $J22$ also effect the SAS region. The net SAS region (Figure D-9) is also an improvement over the baseline since it is more equally proportioned in the vertical and horizontal directions.

5.3.5 Intermediate Finger-Bias (Maximum) Grasp. Since a finger-bias grasp is a slight improvement over a neutral-bias grasp, a fair question is; will a further finger-bias grasp correspond to a larger net SAS region? To examine this question, d_3 is set to its maximum (62.2 mm). The cylinder rotation is sampled at same eight rotation angles as before in Section 5.3.4. The resulting SAS regions are shown in Figures E-1 through E-8.

Compared to the "standard" intermediate finger-bias grasp, the first half of rotation results in similar SAS regions. However, the SAS region reduces in size at a comparatively faster rate in the second half of rotation. Note that in the second half of rotation $J20$ and $J21$ both have a significant effect on the SAS region. At the end of rotation, the SAS region is reduced to a small group of points.

If the grasp focus can be positioned at a single point within the net SAS region, the c_{map} value (0.3261) is very close to the optimum setting for this grasp and rotation range. This assumes that the *optimum* setting is one in which the net SAS region is as small as possible. However, this is more of an "idealization" since a small net SAS region leaves little room for focus positioning error.

5.3.6 Advantages and Disadvantages of Finger-Bias Grasps. From these last two finger-bias grasps, it is apparent that biasing the cylinder towards Fingers 1 and 2 can increase the size of the SAS region. This is especially true during the first half of

rotation. There is point however, where the advantage is lost. Past this point the net SAS region degrades rapidly, as was demonstrated by the maximum finger bias grasp.

From the constraint maps, one can deduce that a properly positioned finger-bias grasp (assuming a constant value for d_4) reduces the torque at joint two on Finger 0. This is important since this particular joint has the greatest influence on the size of the SAS region. For the grasp parameters used, the *best* for the finger-bias grasp is the one at which the torque at joint two on Finger 0 is minimized.

The easiest way to determine this position is through the use of the computer model. Using the computer model is the preferred method since the optimum cylinder bias parameter (d_3) is dependent on the remaining kinematic parameters (specifically d_4 and rotation range). For an intermediate grasp, the optimum finger-bias position is the "standard" finger-bias position presented in Section 5.3.3.

5.4 Increasing Torquing Capability

From the preceding graphical analysis, it was discovered that a retracted grasp configuration corresponds to a large net SAS region. In addition it is apparent that for the baseline contact configuration $\{\psi_0 = 90^\circ, \psi_1 = -50^\circ, \psi_2 = -130^\circ\}$, the net SAS region can be maximized by biasing the cylinder towards Fingers 1 and 2. This information will be combined and used to design a robust grasp for high torque applications.

5.4.1 Single Point Grasp Focus. Assume an ideal situation where the grasp focus can be positioned at a single point; therefore the net SAS region corresponding to the greatest torquing capability for the specific grasp would be as small as possible. Combining the above relationships, we will examine the ideal case using a retracted finger-bias grasp with

semi-symmetric contact locations. For a coarse setting the stable region is reduced by increasing M_{Bz} until the stable region encompasses an area about the size of the cylinder center cross-hair in the previous maps. This corresponds to a new c_{map} value of 0.4891 ($M_{Bz} = .9$ Nm, $m_g = 67$ N, $r_c = 27.46$ mm). The stable region can be reduced further, but we want to be able to visually examine the evolution of the SAS region. Holding c_{map} and r_c constant so that the size of the stable region remains constant, M_{Bz} and m_g are increased proportionally until the desired net SAS region is obtained.

$$M_{Bz_{new}} = (c_{map} r_c) m_{g_{new}} \quad \text{where } c_{map} r_c = \text{const} \quad (5.1)$$

The final values for M_{Bz} and m_g are 1.07 Nm and 79.65, respectively. The constraint maps for $\phi_b = 50^\circ$, -20° , -30° and -50° are shown in Figures 5-10 through 5-13. The maps prior to $\phi_b = -20^\circ$ were omitted since the SAS does not change until after this point.

At the end of rotation ($\phi_b = -50^\circ$) the SAS region is reduced to a few pixel points. This corresponds to the desired net SAS region. Given the focus assumption and contact locations, the selected value of c_{map} provides the maximum torquing capability for a retracted finger-bias grasp over a 100° cylinder rotation range.

5.4.2 Designing a Robust Grasp for High Torque Applications. Using the same grasp and contact configuration, assume that only a 50° cylinder rotation range is required. In addition, assume that the desired focus position is the cylinder center, plus or minus one millimeter (approximately one-quarter of the cross-hair area). Using Equation 5-1 and the same c_{map} value, M_{Bz} and m_g are increased proportionally until the desired net SAS region

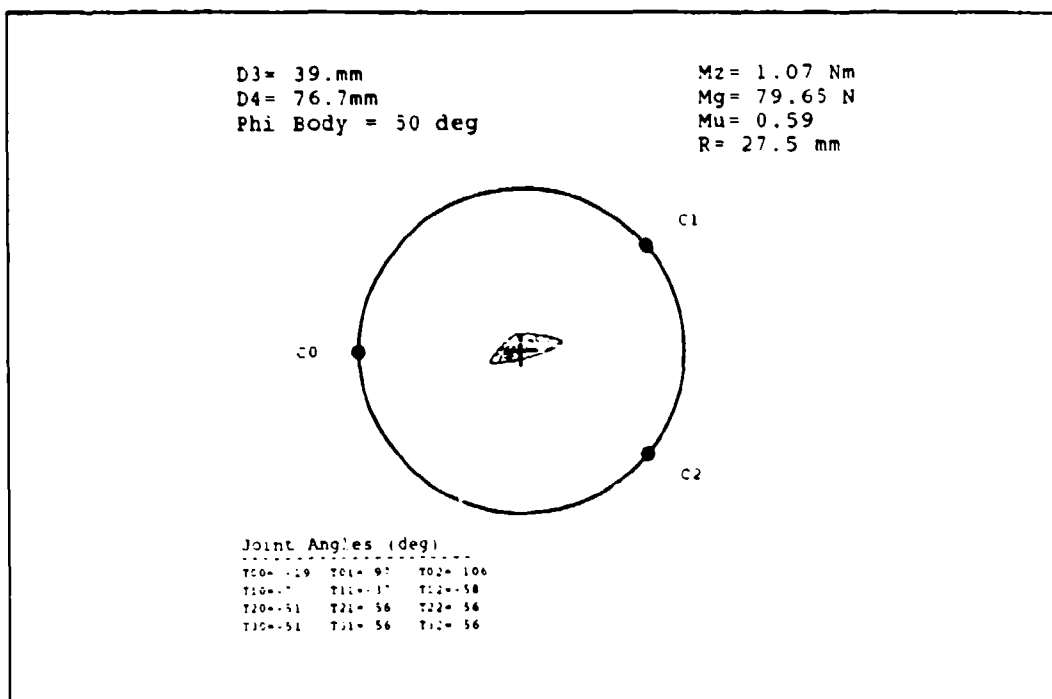


Figure 5-10. Retracted Finger-Bias, $\phi_b = 50^\circ$; Max. Torque, 100° Rotation

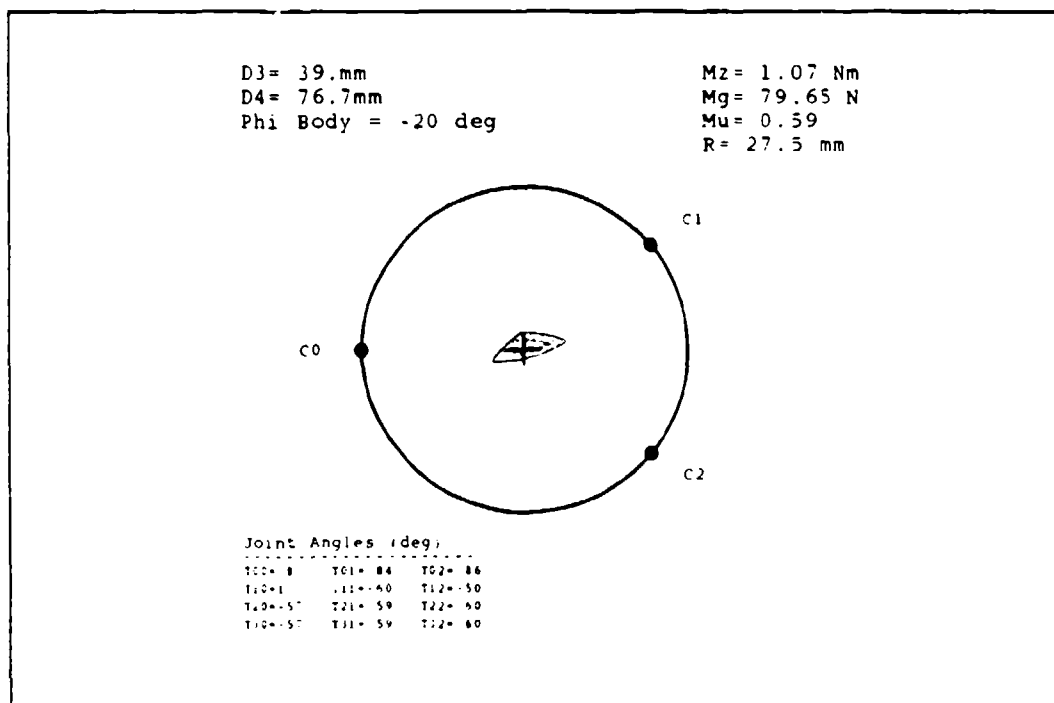


Figure 5-11. Retracted Finger-Bias, $\phi_b = -20^\circ$; Max. Torque, 100° Rotation

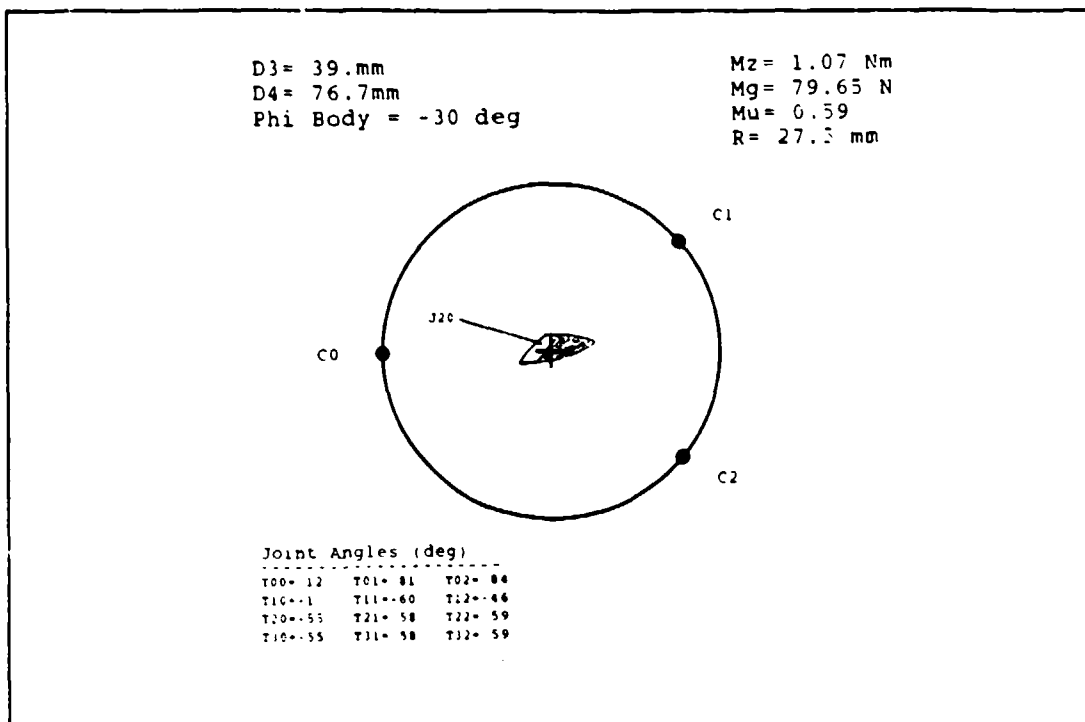


Figure 5-12. Retracted Finger-Bias, $\phi_b = -30^\circ$; Max. Torque, 100° Rotation

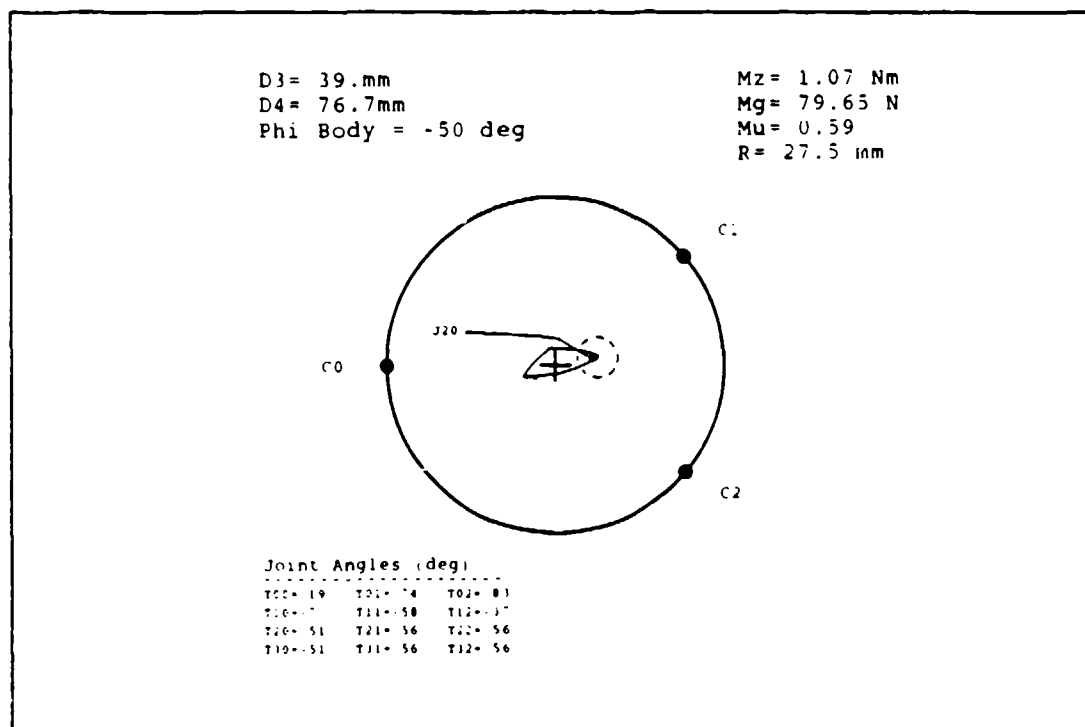


Figure 5-13. Retracted Finger-Bias, $\phi_b = -50^\circ$; Max. Torque, 100° Rotation

is obtained. This results in $M_{B_z} = 1.2 \text{ Nm}$ and $m_g = 89.33 \text{ N}$. Note that decreasing the rotation range by one-half, only increases that torquing capability by approximately 12 percent.

The constraint maps for $\phi_b = 50^\circ, 30^\circ, 20^\circ, 5^\circ$ and 0° are shown in Figures 5-14 through 5-18. Figure 5-19 shows the resulting net SAS region. Examining the net SAS region, it is bounded on the left and along the bottom edge by torque limit lines. The distance from these two boundaries to the cylinder center is approximately one millimeter, as required. However, there is a larger usable area to the upper-left of the center point. From a robustness perspective, the best location for the grasp focus is in the geometric center of the SAS region. From this point, larger focus positioning errors can be absorbed by the grasp and contact configuration without violating stability or joint limit criteria. As mentioned in Section 5.2, an ideal grip (geometric center of net SAS end error region co-located over the cylinder center point) cannot be achieved for the hand model. In this example, the net SAS region satisfies the specified degree of robustness while preserving the cylinder center point; thus the grasp is acceptable. Section 5.6 will examine in greater detail why the cylinder center point is the desirable location for the grasp focus.

5.5 Effects of Contact Location on SAS Region

The results so far are only applicable to a specific contact configuration $\{\psi_0 = 90^\circ, \psi_1 = -50^\circ, \psi_2 = -130^\circ\}$. The question is whether a different contact configuration will provide similar results. Generally speaking, the retracted grasp is still preferred over an intermediate or extended grasp, regardless of the contact configuration. This is due to the shorter moment arm, and thus smaller joint torques. The real question is whether a finger-bias grasp still results in a larger net SAS region.

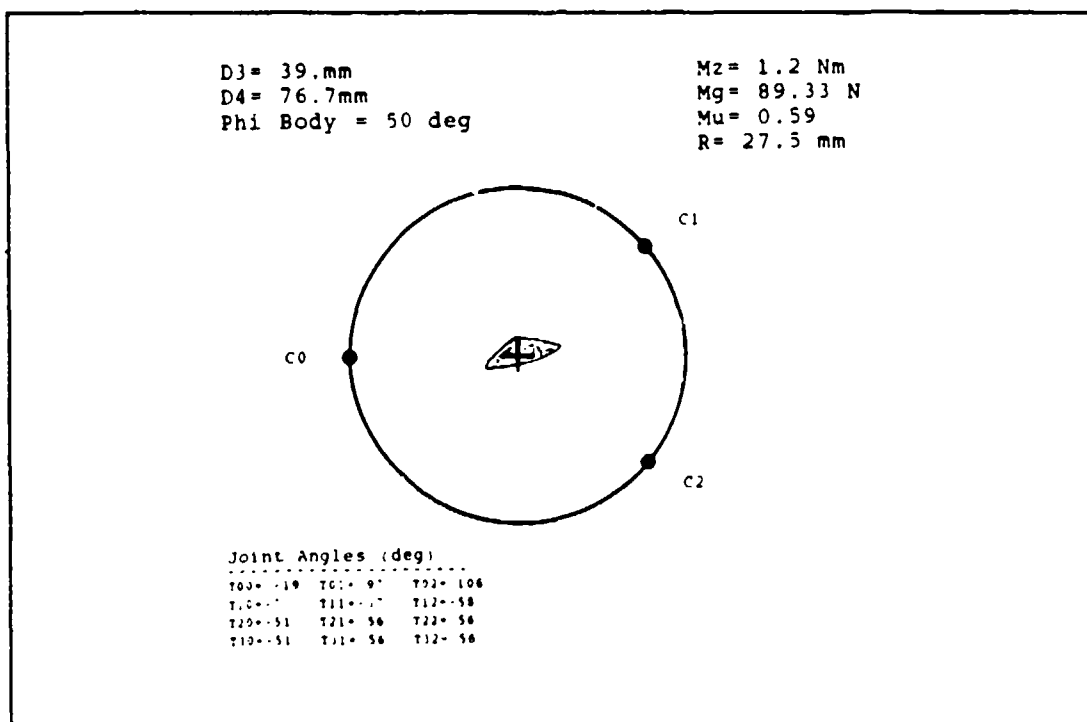


Figure 5-14. Retracted Finger-Bias, $\phi_b = 50^\circ$; Max. Torque, 50° Rotation

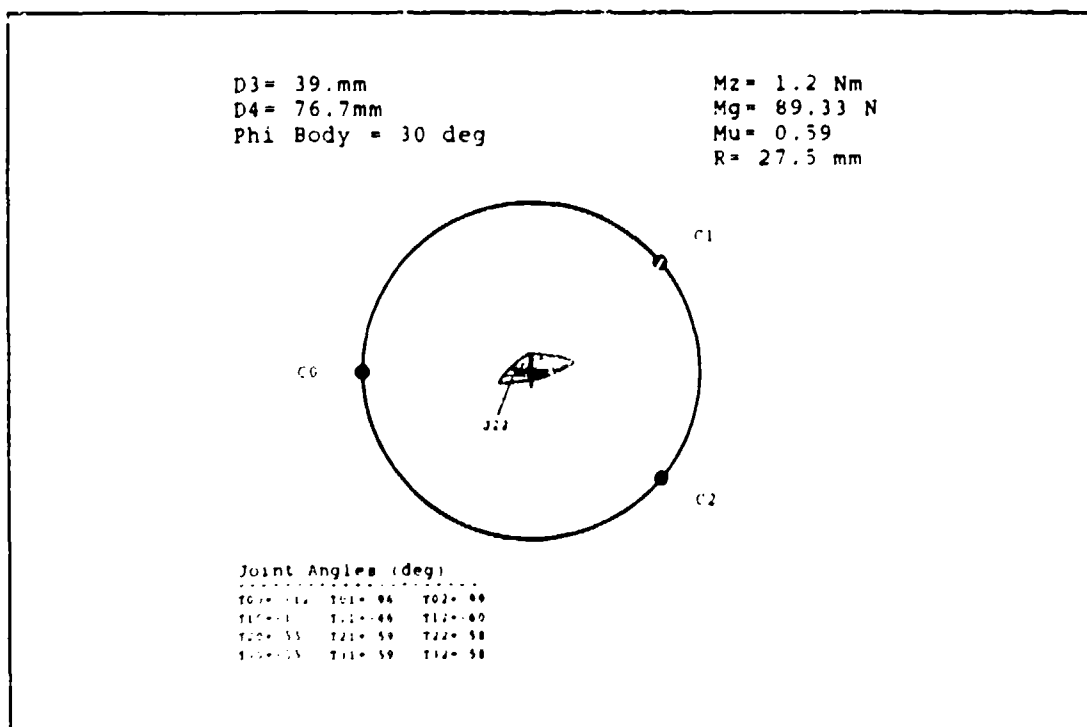


Figure 5-15. Retracted Finger-Bias, $\phi_b = 30^\circ$; Max. Torque, 50° Rotation

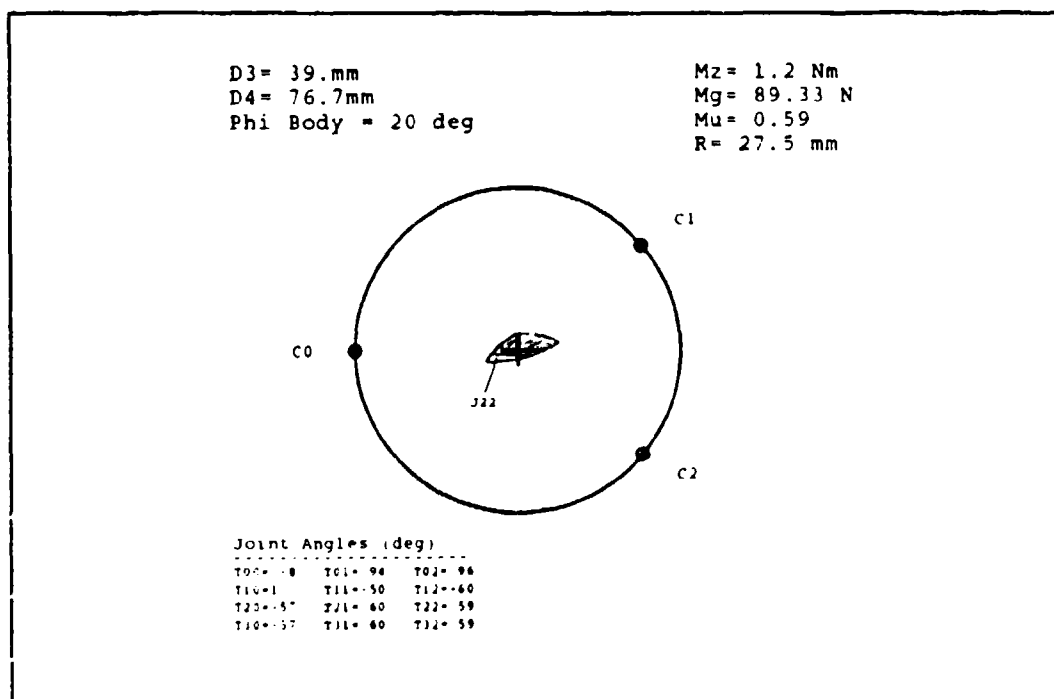


Figure 5-16. Retracted Finger-Bias, $\phi_b = 20^\circ$; Max. Torque, 50° Rotation

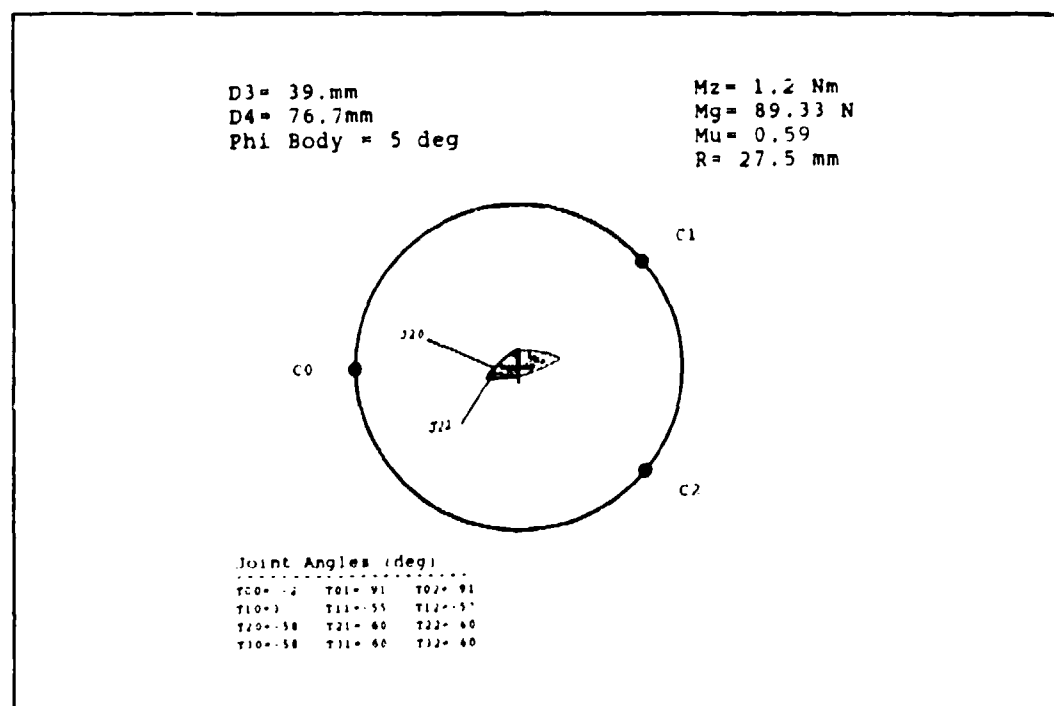


Figure 5-17. Retracted Finger-Bias, $\phi_b = 5^\circ$; Max. Torque, 50° Rotation

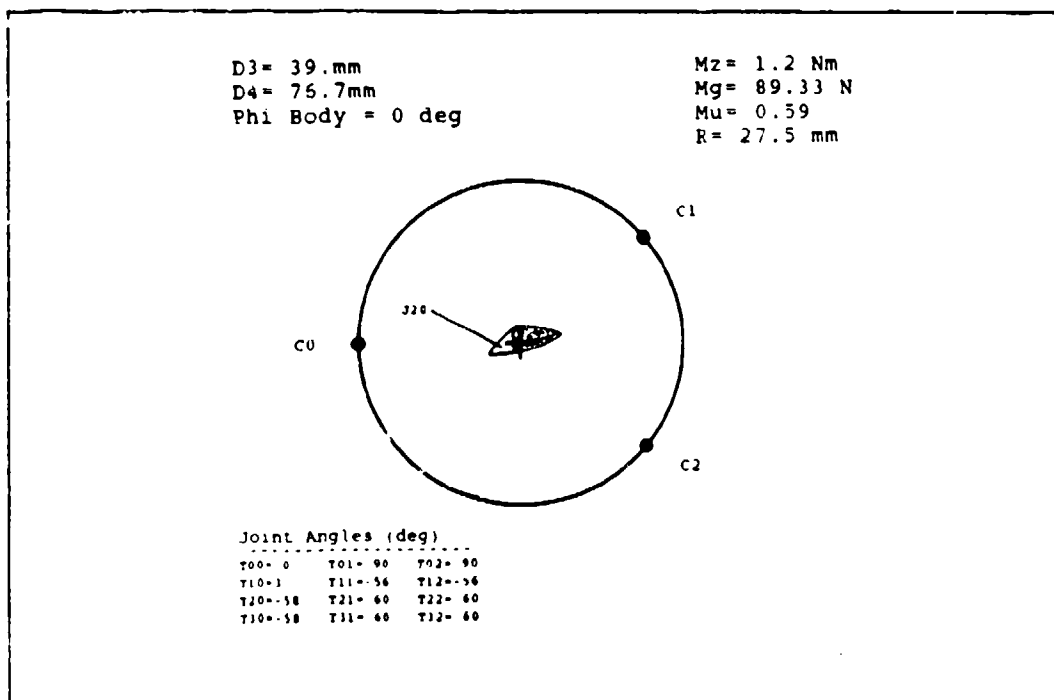


Figure 5-18. Retracted Finger-Bias, $\phi_b = 0^\circ$; Max. Torque, 50° Rotation

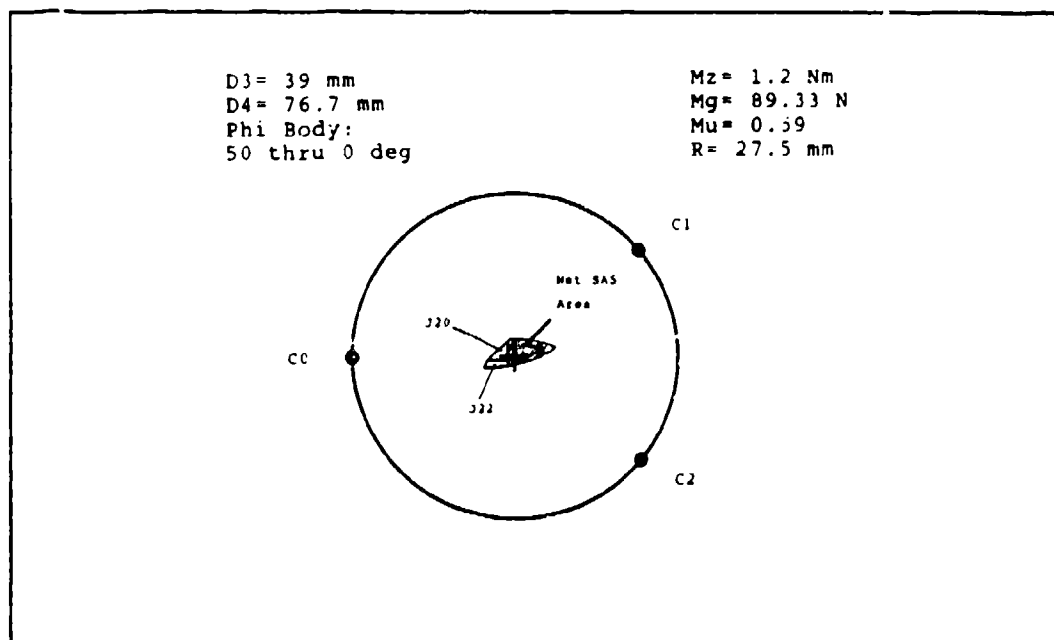


Figure 5-19. Net SAS Region for Retracted Finger-Bias Grasp; Maximum Torque, 50° Rotation

5.5.1 Retracted Finger-Bias Grasp with Symmetric Contacts. To examine this question the contact locations are changed to $\{\psi_0 = 90^\circ, \psi_1 = -30^\circ, \psi_2 = -150^\circ\}$ or to *symmetric* contacts. The cylinder is aligned using the same retracted finger-bias grasp and c_{map} value of .4891 ($M_{Bz} = 1.07 \text{ Nm}$, $m_g = 79.65 \text{ N}$, $r_c = 27.46 \text{ mm}$) that was used in Section 5.4.2. Constraint maps are generated for $\phi_b = 30^\circ, 20^\circ, -20^\circ$, and -30° , and Figures 5-20 through 5-23 depict the resulting constraint maps.

The obvious difference is the shape of the stable region. Its symmetric shape corresponds with the contact symmetry. However, the symmetry is a mirror image about the vertical axis. This type of phenomena is characterized by Edwards [3:p4-2 to 4-7]. At a smaller external moment magnitude, the stable region is completely symmetric (i.e. not a mirror image). As the external moment is increased, the stability or 111 contact code boundary lines move inward at equal rates from the corresponding contacts towards the center. This in essence "chops" the corners of the original triangular shape and results in a mirror image.

The other notable difference is the SAS region is smaller in the first half of rotation than the second half of rotation. There is an opposite trend from the previous contact configuration. Note that the reduction is caused by J_{22} and not J_{20} . This suggests that the cylinder is biased too far towards Fingers 1 and 2.

Before examining another bias position, we should compare the net SAS region (identical to Figure 5-20) with the corresponding "equivalent" region using the previously examined contact configuration. An equivalent comparison can be made by examining the SAS region over the same rotation range (60°). Figures 5-10 and 5-11 ($\phi_b = 50^\circ$ to -20°) show that the SAS region is the same size as the stable region for a minimum rotation range of 70 degrees. This results in a far better net SAS region than the net SAS

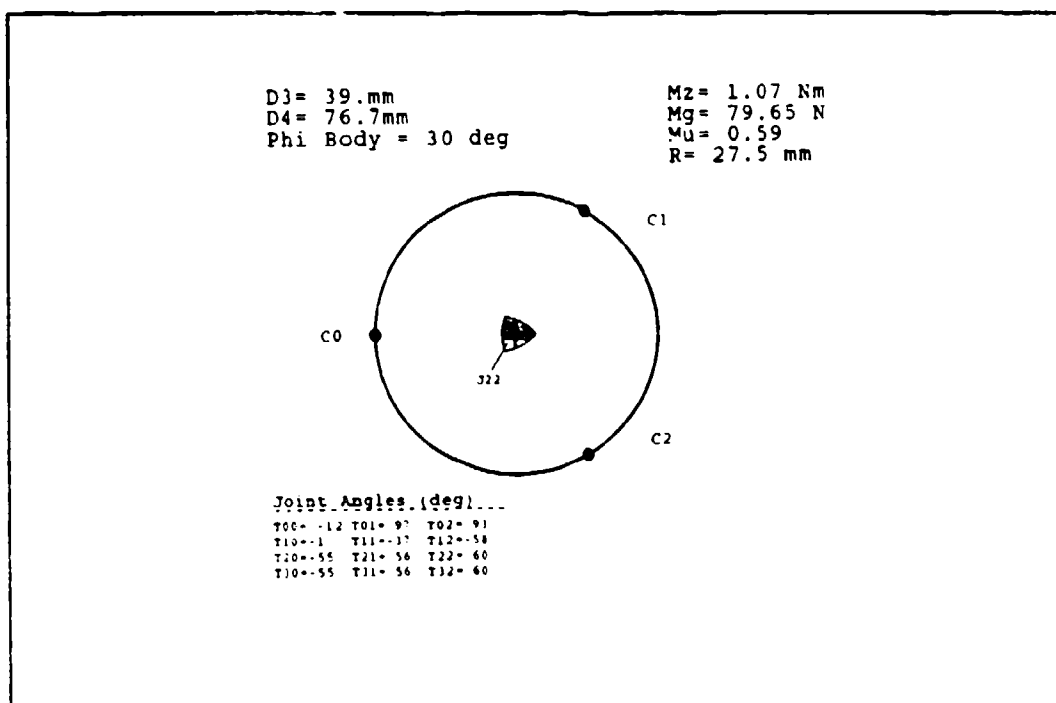


Figure 5-20. Retracted Finger-Bias Grasp, Symmetric Contacts; $\phi_b = 30^\circ$

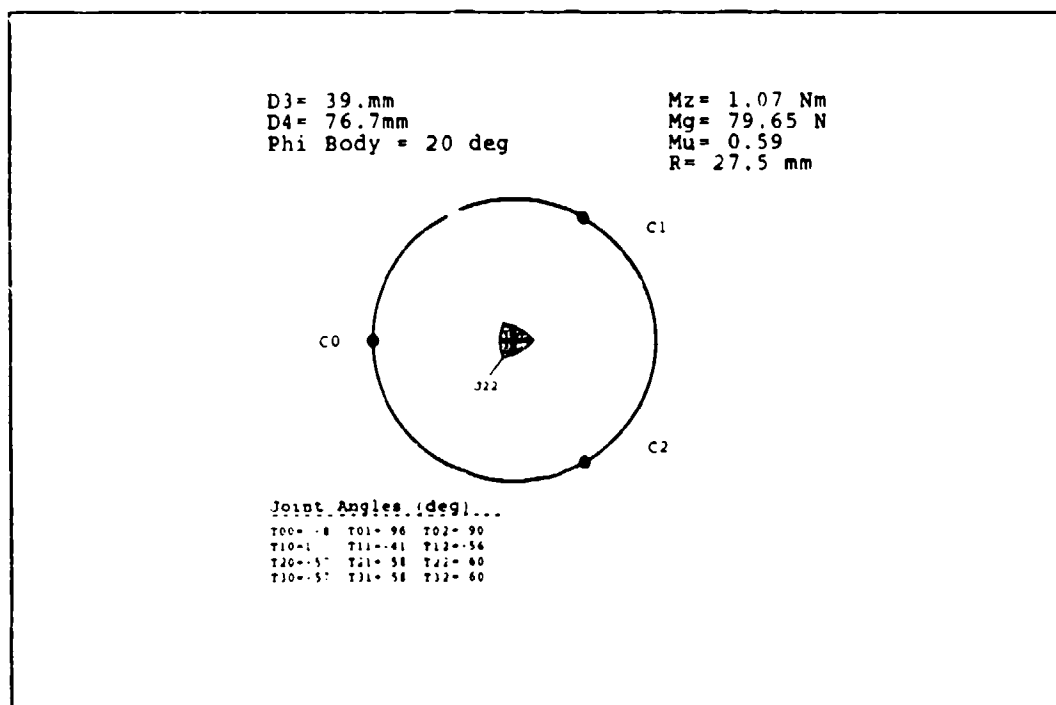


Figure 5-21. Retracted Finger-Bias Grasp, Symmetric Contacts; $\phi_b = 20^\circ$

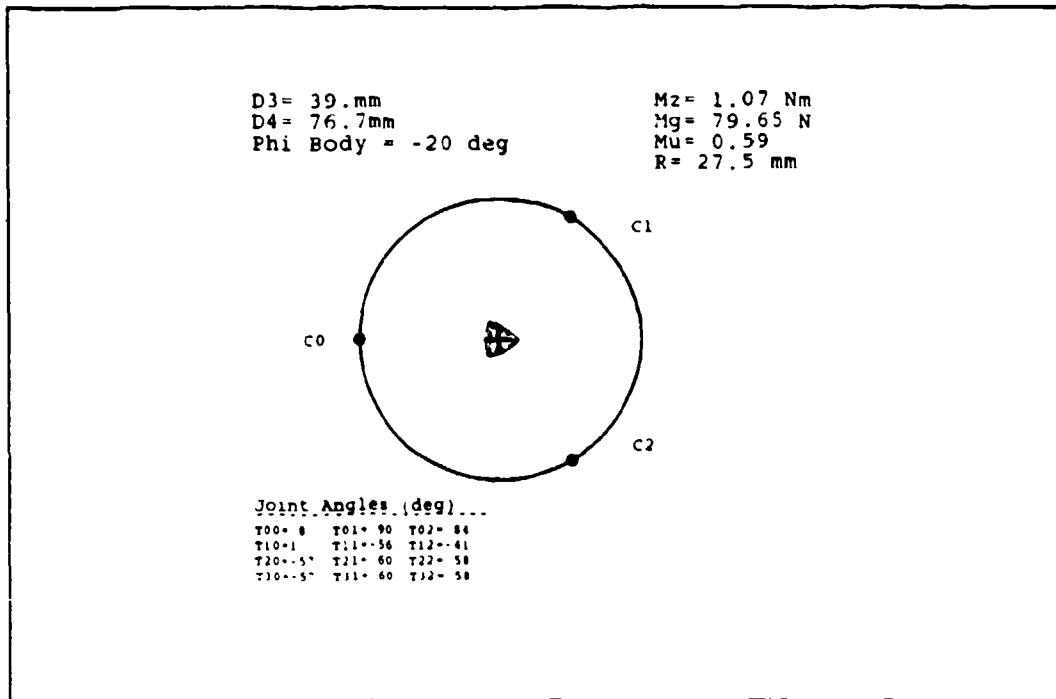


Figure 5-22. Retracted Finger-Bias Grasp, Symmetric Contacts; $\phi_b = -20^\circ$

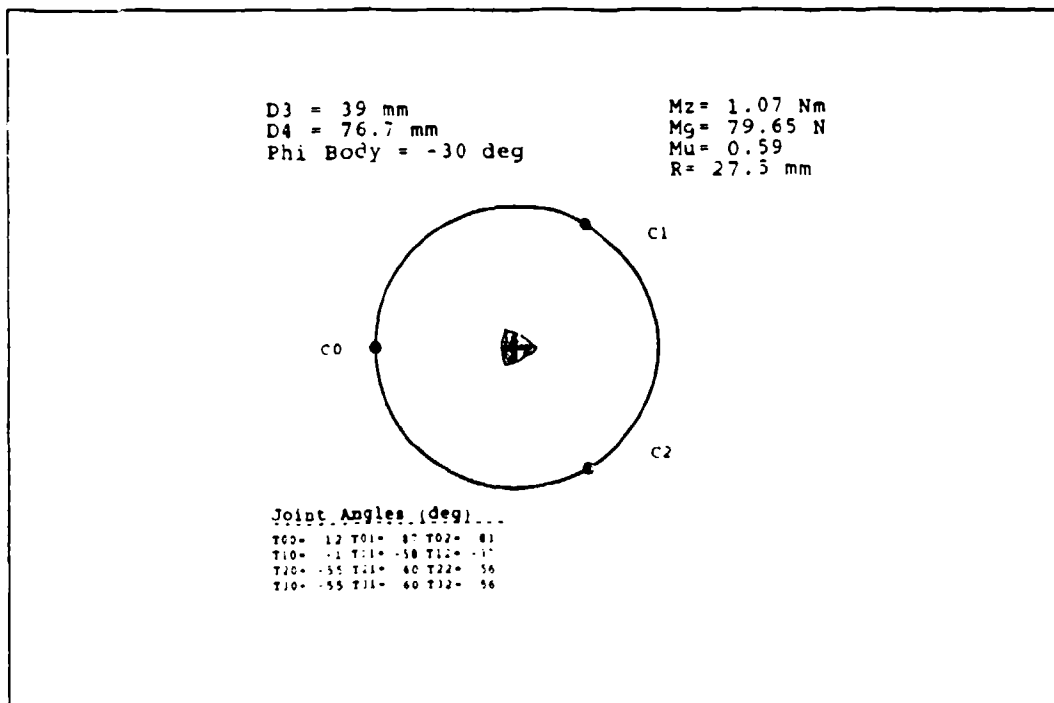


Figure 5-23. Retracted Finger-Bias Grasp, Symmetric Contacts; $\phi_b = -30^\circ$

region using a symmetric contact configuration. This also suggests that the symmetric contact grasp is not properly positioned.

5.5.2 Retracted Thumb-Bias Grasp with Symmetric Contacts. Using the same c_{map} value, the grasp is repositioned to a retracted thumb-bias grasp (slightly thumb-bias, $d_3=28$ mm). Figures 5-24 and 5-25 show the resulting maps for $\phi_b = \{30^\circ, -30^\circ\}$. Only two samples are necessary since the SAS region remains unchanged over the entire rotation range. In fact, the SAS region is the same as the stable region. This is a significant improvement over the finger-bias grasp. This confirms the suspicion that a finger-bias grasp is not necessarily the best cylinder position for all contact configurations.

This time the maximum torque case for the finger-bias grasp in Section 5.4.2 will be compared with the thumb-bias grasp with symmetric contacts. The contact configuration for the finger bias grasp $\{\psi_0 = 90^\circ, \psi_1 = -50^\circ, \psi_2 = -130^\circ\}$ is termed *semi-symmetric* since two of the three contact separation angles are the same. To equally compare the two different contact configurations, we will make the same focus positioning assumptions made in Section 5.4.2. Using the same c_{map} value ($M_{Bz} = 1.2$ Nm and $m_g = 89.33$ N) two sample maps are generated at $\phi_b = \{30^\circ, -30^\circ\}$. The two maps (Figures 5-26 and 5-27, RTB=Retracted Thumb-Bias) correspond to the two extremes for the SAS region.

The net SAS region for the symmetric contact grasp is shown in Figure 5-28. The net region is smaller than the net region in Figure 5-19, which is based on semi-symmetric contacts. However, the proportional area surrounding the cylinder center point is slightly larger. In addition the net region for the symmetric contact case is valid for a 60° rotation range. The net region for the semi-symmetric contact case is only valid for a 50° rotation;

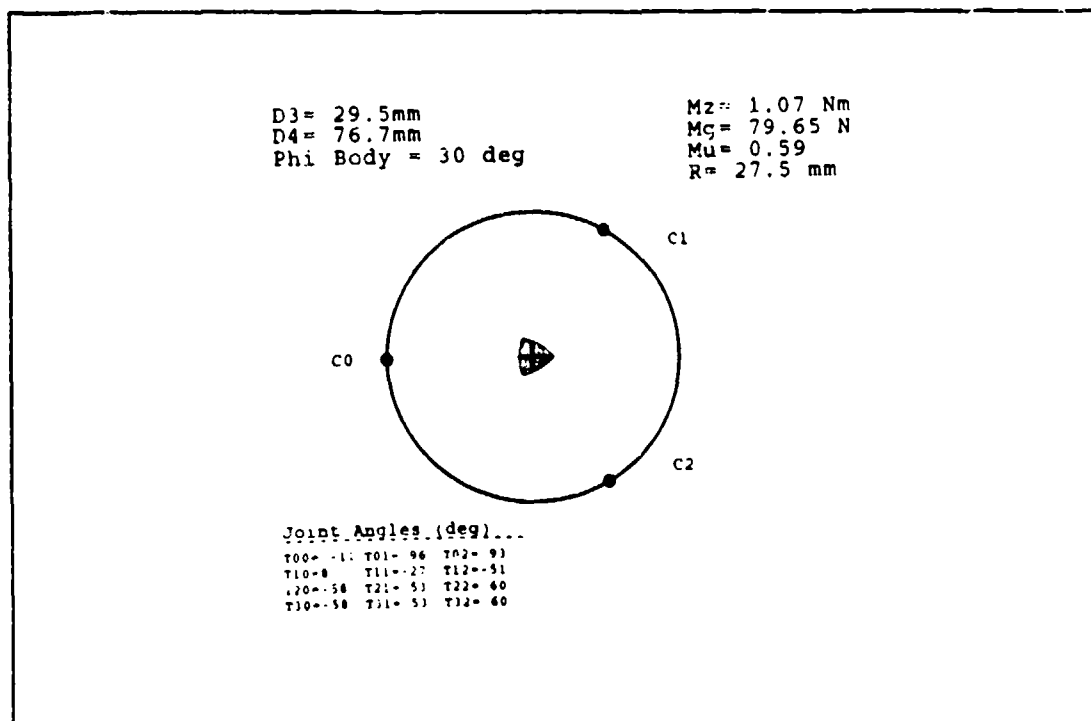


Figure 5-24. Retracted Thumb-Bias Grasp, Symmetric Contacts; $\phi_b = 30^\circ$

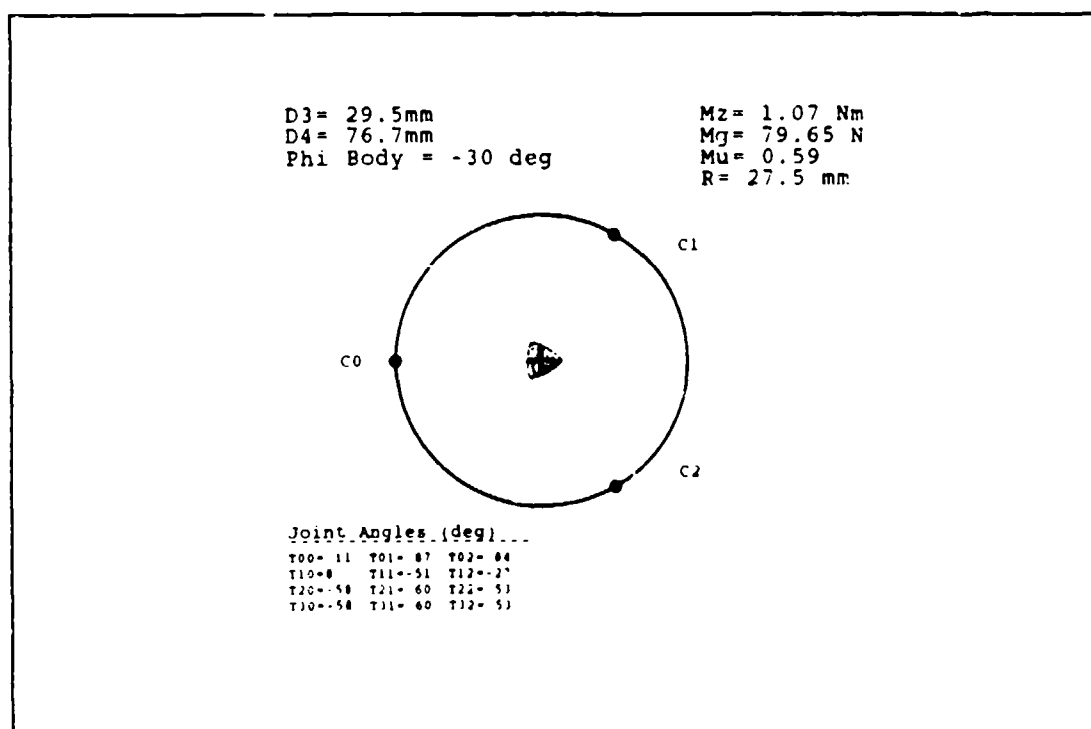


Figure 5-25. Retracted Thumb-Bias Grasp, Symmetric Contacts; $\phi_b = -30^\circ$

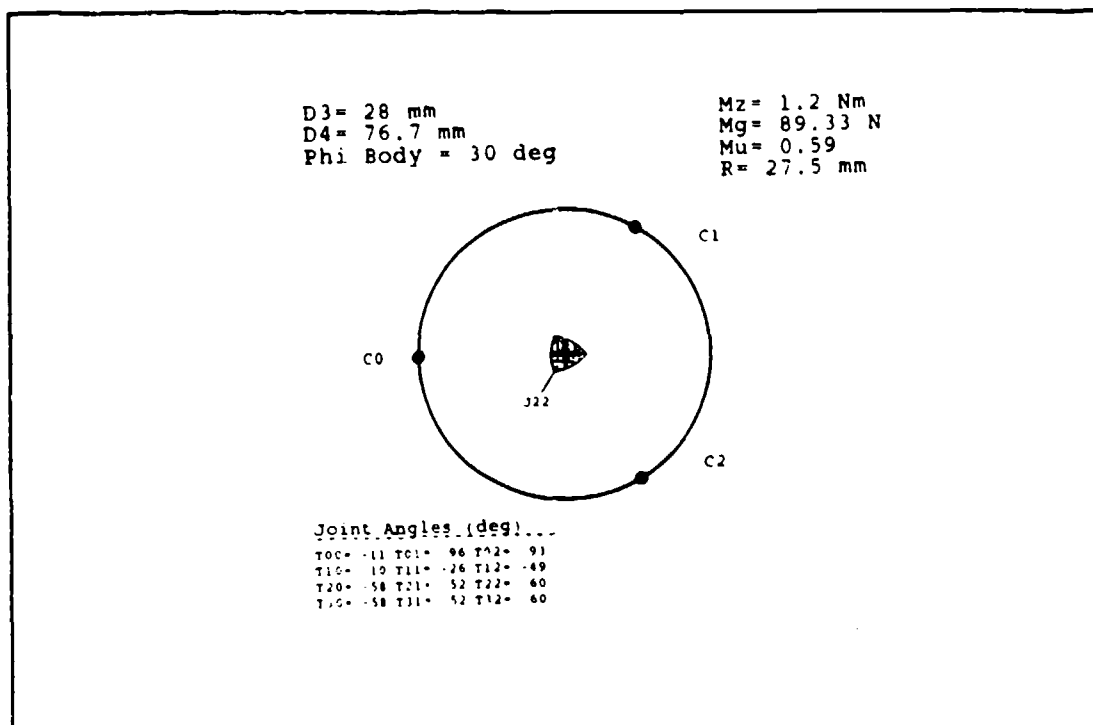


Figure 5-26. RTB Grasp. Symmetric Contacts, $\phi_b = 30^\circ$; High Torque

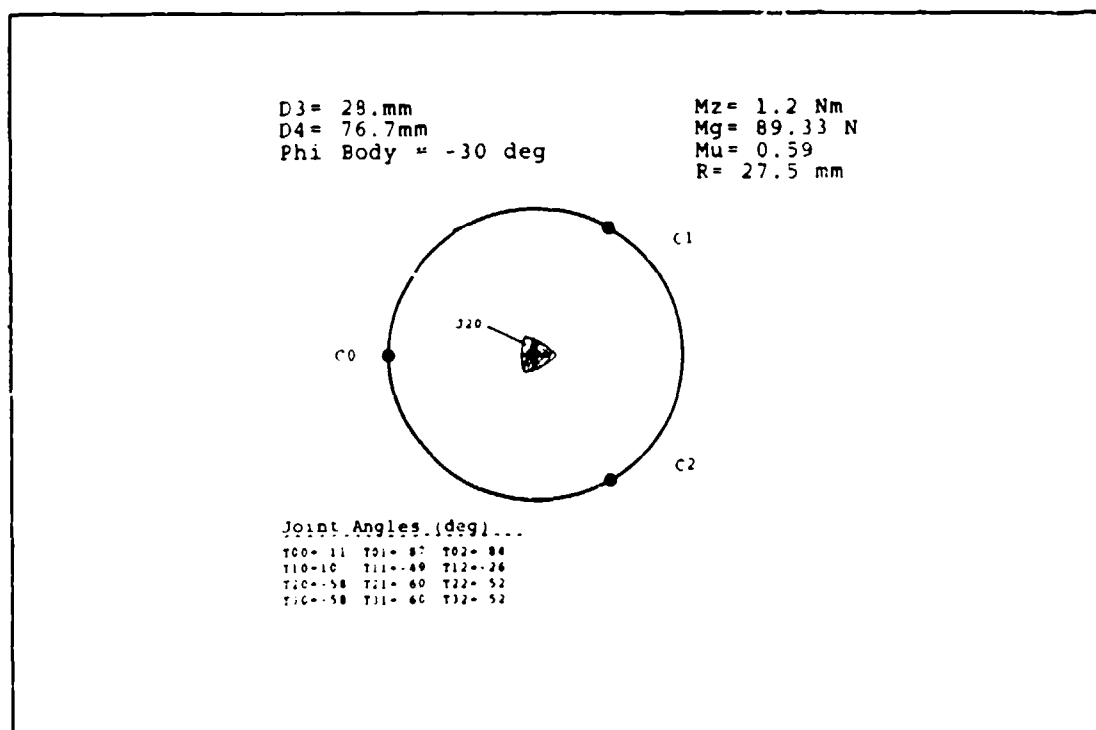


Figure 5-27. RTB Grasp. Symmetric Contacts, $\phi_b = -30^\circ$; High Torque

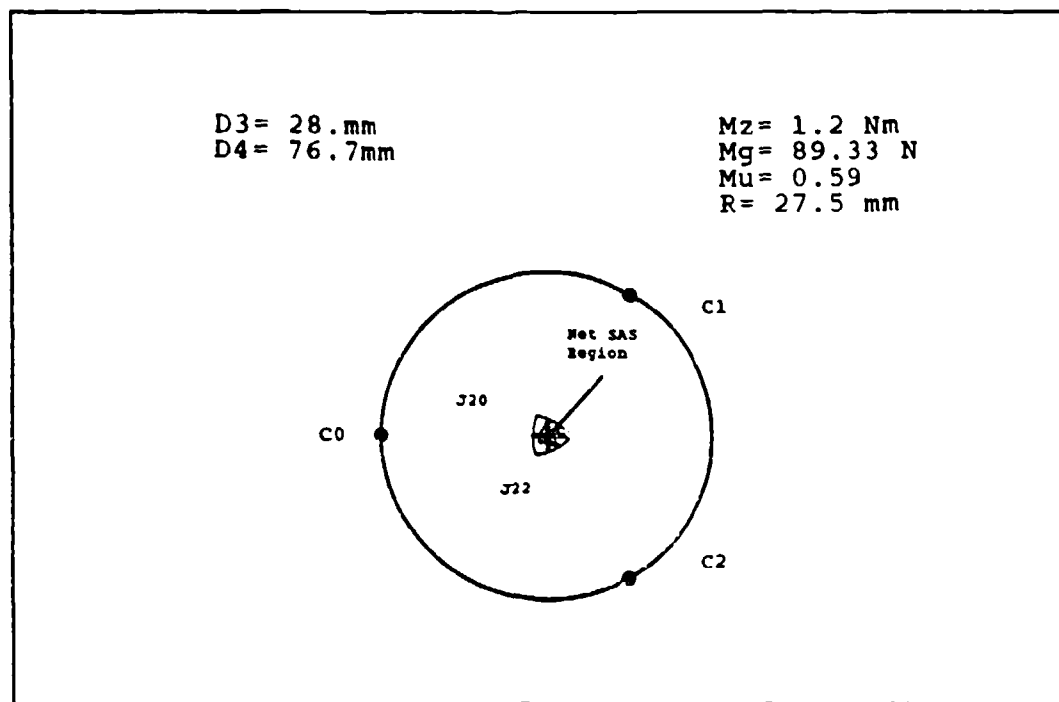


Figure 5-28. Net SAS Region for Retracted Thumb-Bias Grasp w/Symmetric Contacts

although the range can be increased since the net region is larger than the net region for the symmetric contact grasp.

Choosing between the two contact configurations is dependent on where one specifies the desired focus point location, since their rotation ranges are similar. If center point focus location is specified then symmetric contact are preferred, since there is more room for error. If the focus can be positioned in the center of the net SAS region to maximize robustness, then semi-symmetric contact might be preferred since the region is wider. This leads us into the last section of this chapter to determine the advantages and disadvantages of focus location.

5.6 Locating the Grasp Focus

The previous sections provided the understanding of how the SAS net region evolves as the cylinder is rotated using different grasp and contact configurations. We will now sample different focus locations within the stable region to determine the relationship between contact forces and focus location. As mentioned at the beginning of this chapter, the objective is two-fold. The first is to gain some insight as to what determines the shape of the SAS region. The second is to prove that the cylinder center point is the optimal focus location for increased torquing capability.

A comparison is made between the stable regions for the finger-bias grasp with semi-symmetric contacts in Section 5.4.2 and the thumb-bias grasp with symmetric contacts in the Section 5.5.2. An equally spaced 9-point grid is overlaid over the two regions in the same manner. The square grid is positioned over the cylinder center and the grid point spacing is such that its's outer points reach to or slightly past the stable region boundary line. The identical grid overlays for the two regions are shown in Figures 5-29 and 5-30.

Each of the grid points are numbered from left to right, starting at the top of the grid. Tables 5-1 and 5-2 list the discrete values for the forces at each contact for the semi-symmetric contact grasp. Tables 5-3 and 5-4 list the discrete values for the forces at each contact for the symmetric contact grasp. For both contact configurations the total tangential force component must satisfy the stability constraint:

$$X_{JT} \leq \mu Z_{JT} \quad (5.2)$$

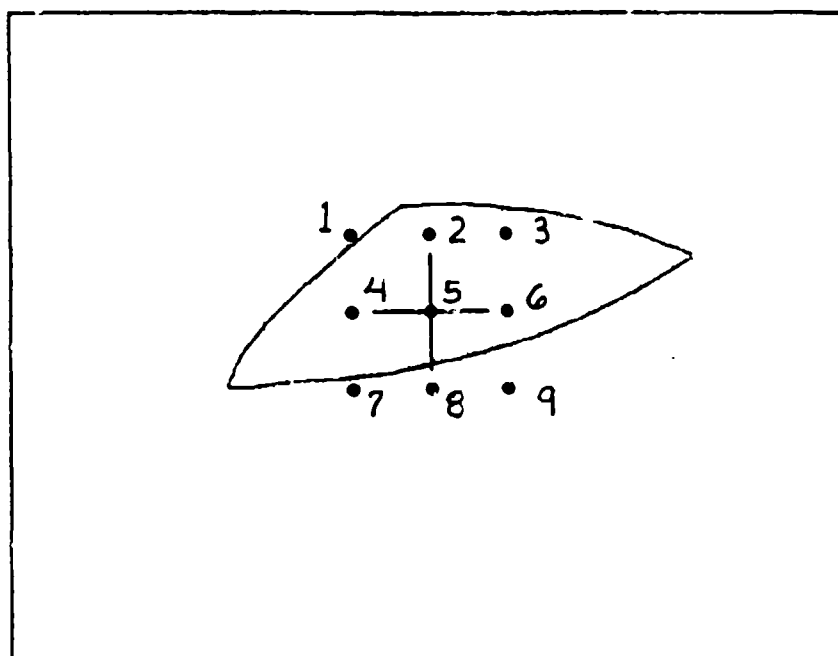


Figure 5-29. Stable Region Grid for Retracted Finger-Bias Grasp with Semi-Symmetric Contacts

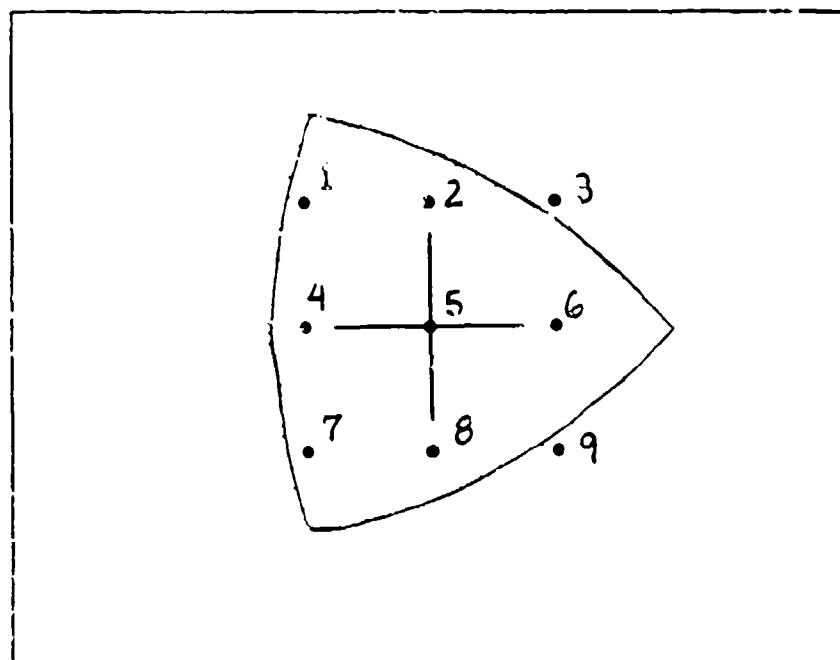


Figure 5-30. Stable Region Grid For Retracted Thumb-Bias Grasp with Symmetric Contacts

Table 5-1. Contact Forces for Grid Points 1 through 5; Semi-Symmetric Contacts

Contact Force Component	Force Magnitude (N) at Grid Point {x,y}				
	1 {-,+}	2 {0,+}	3 {+,+}	4 {-,0}	5 {0,0}
X_{0I}	-3.11	-2.53	-2.57	0	0
X_{0E}	-18.95	-18.95	-18.95	-18.95	-18.95
X_{0T}	-22.06	-21.78	-21.52	-18.95	-18.95
Z_{0I}	39.64	38.87	37.93	39.53	38.75
$\frac{ X_{0T}/Z_{0I} }{\mu}$	0.94	0.95	0.96	0.81	0.83
X_{1I}	2.95	1.7	0.29	1.1	0
X_{1E}	-12.37	-12.37	-12.37	-12.37	-12.37
X_{1T}	-9.42	-10.67	-12.08	-11.27	-12.37
Z_{1I}	28.99	29.03	29.13	24.89	25.29
$\frac{ X_{1T}/Z_{1I} }{\mu}$	0.55	0.62	0.70	0.77	0.83
X_{2I}	0.17	1.13	2.28	-1.1	0
X_{2E}	-12.37	-12.37	-12.37	-12.37	-12.37
X_{2T}	-12.2	-11.24	-10.09	-13.47	-12.37
Z_{2I}	20.43	21.25	22.06	24.88	25.29
$\frac{ X_{2T}/Z_{2I} }{\mu}$	1.01	0.90	0.77	0.92	0.83

Table 5-2. Contact Forces for Grid Points 6 through 9; Semi-Symmetric Contacts

Contact Force Component	Force Magnitude (N) at Grid Point {x,y}			
	6 {+,0}	7 {-,-}	8 {0,-}	9 {+,-}
X_{0I}	0	3.11	2.83	2.57
X_{0E}	-18.95	-18.95	-18.95	-18.95
X_{0T}	-18.95	-15.84	-16.12	-16.38
Z_{0I}	37.79	39.64	38.87	37.93
$\frac{ X_{0T}/Z_{0I} }{\mu}$	0.85	0.68	0.70	0.73
X_{1I}	-1.28	-0.17	-1.13	-2.28
X_{1E}	-12.37	-12.37	-12.37	-12.37
X_{1T}	-13.65	-12.54	-13.50	-14.65
Z_{1I}	25.74	20.43	21.25	22.06
$\frac{ X_{1T}/Z_{1I} }{\mu}$	0.90	1.04	1.08	1.13
X_{2I}	1.28	-2.95	-1.7	-0.29
X_{2E}	-12.37	-12.37	-12.37	-12.37
X_{2T}	-11.09	-15.32	-14.07	-12.66
Z_{2I}	25.74	28.99	29.03	29.13
$\frac{ X_{2T}/Z_{2I} }{\mu}$	0.73	0.89	0.82	0.74

Table 5-3. Contact Forces for Grid Points 1 through 5; Symmetric Contacts

Contact Force Component	Force Magnitude (N) at Grid Point {x,y}				
	1 {-,+}	2 {0,+}	3 {+,+}	4 {-,0}	5 {0,0}
X_{0I}	-2.5	-2.18	-1.87	0	0
X_{0E}	-14.56	-14.56	-14.56	-14.56	-14.56
X_{0T}	-17.06	-16.74	-16.43	-14.56	-14.56
Z_{0I}	31.87	29.9	27.52	31.76	29.78
$\frac{ X_{0T}/Z_{0I} }{\mu}$	0.91	0.95	1.01	0.96	0.83
X_{1I}	3.14	1.23	-0.96	1.75	0
X_{1E}	-14.56	-14.56	-14.56	-14.56	-14.56
X_{1T}	-11.42	-13.33	-15.52	-12.81	-14.56
Z_{1I}	30.76	31.54	32.41	28.73	29.78
$\frac{ X_{1T}/Z_{1I} }{\mu}$	0.63	0.72	0.81	0.76	0.83
X_{2I}	-0.64	0.95	2.83	-1.75	0
X_{2E}	-14.56	-14.56	-14.56	-14.56	-14.56
X_{2T}	-15.12	-13.61	-11.73	-16.31	-14.56
Z_{2I}	26.42	27.77	29.18	28.73	29.78
$\frac{ X_{2T}/Z_{2I} }{\mu}$	0.97	0.83	0.68	0.78	0.83

Table 5-4. Contact Forces for Grid Points 6 through 9; Symmetric Contacts

Contact Force Component	Force Magnitude (N) at Grid Point {x,y}			
	6 {+,0}	7 {-,-}	8 {0,-}	9 {+,-}
X_{0I}	0	2.5	2.18	1.87
X_{0E}	-14.56	-14.56	-14.56	-14.56
X_{0T}	-14.56	-12.06	-12.38	-12.69
Z_{0I}	27.39	31.87	29.9	27.52
$\frac{ X_{0T}/Z_{0I} }{\mu}$	0.90	0.64	0.70	0.78
X_{1I}	-2.02	0.64	-0.95	-2.83
X_{1E}	-14.56	-14.56	-14.56	-14.56
X_{1T}	-16.58	-13.92	-15.51	-17.39
Z_{1I}	30.9	26.43	27.77	29.18
$\frac{ X_{1T}/Z_{1I} }{\mu}$	0.91	0.89	0.95	1.01
X_{2I}	2.02	-3.14	-1.23	0.96
X_{2E}	-14.56	-14.56	-14.56	-14.56
X_{2T}	-12.54	-17.70	-15.79	-13.60
Z_{2I}	30.9	30.76	31.54	32.42
$\frac{ X_{2T}/Z_{2I} }{\mu}$	0.69	0.97	0.85	0.71

where

$$X_{jT} = X_{jI} + X_{jE} \quad j = 0, 1, 2$$

$$Z_{jT} = Z_{jI}$$

The shaded boxes in Tables 5-1 through 5-4 represent the contact locations which violate Equation 5-2. This is graphically confirmed by the constraint maps in Figures 5-29 and 5-30. A simple method to interpret the contact force information in the tables is to calculate and compare the value of X_{jT}/Z_{jT} to the friction coefficient μ . Rearranging equation 5.2 and realizing that Z_{jT} is equal to Z_{jI} (reference Section 3.5):

$$\frac{|X_{jT}/Z_{jI}|}{\mu} < 1.0$$

The ratio in Equation 5.3 must be less than one to avoid contact slip. As the ratio approaches one, the potential for slip increases; for discussion define the calculated ratio as the *slip potential* for the contact point. Since the contact point will not actually slip until the ratio equals one, the slip potential is merely a quality measure for comparison purposes. The slip potential is calculated for each of the nine grid points and listed in Tables 5-1 through 5-4.

Using the definition of the slip potential, there are several key items to note concerning focus location. Most notable is that at the cylinder center point (grid point five), each of the contacts points have the same slip potential. This is true regardless of contact configuration. Having equal potentials implies that when the conditions for slip exist, all three contact points will slip at the same time. This is a predictable feature; a

feature which does not require advance calculation since it is independent of contact configuration.

At point locations other than the cylinder center, the slip potential for a given contact is different from the other two contacts. The resulting values are unique for each contact point and a function of contact configuration. For example, compare grid point seven for the two contact configurations. The slip potential for each contact using semi-symmetric contacts (reference Table 5-2) changes significantly if the contact configuration is switched to symmetric contacts (Table 5-4) even though the focus location is the same. Also note that in the semi-symmetric case, Finger 1 has the highest slip potential. At the same point using symmetric contacts, Finger 2 has the highest slip potential. Unlike the cylinder center point, which finger will slip first cannot be predicted without discrete calculations at the specific focus point.

The cylinder center point also has a computational advantage over any other point in the grasp plane. Since the slip potential is the same for each contact, the value need only be calculated once. With this value the contact forces for the remaining two contact points can be easily calculated. Equations 3.5 and 3.10 are normally required to calculate the total contact force. Equation 3.10 is complex, but can be avoided for the other two contact points. Equation 3.5 can be used to calculate X_{jE} , which is equal to X_{jT} . Using the calculated value for the slip potential and Equation 5.3, $Z_{jI}=Z_{jT}$ can be easily calculated.

At the cylinder center point, the x-component of the homogeneous or internal contact force solution is zero for each of the three contact points. Again, this is independent of contact configuration. At this point the x-component of the total contact force is equal to X_{jE} only; the force necessary to oppose the external moment. Therefore, the total contact

force is used only to oppose the external moment (X_{jE}) or to maintain grasp stability (Z_{jI}). At any other point, the x-component of the internal contact force exists for at least two of the fingers. This implies that part of the internal grasp force is used to do non-useful work; i.e. the fingers are working against each other. A conclusion can be made that the cylinder center point is the most efficient point for locating the grasp focus. This confirms Edwards' statement that the cylinder center point is the optimal focus location for increased torquing capability.

The slip potential can also be used to examine the shape of the stable region for each of the contact configurations. We will examine the slip potential as a function of grid point location. First select the contact point with the maximum slip potential at each grid point location. These values are listed in bold type in Table 5-1 through 5-4. Now compare these values with the shape of the corresponding stable region shown in Figure 5-29 or Figure 5-30. Note that the values match the shape of the region. This is as expected since, by definition, the shape of the stable region is determined by the no-contact-slip stability criteria.

Due to the complexity of the grasp equations (Equation 3.5 and 3.10) and the inclusion of the external moment, it is difficult to explain exactly why the stable region is shaped as it is. In addition, it is the shape of net SAS region which ultimately defines whether the grasp can successfully complete the task. If joint torque limits are violated, any symmetry contained in the stable region is removed by torque limit lines. However, a basic understanding of how contact configuration effects the shape of the stable region is still important for grasp planning purposes. Two general statements can be made concerning the relationship between contact configuration and the shape of the stable region:

1) If the contact locations are symmetric, the stable region will be symmetric about the horizontal axis of the contact plane (axis containing contact point for Finger 0 and the cylinder center point) and will enclose the cylinder center point.

2) If the contact locations are semi-symmetric, the stable region will have no symmetry, but will enclose the cylinder center point. In addition, if the external moment is counter-clockwise, the region will be bias towards Finger 1; if it is clockwise, the region will be bias towards Finger 2

5.7 Summary

Generating constraint maps for various grasp configurations provides a basic understanding of how the SAS region evolves over a given cylinder rotation range. Three primary grasp configurations (retracted, intermediate, and extended) were examined to determine the effects of cylinder proximity on the net SAS region. In addition, three different types of bias-grasps were examined to determine the effects of cylinder biasing on the net SAS region. The graphical analysis revealed that positioning the cylinder as close as possible to the palm results in a large SAS region. However, biasing the cylinder towards a specific finger to maximize the size of the net SAS region is dependent on the grasp configuration.

Adjusting the grasp such that the net SAS region is maximized is desirable since it implies that the grasp configuration is then capable of opposing a highest level of external torque. In addition, designing the grasp such that the net SAS region encloses the specified error insures that the grasp is robust for the entire manipulation task. The

general relationships for cylinder proximity and cylinder bias were used to demonstrate a method for designing a robust grasp for high torque applications.

The results also determine the effects of contact configuration on the net SAS region. Two different contact configurations, semi-symmetric and symmetric, were compared. It was determined that for semi-symmetric contact locations, a finger-bias grasp maximizes the net SAS region. However, if symmetric contacts are used then the maximum net SAS region occurs with a thumb bias grasp. The comparison was made using equal external moment and grasp force magnitudes, along with similar rotation ranges. The maximum net SAS region for the semi-symmetric contact grasp is larger than the corresponding region for the symmetric contact grasp; although the proportional area about the cylinder center point is slightly smaller than the same area type using symmetric contacts.

The evolution of the SAS region was also shown to be dependent on the contact configuration. For a finger-bias grasp with semi-symmetric contacts, the SAS region reduces in size as the fingers rotate the cylinder. In general, the size SAS region is at a maximum during the first phase of rotation and decreases to a minimum size at the final phase. This implies that the maximum torquing capability of this grasp and contact configuration is at the beginning of the cylinder rotational movement.

For a thumb-bias grasp with symmetric contacts, the size of the SAS region reaches a maximum during the mid-point phase of rotation. At the start of rotation, the SAS region is reduced in size by the second joint on Finger 2. At the end of rotation, the SAS region is similarly reduced in size, but this time by the second joint on Finger 0. This type of trend suggests that the net SAS region can be maximized by using a thumb-bias

grasp during the first phase of rotation and then transitioning to a finger-bias grasp as the cylinder progresses towards the final phase of rotation.

An examination of the contact forces at specific points revealed that the cylinder center point is the most efficient location for the grasp focus. In addition, at the cylinder center point the slip potential is the same for each of the three contact points. This implies that all three contact points will approach the point of slip at the same rate. The feature of equal slip potentials can be exploited to ease the computational burden in calculating the total contact force for two of the three contact locations. All of these statements are true regardless of contact configuration.

VI. Conclusions

The study conclusions are partially restricted since they pertain to a specific hand model, and a limited number of grasp and contact configurations. However, the hand model employed is based on one of the few existing robotic hands actively utilized in robotic research. In addition, the types of grasp and contact configurations examined are common to those used for typical task applications. Therefore, the results and techniques presented provide useful information and general relationships for use in grasp planning. Given a specific task, the constraint mapping procedure can be used to determine single grasp focus location which satisfies all grasp criteria.

Constraint maps were used to determine how the safe and stable region evolves as the fingers rotate the cylinder about its transverse axis, while opposing an external torque. The safe and stable region (SAS) represents an area of all possible grasp force focus locations which satisfy grasp stability and joint torque limit criteria at a specific rotation increment. The intersection of all SAS regions at each rotation increment results in a net SAS region in which all points satisfy the criteria over the entire rotation range.

Examining retracted, intermediate, and extended three-finger precision grasps determined the relationship between cylinder proximity and the evolution of the SAS region over the cylinder rotation range. The graphical analysis revealed that the net SAS region is smallest in size for an extended grasp, and largest in size when the grasp is in a retracted configuration. This implies that a retracted grasp is the "strongest" single grasp type for applying torque as the cylinder is rotated. Presented the option, the best way to

improve the torquing capability of a given grasp is position the cylinder as close as possible to the hand. This particular relationship is independent of hand design.

Minor improvements in the size of the net SAS region can be obtained by biasing the cylinder towards the thumb, opposing fingers, or leaving it in a neutral-bias to position. Which type of bias position to use is dependent on the type of contact configuration. For the study hand model, the results demonstrated that a finger-bias position will maximize the net SAS region if the contact locations are semi-symmetric. For symmetric contact locations, a thumb-bias cylinder position will maximize the net SAS region.

The analysis consistently demonstrated that, regardless of grasp or contact configuration, the second joint on the thumb or "Finger 0" was the most sensitive to the commanded contact force. At high c_{map} values, the joint exceeds its' torque limit and reduces the size of the net SAS region. This characteristic is unique to the hand model dimensions and joint torque limits employed. Different model or limit parameters will reveal different results. If one was to redesign the hand based on this study, the results imply that the last two links on the thumb should be reduced in length or the maximum tendon tension for joint two should be increased.

Choosing between symmetric or semi-symmetric contact locations is dependent on the specific task application and where the desired focus location resides. If the primary task objective is to maximize the cylinder rotation range, clearly semi-symmetric contacts are preferred. This assumes that the rotation range is limited by not allowing the contact point to rotate onto the top or "fingernail" portion of the finger-tip. It was also observed that semi-symmetric contacts also possess a unique quality: the SAS region is largest in

size during the beginning phase of rotation. This attribute can be exploited for task applications which require high torquing capability at the start of rotation, such as loosening an oil filter. Once the filter breaks free, the contact layout allows for large rotation ranges for rapidly removing the filter.

Symmetric contact configurations are useful for tasks in which there may be significant external disturbances. The symmetric layout of the contacts allow for equal resistance to disturbances in both directions of the grasp plane. This configuration is most applicable to mating tasks such as attaching an oil filter onto a threaded post. The evolution of the SAS region for symmetric contacts also suggests that a larger net SAS region can be obtained by changing the cylinder-bias during the rotational movement. At the beginning of rotation, a thumb-bias grasp will maximize the SAS region; at the end of rotation, a finger-bias grasp will maximize the SAS region. The results also demonstrated that symmetric contacts are preferred if the grasp focus is to be located at the cylinder center.

The analysis revealed that the cylinder center point is the most efficient location for the grasp focus. At this point the contact forces are used purely to do useful work by holding the cylinder and opposing the external moment. With a high grasp efficiency, the fraction of contact force available for opposing external moments and disturbances is at a maximum. In addition, if the focus is located at the center point, all three contact points will approach the point of slip at the same rate. This characteristic can be exploited to ease the computational burden in calculating the total contact force for two of the three contact locations. Each of these attributes are independent of contact configuration.

For an ideal grip, the net SAS region is equal in size and shape to that for the error region. With this condition, the two regions can be centered directly over the center of the

cylinder to achieve the maximum combination of grasp torquing capability and robustness. The results demonstrated that the ideal grip cannot be achieved with the hand model employed. However, using the constraint mapping procedure and the general relationships presented, an acceptable grasp configuration can always be achieved. The general relationships between the simulated cylinder threading task and the grasp parameters are listed in Table 6-1.

The relationships in Table 6-1 can be used to design a robust grasp with high torquing capability. The retracted grasp configuration is the best grasp for positioning the cylinder relative to the hand. This provides the greatest gain towards increasing the size of the net SAS region. The contact configuration can be matched to the task application, and the correct cylinder-biasing can be derived to maximize the size of the net SAS region. Designing a robust grasp for high torque applications is accomplished by maximizing the ratio of the external moment to the grasp force magnitude and cylinder radius ($M_{Bz}/m_g r_c$). The "target" size of the net region corresponds to the amount of focus positioning error inherent in the actual hand controller. The error region is centered over the cylinder center point to maximize grasp efficiency and take advantage of the predictable contact slip characteristics unique to this point. The constraint mapping procedure can be used to methodically reduce the net SAS region and encompass the error region. The resulting grasp is robust and stable throughout the manipulation task.

The study objective was to develop a planning procedure for grasping and manipulating a cylinder using a three-finger precision grasp. The objective was successfully accomplished and demonstrated using a model of the Utah/MIT Dexterous Hand. The analysis simulated the task of rotating a cylinder about a threaded post while opposing an external moment. The combined effects of applied torque, contact location,

Table 6-1. Threading Task Characteristics VS Grasp Parameters

CHAR. PARAM.	Torque Capability	Rotation Range	Robustness
Cylinder Bias Thumb Bias - Neutral Bias - Finger Bias	Use to Maximize Dependent on: - Hand Design - Contact Location	-----	Use to Maximize Dependent on: - Hand Design - Contact Location
Cylinder Proximity - Retracted - Intermediate Extended	Retracted Strongest Extended Weakest	-----	Use Retracted Grasp
Focus Location	Optimum Point at Object Center	Not Effected if Located In Net SAS Region	Opt. Point at Center of Net SAS Region
Contact Location	Use Symmetric for Mating Tasks Use Semi-Symmetric to Loosen/Tighten or for Quick Removal Tasks	Use Semi-Symmetric for Maximum Rotation Range	Use Symmetric to Preserve Area About Object Center Point

and object position and orientation on grasp stability and robustness were analyzed using the method of grasp force focus positioning. The procedure from this study can be used to determine a single grip which guarantees grasp stability, robustness, and high torquing capability for the task. The procedure can also be used to analyze the resulting effects of hand design changes or new hand designs.

VII. Recommendations

7.1 Verification of Procedure

The results of this study would be put to greatest use by verifying the relationships and procedure presented. This could be accomplished using the Utah/MIT Dexterous Hand, which is readily available in the AFIT Robotics Lab. The most difficult aspect of the verification would be determining where the actual robot hand is positioning the grasp focus. A thorough understanding of the sensor and controller limitations is required.

7.2 Examining Additional Model Parameters

There are several more parameters which can be examined in a future study. An interesting and useful parameter to include is the modelling of rolling contacts. For large cylinder rotation angles, rolling contacts can have a significant effect on the size and shape of the safe and stable region. Even an approximate model would be useful since it is a closer representation of the actual hand than a point contact model assumption. There are several other items which can be examined. One is the effects of non-symmetric contact locations on the SAS region. The other is the effects of biasing the cylinder in a direction which is parallel a line joining the base joints of Fingers 1 and 2 (orthogonal direction to the bias studied). Different hand dimensions can also be examined. One idea is to design a several hands for specific cylinder sizes.

7.3 Customizing Joint Torque Limits

The joint torque limitations were constant in this study and assumed zero co-contraction of the tendons. With a zero co-contraction setting, the fingers of the hand have no stiffness. For real-time implementation tasks, finger stiffness is required. Therefore, a useful update to the grasp planning procedure would be the inclusion of stiffness criteria.

For the limits used in this study, joint two of the fingers was typically the weakest joint. This implies that the joint limits for other joints are set too high. The constraint mapping technique can be used to adjust the joint torque limits for each individual joint. One method is to overlay a series of joint torque limit lines for each joint onto a map of the stable region and desired error region. Each joint torque limit line is based on a specific joint torque limit. The lines closest to the error region correspond to the desired joint torque limit values. The reduced joint torque margin for each joint can be redistributed to satisfy a specified stiffness criteria.

The effects of adjusting the joint torque limits on the size and shape of the net SAS region can also be examined. The primary goal would be to make the size and shape of the net SAS region identical to that for the error region. In addition, the geometric center of the two regions should be collocated over the cylinder center point. This would result in a grasp which maximizes the combination of grasp efficiency (and thus, torquing capability) and robustness. The constraint mapping method described in the previous paragraph can also be used for this case study.

Appendix A. *Constraint Map Set #2*

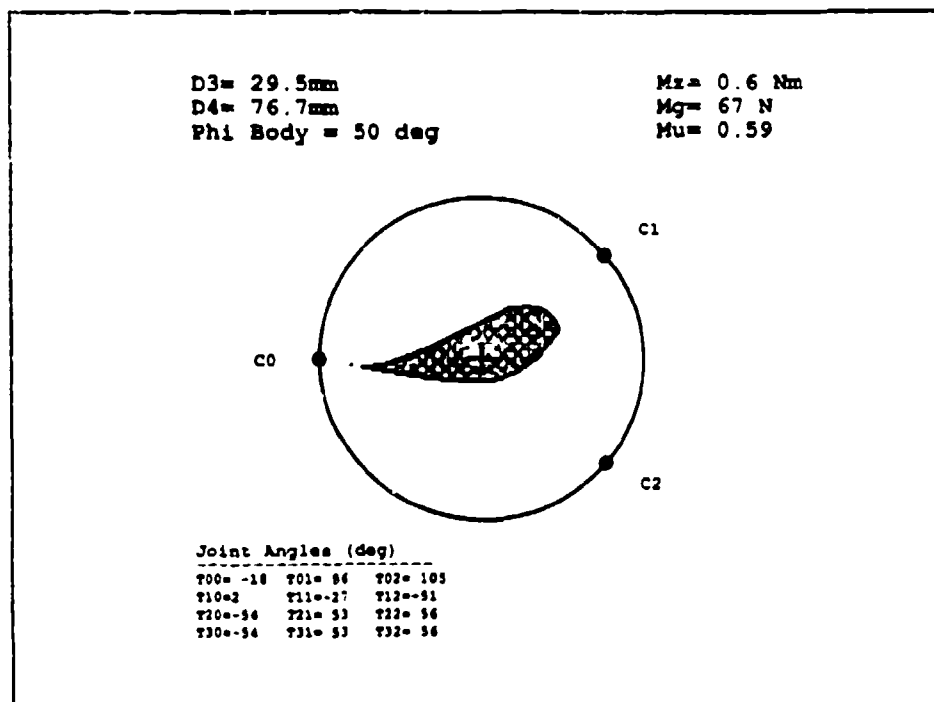


Figure A-1. Retracted Neutral-Bias Grasp, $\phi_b = 50^\circ$

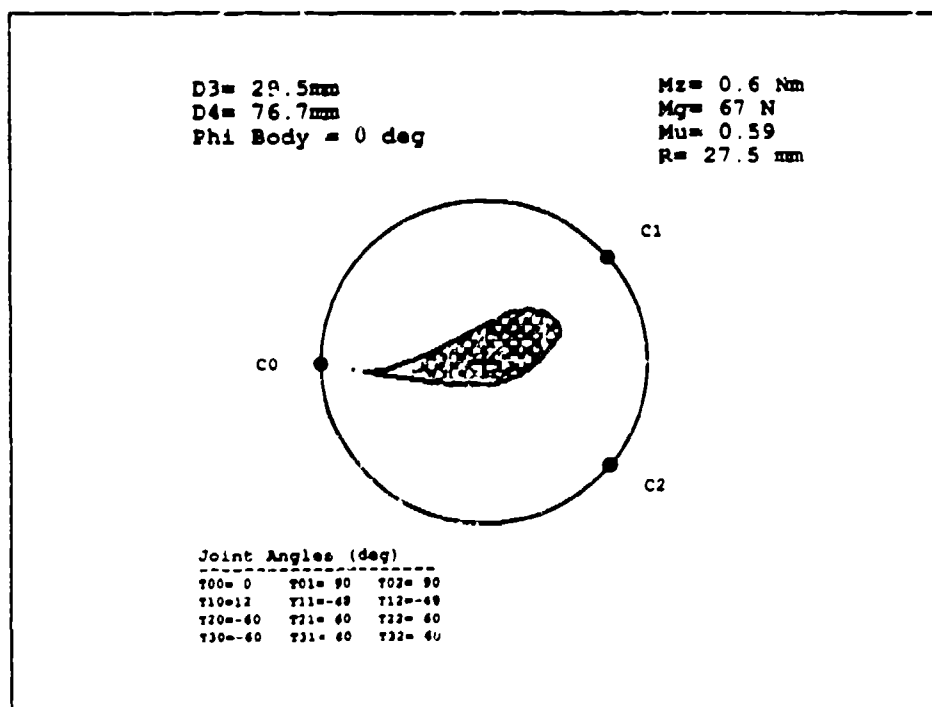


Figure A-2. Retracted Neutral-Bias Grasp, $\phi_b = 0^\circ$

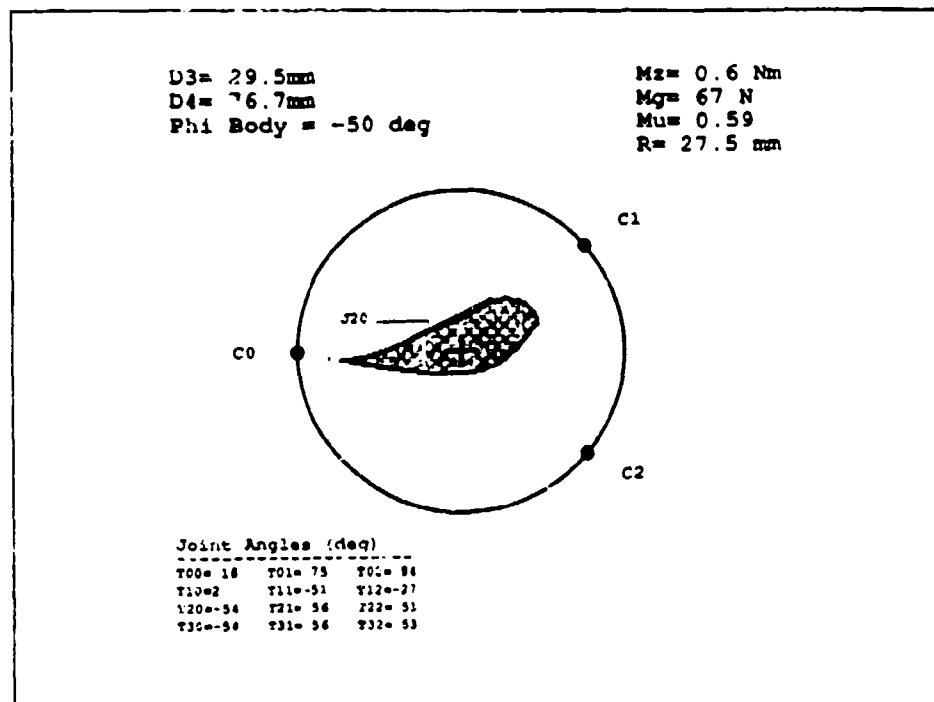


Figure A-3. Retracted Neutral-Bias Grasp, $\phi_b = -50^\circ$

Appendix B. *Constraint Map Set #3*

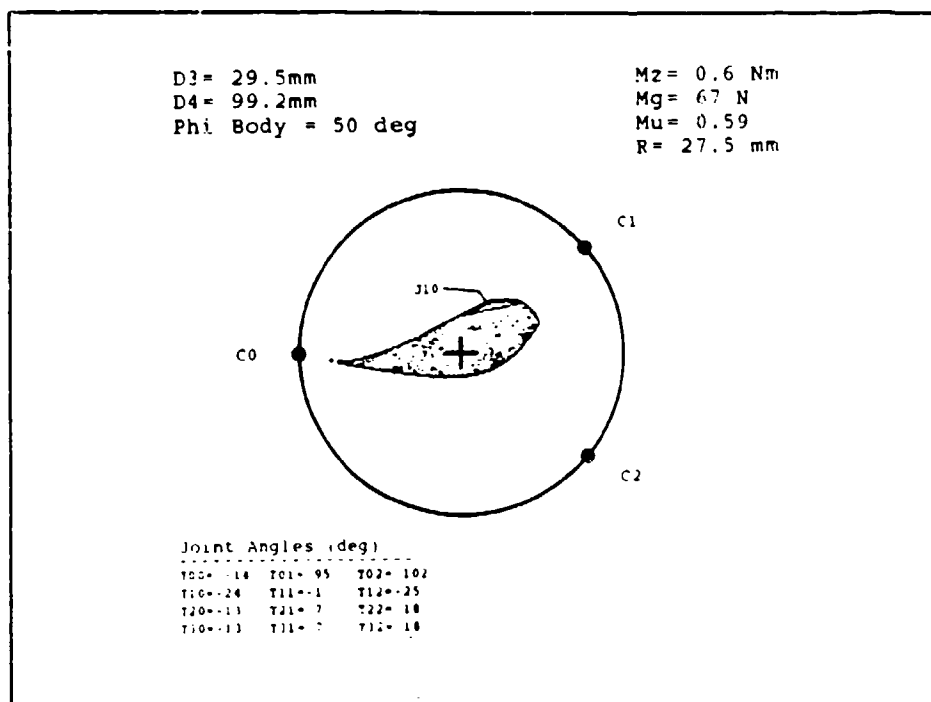


Figure B-1. Extended Neutral-Bias Grasp, $\phi_b = 50^\circ$

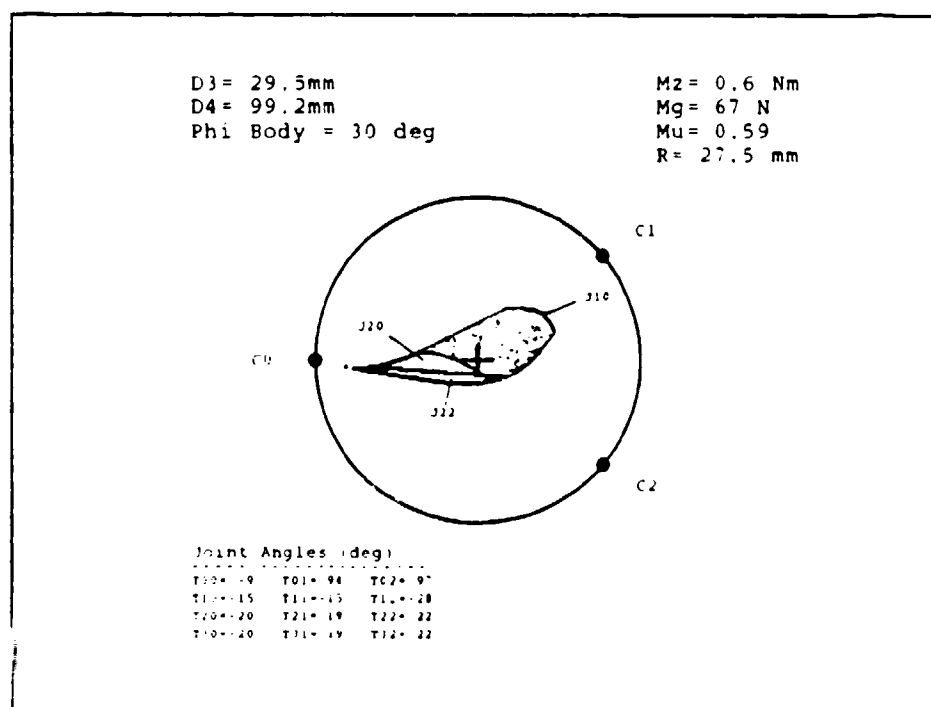


Figure B-2. Extended Neutral-Bias Grasp, $\phi_b = 30^\circ$

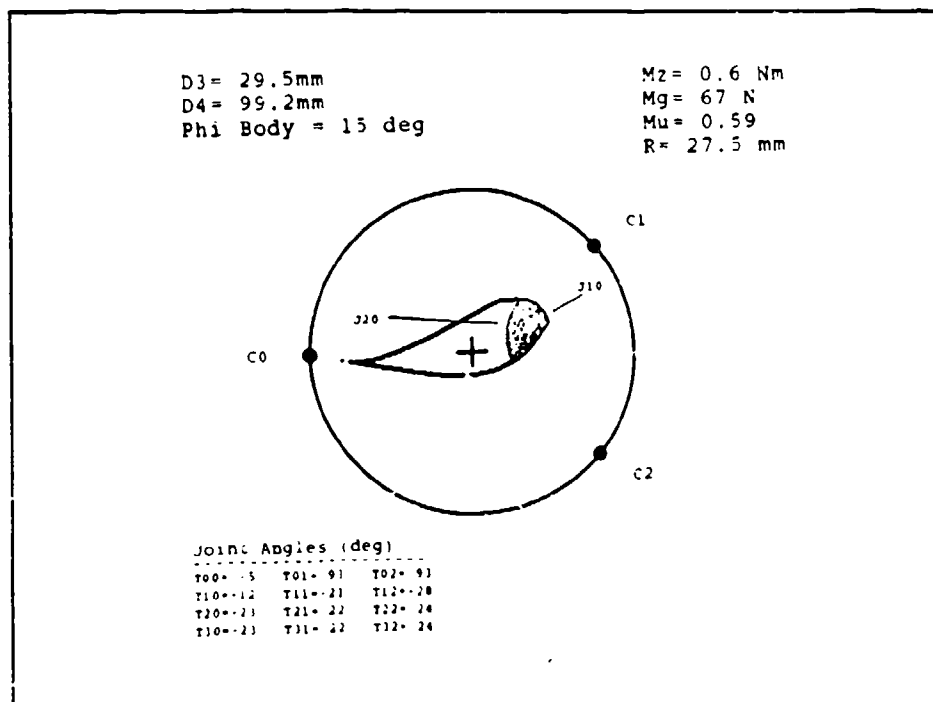


Figure B-3. Extended Neutral-Bias Grasp, $\phi_b = 15^\circ$

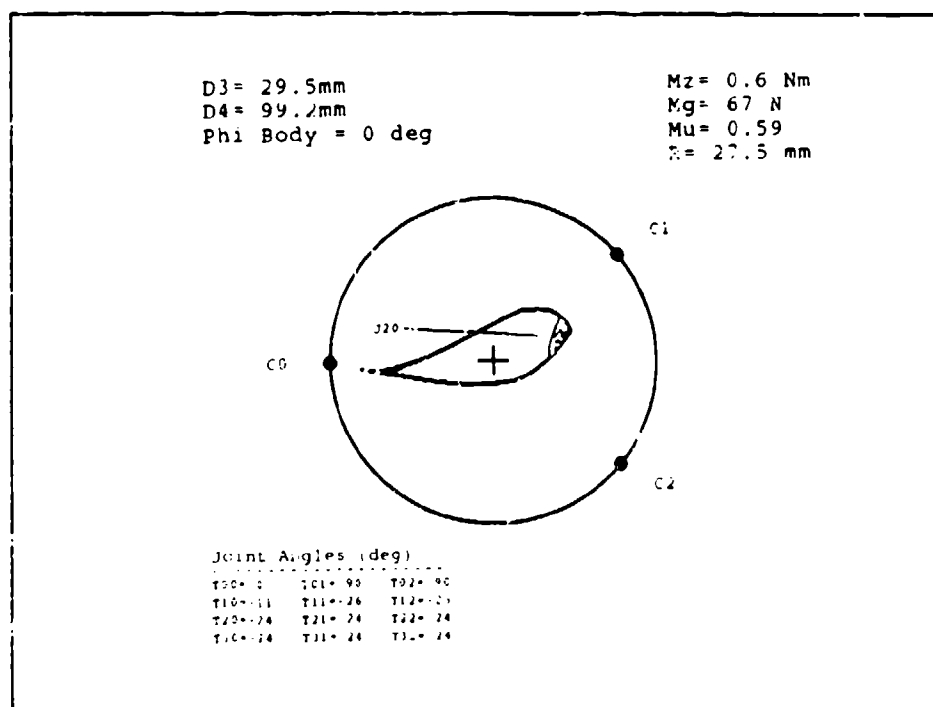


Figure B-4. Extended Neutral-Bias Grasp, $\phi_b = 0^\circ$

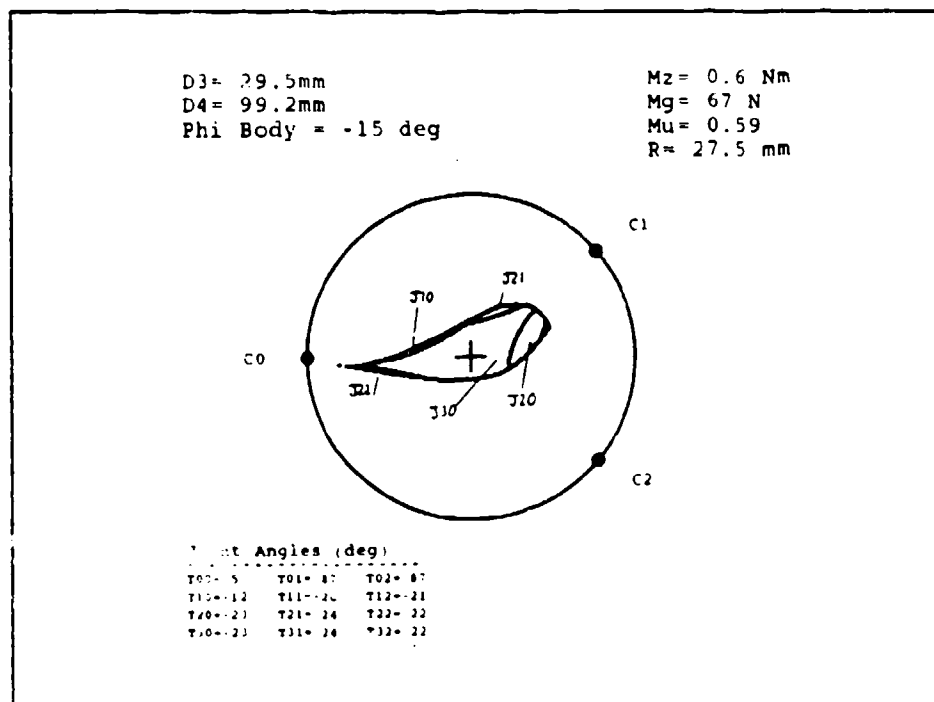


Figure B-5. Extended Neutral-Bias Grasp, $\phi_b = -15^\circ$

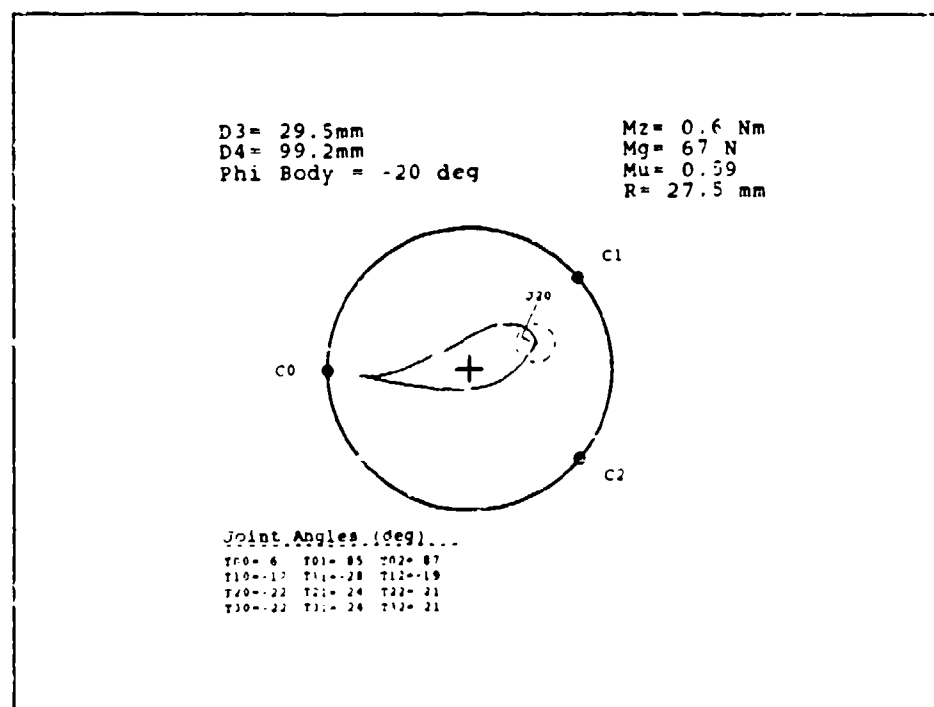


Figure B-6. Extended Neutral-Bias Grasp, $\phi_b = -20^\circ$

Appendix C. *Constraint Map Set #4*

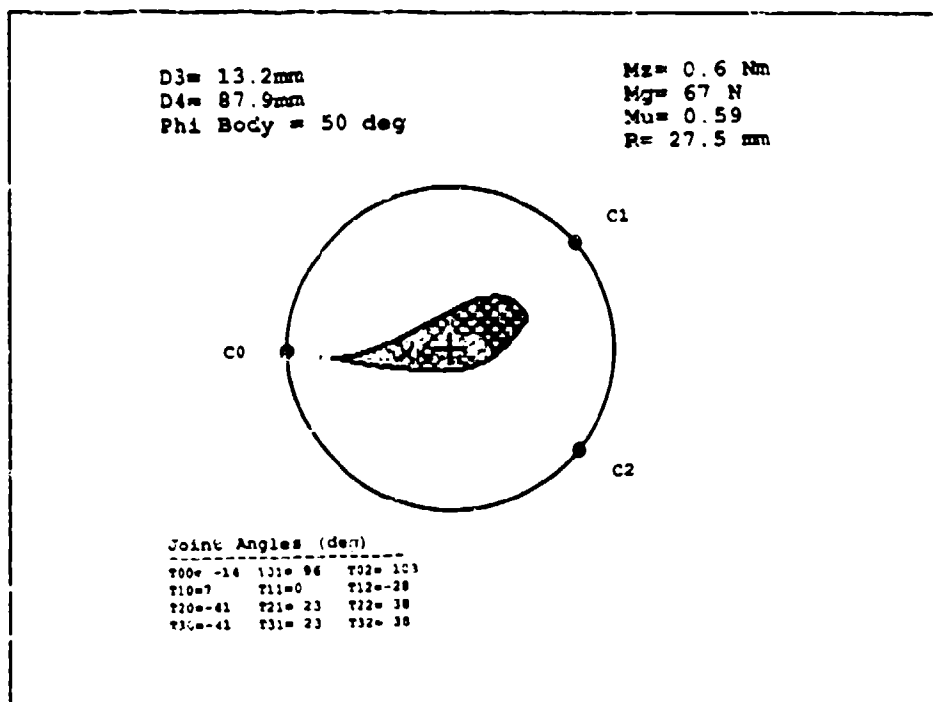


Figure C-1. Intermediate Thumb-Bias Grasp, $\phi_b = 50^\circ$

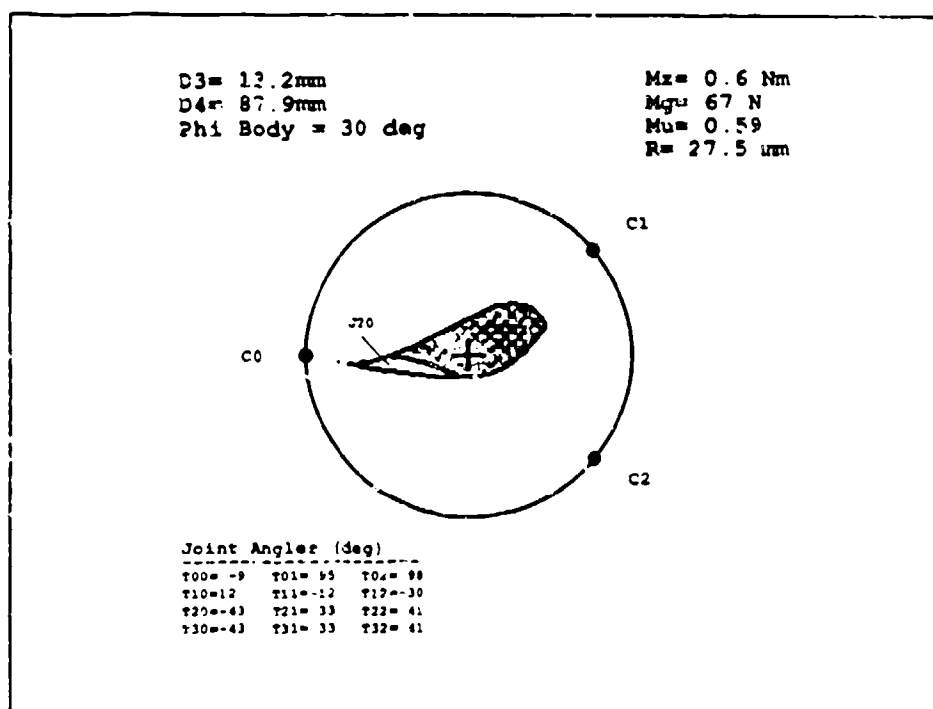


Figure C-2. Intermediate Thumb-Bias Grasp, $\phi_b = 30^\circ$

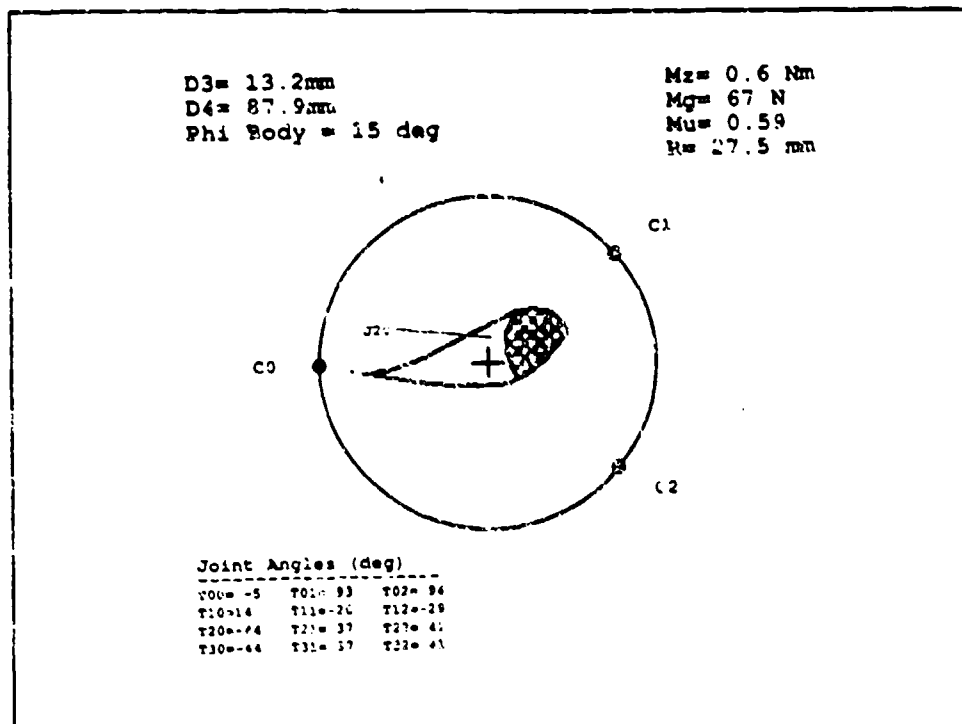


Figure C-3. Intermediate Thumb-Bias Grasp, $\phi_b = 15^\circ$

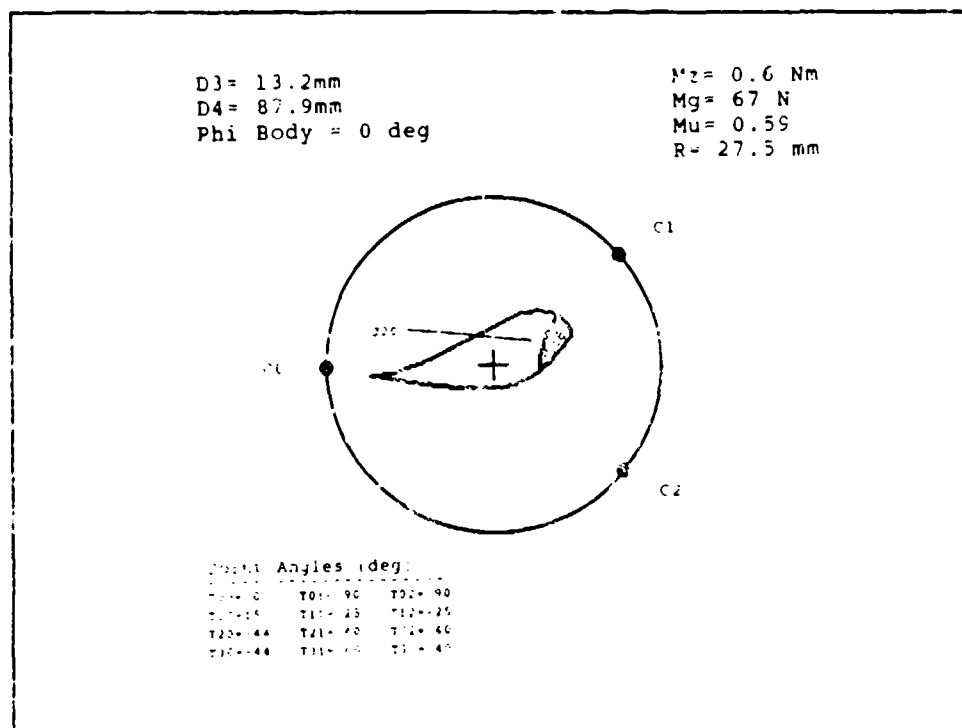


Figure C-4. Intermediate Thumb-Bias Grasp, $\phi_b = 0^\circ$

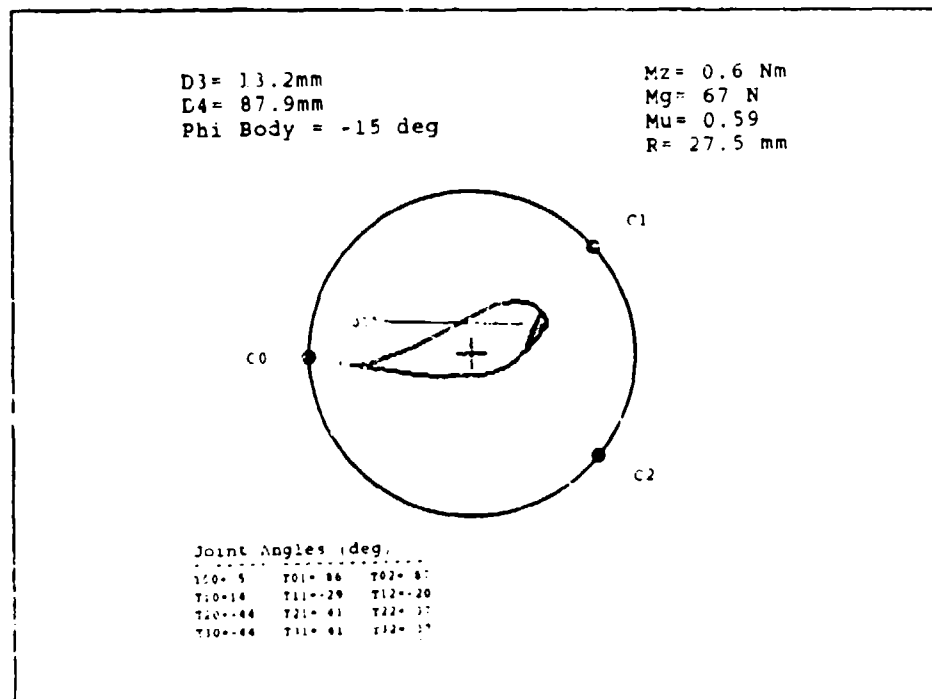


Figure C-5. Intermediate Thumb-Bias Grasp, $\phi_b = -15^\circ$

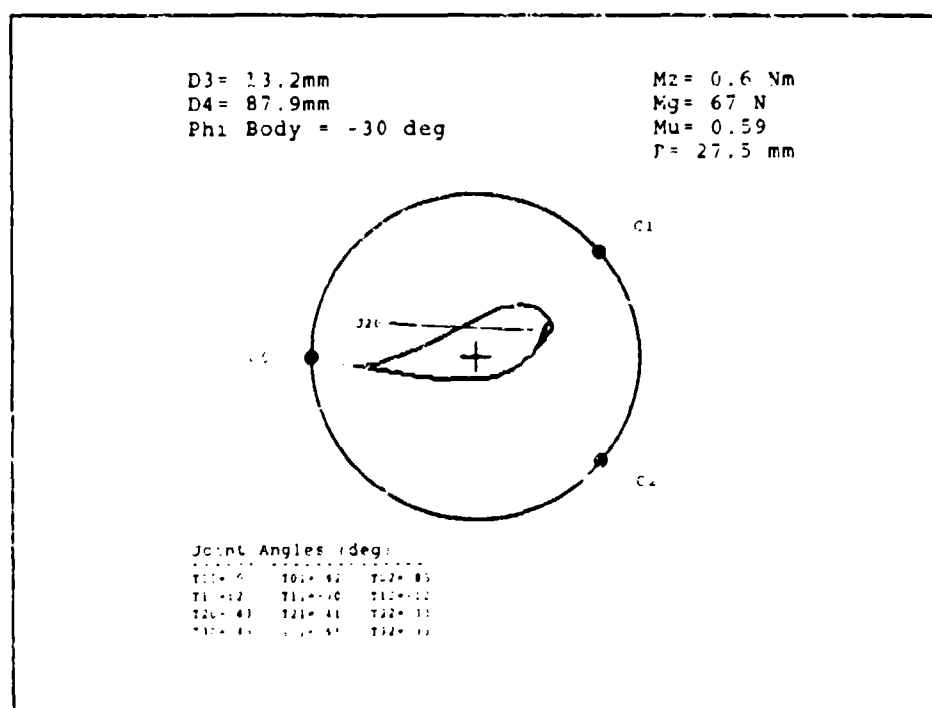


Figure C-6. Intermediate Thumb-Bias Grasp, $\phi_b = -30^\circ$

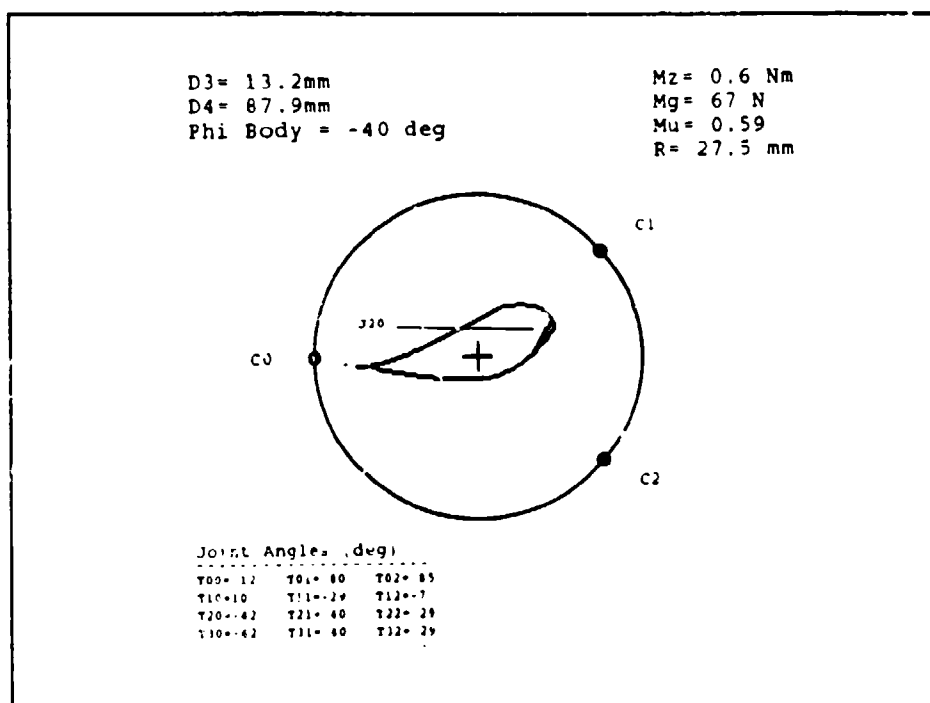


Figure C-7. Intermediate Thumb-Bias Grasp, $\phi_h = -40^\circ$

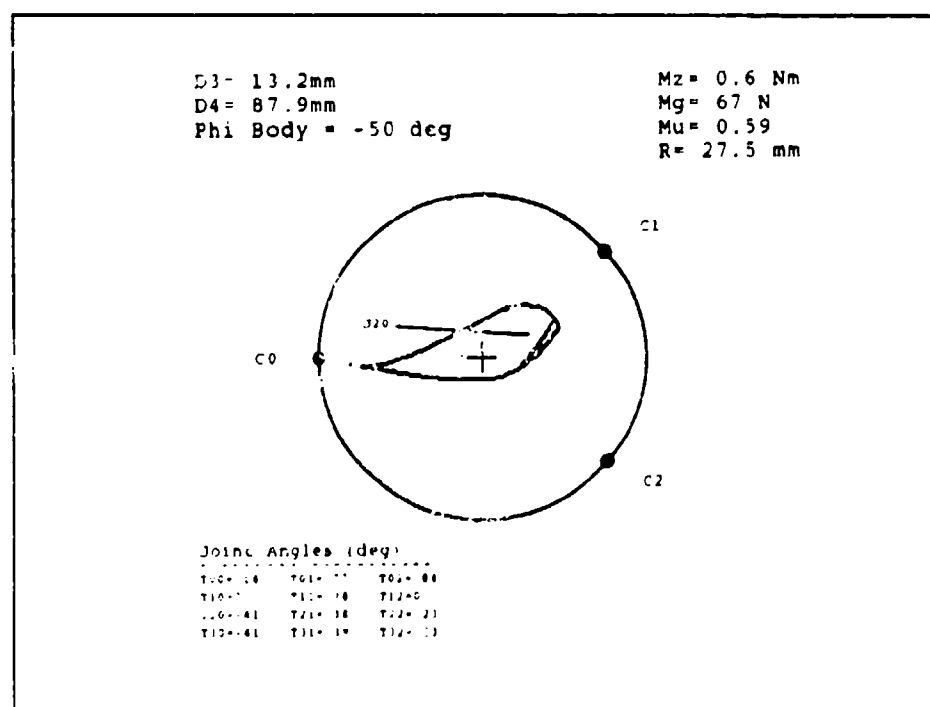


Figure C-8. Intermediate Thumb-Bias Grasp, $\phi_b = -50^\circ$

Appendix D. *Constraint Map Set #5*

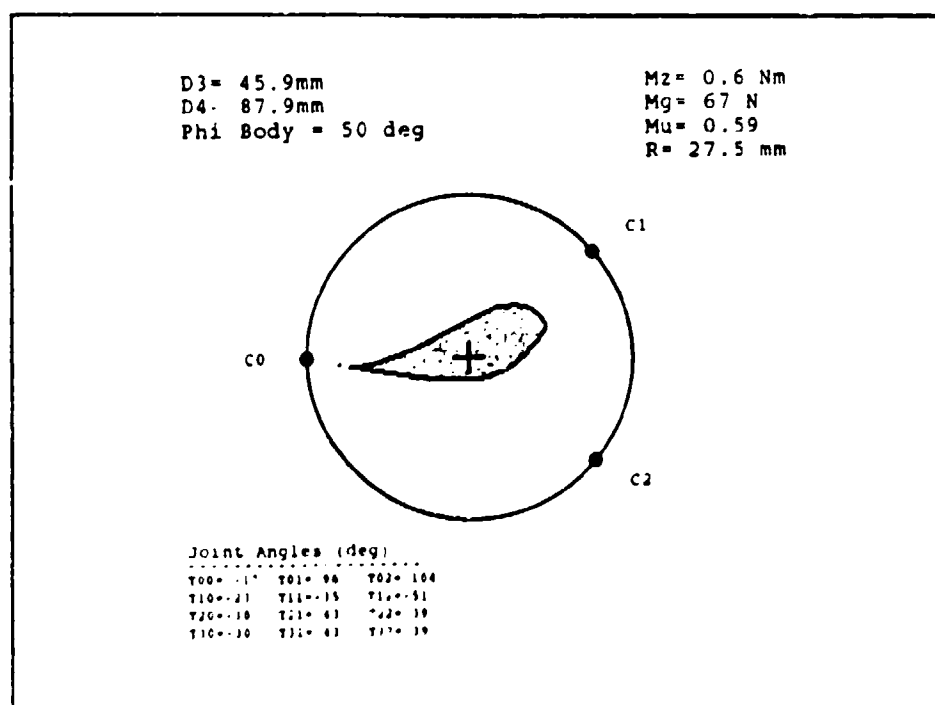


Figure D-1. Intermediate Finger-Bias Grasp, $\phi_b = 50^\circ$

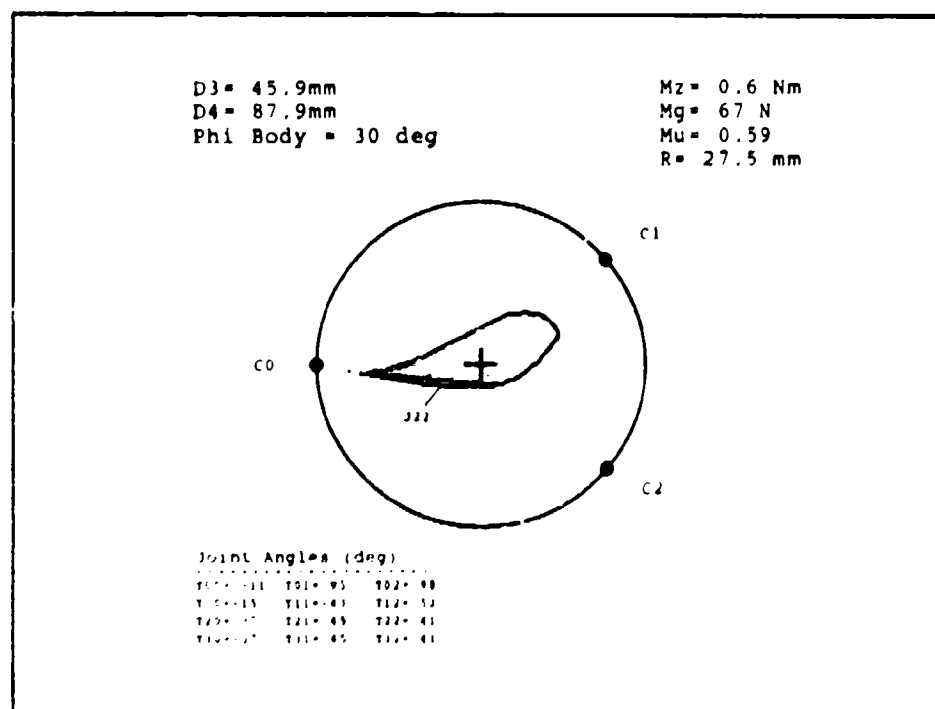


Figure D-2. Intermediate Finger-Bias Grasp, $\phi_b = 30^\circ$

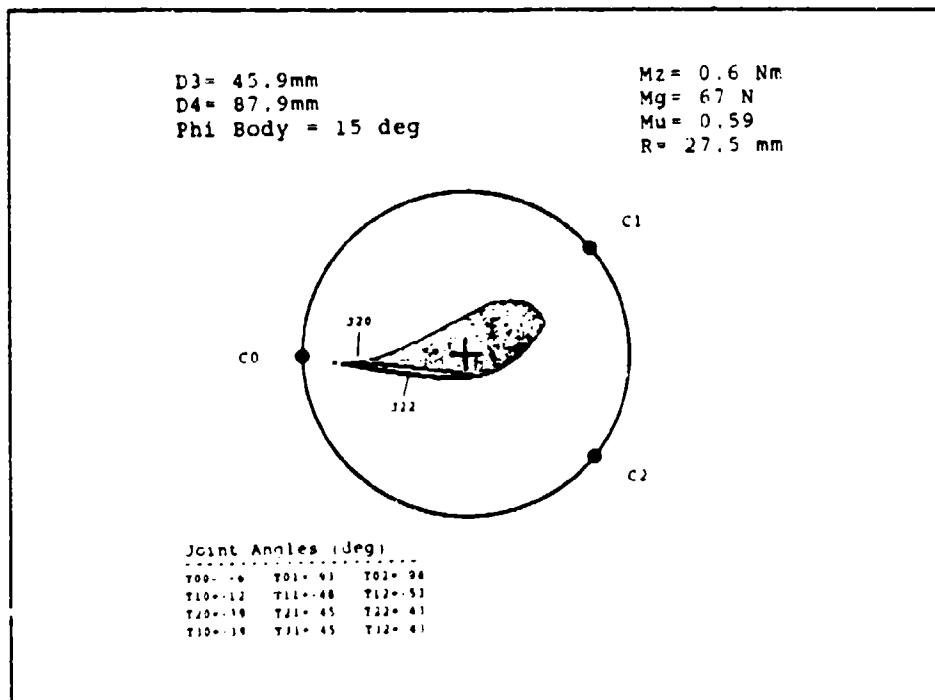


Figure D-3. Intermediate Finger-Bias Grasp, $\phi_b = 15^\circ$

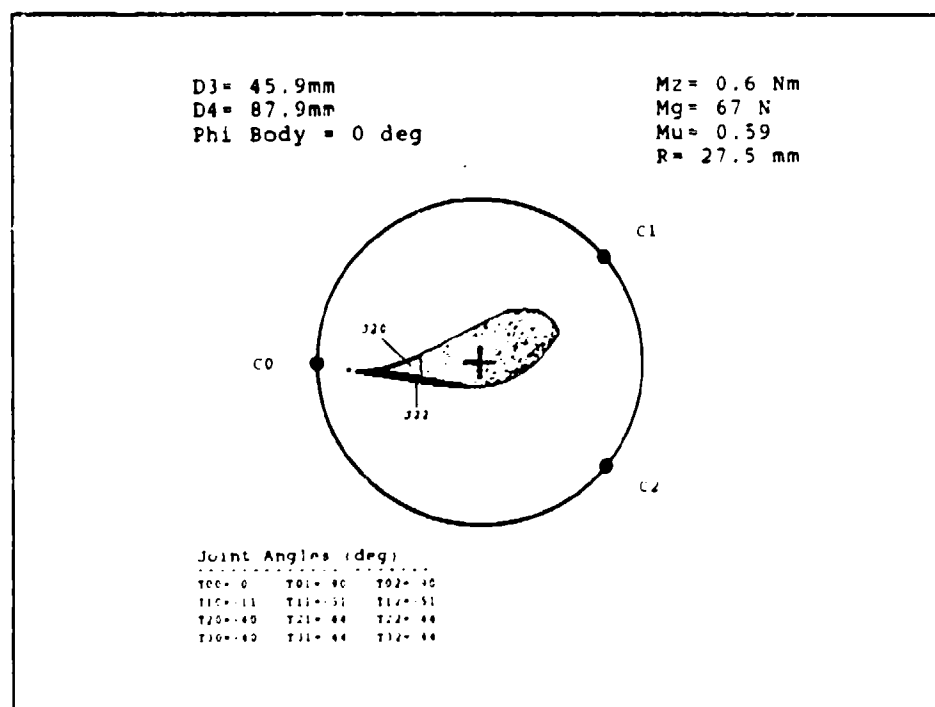


Figure D-4. Intermediate Finger-Bias Grasp, $\phi_b = 0^\circ$

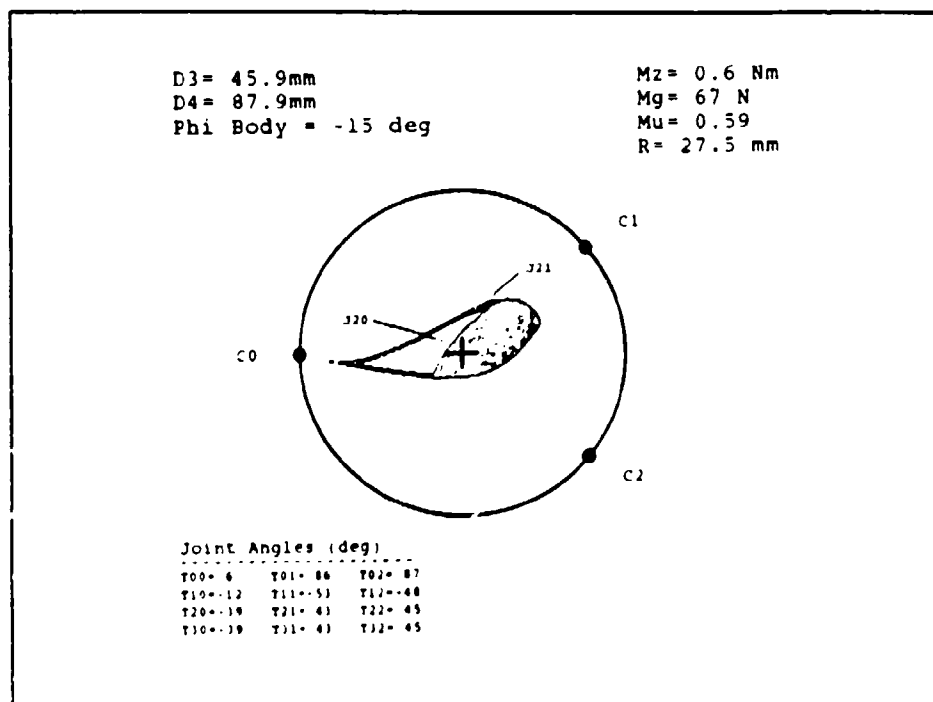


Figure D-5. Intermediate Finger-Bias Grasp, $\phi_b = -15^\circ$

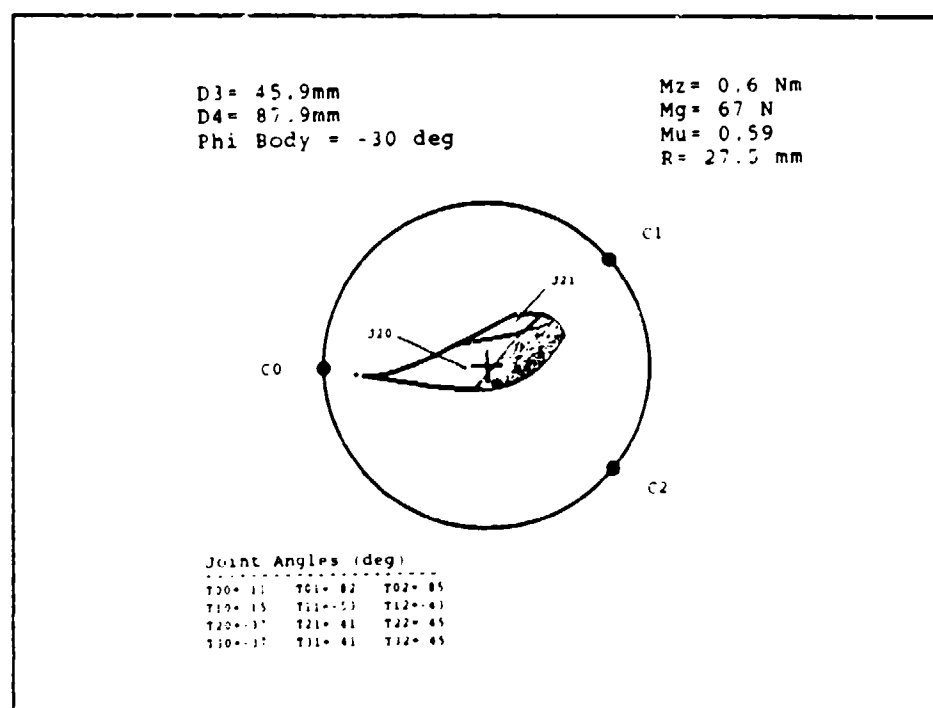


Figure D-6. Intermediate Finger-Bias Grasp, $\phi_b = -30^\circ$

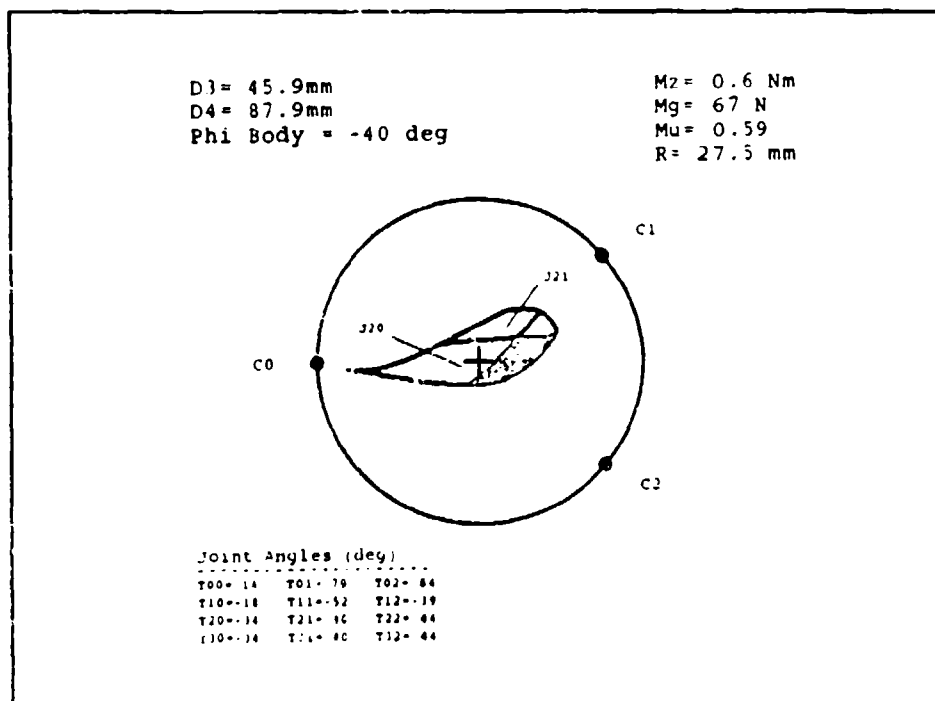


Figure D-7. Intermediate Finger-Bias Grasp, $\phi_b = -40^\circ$

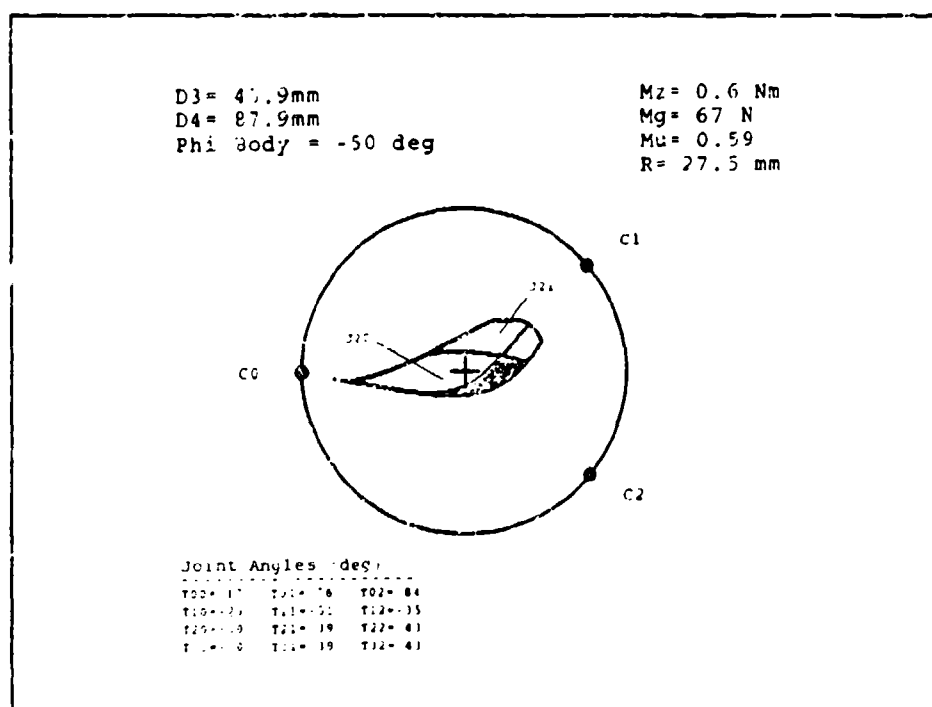


Figure D-8. Intermediate Finger-Bias Grasp, $\phi_b = -50^\circ$

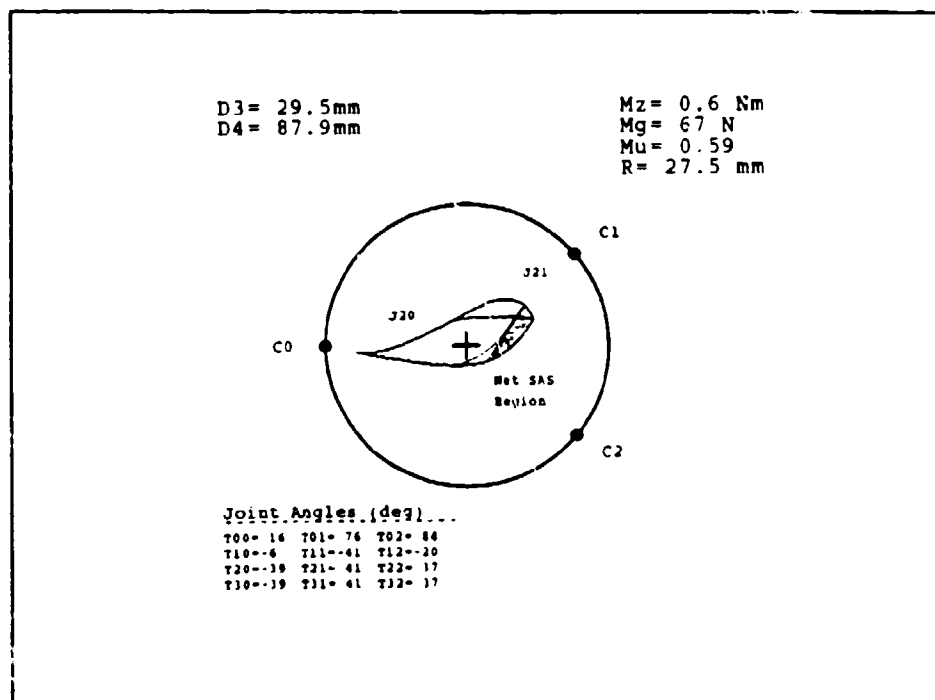


Figure D-9. Net SAS Region for Intermediate Finger-Bias Grasp

Appendix E. *Constraint Map Set #6*

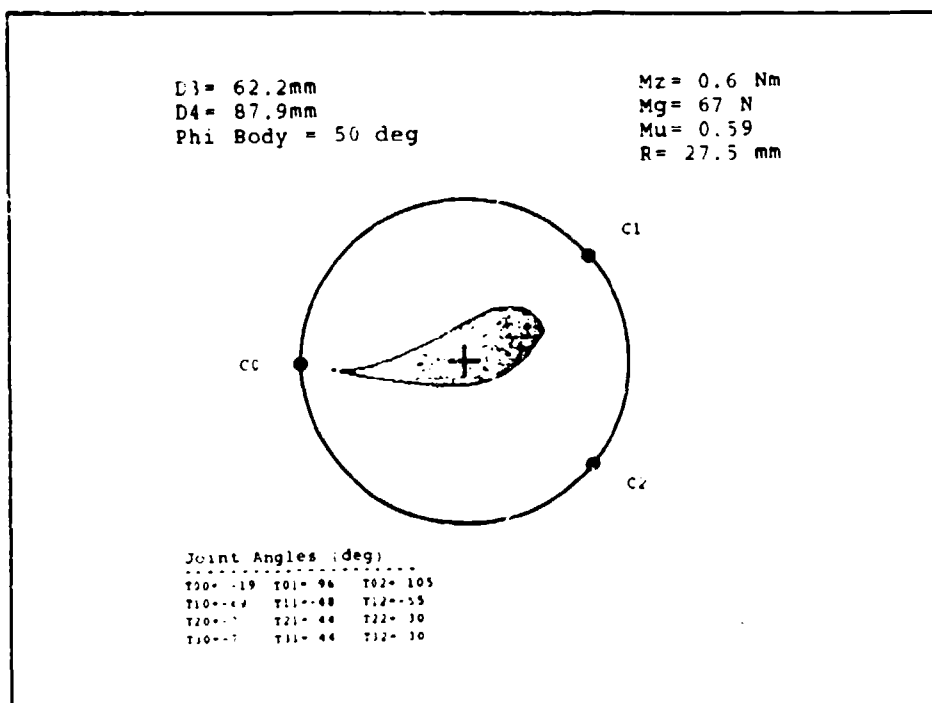


Figure E-1. Intermediate Finger-Bias Grasp (Max. Bias), $\phi_b = 50^\circ$

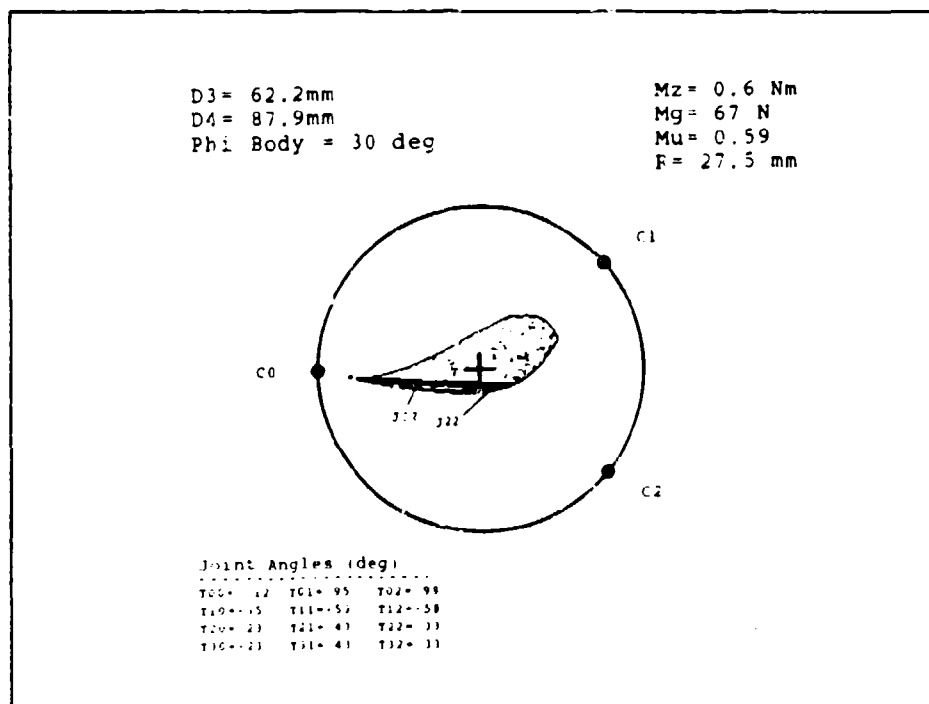


Figure E-2. Intermediate Finger-Bias Grasp (Max. Bias), $\phi_b = 30^\circ$

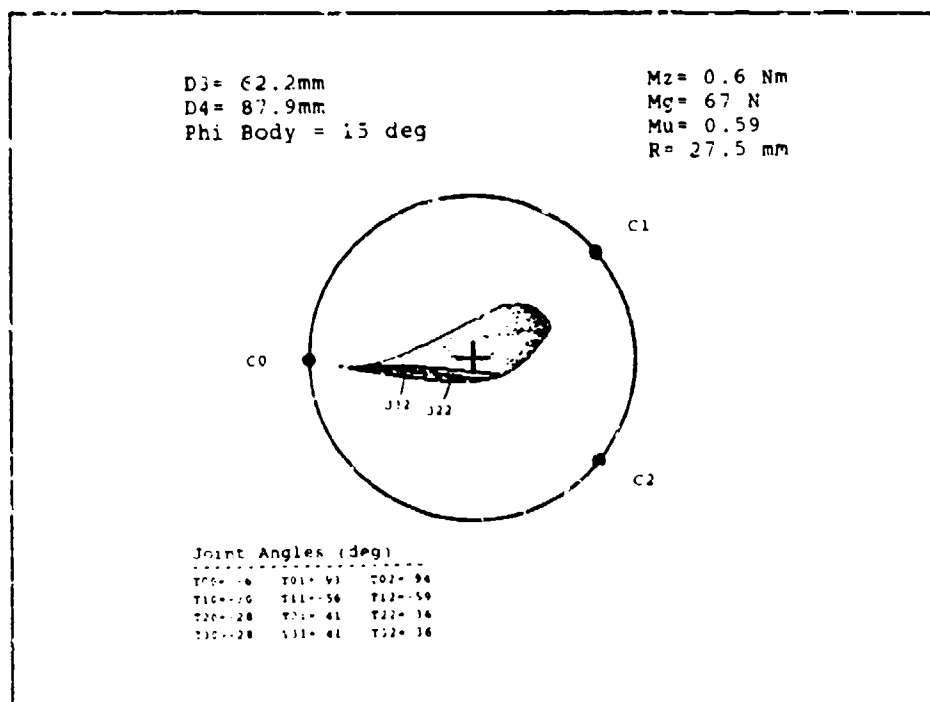


Figure E-3. Intermediate Finger-Bias Grasp (Max. Bias), $\phi_b = 15^\circ$

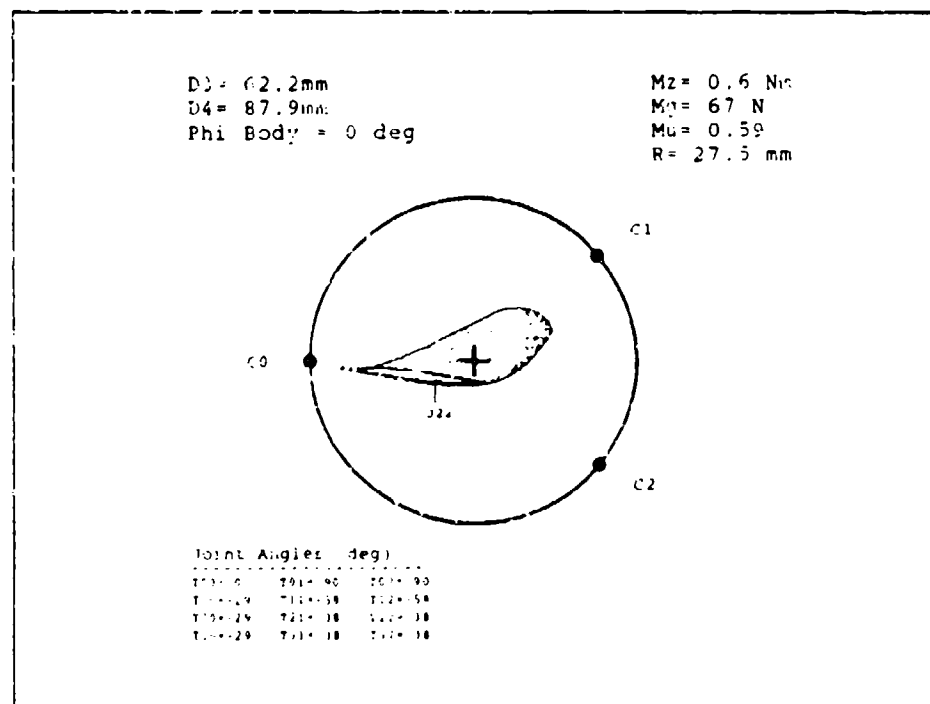


Figure E-4. Intermediate Finger-Bias Grasp (Max. Bias), $\phi_b = 0^\circ$

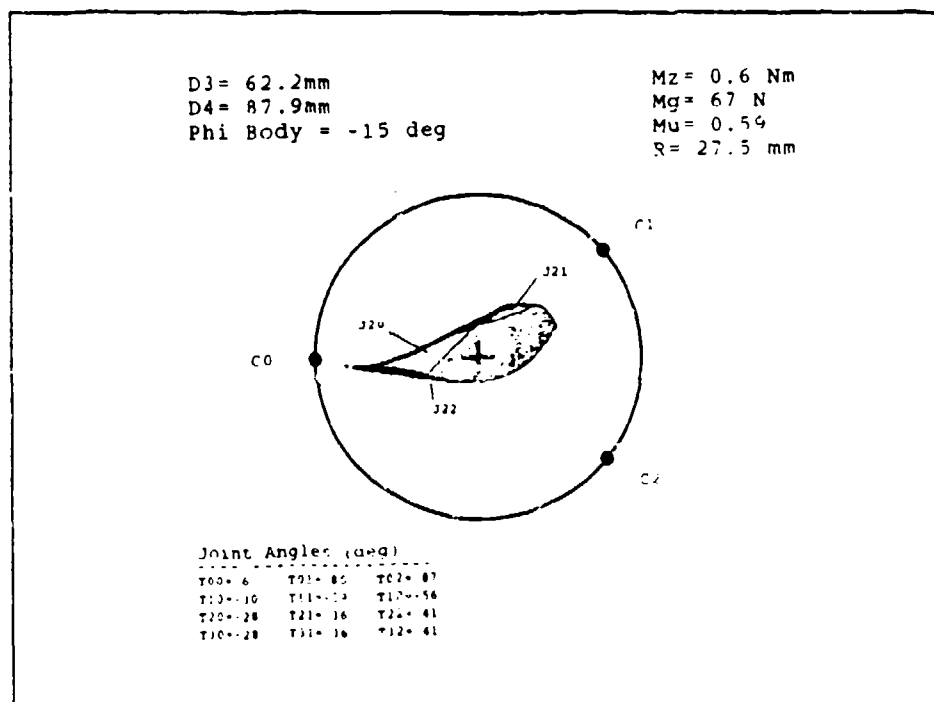


Figure E-5. Intermediate Finger-Bias Grasp (Max. Bias), $\phi_b = -15^\circ$

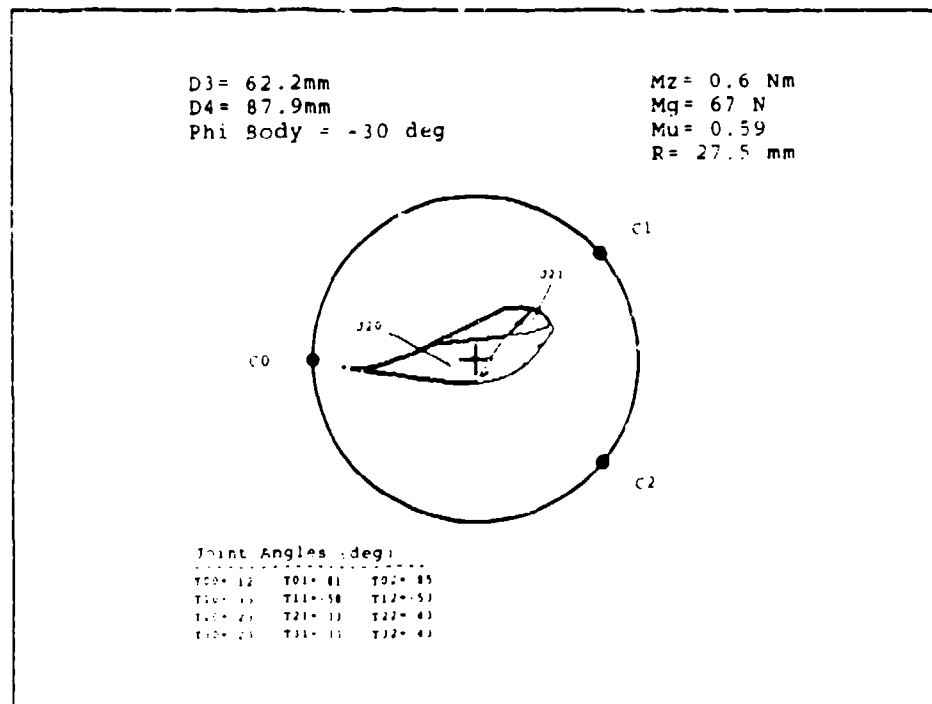


Figure E-6. Intermediate Finger-Bias Grasp (Max. Bias), $\phi_b = -30^\circ$

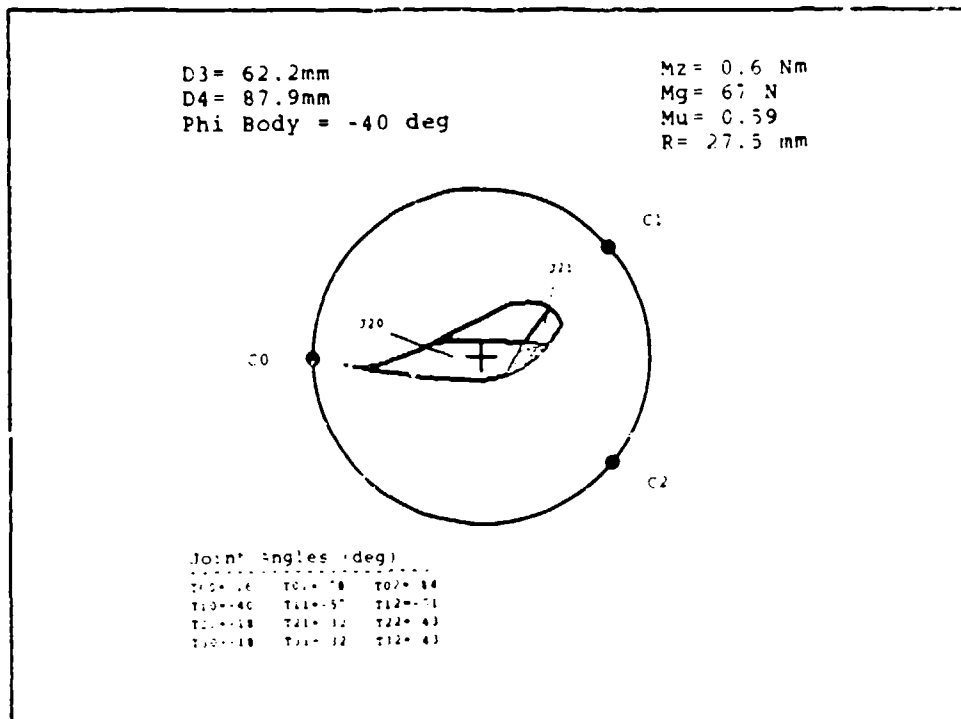


Figure E-7. Intermediate Finger-Bias Grasp (Max. Bias), $\phi_b = -40^\circ$

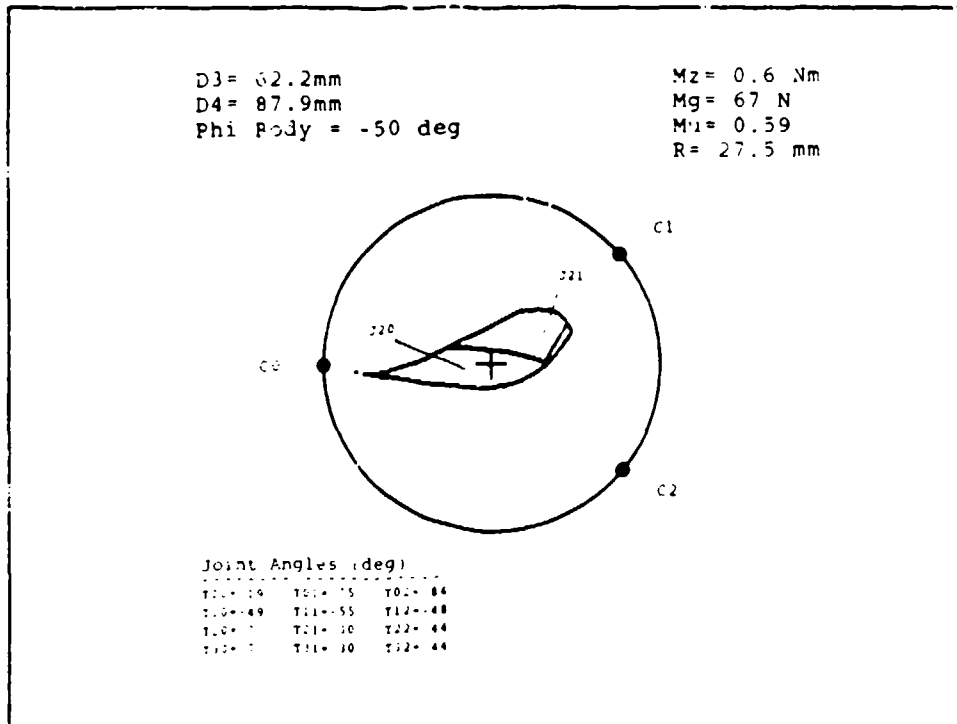


Figure E-8. Intermediate Finger-Bias Grasp (Max. Bias), $\phi_b = -50^\circ$

Appendix F. *Inverse Kinematics Computer Program*

Inverse Kinematics Fortran Program

Character Yes*1,SYes*1,Ans*1

Integer K,N

Real Alpha,D3,D4,L1,L2,L3,Lc,Lp,RotInc,Psi0,Psi1,Psi2,
PBPsi0,PBPsi1,PBPsi2,PhiB

Double Precision X0C1,Y0C1,Z0C1,X1C1,Y1C1,Z1C1,X2C1,Y2C1,Z2C1,
X0C3,Y0C3,Z0C3,X1C3,Y1C3,Z1C3,X2C3,Y2C3,Z2C3,
X0C2,Y0C2,Z0C2,X1C2,Y1C2,Z1C2,X2C2,Y2C2,Z2C2,
T00,T10,T20,T01,T11,T21,T02,T12,T22,Deg,BB0,
BB1,BB2

Type *,'

Type *,'

Type *,'

Type *,'

Type *,'

Type *,'*****'

Type *,'*****'

Type *,'

Type *,' Inverse Kinematics Program

Type *,' for an

Type *,' End Grasp of a Cylinder

Type *,' using the

Type *,' UMDH Point Contact Model

Type *,'

Type *,'*****'

Type *,'*****'

CCCCCCCCCCCCCCCCCCCCCCCC

C

C Establish Constant Values

C

CCCCCCCCCCCCCCCCCCCCCCCC

Rpb = 0.695

R = 1.08122806

L1 = 1.7

L2 = 1.3

L3 = 0.735

Lo = 1.2

```

Lp = 1.05
Rp0 = 0.695
Rp1 = 0.0
Rp2 = 1.39
Deg = 3.141592654/180.0
Pp = 12.0*Deg
Po = 30*Deg
Hp = 0.95
Ho = 0.4
Warn=0.0

```

```

CCCCCCCCCCCCCCCCCCCCCCCCCCCCCCCCCCCCCCCCCCCC
C
C   Use Open Statements to associate filenames
C   with various logical unit numbers
C
CCCCCCCCCCCCCCCCCCCCCCCCCCCCCCCCCCCCCCCCCCCC

```

```

      Open(12,File='Fing0.DAT',Status='Old',
# Access='Sequential', Form='Formatted')

```

```

      Open(13,File='Fing1.DAT',Status='Old',
# Access='Sequential', Form='Formatted')

```

```

      Open(14,File='Fing2.DAT',Status='Old',
# Access='Sequential', Form='Formatted')

```

```

      Open(15,File='D3Curve.DAT',Status='Old',
# Access='Sequential', Form='Formatted')

```

```

      Open(16,File='Hand.dat',Status='Old',
# Access='Sequential', Form='Formatted')

```

```

CCCCCCCCCCCCCCCCCCCCCCCCCCCCCCCCCCCCCCCCCCCC
C
C   Prompt for input variables Psi0, Psi1, and Psi2
C
CCCCCCCCCCCCCCCCCCCCCCCCCCCCCCCCCCCCCCCCCCCC

```

```

1   Type *, ' '
    Type *, ' '
    Type *, 'Input Psi0 (Fing 0), Psi1 (Fing 1), Psi2
#(Fing 2) (Deg);'
    Accept *, Psi0,Psi1,Psi2
    Write(*,3)Psi0,Psi1,Psi2
3   Format(/'Psi0=',F9.4,' Psi1=',F9.4,' Psi2=',F9.4)

```


CCCCCCCCCCCCCCCCCCCCCCCCCCCCCCCCCCCC

C

C Prompt for Body Rotation Increment (deg)

C

CCCCCCCCCCCCCCCCCCCCCCCCCCCCCCCCCCCC

Type *,' '

Type *,' '

Type *,'Input Body Rotation Increment (Pos # deg)'

Accept *, RotInc

Write (*,4) RotInc

4 Format('/RotInc (Deg) = ',F7.4)

CCCCCCCCCCCCCCCCCCCCCCCCCCCCCCCCCCCC

C

C Prompt for input variables Alpha, D3, and D4

C

CCCCCCCCCCCCCCCCCCCCCCCCCCCCCCCCCCCC

Type *,' '

Type *,' '

* Type *,'Input Alpha (Deg), D3 (Pos # inches), D4 (Pos #
* # inches);'

Type *,'Input D3 and D4 (inches)'

* Accept *, Alpha,D3,D4

Accept *,D3,D4

Alpha=-24.07773221758005

Write(*,5)Alpha,D3,D4

5 Format('/Alpha (Deg) = ',F9.4,' D3 = ',F9.4,' D4 = ',F9.4)

DAlpha = Alpha

Alpha = Alpha*Deg

Type *,' '

Type *,' '

Type *,'Input Discrete Body Rotation Angle (Deg) at'

Type *,'which to Output Data to Hand.dat File'

Accept *,DiscPhi

Write(*,7)DiscPhi

7 Format('Discrete Phi Body (Deg) = ',F9.4)

6 Type*,' '

Type *,' '

Type *,'Beginning Program'

Write(*,3)Psi0,Psi1,Psi2

Write(*,4)RotInc

Write(*,8)Alpha,D3,D4

```

Write(12,8)Alpha,D3,D4
Write(13,8)Alpha,D3,D4
Write(14,8)Alpha,D3,D4

8   Format(i'Alpha (Rad) =',F9.4,' D3=',F9.4,' D4=',F9.4///)

    If (RotInc .EQ. 0.0) Then
        K=0
    Else
        K=170.0/RotInc
    EndIf

    N=1
    PhiB = 0.0
    Q=0

CCCCCCCCCCCCCCCCCCCCCCCCCCCCCCCCCCCCCCCC
C
C   Begin Loop to Determine Max Body Rotation Angle,
C   Given a Fixed Value for D3 and D4
C
C   First Pass (N=1) Determines Max Left (CCW)
C   Rotation Angle
C
C   Second Pass (N=-1) Determines Max Right (CW)
C   Rotation Angle
C
CCCCCCCCCCCCCCCCCCCCCCCCCCCCCCCCCCCCCCCC

10  Do 400 i=0,K,N

CCCCCCCCCCCCCCCCCCCCCCCCCCCCCCCCCCCCCCCCCCCCCCCCCCCCCCCCCCCC
C
C   Convert Angles (Psi0,Psi1,Psi2) to Radians and Define Their
C   Respective Sums as:
C
C   PBPsi(j) = PhiB*Deg + Psi(j)*Deg, where j=1,2,3
C
CCCCCCCCCCCCCCCCCCCCCCCCCCCCCCCCCCCCCCCCCCCCCCCCCCCCCCCCCCCC

    PBPsi0 = PhiB*Deg + Psi0*Deg
    PBPsi1 = PhiB*Deg + Psi1*Deg
    PBPsi2 = PhiB*Deg + Psi2*Deg

CCCCCCCCCCCCCCCCCCCCCCCCCCCCCCCCCCCCCCCC
C
C   Calculate contact position w.r.t Palm Frame

```

C (X0Ci,Y0Ci,Z0Ci), where i=1,2,3

C

CCCCCCCCCCCCCCCCCCCCCCCCCCCCCCCCCCCC

$$X0C1 = \cos(\alpha) \cdot (D3 - R \cdot \sin(PB\psi_0)) - D4 \cdot \sin(\alpha)$$

$$Y0C1 = R_{pb} - R \cdot \cos(PB\psi_0)$$

$$Z0C1 = D4 \cdot \cos(\alpha) + \sin(\alpha) \cdot (D3 - R \cdot \sin(PB\psi_0))$$

$$X0C2 = \cos(\alpha) \cdot (D3 - R \cdot \sin(PB\psi_1)) - D4 \cdot \sin(\alpha)$$

$$Y0C2 = R_{pb} - R \cdot \cos(PB\psi_1)$$

$$Z0C2 = D4 \cdot \cos(\alpha) + \sin(\alpha) \cdot (D3 - R \cdot \sin(PB\psi_1))$$

$$X0C3 = \cos(\alpha) \cdot (D3 - R \cdot \sin(PB\psi_2)) - D4 \cdot \sin(\alpha)$$

$$Y0C3 = R_{pb} - R \cdot \cos(PB\psi_2)$$

$$Z0C3 = D4 \cdot \cos(\alpha) + \sin(\alpha) \cdot (D3 - R \cdot \sin(PB\psi_2))$$

CCCCCCCCCCCCCCCCCCCCCCCCCCCCCCCCCCCC

C

C Calculate Finger i contact position w.r.t

C its' Frame 1, (X1Ci, Y1Ci, Z1Ci), where i=1,2,3

C

CCCCCCCCCCCCCCCCCCCCCCCCCCCCCCCCCCCC

$$X1C1 = Z0C1$$

$$Y1C1 = R_{p0} - Y0C1$$

$$Z1C1 = X0C1$$

* Write(*,15)X1C1,Y1C1,Z1C1

*15 Format('X1C1=',F7.4,3X,'Y1C1=',F7.4,3X,'Z1C1=',F7.4)

$$X1C2 = -R_{p1} + Y0C2$$

$$\begin{aligned} Y1C2 &= H_p \cdot \cos(P_p) + Z0C2 \cdot \cos(P_p) + X0C2 \cdot \sin(P_p) - \\ \# \quad &L_p \cdot \cos(P_p) \cdot \tan(P_p) \end{aligned}$$

$$\begin{aligned} Z1C2 &= X0C2 \cdot \cos(P_p) - H_p \cdot \sin(P_p) - Z0C2 \cdot \sin(P_p) + \\ \# \quad &L_p \cdot \sin(P_p) \cdot \tan(P_p) \end{aligned}$$

* Write(*,16)X1C2,Y1C2,Z1C2

*16 Format('X1C2=',F7.4,3X,'Y1C2=',F7.4,3X,'Z1C2=',F7.4)

$$X1C3 = -R_{p2} + Y0C3$$

$$\begin{aligned} Y1C3 &= H_p \cdot \cos(P_p) + Z0C3 \cdot \cos(P_p) + X0C3 \cdot \sin(P_p) - \\ \# \quad &L_p \cdot \cos(P_p) \cdot \tan(P_p) \end{aligned}$$

```

      Z1C3 = X0C3*cos(Pp) - Hp*sin(Pp) - Z0C3*sin(Pp) +
#      Lp*sin(Pp)*tan(Pp)
*      Write(*,17)X1C3,Y1C3,Z1C3
*17   Format('X1C3=',F7.4,3X,'Y1C3=',F7.4,3X,'Z1C3=',F7.4)

```

```

CCCCCCCCCCCCCCCCCCCCCCCCCCCC
C
C   Calculate Theta 0i (T0i)
C   where i=1,2,3
C
CCCCCCCCCCCCCCCCCCCCCCCCCCCC

```

```

      If(X1C1 .EQ. 0.0) Then
          T00=90*Deg
      Else
          T00 = DATan(Y1C1/X1C1)
      EndIf

```

```

      If(X1C2 .EQ. 0.0) Then
          T01=90*Deg
      ElseIf(X1C2 .LT. 0.0) Then
          T01 = 180* Deg + DATan(Y1C2/X1C2)
      Else
          T01 = DATan(Y1C2/X1C2)
      EndIf

```

```

      If(X1C3 .EQ. 0.0) Then
          T02=90*Deg
      ElseIf(X1C3 .LT. 0.0) Then
          T02 = 180* Deg + DATan(Y1C3/X1C3)
      Else
          T02 = DATan(Y1C3/X1C3)
      EndIf

```

```

CCCCCCCCCCCCCCCCCCCCCCCCCCCCCCCCCCCCCCCCCCCCCCCCCCCCCCCCCCCC
C
C   Step 3: Calculate Finger i contact position w.r.t
C   its' Frame 2 (X2Ci, Y2Ci, Z2Ci), where i=1,2,3
C
CCCCCCCCCCCCCCCCCCCCCCCCCCCCCCCCCCCCCCCCCCCCCCCCCCCCCCCCCCCC

```

```

      X2C1 = -Ho + X1C1*cos(T00) + Y1C1*sin(T00)
      Y2C1 = -Z1C1
      Z2C1 = Y1C1*cos(T00) - X1C1*sin(T00)

```

$X2C2 = X1C2 * \cos(T01) - Lo * \sin(Po) + Y1C2 * \sin(T01)$
 $Y2C2 = -Z1C2 + Lo * \cos(Po) + Lp / \cos(Pp)$
 $Z2C2 = Y1C2 * \cos(T01) - X1C2 * \sin(T01)$

$X2C3 = X1C3 * \cos(T02) - Lo * \sin(Po) + Y1C3 * \sin(T02)$
 $Y2C3 = -Z1C3 + Lo * \cos(Po) + Lp / \cos(Pp)$
 $Z2C3 = Y1C3 * \cos(T02) - X1C3 * \sin(T02)$

CC

C
 C Determine if Contact 1 location is a reachable point
 C (RMax based on T20 = T30 = -6.5 degrees
 C RMin based on T20 = T30 = -90 degrees)

C
 CCC

RMax0=3.720951385087795
 RMin0=1.619019765166565
 CDist0=Sqrt(X2C1**2 + Y2C1**2)
 If(CDist0 .LT. RMin0) Then
 Type *, 'Contact 1 location is too close to Finger 0 and'
 Warn=1
 ElseIf(CDist0 .GT. RMax0) Then
 Type *, 'Contact 1 location is too far from Finger 0 and'
 Warn=1
 EndIf

CC

C
 C Determine if Contact 2 location is a reachable point
 C (RMax based on T21 = T31 = 6.5 degrees
 C RMin based on T21 = T31 = 90 degrees)

C
 CCC

RMax1=3.720951385087795
 RMin1=1.619019765166565
 CDist1=Sqrt(X2C2**2 + Y2C2**2)
 If(CDist1 .LT. RMin1) Then
 Type *, 'Contact 2 location is too close to Finger 1 and'
 Warn=1
 ElseIf(CDist1 .GT. RMax1) Then
 Type *, 'Contact 2 location is too far from Finger 1 and'
 Warn=1
 EndIf

```

CCCCCCCCCCCCCCCCCCCCCCCCCCCCCCCCCCCCCCCCCCCC
C
C   Determine if Contact 3 location is a reachable point
C   (RMax2 based on T22 = T32 = 6.5 degrees
C   RMin2 based on T22 = T32 = 90 degrees)
C
CCCCCCCCCCCCCCCCCCCCCCCCCCCCCCCCCCCCCCCCCCCC

```

```

RMax2=3.720951385087795
RMin2=1.619019765166565
CDist2=Sqrt(X2C3**2 + Y2C3**2)

```

```

If(CDist2 .LT. RMin2) Then
    Warn=1
    Type *, 'Contact 3 location is too close to Finger 2 and'
ElseIf(CDist2 .GT. RMax2) Then
    Type *, 'Contact 3 location is too far from Finger 2 and'
    Warn=1
EndIf

```

```

CCCCCCCCCCCCCCCCCCCCCCCCCCCCCCCCCCCCCCCCCCCC
C
C   If any of the contacts are not reachable given a
C   neutral body position (zero rotation), then
C   start over and request new inputs
C
CCCCCCCCCCCCCCCCCCCCCCCCCCCCCCCCCCCCCCCCCCCC

```

```

If((Warn .EQ. 1) .AND. (PhiB .EQ. 0.0)) Then
    Type *, ' '
    Type *, ' '
    Type *, 'Input parameters are invalid'
    Type *, ' '
    Type *, 'Starting Over'
    Warn=0.0
    Type *, ' '
    Type *, 'Requesting new inputs'
    Type *, ' '
    Go to 1
EndIf

```

```

CCCCCCCCCCCCCCCCCCCCCCCCCCCCCCCCCCCCCCCCCCCC
C
C   Calculate Theta 20 (T20)
C
C   Calculate Theta 10 (T10)
C

```

CCCCCCCCCCCCCCCCCCCCCCCCCCCC

BB0 = (-2*L2*(L1 + L3)/(L1*L3) + Sqrt(4*L2**2*(L1
+ L3)**2/(L1**2*L3**2) - 16*(L1**2 + L2**2
- 2*L1*L3 + L3**2 - X2C1**2 - Y2C1**2)/(L1*L3)))/8

T20 = DATan(-Sqrt(Abs(1-BB0**2))/BB0)

T10 = DATan(Y2C1/X2C1) - DATan((L2*Sin(T20) +
L3*Sin(2*T20))/(L1 + L2*Cos(T20) + L3*Cos(2*T20)))

CCCCCCCCCCCCCCCCCCCCCCCCCCCC

C

C Calculate Theta 21 (T21)

C

C Calculate Theta 11 (T11)

C

CCCCCCCCCCCCCCCCCCCCCCCCCCCC

BB1 = (-2*L2*(L1 + L3)/(L1*L3) + Sqrt(4*L2**2*(L1
+ L3)**2/(L1**2*L3**2) - 16*(L1**2 + L2**2
- 2*L1*L3 + L3**2 - X2C2**2 - Y2C2**2)/(L1*L3)))/8

T21 = DATan(Sqrt(Abs(1-BB1**2))/BB1)

T11 = DATan(Y2C2/X2C2) - DATan((L2*Sin(T21) +
L3*Sin(2*T21))/(L1 + L2*Cos(T21) + L3*Cos(2*T21)))

CCCCCCCCCCCCCCCCCCCCCCCCCCCC

C

C Calculate Theta 22 (T22)

C

C Calculate Theta 12 (T12)

C

CCCCCCCCCCCCCCCCCCCCCCCCCCCC

BB2 = (-2*L2*(L1 + L3)/(L1*L3) + Sqrt(4*L2**2*(L1
+ L3)**2/(L1**2*L3**2) - 16*(L1**2 + L2**2
- 2*L1*L3 + L3**2 - X2C3**2 - Y2C3**2)/(L1*L3)))/8

T22 = DATan(Sqrt(Abs(1-BB2**2))/BB2)

T12 = DATan(Y2C3/X2C3) - DATan((L2*Sin(T22) +
L3*Sin(2*T22))/(L1 + L2*Cos(T22) + L3*Cos(2*T22)))

CCCCCCCCCCCCCCCCCCCC

C

C Convert angles to Degrees

C

CCCCCCCCCCCCCCCCCCCC

PBPsi0 = PBPsi0/Deg

PBPsi1 = PBPsi1/Deg

PBPsi2 = PBPsi2/Deg

T00 = T00/Deg

T10 = T10/Deg

T20 = T20/Deg

T01 = T01/Deg

T11 = T11/Deg

T21 = T21/Deg

T02 = T02/Deg

T12 = T12/Deg

T22 = T22/Deg

CCCCCCCCCCCCCCCCCCCCCCCCCCCCCCCC

C

C Check for Joint Angle Limit Violations

C

CCCCCCCCCCCCCCCCCCCCCCCCCCCCCCCC

IF(Abs(T00) .GT. 45) Then

Type *, 'T00 Exceeds Limit'

Warn = 1

ElseIf((T10 .LT. -60.0) .OR. (T10 .GT. 15)) Then

Type *, 'T10 Exceeds Limit'

Warn = 1

ElseIf((T20 .LT. -90) .OR. (T20 .GT. -6.5)) Then

Type *, 'T20 Exceeds Limit'

Warn = 1

ElseIf((T01 .GT. 115) .OR. (T01 .LT. 65)) Then

Type *, 'T01 Exceeds Limit'

Warn = 1

ElseIf((T11 .GT. 11) .OR. (T11 .LT. -60)) Then

Type *, 'T11 Exceeds Limit'

Warn = 1

ElseIf((T21 .GT. 90) .OR. (T21 .LT. 3.5)) Then

Type *, 'T21 Exceeds Limit'

ElseIf((T02 .GT. 115) .OR. (T02 .LT. 65)) Then

Type *, 'T02 Exceeds Limit'

Warn = 1


```

ElseIf((T12 .GT. 11) .OR. (T12 .LT. -50)) Then
    Type *, 'T12 Exceeds Limit'
    Warn=1
ElseIf((T22 .GT. 90) .OR. (T22 .LT. 3.5)) Then
    Type *, 'T22 Exceeds Limit'
    Warn=1
EndIf

If((Warn .EQ. 1) .AND. (PhiB .EQ. 0.0)) Then
    Type *, ' '
    Type *, ' '
    Type *, 'Input parameters are invalid'
    Write(*,22) T00,T10,T20,T01,T11,T21,T02,T12,T22
    Write(*,19) X2C1,Y2C1,X2C2,Y2C2,X2C3,Y2C3
    Type *, ' '
    Type *, 'Starting Over'
    Warn=0.0
    Type *, ' '
    Type *, 'Requesting new inputs'
    Type *, ' '
    Go to 1

ElseIf((Warn .EQ. 1) .AND. (N .EQ. -1))Then
    Type *, 'at end of right rotation'
    Write(*,22) T00,T10,T20,T01,T11,T21,T02,T12,T22
    Write(*,19) X2C1,Y2C1,X2C2,Y2C2,X2C3,Y2C3
    Write(*,20)RRMax
    Write(12,22) T00,T10,T20,T01,T11,T21,T02,T12,T22
    Write(12,19) X2C1,Y2C1,X2C2,Y2C2,X2C3,Y2C3
    Write(13,22) T00,T10,T20,T01,T11,T21,T02,T12,T22
    Write(13,19) X2C1,Y2C1,X2C2,Y2C2,X2C3,Y2C3
    Write(14,22) T00,T10,T20,T01,T11,T21,T02,T12,T22
    Write(14,19) X2C1,Y2C1,X2C2,Y2C2,X2C3,Y2C3
    Write(12,20)RRMax
    Write(13,20)RRMax
    Write(14,20)RRMax
    Go to 500

ElseIf((Warn .EQ. 1) .AND. (N .EQ. 1)) Then
    Type *, 'at end of left rotation'
    Write(*,22) T00,T10,T20,T01,T11,T21,T02,T12,T22
    Write(*,19) X2C1,Y2C1,X2C2,Y2C2,X2C3,Y2C3
    Write(*,21)RLMax
    Write(12,22) T00,T10,T20,T01,T11,T21,T02,T12,T22
    Write(12,19) X2C1,Y2C1,X2C2,Y2C2,X2C3,Y2C3
    Write(13,22) T00,T10,T20,T01,T11,T21,T02,T12,T22
    Write(13,19) X2C1,Y2C1,X2C2,Y2C2,X2C3,Y2C3
    Write(14,22) T00,T10,T20,T01,T11,T21,T02,T12,T22

```

```

Write(14,19) X2C1,Y2C1,X2C2,Y2C2,X2C3,Y2C3
Write(12,21)RLMax
Write(13,21)RLMax
Write(14,21)RLMax
Go to 450
EndIf

```

```

19  Format('/Frame 2 Contact Positions at Point of Violation are; '
#  //'{X2Ci,Y2Ci} = > ',2('{',F7.4,',',F7.4,'}; '), '{',F7.4,',',
#  ',F7.4,'}')
20  Format('Max Safe Right Rotation is ',F7.2, ' Degrees'//)
21  Format('Max Safe Left Rotation is ',F7.2, ' Degrees'//)

22  Format('/Joint Angles at Point of Violation are; '
#  '/3(F8.3,3X),/3(F8.3,3X),/3(F8.3,3X))

```

```

CCCCCCCCCCCCCCCCCCCCCCCCCCCCCCCCCCCC
C
C  Write Finger Data to the Respective Data File
C
CCCCCCCCCCCCCCCCCCCCCCCCCCCCCCCCCCCC

```

```

Write(12,30) PhiB,X1C1,Y1C1,Z1C1,PBPsi0,T00,T10,T20
Write(13,30) PhiB,X1C2,Y1C2,Z1C2,PBPsi1,T01,T11,T21
Write(14,30) PhiB,X1C3,Y1C3,Z1C3,PBPsi2,T02,T12,T22

```

```

If((PhiB .EQ. DiscPhi) .AND. Q .EQ. 0) Then
Write(16,31)DAlpha
Write(16,31)R
Write(16,31)Rpb
Write(16,31)D3
Write(16,31)D4
Write(16,31)PhiB
Write(16,31)Psi0
Write(16,31)Psi1
Write(16,31)Psi2
Write(16,31)T00
Write(16,31)T10
Write(16,31)T20
Write(16,31)T01
Write(16,31)T11
Write(16,31)T21
Write(16,31)T02
Write(16,31)T12
Write(16,31)T22

```

```

CntAng1 = T10 + 90 + 2*T20-DAlpha
CntAng2 = -(T11 + 78 + 2*T21-DAlpha-180)
CntAng3 = -(T12 + 78 + 2*T22-DAlpha-180)

```

```

A00=T00
A10=T10
A20=T20
A01=T01
A11=T11
A21=T21
A02=T02
A12=T12
A22=T22

```

```

      Q=1
EndIf

```

```

30  Format(4(F8.3,3X),/4(F8.3,3X)/)
31  Format(F10.5)

```

```

      If (N .EQ. 1) Then
          RLMax = PhiB
      Else
          RRMMax = PhiB
      EndIf

```

```

      PhiB = RotInc*N + PhiB

```

```

400  Continue

```

```

CCCCCCCCCCCCCCCCC
C
C  End Do Loop
C
CCCCCCCCCCCCCCCCC

```

```

450  If((N .EQ. 1) .AND. (RotInc .GT. 0.))Then
      N=-1
      K=-K
      Warn=0.0
      PhiB=0.0
      Go to 10
    EndIf

```

```

500  RotMax = RLMax - RRMMax

```

```

Type *, '
Type *, '*****
Type *, '*****
Write(*,505)RotMax
Write(12,505)RotMax
Write(13,505)RotMax
Write(14,505)RotMax
Type *, '*****
Type *, '*****
Type *, '
Type *, '
Type *, '
505 Format('Total Max Safe Rotation is ',F6.2, ' Degrees')

Write(15,520)D3,RotMax
520 Format(F9.4,',',F9.4)

Write(*,545)CntAng1
Type *, '
Write(*,550)CntAng2
Type *, '
Write(*,555)CntAng3
Type *, '
Type *, '
Write(*,22) A00,A10,A20,A01,A11,A21,A02,A12,A22
Type *, '
IF((CntAng1 .LT. 0) .OR. (CntAng2 .LT. 0) .OR.
# (CntAng3 .LT. 0)) Then
    Type *, 'Body is Too Close to Hand'
    Type *, '
    Type *, '
    EndIf

Type*, 'Do you wish to start over with a new value for
# D3 (Y/N)?'
Read(5,530)Ans
530 Format(A)
Yes = 'Y'
SYes = 'y'

If((Ans .EQ. Yes) .OR. (Ans .EQ. SYes))Then
    Type *, '
    Type *, 'Input New Value for D3'
    Accept *.D3
    Type*, '
    Write(*,540)D3
540 Format('D3 = ',F9.4)

```

```

Warn=0.0
Go to 6
EndIf
545 Format(1X,'Contact Angle 1 is ',F8.3)
550 Format(1x,'Contact Angle 2 is ',F8.3)
555 Format(1x,'Contact Angle 3 is ',F8.3)
Type*,'Ending Program'
Type*,' '

Close(12,Status='Keep')
Close(13,Status='Keep')
Close(14,Status='Keep')
Close(15,Status='Keep')
Close(16,Status='Keep')

Stop
End

```

Appendix G. *Grasp Analysis Computer Program*

C Program Mapper

CC

CC This Is Mapper. It Is A Fortran Program That Generates
CC Data For Constraint Maps. No Subroutines Are Called, It
CC Just Runs Straight Through...it is Explained Well With
CC Comments Though, So I Don't Want To Hear Any Complair.ts
CC About Not Being Able To Decipher My Code.

CC

CC Inputs:

CC

CC Psi0,Psi1,Psi2.....Contact Point Locations From
CC Vertical, Going Clkwise

CC

CC Mz.....External Moment Applied

CC

CC Mg.....Grasp Force Magnitude

CC

CC R.....Cylinder Radius

CC

CC Mu.....Friction Coefficient (static

CC

CC S.....Scale Of Map (Number Of
CC Cylinder Radii from the Center
CC to the Edge of the Map)

CC

CC Run.....A Two Digit Character String
CC Used to I.d. Generated Files

CC

CC ResX,ResY.....Map Resolution (horiz & vert)
CC Whole Number Representing the
CC Number of Pixels per X-Scale
CC & Y-Scale of Map

CC

CC Inputs From Hand.dat:

CC

CC L1,L2.....1st And 2nd Finger Lengths

CC

CC Theta1,2,3.....D&H Link Position Angles

CC

CC Output Files: (## = Run Number)

CC

CC Stable##.dat.....Data Points Indicating Areas

CC

CC With A Stable Code (111)

CC

CC Bdry##.dat.....Data Points For Boundaries
CC Between Different Code Areas

CC

C Prompt For Various Inputs

C

CCCCCCCCCCCCCCCCCCCCCCCCCCCCCCCC

```

    Type *, 'Input External Moment Magnitude (N-m);'
    Accept *, Mz
    Write(*,5)Mz
5   Format(F7.3,3X,F7.3//)
    Type *, ' '
    Type *, 'Input Grasp Force Magnitude (N);'
    Accept *, Mg
    Write(*,5)Mg
    Type *, 'Input Friction Coefficient;'
    Accept *, Mu
    Write(*,5)Mu
    Type *, 'Map Scale ?'
    Accept *, S
    Write(*,5)S
    Type *, 'Run Number ? (2-digit)'
    Read(5,10)Run
    Write(*,10)Run
10  Format(A)
    Type *, 'X-Resolution,Y-Resolution (whole numbers > 1);'
    Type *, 'Note: Using Odd Numbers Will Include Cylinder Center'
    Accept *, ResX,ResY
    Write(*,5)ResX,ResY
    Type *, 'Do You Want Extra Boundary Resolution (Y/N)?'
    Read(5,20)Ans
20  Format(A)
    Yes = 'Y'
    SYes = 'y'
```

CC

C

C Use Open Statements To Associate Filenames

C With Various Logical Unit Numbers

C

CC

```

    Open(12,File='Hand.dat',Status='Old',
1      Access='Sequential',
1      Form='Formatted')

    Open(13,File='Torq00'//Run//'.dat',Status='New',
1      Access='Sequential',
1      Form='Formatted')
```

```
Open(14,File='Torq10'//Run//'.dat',Status='New',  
1    Access='Sequential',  
1    Form='Formatted')
```

```
Open(15,File='Torq20'//Run//'.dat',Status='New',  
1    Access='Sequential',  
1    Form='Formatted')
```

```
Open(16,File='Torq30'//Run//'.dat',Status='New',  
1    Access='Sequential',  
1    Form='Formatted')
```

```
Open(17,File='Torq01'//Run//'.dat',Status='New',  
1    Access='Sequential',  
1    Form='Formatted')
```

```
Open(18,File='Torq11'//Run//'.dat',Status='New',  
1    Access='Sequential',  
1    Form='Formatted')
```

```
Open(19,File='Torq21'//Run//'.dat',Status='New',  
1    Access='Sequential',  
1    Form='Formatted')
```

```
Open(20,File='Torq31'//Run//'.dat',Status='New',  
1    Access='Sequential',  
1    Form='Formatted')
```

```
Open(21,File='Torq02'//Run//'.dat',Status='New',  
1    Access='Sequential',  
1    Form='Formatted')
```

```
Open(22,File='Torq12'//Run//'.dat',Status='New',  
1    Access='Sequential',  
1    Form='Formatted')
```

```
Open(23,File='Torq22'//Run//'.dat',Status='New',  
1    Access='Sequential',  
1    Form='Formatted')
```

```
Open(24,File='Torq32'//Run//'.dat',Status='New',  
1    Access='Sequential',  
1    Form='Formatted')
```

```
Open(25,File='Stable'//Run//'.dat',Status='New',  
1    Access='Sequential',  
1    Form='Formatted')
```

```
Open(26,File='Brdry'//Run//'.dat',Status='New',
```

```

1      Access='Sequential',
1      Form='Formatted')

Open(27,File='C:\ntcts\Run\'.dat',Status='New',
1      Access='Sequential',
1      Form='Formatted')

Open(28,File='SAS\Run\'.dat',Status='New',
1      Access='Sequential',
1      Form='Formatted')

Open(29,File='S:\bnd\Run\'.dat',Status='New',
1      Access='Sequential',
1      Form='Formatted')

```

```

Write(13,235)
Write(14,235)
Write(15,235)
Write(16,235)
Write(17,235)
Write(18,235)
Write(19,235)
Write(20,235)
Write(21,235)
Write(22,235)
Write(23,235)
Write(24,235)
Write(26,235)
Write(27,235)
Write(28,235)
Write(29,235)

```

```

CCCCCCCCCCCCCCCCCCCCCCCCCCCC
C
C   Input Data From Hand.dat File
C
CCCCCCCCCCCCCCCCCCCCCCCCCCCC

```

```

Read(12,30)Alpha
Read(12,30)R
Read(12,30)Rpb
Read(12,30)D3
Read(12,30)D4
Read(12,30)PhiB
Read(12,30)Psi0
Read(12,30)Psi1
Read(12,30)Psi2
Read(12,30)T00

```

```

Read(12,30)T10
Read(12,30)T20
Read(12,30)T01
Read(12,30)T11
Read(12,30)T21
Read(12,30)T02
Read(12,30)T12
Read(12,30)T22

```

```

Write(*,31)Alpha,R,Rpb
Write(*,31)D3,D4,PhiB
Write(*,31)Psi0,Psi1,Psi2
Write(*,31)T00,T10,T20
Write(*,31)T01,T11,T21
Write(*,31)T02,T12,T22

```

30 Format(F10.6)

31 Format(/3(F10.5,3X))

```

CCCCCCCCCCCCCCCCCCCC
C
C Convert To Meters
C
CCCCCCCCCCCCCCCCCCCC

```

```

R = R * (0.0254)
Rpb = Rpb * (0.0254)

```

```

CCCCCCCCCCCCCCCCCCCCCCCCCCCCCCCCCCCCCCCCCCCCCCCCCCCC
C
C Establish Constant Values For Hand (Metric)
C
CCCCCCCCCCCCCCCCCCCCCCCCCCCCCCCCCCCCCCCCCCCCCCCCCCCC

```

```

L1 = 1.7 * (0.0254)
L2 = 1.3 * (0.0254)
L3 = 0.735 * (0.0254)
Lo = 1.2 * (0.0254)
Ho = 0.4 * (0.0254)
Write(*,30)L1,L2,L3,Lo,Ho

```

```

Deg = 3.141592654/180.0
Pp = 12.0*Deg
Po = 30*Deg

```

```

Tau0MX = 2.958
Tau1MX = 2.958

```

Tau2MX = 1.139

Tau3MX = .427

CCCCCCCCCCCCCCCCCCCC

C

C Convert To Radians

C

CCCCCCCCCCCCCCCCCCCC

Alpha=Alpha*Deg

PhiB=PhiB*Deg

Psi0=Psi0*Deg

Psi1=Psi1*Deg

Psi2=Psi2*Deg

T00=T00*Deg

T10=T10*Deg

T20=T20*Deg

T01=T01*Deg

T11=T11*Deg

T21=T21*Deg

T02=T02*Deg

T12=T12*Deg

T22=T22*Deg

CCCCCCCCCCCCCCCCCCCC

C

C Set Toggle Switches To Zero

C

CCCCCCCCCCCCCCCCCCCC

ToglA0=0

ToglB0=0

ToglC0=0

ToglD0=0

ToglE0=0

ToglF0=0

ToglG0=0

ToglH0=0

ToglA1=0

ToglB1=0

ToglC1=0

ToglD1=0

ToglE1=0

ToglF1=0

ToglG1=0

ToglH1=0

ToglA2=0
 ToglB2=0
 ToglC2=0
 ToglD2=0
 ToglF2=0
 ToglF2=0
 ToglG2=0
 ToglH2=0

ToglZZ=0

CC

C

C Calculate 'External' Or Balancing Forces

C

CC

$B1 = \cos(\Psi1) - \cos(\Psi0)$
 $B2 = \cos(\Psi1) - \cos(\Psi2)$
 $B3 = \cos(\Psi2) - \cos(\Psi0)$
 $B4 = \sin(\Psi0 - \Psi2) - \sin(\Psi0 - \Psi1) - \sin(\Psi1 - \Psi2)$
 $B5 = -Mz * \cos(\Psi1) / R$
 $B6 = Mz * \cos(\Psi0) / R$
 $B7 = Mz * \sin(\Psi0 - \Psi1) / R$

$X1E = B5 / B1 - (B2 * B7) / (B1 * B4)$
 $X2E = B6 / B1 - (B3 * B7) / (B1 * B4)$
 $X3E = B7 / B4$

CC

C

C Calculate Terms Needed For Joint Torque Determination

C

CC

$D10 = L1 * \cos(T10) + L2 * \cos(T10 + T20) + L3 * \cos(T10 + 2 * T20)$
 $D20 = L1 * \sin(T10) + L2 * \sin(T10 + T20) + L3 * \sin(T10 + 2 * T20)$
 $D30 = L2 * \cos(T10 + T20) + L3 * \cos(T10 + 2 * T20)$
 $D40 = L2 * \sin(T10 + T20) + L3 * \sin(T10 + 2 * T20)$
 $D50 = L3 * \cos(T10 + 2 * T20)$
 $D60 = L3 * \sin(T10 + 2 * T20)$

$D11 = L1 * \cos(T11) + L2 * \cos(T11 + T21) + L3 * \cos(T11 + 2 * T21)$
 $D21 = L1 * \sin(T11) + L2 * \sin(T11 + T21) + L3 * \sin(T11 + 2 * T21)$
 $D31 = L2 * \cos(T11 + T21) + L3 * \cos(T11 + 2 * T21)$
 $D41 = L2 * \sin(T11 + T21) + L3 * \sin(T11 + 2 * T21)$
 $D51 = L3 * \cos(T11 + 2 * T21)$
 $D61 = L3 * \sin(T11 + 2 * T21)$

```

D12=L1*Cos(T12) + L2*Cos(T12 + T22) + L3*Cos(T12 + 2*T22)
D22=L1*Sin(T12) + L2*Sin(T12 + T22) + L3*Sin(T12 + 2*T22)
D32=L2*Cos(T12 + T22) + L3*Cos(T12 + 2*T22)
D42=L2*Sin(T12 + T22) + L3*Sin(T12 + 2*T22)
D52=L3*Cos(T12 + 2*T22)
D62=L3*Sin(T12 + 2*T22)

```

```

CCCCCCCCCCCCCCCCCCCCCCCCCCCCCCCCCCCCCCCC

```

```

C
C  Calculate Some Needed Trig Terms and
C  Initialize the Comparison Code Term
C
CCCCCCCCCCCCCCCCCCCCCCCCCCCCCCCCCCCCCCCC

```

```

P1=-1.0*Cos(Psi0)
P2=Sin(Psi0)
P3=-1.0*Cos(Psi1)
P4=Sin(Psi1)
P5=-1.0*Cos(Psi2)
P6=Sin(Psi2)

```

```

Codepr=0.0

```

```

CCCCCCCCCCCCCCCCCCCCCCCCCCCCCCCCCCCCCCCC

```

```

C
C  Iteration Loop to Calculate Internal Forces,
C  Generate Contact Codes, Calculate Required
C  Joint Torques, Etc.
C  (One Iteration Per Point on Grasp Plane)
C  *****Start Here*****
C

```

```

CCCCCCCCCCCCCCCCCCCCCCCCCCCCCCCCCCCCCCCC

```

```

Type *, 'Beginning Primary Loop'
Type *, ' '

```

```

Do 150 V=i.0,ResY,1.0

```

```

*   J=ResY-V+1
*   Write(6,200)J

```

```

CCCCCCCCCCCCCCCCCCCCCCCCCCCCCCCCCCCCCCCC

```

```

C
C  Set Flags to Determine Boundries of Joint-Torque
C  Limit Exceedence in Stable Map (Code=111)
C

```

```

CCCCCCCCCCCCCCCCCCCCCCCCCCCCCCCCCCCCCCCC

```

```

Flag00=1
Flag10=1

```

Flag20=1
Flag30=1

Flag01=1
Flag11=1
Flag21=1
Flag31=1

Flag02=1
Flag12=1
Flag22=1
Flag32=1

FlgA00=0
FlgB00=1

FlgA10=0
FlgB10=1

FlgA20=0
FlgB20=1

FlgA30=0
FlgB30=1

FlgA01=0
FlgB01=1

FlgA11=0
FlgB11=1

FlgA21=0
FlgB21=1

FlgA31=0
FlgB31=1

FlgA02=0
FlgB02=1

FlgA12=0
FlgB12=1

FlgA22=0
FlgB22=1

FlgA32=0
FlgB32=1


```

Do 140 U=1.0,ResX,1.0
  Xg=((U-1.0-ResX/2.0+0.5)*S*R)/(ResX/2.0-0.5)
  Yg=((1.0-V+ResY/2.0-0.5)*S*R)/(ResY/2.0-0.5)

  P7=Xg*Sin(Psi1)-Yg*Cos(Psi1)+R
  P8=Xg*Cos(Psi1)+Yg*Sin(Psi1)
  P9=Xg*Sin(Psi2)-Yg*Cos(Psi2)+R
  P10=Xg*Cos(Psi2)+Yg*Sin(Psi2)

  Q1=P3-P1
  Q2=P5-P1
  Q3=P4*P2+P1*P3-P2**2.0-P1**2.0
  Q4=P4*P1-P3*P2
  Q5=P6*P2+P1*P5-P2**2.0-P1**2.0
  Q6=P1*P6-P5*P2

  R1=P4*Q3-Q1*Q4
  R2=Q2*Q3-Q1*Q5
  R3=P6*Q3-Q1*Q6
  R4=P8*Q3-P7*Q4
  R5=-1.0*Q5*P7
  R6=-1.0*Q6*P7

  U1=Q3*R4-Q5*R4+Q4*R5
  U2=Q4*R6-Q6*R4
  U3=R2*R4-R1*R5
  U4=R3*R4-R1*R6
  U5=Q5*R4-Q4*R5
  U6=Q6*R4-Q4*R6

  V1=U1*P10-U2*P9
  V2=U3*P10-U4*P9
  V3=U5*P10-U6*P9
  V4=R5*P10-R6*P9

  W1=V1/(P9*Q3*R4)
  W2=V2/(P2*P9*Q3*R4)
  W3=V3/(P9*Q3*R4)
  W4=V4/(P9*R4)
  W5=-1.0*P10/P9

  Z3I=Mg/(Sqrt(W1**2+W2**2)+Sqrt(W3**2+W4**2)+Sqrt(W5**2+1.0))
  X1I=W1*Z3I
  Z1I=W2*Z3I
  X2I=W3*Z3I
  Z2I=W4*Z3I
  X3I=W5*Z3I

```

CCCCCCCCCCCCCCCCCCCCCCCCCCCCCCCCCCCC

C

C Calculate Total Contact Forces Needed

C at Each Contact Point

C

CCCCCCCCCCCCCCCCCCCCCCCCCCCCCCCCCCCC

$X1T = X1E + X1I$

$X2T = X2E + X2I$

$X3T = X3E + X3I$

$Z1T = Z1I$

$Z2T = Z2I$

$Z3T = Z3I$

CCCCCCCCCCCCCCCCCCCCCCCCCCCCCCCCCCCC

C

C Test for Constraint Compliance

C

CCCCCCCCCCCCCCCCCCCCCCCCCCCCCCCCCCCC

Unstab=0.0

If (Z1T .LE. 0) Then

Code1=300

Unstab=1.0

Else If (ABS(X1T) .GE. (Z1T*Mu)) Then

Code1=200

Else

Code1=100

End If

If (Z2T .LE. 0) Then

Code2=300

Unstab=1.0

Else If (ABS(X2T) .GE. (Z2T*Mu)) Then

Code2=200

Else

Code2=100

End If

If (Z3T .LE. 0) Then

Code3=300

Unstab=1.0

Else If (ABS(X3T) .GE. (Z3T*Mu)) Then

Code3=200

Else

Code3=100

End If

CCCCCCCCCCCCCCCCCCCC

C

C Calculate Contact Code

C

CCCCCCCCCCCCCCCCCCCC

Code = Code1 + Code2 + Code3

CC

C

C Output Coordinates to 'Stable##.dat' if the

C Contact Code = 111.

C

C This Group of points represents the Grasp

C Force Focus Map if Torque Limitations are

C not Considered.

C

CC

If (Code .EQ. 111) Then

Write(25,220)Xg,Yg

Endif

CC

C

C Do A Left-to-right Search For Code Boundaries

C

CC

If (U .EQ. 1.0) Go To 130

If ((Code .EQ. 111) .AND. (Code-Codepr) .NE. 0)

Write(29,220)Xg,Yg

If ((Codepr .EQ. 111) .AND. Codepr) .NE. 0)

Write(29,220)Xgpr,Yg

If((Code-Codepr) .NE.0)Then

Xadj = Xg - R*S/ResX

Write(26,220)Xadj,Yg

EndIf

CC

C

C Calculate the Joint Torques Required to

C Exert the Forces K1T,Z1T,X2T,Z2T,X3T,Z3T

C on the Object. Output the X & Y Coords

C If Joint Torque Limits are Exceeded.

C

CC

E10=-(Z1T*Cos(PhiB + Psi0)) - X1T*Sin(PhiB + Psi0)
 E20=-(X1T*Cos(PhiB + Psi0)*Sin(Alpha)) + Z1T*Sin(Alpha)*
 # Sin(PhiB + Psi0)
 E30=-(X1T*Cos(Alpha)*Cos(PhiB + Psi0)) + Z1T*Cos(Alpha)*
 # Sin(PhiB + Psi0)

E11=Z2T*Cos(PhiB + Psi1) + X2T*Sin(PhiB + Psi1)
 E21=-(X2T*Cos(PhiB + Psi1)*Sin(Alpha + Pp)) +
 # Z2T*Sin(Alpha + Pp)*Sin(PhiB + Psi1)
 E31=-(X2T*Cos(Alpha + Pp)*Cos(PhiB + Psi1)) +
 # Z2T*Cos(Alpha + Pp)*Sin(PhiB + Psi1)

E12=Z3T*Cos(PhiB + Psi2) + X3T*Sin(PhiB + Psi2)
 E22=-(X3T*Cos(PhiB + Psi2)*Sin(Alpha + Pp)) +
 # Z3T*Sin(Alpha + Pp)*Sin(PhiB + Psi2)
 E32=-(X3T*Cos(Alpha + Pp)*Cos(PhiB + Psi2)) +
 # Z3T*Cos(Alpha + Pp)*Sin(PhiB + Psi2)

Tau00 = Cos(T00)*(Ho + D10*E00) - (Ho + D10)*E20*Sin(T00)
 Tau10 = -(D10*E30) - Cos(T00)*E00*D20 - E10*Sin(T00)*D20
 Tau20 = -(D30*E30) - Cos(T00)*E20*D40 - E10*Sin(T00)*D40
 Tau30 = -(D50*E30) - Cos(T00)*E20*D60 - E10*Sin(T00)*D60

Tau01 = Cos(T01)*(D11 + Lo*Sin(Po))*E21 - (D11 + Lo*Sin(Po))*E11*Sin(T01)
 Tau11 = -(D11*E31) - Cos(T01)*E11*D21 - E21*Sin(T01)*D21
 Tau21 = -(D31*E31) - Cos(T01)*E11*D41 - E21*Sin(T01)*D41
 Tau31 = -(D51*E31) - Cos(T01)*E11*D61 - E21*Sin(T01)*D61

Tau02 = Cos(T02)*(D12 + Lo*Sin(Po))*E22 - (D12 + Lo*Sin(Po))*E12*Sin(T02)
 Tau12 = -(D12*E32) - Cos(T02)*E12*D22 - E22*Sin(T02)*D22
 Tau22 = -(D32*E32) - Cos(T02)*E12*D42 - E22*Sin(T02)*D42
 Tau32 = -(D52*E32) - Cos(T02)*E12*D62 - E22*Sin(T02)*D62

CC

C

C Reset Toggles Ij, Jj, Kj, Lj & WW to zero

C where j = 0, 1, 2

C

CC

TogI10=0

TogI10=0

TogIK0=0

TogILO=0

TogI11=0

ToglJ1=0
ToglK1=0
ToglL1=0

ToglI2=0
ToglJ2=0
ToglK2=0
ToglL2=0

ToglWW=0

CC

C

C Check for Torque Limit Exceedence in Total Map Area
C (Checks All Map Points)

C

C ToglAj/Bj/Cj/Dj = 1 indicates that the Torque Limit was
C exceeded for some point in the Map Area

C

C Note: This two Toggle Type is never reset to zero

C

CC

If (ABS(Tau00) .GT. Tau0MX) Then

 ToglA0= 1

EndIf

If (ABS(Tau10) .GT. Tau1MX) Then

 ToglB0= 1

EndIf

If (ABS(Tau20) .GT. Tau2MX) Then

 ToglC0= 1

EndIf

If (ABS(Tau30) .GT. Tau3MX) Then

 ToglD0= 1

Endif

if (ABS(Tau01) .GT. Tau0MX) Then

 ToglA1= 1

EndIf

If (ABS(Tau11) .GT. Tau1MX) Then

 ToglB1= 1

EndIf

If (ABS(Tau21) .GT. Tau2MX) Then

 ToglC1= 1

EndIf

If (ABS(Tau31) .GT. Tau3MX) Then

 ToglD1= 1

Endif

```

If (ABS(Tau02) .GT. Tau0MX) Then
  ToglA2=1
EndIf
If (ABS(Tau12) .GT. Tau1MX) Then
  ToglB2=1
EndIf
If (ABS(Tau22) .GT. Tau2MX) Then
  ToglC2=1
EndIf
If (ABS(Tau32) .GT. Tau3MX) Then
  ToglD2=1
EndIf

```

CC

```

C
C Check for Torque Limit exceedence in the Stable Map
C (Code = 111) Area
C
C ToglEj/Fj/Gj/Hj = 1 indicates that the Torque Limit was
C exceeded for some point in Stable Map (Code=111)
C
C Note: These Toggle Types are never reset to zero
C
C ToglIj/Jj/Kj/Lj = 1 indicates that the Torque Limit was
C exceeded at the particular Stable Grasp Focus point being
C analyzed in the Stable Map Area
C
C Note: These Toggle Types, Along with ToglWW, are Reset for
C Each Iteration
C

```

CC

```

If ((ABS(Tau00) .GT. Tau0MX) .AND. (Code.EQ. 111)) Then
  ToglE0=1
  ToglI0=1
  ToglWW=1
EndIf
If ((ABS(Tau10) .GT. Tau1MX) .AND. (Code .EQ. 111)) Then
  ToglF0=1
  ToglJ0=1
  ToglWW=1
EndIf
If ((ABS(Tau20) .GT. Tau2MX) .AND. (Code .EQ. 111)) Then
  ToglG0=1
  ToglK0=1
  ToglWW=1
EndIf
If ((ABS(Tau30) .GT. Tau3MX) .AND. (Code .EQ. 111)) Then

```

```

    ToglH0=1
    ToglL0=1
    ToglWW=1
Endif

If ((ABS(Tau01) .GT. Tau0MX) .AND. (Code .EQ. 111)) Then
    ToglE1=1
    ToglI1=1
    ToglWW=1
EndIf
If ((ABS(Tau11) .GT. Tau1MX) .AND. (Code .EQ. 111)) Then
    ToglF1=1
    ToglJ1=1
    ToglWW=1
EndIf
If ((ABS(Tau21) .GT. Tau2MX) .AND. (Code .EQ. 111)) Then
    ToglG1=1
    ToglK1=1
    ToglWW=1
EndIf
If ((ABS(Tau31) .GT. Tau3MX) .AND. (Code .EQ. 111)) Then
    ToglH1=1
    ToglL1=1
    ToglWW=1
Endif

If ((ABS(Tau02) .GT. Tau0MX) .AND. (Code .EQ. 111)) Then
    ToglE2=1
    ToglI2=1
    ToglWW=1
EndIf
If ((ABS(Tau12) .GT. Tau1MX) .AND. (Code .EQ. 111)) Then
    ToglF2=1
    ToglJ2=1
    ToglWW=1
EndIf
If ((ABS(Tau22) .GT. Tau2MX) .AND. (Code .EQ. 111)) Then
    ToglG2=1
    ToglK2=1
    ToglWW=1
EndIf
If ((ABS(Tau32) .GT. Tau3MX) .AND. (Code .EQ. 111)) Then
    ToglH2=1
    ToglL2=1
    ToglWW=1
Endif

```

CC

```

C
C Check for Torque Limit exceedence in the Stable Map Area
C (For All Points in Area; Code=111). If True, Write Grasp
C Focus BOUNDARY Point to the Respective Finger-Joint File.
C
CCCCCCCCCCCCCCCCCCCCCCCCCCCCCCCCCCCCCCCCCCCCCCCCCCCCCCCC

```

```

      If ((TogII0 .EQ. 1) .AND. ((Flag00 - FlgA00) .NE. 0)) Then
        Write(13,220)Xg,Yg
        Flag00 = 0
      EndIf

```

```

      If ((TogII0 .EQ. 0) .AND. (Code .EQ. 111) .AND.
# ((FlgB00 - Flag00) .NE. 0)) Then
        Write(13,220)Xg,Yg
        Flag00 = 1
      EndIf

```

```

      If ((TogIA0 .EQ. 1) .AND. (Code .NE. 111) .AND.
# (Codepr .EQ. 111) .AND. (Flag00 .EQ. 0)) Then
        Write(13,220)Xgpr,Yg
        Flag00 = 1
      EndIf

```

```

      If ((TogIJ0 .EQ. 1) .AND. ((Flag10 - FlgA10) .NE. 0)) Then
        Write(14,220)Xg,Yg
        Flag10 = 0
      EndIf

```

```

      If ((TogIJ0 .EQ. 0) .AND. (Code .EQ. 111) .AND.
# ((FlgB10 - Flag10) .NE. 0)) Then
        Write(14,220)Xg,Yg
        Flag10 = 1
      EndIf

```

```

      If ((TogIB0 .EQ. 1) .AND. (Code .NE. 111) .AND.
# (Codepr .EQ. 111) .AND. (Flag10 .EQ. 0)) Then
        Write(14,220)Xgpr,Yg
        Flag10 = 1
      EndIf

```

```

      If ((TogIK0 .EQ. 1) .AND. ((Flag20 - FlgA20) .NE. 0)) Then
        Write(15,220)Xg,Yg
        Flag20 = 0
      EndIf

```

```

      If ((TogIK0 .EQ. 0) .AND. (Code .EQ. 111) .AND.
# ((FlgB20 - Flag20) .NE. 0)) Then

```



```

    Write(15,220)Xg,Yg
    Flag20 = 1
EndIf

If ((ToglC0 .EQ. 1) .AND. (Code .NE. 111) .AND.
# (Codepr .EQ. 111) .AND. (Flag20 .EQ. 0)) Then
    Write(15,220)Xgpr,Yg
    Flag20 = 1
EndIf

If ((ToglL0 .EQ. 1) .AND. ((Flag30 - FlgA30) .NE. 0)) Then
    Write(16,220)Xg,Yg
    Flag30 = 0
EndIf

If ((ToglL0 .EQ. 0) .AND. (Code .EQ. 111) .AND.
# ((FlgB30 - Flag30) .NE. 0)) Then
    Write(16,220)Xg,Yg
    Flag30 = 1
EndIf

If ((ToglD0 .EQ. 1) .AND. (Code .NE. 111) .AND.
# (Codepr .EQ. 111) .AND. (Flag30 .EQ. 0)) Then
    Write(16,220)Xgpr,Yg
    Flag30 = 1
EndIf

If ((ToglI1 .EQ. 1) .AND. ((FlagC1 - FlgA01) .NE. 0)) Then
    Write(17,220)Xg,Yg
    Flag01 = 0
EndIf

If ((ToglI1 .EQ. 0) .AND. (Code .EQ. 111) .AND.
# ((FlgB01 - Flag01) .NE. 0)) Then
    Write(17,220)Xg,Yg
    Flag01 = 1
EndIf

If ((ToglA1 .EQ. 1) .AND. (Code .NE. 111) .AND.
# (Codepr .EQ. 111) .AND. (Flag01 .EQ. 0)) Then
    Write(17,220)Xgpr,Yg
    Flag01 = 1
EndIf

If ((ToglJ1 .EQ. 1) .AND. ((Flag11 - FlgA11) .NE. 0)) Then
    Write(18,220)Xg,Yg
    Flag11 = 0

```

```

EndIf

If ((ToglJ1 .EQ. 0) .AND. (Code .EQ. 111) .AND.
# ((FlgB11 - Flag11) .NE. 0)) Then
    Write(18,220)Xg,Yg
    Flag11 = 1
EndIf

If ((ToglB1 .EQ. 1) .AND. (Code .NE. 111) .AND.
# (Codepr .EQ. 111) .AND. (Flag11 .EQ. 0)) Then
    Write(18,220)Xgpr,Yg
    Flag11 = 1
EndIf

If ((ToglK1 .EQ. 1) .AND. ((Flag21 - FlgA21) .NE. 0)) Then
    Write(19,220)Xg,Yg
    Flag21 = 0
EndIf

If ((ToglK1 .EQ. 0) .AND. (Code .EQ. 111) .AND.
# ((FlgB21 - Flag21) .NE. 0)) Then
    Write(19,220)Xg,Yg
    Flag21 = 1
EndIf

If ((ToglC1 .EQ. 1) .AND. (Code .NE. 111) .AND.
# (Codepr .EQ. 111) .AND. (Flag21 .EQ. 0)) Then
    Write(19,220)Xgpr,Yg
    Flag21 = 1
EndIf

If ((ToglL1 .EQ. 1) .AND. ((Flag31 - FlgA31) .NE. 0)) Then
    Write(20,220)Xg,Yg
    Flag31 = 0
EndIf

If ((ToglL1 .EQ. 0) .AND. (Code .EQ. 111) .AND.
# ((FlgB31 - Flag31) .NE. 0)) Then
    Write(20,220)Xg,Yg
    Flag31 = 1
EndIf

If ((ToglD1 .EQ. 1) .AND. (Code .NE. 111) .AND.
# (Codepr .EQ. 111) .AND. (Flag31 .EQ. 0)) Then
    Write(20,220)Xgpr,Yg
    Flag31 = 1
EndIf

```

```

If ((TogI12 .EQ. 1) .AND. ((Flag02 - FlgA02) .NE. 0)) Then
  Write(21,220)Xg,Yg
  Flag02 = 0
EndIf

If ((TogI12 .EQ. 0) .AND. (Code .EQ. 111) .AND.
# ((FlgB02 - Flag02) .NE. 0)) Then
  Write(21,220)Xg,Yg
  Flag02 = 1
EndIf

If ((TogI12 .EQ. 1) .AND. (Code .NE. 111) .AND.
# (Codepr .EQ. 111) .AND. (Flag02 .EQ. 0)) Then
  Write(21,220)Xgpr,Yg
  Flag02 = 1
EndIf

If ((TogI12 .EQ. 1) .AND. ((Flag12 - FlgA12) .NE. 0)) Then
  Write(22,220)Xg,Yg
  Flag12 = 0
EndIf

If ((TogI12 .EQ. 0) .AND. (Code .EQ. 111) .AND.
# ((FlgB12 - Flag12) .NE. 0)) Then
  Write(22,220)Xg,Yg
  Flag12 = 1
EndIf

If ((TogI12 .EQ. 1) .AND. (Code .NE. 111) .AND.
# (Codepr .EQ. 111) .AND. (Flag12 .EQ. 0)) Then
  Write(22,220)Xgpr,Yg
  Flag12 = 1
EndIf

If ((TogIK2 .EQ. 1) .AND. ((Flag22 - FlgA22) .NE. 0)) Then
  Write(23,220)Xg,Yg
  Flag22 = 0
EndIf

If ((TogIK2 .EQ. 0) .AND. (Code .EQ. 111) .AND.
# ((FlgB22 - Flag22) .NE. 0)) Then
  Write(23,220)Xg,Yg
  Flag22 = 1
EndIf

If ((TogIC2 .EQ. 1) .AND. (Code .NE. 111) .AND.
# (Codepr .EQ. 111) .AND. (Flag22 .EQ. 0)) Then
  Write(23,220)Xgpr,Yg

```

```
Flag22 = 1
EndIf
```

```
If ((ToglL2 .EQ. 1) .AND. ((Flag32 - FlgA32) .NE. 0)) Then
  Write(24,220)Xg,Yg
  Flag32 = 0
EndIf
```

```
If ((ToglL2 .EQ. 0) .AND. (Code .EQ. 111) .AND.
# ((FlgB32 - Flag32) .NE. 0)) Then
  Write(24,220)Xg,Yg
  Flag32 = 1
EndIf
```

```
If ((ToglD2 .EQ. 1) .AND. (Code .NE. 111) .AND.
# (Codepr .EQ. 111) .AND. (Flag32 .EQ. 0)) Then
  Write(24,220)Xgpr,Yg
  Flag32 = 1
EndIf
```

```
CCCCCCCCCCCCCCCCCCCCCCCCCCCCCCCCCCCCCCCCCCCCCCCCCCCC
```

```
C
C Output Coordinates To 'SAS##.dat' If
C the Contact Code is 111 and None of
C Torque Limits are Exceeded.
C
C This group of points is the Net,
C Usable Grasp Force Focus Map.
C
```

```
CCCCCCCCCCCCCCCCCCCCCCCCCCCCCCCCCCCCCCCCCCCCCCCCCCCC
```

```
If ((Code .EQ. 111) .AND. (ToglWW .EQ. 0)) Then
  ToglZZ = 1
  Write(28,220)Xg,Yg
```

```
Endif
```

```
CCCCCCCCCCCCCCCCCCCCCCCCCCCCCCCCCCCCCCCCCCCCCCCCCCCC
```

```
C
C *****Stop Here*****
C Update Codepr And Return To Beginning Of Loop
C
```

```
CCCCCCCCCCCCCCCCCCCCCCCCCCCCCCCCCCCCCCCCCCCCCCCCCCCC
```

```
130 Codepr=Code
```

```

      Xgpr=Xg
140 Continue
150 Continue

```

```

CCCCCCCCCCCCCCCCCCCCCCCCCCCCCCCCCCCCCCCCCCCCCCCCCCCCCCCC
C
C Now Look For Horizontal Boundary Lines That Would Not
C Show Up With A Left To Right Type Of Search. Write
C These Boundary Points To 'bndry##.dat'
C *****Start Here*****
C
CCCCCCCCCCCCCCCCCCCCCCCCCCCCCCCCCCCCCCCCCCCCCCCCCCCCCCCC

```

```

      If ((Ans .NE. Yes) .AND. (Ans .NE. SYes)) Go To 210
      Codepr=0

```

```

      Type *, 'Beginning Top-to-Bottom Boundary Search'
      Type *, ' '
      Do 180 U=1.0,ResX,1.0
*       J=ResX-U+1
*       Write(6,200)J

```

```

CCCCCCCCCCCCCCCCCCCCCCCCCCCCCCCCCCCCCCCCCCCCCCCCCCCCCCCC
C
C Set Flags to Determine Boundries of Joint-Torque
C Limit Exceedence in Stable Map (Code=111)
C
CCCCCCCCCCCCCCCCCCCCCCCCCCCCCCCCCCCCCCCCCCCCCCCCCCCCCCCC

```

```

      Flag00=1
      Flag10=1
      Flag20=1
      Flag30=1

```

```

      Flag01=1
      Flag11=1
      Flag21=1
      Flag31=1

```

```

      Flag02=1
      Flag12=1
      Flag22=1
      Flag32=1

```

```

      FlgA00=0
      FlgB00=1

```

```

      FlgA10=0

```

FlgB10=1

FlgA20=0

FlgB20=1

FlgA30=0

FlgB30=1

FlgA01=0

FlgB01=1

FlgA11=0

FlgB11=1

FlgA21=0

FlgB21=1

FlgA31=0

FlgB31=1

FlgA02=0

FlgB02=1

FlgA12=0

FlgB12=1

FlgA22=0

FlgB22=1

FlgA32=0

FlgB32=1

Do 170 V=1.0,ResY,1.0

$Xg = ((U - 1.0 - ResX/2.0 + 0.5) * S * R) / (ResX/2.0 - 0.5)$

$Yg = ((1.0 - V + ResY/2.0 - 0.5) * S * R) / (ResY/2.0 - 0.5)$

$P7 = Xg * Sin(Psi1) - Yg * Cos(Psi1) + R$

$P8 = Xg * Cos(Psi1) + Yg * Sin(Psi1)$

$P9 = Xg * Sin(Psi2) - Yg * Cos(Psi2) + R$

$P10 = Xg * Cos(Psi2) + Yg * Sin(Psi2)$

$Q1 = P3 - P1$

$Q2 = P5 - P1$

$Q3 = P4 * P2 + P1 * P3 - P2 ** 2.0 - P1 ** 2.0$

$Q4 = P4 * P1 - P3 * P2$

$Q5 = P6 * P2 + P1 * P5 - P2 ** 2.0 - P1 ** 2.0$

$Q6 = P1 * P6 - P5 * P2$

$R1 = P4 * Q3 - Q1 * Q4$
 $R2 = Q2 * Q3 - Q1 * Q5$
 $R3 = P6 * Q3 - Q1 * Q6$
 $R4 = P8 * Q3 - P7 * Q4$
 $R5 = -1.0 * Q5 * P7$
 $R6 = -1.0 * Q6 * P7$

$U1 = Q3 * R4 - Q5 * R4 + Q4 * R5$
 $U2 = Q4 * R6 - Q6 * R4$
 $U3 = R2 * R4 - R1 * R5$
 $U4 = R3 * R4 - R1 * R6$
 $U5 = Q5 * R4 - Q4 * R5$
 $U6 = Q6 * R4 - Q4 * R6$

$V1 = U1 * P10 - U2 * P9$
 $V2 = U3 * P10 - U4 * P9$
 $V3 = U5 * P10 - U6 * P9$
 $V4 = R5 * P10 - R6 * P9$

$W1 = V1 / (P9 * Q3 * R4)$
 $W2 = V2 / (P2 * P9 * Q3 * R4)$
 $W3 = V3 / (P9 * Q3 * R4)$
 $W4 = V4 / (P9 * R4)$
 $W5 = -1.0 * P10 / P9$

$Z3I = Mg / (\text{Sqrt}(W1 ** 2 + W2 ** 2) + \text{Sqrt}(W3 ** 2 + W4 ** 2) + \text{Sqrt}(W5 ** 2 + 1.0))$
 $X1I = W1 * Z3I$
 $Z1I = W2 * Z3I$
 $X2I = W3 * Z3I$
 $Z2I = W4 * Z3I$
 $X3I = W5 * Z3I$

CC

C
 C Calculate Total Contact Forces Needed
 C At Each Contact Point
 C

CC

$X1T = X1E + X1I$
 $X2T = X2E + X2I$
 $X3T = X3E + X3I$
 $Z1T = Z1I$
 $Z2T = Z2I$
 $Z3T = Z3I$

CC

C

C Test For Constraint Compliance

C

CCCCCCCCCCCCCCCCCCCCCCCCCCCCCCCCCCCC

 If (Z1T .LE. 0) Then

 Code1 = 300

 Else If (ABS(X1T) .GE. (Z1T*Mu)) Then

 Code1 = 200

 Else

 Code1 = 100

End If

 If (Z2T .LE. 0) Then

 Code2 = 30

 Else If (ABS(X2T) .GE. (Z2T*Mu)) Then

 Code2 = 20

 Else

 Code2 = 10

End If

 If (Z3T .LE. 0) Then

 Code3 = 3

 Else If (ABS(X3T) .GE. (Z3T*Mu)) Then

 Code3 = 2

 Else

 Code3 = 1

End If

CCCCCCCCCCCCCCCCCCCCCCCCCCCCCCCCCCCC

C

C Calculate Contact Code

C

CCCCCCCCCCCCCCCCCCCCCCCCCCCCCCCCCCCC

 Code = Code1 + Code2 + Code3

CCCCCCCCCCCCCCCCCCCCCCCCCCCCCCCCCCCC

C

C Do A Search For Code Boundaries

C

CCCCCCCCCCCCCCCCCCCCCCCCCCCCCCCCCCCC

 If (V .EQ. 1.0) Go To 165

 If ((Code .EQ. 111) .AND. (Code-Codepr) .NE. 0)
 # Write(29,220)Xg,Yg


```

If ((Codepr .EQ. 111) .AND. (Code-Codepr) .NE. 0)
# Write(29,220)Xg,Ygpr

```

```

If ((Code-Codepr) .NE. 0) Then
  Yadj = Yg + R*S/ResY
  Write(26,220)Xg,Yadj
Endif

```

```

CCCCCCCCCCCCCCCCCCCCCCCCCCCCCCCCCCCCCCCCCCCCCCCCCCCCCCCC

```

```

C
C Calculate the Joint Torques Required to
C Exert the Forces X1T,Z1T,X2T,Z2T,X3T,Z3T
C on the Object. Output the X & Y Coords
C If Joint Torque Limits are Exceeded.
C

```

```

CCCCCCCCCCCCCCCCCCCCCCCCCCCCCCCCCCCCCCCCCCCCCCCCCCCCCCCC

```

```

E10=-(Z1T*cos(PhiB + Psi0)) - X1T*sin(PhiB + Psi0)
E20=-(X1T*cos(PhiB + Psi0)*sin(Alpha)) + Z1T*sin(Alpha)*
# Sin(PhiB + Psi0)
E30=-(X1T*cos(Alpha)*cos(PhiB + Psi0)) + Z1T*cos(Alpha)*
# Sin(PhiB + Psi0)

```

```

E11=Z2T*cos(PhiB + Psi1) + X2T*sin(PhiB + Psi1)
E21=-(X2T*cos(PhiB + Psi1)*sin(Alpha + Pp)) +
# Z2T*sin(Alpha + Pp)*sin(PhiB + Psi1)
E31=-(X2T*cos(Alpha + Pp)*cos(PhiB + Psi1)) +
# Z2T*cos(Alpha + Pp)*sin(PhiB + Psi1)

```

```

E12=Z3T*cos(PhiB + Psi2) + X3T*sin(PhiB + Psi2)
E22=-(X3T*cos(PhiB + Psi2)*sin(Alpha + Pp)) +
# Z3T*sin(Alpha + Pp)*sin(PhiB + Psi2)
E32=-(X3T*cos(Alpha + Pp)*cos(PhiB + Psi2)) +
# Z3T*cos(Alpha + Pp)*sin(PhiB + Psi2)

```

```

Tau00 = Cos(T00)*(Ho + D10)*E10 - (Ho + D10)*E20*sin(T00)
Tau10 = -(D10*E30) - Cos(T00)*E20*D20 - E10*sin(T00)*D20
Tau20 = -(D30*E30) - Cos(T00)*E20*D40 - E10*sin(T00)*D40
Tau30 = -(D50*E30) - Cos(T00)*E20*D60 - E10*sin(T00)*D60

```

```

Tau01=Cos(T01)*(D11+Lo*sin(Po))*E21-(D11+Lo*sin(Po))*E11*sin(T01)
Tau11 = -(D11*E31) - Cos(T01)*E11*D21 - E21*sin(T01)*D21
Tau21 = -(D31*E31) - Cos(T01)*E11*D41 - E21*sin(T01)*D41
Tau31 = -(D51*E31) - Cos(T01)*E11*D61 - E21*sin(T01)*D61

```

```

Tau02=Cos(T02)*(D12+Lo*sin(Po))*E22-(D12+Lo*sin(Po))*E12*sin(T02)
Tau12 = -(D12*E32) - Cos(T02)*E12*D22 - E22*sin(T02)*D22
Tau22 = -(D32*E32) - Cos(T02)*E12*D42 - E22*sin(T02)*D42

```

$\text{Tau32} = -(\text{D52} * \text{E32}) - \text{Cos}(\text{T02}) * \text{E12} * \text{D62} - \text{E22} * \text{Sin}(\text{T02}) * \text{D62}$

CC

C

C Reset Toggles Ij, Jj, Kj, Lj & WW to zero

C where j = 0, 1, 2

C

CC

ToglI0=0

ToglJ0=0

ToglK0=0

ToglL0=0

ToglI1=0

ToglJ1=0

ToglK1=0

ToglL1=0

ToglI2=0

ToglJ2=0

ToglK2=0

ToglL2=0

ToglWW=0

CC

C

C Check for Torque Limit Exceedence in Total Map Area

C (Checks All Map Points)

C

C ToglAj/Bj/Cj/Dj = 1 indicates that the Torque Limit was

C exceeded for some point in the Map Area

C

C Note: This two Toggle Type is never reset to zero

C

CC

If (ABS(Tau00) .GT. Tau0MX) Then

ToglA0=1

EndIf

If (ABS(Tau10) .GT. Tau1MX) Then

ToglB0=1

EndIf

If (ABS(Tau20) .GT. Tau2MX) Then

ToglC0=1

EndIf

If (ABS(Tau30) .GT. Tau3MX) Then

```

    ToglD0=1
  Endif

  If (ABS(Tau01) .GT. Tau0MX) Then
    ToglA1=1
  EndIf
  If (ABS(Tau11) .GT. Tau1MX) Then
    ToglB1=1
  EndIf
  If (ABS(Tau21) .GT. Tau2MX) Then
    ToglC1=1
  EndIf
  If (ABS(Tau31) .GT. Tau3MX) Then
    ToglD1=1
  Endif

```

```

  If (ABS(Tau02) .GT. Tau0MX) Then
    ToglA2=1
  EndIf
  If (ABS(Tau12) .GT. Tau1MX) Then
    ToglB2=1
  EndIf
  If (ABS(Tau22) .GT. Tau2MX) Then
    ToglC2=1
  EndIf
  If (ABS(Tau32) .GT. Tau3MX) Then
    ToglD2=1
  Endif

```

CC

C
 C Check for Torque Limit exceedence in the Stable Map
 C (Code = 111) Area
 C
 C ToglEj/Fj/Gj/Hj = 1 indicates that the Torque Limit was
 C exceeded for some point in Stable Map (Code=111)
 C
 C Note: These Toggle Types are never reset to zero
 C
 C ToglIj/Jj/Kj/Lj = 1 indicates that the Torque Limit was
 C exceeded at the particular Stable Grasp Focus point being
 C analyzed in the Stable Map Area
 C
 C Note: These Toggle Types, Along with ToglWW, are Reset for
 C Each Iteration
 C

CC

```

If ((ABS(Tau00) .GT. Tau0MX) .AND. (Code.EQ. 111)) Then
  ToglE0= 1
  ToglI0= 1
  ToglWW= 1
EndIf
If ((ABS(Tau10) .GT. Tau1MX) .AND. (Code .EQ. 111)) Then
  ToglF0= 1
  ToglJ0= 1
  ToglWW= 1
EndIf
If ((ABS(Tau20) .GT. Tau2MX) .AND. (Code .EQ. 111)) Then
  ToglG0= 1
  ToglK0= 1
  ToglWW= 1
EndIf
If ((ABS(Tau30) .GT. Tau3MX) .AND. (Code .EQ. 111)) Then
  ToglH0= 1
  ToglL0= 1
  ToglWW= 1
Endif

If ((ABS(Tau01) .GT. Tau0MX) .AND. (Code .EQ. 111)) Then
  ToglE1= 1
  ToglI1= 1
  ToglWW= 1
EndIf
If ((ABS(Tau11) .GT. Tau1MX) .AND. (Code .EQ. 111)) Then
  ToglF1= 1
  ToglJ1= 1
  ToglWW= 1
EndIf
If ((ABS(Tau21) .GT. Tau2MX) .AND. (Code .EQ. 111)) Then
  ToglG1= 1
  ToglK1= 1
  ToglWW= 1
EndIf
If ((ABS(Tau31) .GT. Tau3MX) .AND. (Code .EQ. 111)) Then
  ToglH1= 1
  ToglL1= 1
  ToglWW= 1
Endif

If ((ABS(Tau02) .GT. Tau0MX) .AND. (Code .EQ. 111)) Then
  ToglE2= 1
  ToglI2= 1
  ToglWW= 1
EndIf
If ((ABS(Tau12) .GT. Tau1MX) .AND. (Code .EQ. 111)) Then

```

```

    ToglF2=1
    ToglJ2=1
    ToglWW=1
  EndIf
  If ((ABS(Tau22) .GT. Tau2MX) .AND. (Code .EQ. 111)) Then
    ToglG2=1
    ToglK2=1
    ToglWW=1
  EndIf
  If ((ABS(Tau32) .GT. Tau3MX) .AND. (Code .EQ. 111)) Then
    ToglH2=1
    ToglL2=1
    ToglWW=1
  EndIf

```

CC

C
 C Check for Torque Limit exceedence in the Stable Map Area
 C (For All Points in Area; Code=111). If True, Write Grasp
 C Focus BOUNDARY Point to the Respective Finger-Joint File.
 C

CC

```

    If ((ToglI0 .EQ. 1) .AND. ((Flag00 - FlgA00) .NE. 0)) Then
      Write(13,220)Xg,Yg
      Flag00 = 0
    EndIf

    If ((ToglI0 .EQ. 0) .AND. (Code .EQ. 111) .AND.
  # ((FlgB00 - Flag00) .NE. 0)) Then
      Write(13,220)Xg,Yg
      Flag00 = 1
    EndIf

    If ((ToglA0 .EQ. 1) .AND. (Code .NE. 111) .AND.
  # (Codepr .EQ. 111) .AND. (Flag00 .EQ. 0)) Then
      Write(13,220)Xg,Ygpr
      Flag00 = 1
    EndIf

    If ((ToglJ0 .EQ. 1) .AND. ((Flag10 - FlgA10) .NE. 0)) Then
      Write(14,220)Xg,Yg
      Flag10 = 0
    EndIf

    If ((ToglJ0 .EQ. 0) .AND. (Code .EQ. 111) .AND.
  # ((FlgB10 - Flag10) .NE. 0)) Then
      Write(14,220)Xg,Yg

```

```

    Flag10 = 1
EndIf

If ((TogIB0 .EQ. 1) .AND. (Code .NE. 111) .AND.
# (Codepr .EQ. 111) .AND. (Flag10 .EQ. 0)) Then
    Write(14,220)Xg,Ygpr
    Flag10 = 1
EndIf

If ((TogIK0 .EQ. 1) .AND. ((Flag20 - FlgA20) .NE. 0)) Then
    Write(15,220)Xg,Yg
    Flag20 = 0
EndIf

If ((TogIK0 .EQ. 0) .AND. (Code .EQ. 111) .AND.
# ((FlgB20 - Flag20) .NE. 0)) Then
    Write(15,220)Xg,Yg
    Flag20 = 1
EndIf

If ((TogIC0 .EQ. 1) .AND. (Code .NE. 111) .AND.
# (Codepr .EQ. 111) .AND. (Flag20 .EQ. 0)) Then
    Write(15,220)Xg,Ygpr
    Flag20 = 1
EndIf

If ((TogIL0 .EQ. 1) .AND. ((Flag30 - FlgA30) .NE. 0)) Then
    Write(16,220)Xg,Yg
    Flag30 = 0
EndIf

If ((TogIL0 .EQ. 0) .AND. (Code .EQ. 111) .AND.
# ((FlgB30 - Flag30) .NE. 0)) Then
    Write(16,220)Xg,Yg
    Flag30 = 1
EndIf

If ((TogID0 .EQ. 1) .AND. (Code .NE. 111) .AND.
# (Codepr .EQ. 111) .AND. (Flag30 .EQ. 0)) Then
    Write(16,220)Xg,Ygpr
    Flag30 = 1
EndIf

If ((TogII1 .EQ. 1) .AND. ((Flag01 - FlgA01) .NE. 0)) Then
    Write(17,220)Xg,Yg
    Flag01 = 0
EndIf

```

```

If ((ToglI1 .EQ. 0) .AND. (Code .EQ. 111) .AND.
# ((FlgB01 - Flag01) .NE. 0)) Then
    Write(17,220)Xg,Yg
    Flag01 = 1
EndIf

If ((ToglA1 .EQ. 1) .AND. (Code .NE. 111) .AND.
# (Codepr .EQ. 111) .AND. (Flag01 .EQ. 0)) Then
    Write(17,220)Xg,Ygpr
    Flag01 = 1
EndIf

If ((ToglJ1 .EQ. 1) .AND. ((Flag11 - FlgA11) .NE. 0)) Then
    Write(18,220)Xg,Yg
    Flag11 = 0
EndIf

If ((ToglJ1 .EQ. 0) .AND. (Code .EQ. 111) .AND.
# ((FlgB11 - Flag11) .NE. 0)) Then
    Write(18,220)Xg,Yg
    Flag11 = 1
EndIf

If ((ToglB1 .EQ. 1) .AND. (Code .NE. 111) .AND.
# (Codepr .EQ. 111) .AND. (Flag11 .EQ. 0)) Then
    Write(18,220)Xg,Ygpr
    Flag11 = 1
EndIf

If ((ToglK1 .EQ. 1) .AND. ((Flag21 - FlgA21) .NE. 0)) Then
    Write(19,220)Xg,Yg
    Flag21 = 0
EndIf

If ((ToglK1 .EQ. 0) .AND. (Code .EQ. 111) .AND.
# ((FlgB21 - Flag21) .NE. 0)) Then
    Write(19,220)Xg,Yg
    Flag21 = 1
EndIf

If ((ToglC1 .EQ. 1) .AND. (Code .NE. 111) .AND.
# (Codepr .EQ. 111) .AND. (Flag21 .EQ. 0)) Then
    Write(19,220)Xg,Ygpr
    Flag21 = 1
EndIf

If ((ToglL1 .EQ. 1) .AND. ((Flag31 - FlgA31) .NE. 0)) Then
    Write(20,220)Xg,Yg

```

```

    Flag31 = 0
EndIf

If ((ToglL1 .EQ. 0) .AND. (Code .EQ. 111) .AND.
# ((FlgB31 - Flag31) .NE. 0)) Then
    Write(20,220)Xg,Yg
    Flag31 = 1
EndIf

If ((ToglD1 .EQ. 1) .AND. (Code .NE. 111) .AND.
# (Codepr .EQ. 111) .AND. (Flag31 .EQ. 0)) Then
    Write(20,220)Xg,Ygpr
    Flag31 = 1
EndIf

If ((ToglI2 .EQ. 1) .AND. ((Flag02 - FlgA02) .NE. 0)) Then
    Write(21,220)Xg,Yg
    Flag02 = 0
EndIf

If ((ToglI2 .EQ. 0) .AND. (Code .EQ. 111) .AND.
# ((FlgB02 - Flag02) .NE. 0)) Then
    Write(21,220)Xg,Yg
    Flag02 = 1
EndIf

If ((ToglA2 .EQ. 1) .AND. (Code .NE. 111) .AND.
# (Codepr .EQ. 111) .AND. (Flag02 .EQ. 0)) Then
    Write(21,220)Xg,Ygpr
    Flag02 = 1
EndIf

If ((ToglJ2 .EQ. 1) .AND. ((Flag12 - FlgA12) .NE. 0)) Then
    Write(22,220)Xg,Yg
    Flag12 = 0
EndIf

If ((ToglJ2 .EQ. 0) .AND. (Code .EQ. 111) .AND.
# ((FlgB12 - Flag12) .NE. 0)) Then
    Write(22,220)Xg,Yg
    Flag12 = 1
EndIf

If ((ToglB2 .EQ. 1) .AND. (Code .NE. 111) .AND.
# (Codepr .EQ. 111) .AND. (Flag12 .EQ. 0)) Then
    Write(22,220)Xg,Ygpr
    Flag12 = 1

```



```

EndIf

If ((TogIK2 .EQ. 1) .AND. ((Flag22 - FlgA22) .NE. 0)) Then
  Write(23,220)Xg,Yg
  Flag22 = 0
EndIf

If ((TogIK2 .EQ. 0) .AND. (Code .EQ. 111) .AND.
# ((FlgB22 - Flag22) .NE. 0)) Then
  Write(23,220)Xg,Yg
  Flag22 = 1
EndIf

If ((TogIC2 .EQ. 1) .AND. (Code .NE. 111) .AND.
# (Codepr .EQ. 111) .AND. (Flag22 .EQ. 0)) Then
  Write(23,220)Xg,Ygpr
  Flag22 = 1
EndIf

If ((TogIL2 .EQ. 1) .AND. ((Flag32 - FlgA32) .NE. 0)) Then
  Write(24,220)Xg,Yg
  Flag32 = 0
EndIf

If ((TogIL2 .EQ. 0) .AND. (Code .EQ. 111) .AND.
# ((FlgB32 - Flag32) .NE. 0)) Then
  Write(24,220)Xg,Yg
  Flag32 = 1
EndIf

If ((TogID2 .EQ. 1) .AND. (Code .NE. 111) .AND.
# (Codepr .EQ. 111) .AND. (Flag32 .EQ. 0)) Then
  Write(24,220)Xg,Ygpr
  Flag32 = 1
EndIf

```

```

CCCCCCCCCCCCCCCCCCCCCCCCCCCCCCCCCCCCCCCCCCCCCCCCCCCCCCCC
C
C   Output Coordinates To 'SAS##.dat' If
C   the Contact Code is 111 and None of
C   Torque Limits are Exceeded.
C
C   This group of points is the Net,
C   Usable Grasp Force Focus Map.
C
CCCCCCCCCCCCCCCCCCCCCCCCCCCCCCCCCCCCCCCCCCCCCCCCCCCCCCCC

```

```

      If ((Code .EQ. 111) .AND. (ToglWW .EQ. 0)) Then
        ToglZZ = 1
        Write(28,220)Xg,Yg

      Endif

CCCCCCCCCCCCCCCCCCCCCCCCCCCCCCCCCCCCCCCCCCCCCCCCCCCCCCCC
C
C      *****Stop Here*****
C    Update Codepr And Return To Beginning Of Loop
C
CCCCCCCCCCCCCCCCCCCCCCCCCCCCCCCCCCCCCCCCCCCCCCCCCCCCCCCC

165  Codepr = Code
      Ygpr = Yg
170  Continue
180  Continue
200  Format(' + '.I3,' Iterations Remaining')

CCCCCCCCCCCCCCCCCCCCCCCCCCCCCCCCCCCCCCCCCCCCCCCCCCCCCCCC
C
C    Generate The Contact Point Data Points And
C    Output Them To The File 'cntcts##.dat'
C
CCCCCCCCCCCCCCCCCCCCCCCCCCCCCCCCCCCCCCCCCCCCCCCCCCCCCCCC

210  X1 = -R*Sin(Psi0)
      Y1 = R*Cos(Psi0)
      X2 = -R*Sin(Psi1)
      Y2 = R*Cos(Psi1)
      X3 = -R*Sin(Psi2)
      Y3 = R*Cos(Psi2)

      Write(27,220)X1,Y1
      Write(27,220)X2,Y2
      Write(27,220)X3,Y3

CCCCCCCCCCCCCCCCCCCCCCCCCCCCCCCCCCCCCCCCCCCCCCCCCCCCCCCC
C
C    Check Toggle Switches And Output
C    Warnings If Joint Torque Limits Exceeded
C      Or Safe Areas Exist
C
CCCCCCCCCCCCCCCCCCCCCCCCCCCCCCCCCCCCCCCCCCCCCCCCCCCCCCCC

      If (ToglA0 .EQ. 1) Type *, 'Finger 0-Joint Zero Torque Limits
# Exceeded'
      If (ToglE0 .EQ. 1) Type *, 'in Stable Area'

```

```

Type *, ''
If (ToglB0.EQ. 1) Type *, 'Finger 0-Joint One Torque Limits
# Exceeded'
If (ToglF0.EQ. 1) Type *, 'in Stable Area'
Type *, ''
If (ToglC0.EQ. 1) Type *, 'Finger 0-Joint Two Torque Limits
# Exceeded'
If (ToglG0.EQ. 1) Type *, 'in Stable Area'
Type *, ''
If (ToglD0.EQ. 1) Type *, 'Finger0-Joint Three Torque Limits
# Exceeded'
If (ToglH0.EQ. 1) Type *, 'in Stable Area'
Type *, ''
Type *, ''
If (ToglA1.EQ. 1) Type *, 'Finger 1-Joint Zero Torque Limits
# Exceeded'
If (ToglE1.EQ. 1) Type *, 'in Stable Area'
Type *, ''
If (ToglB1.EQ. 1) Type *, 'Finger 1-Joint One Torque Limits
# Exceeded'
If (ToglF1.EQ. 1) Type *, 'in Stable Area'
Type *, ''
If (ToglC1.EQ. 1) Type *, 'Finger 1-Joint Two Torque Limits
# Exceeded'
If (ToglG1.EQ. 1) Type *, 'in Stable Area'
Type *, ''
If (ToglD1.EQ. 1) Type *, 'Finger1-Joint Three Torque Limits
# Exceeded'
If (ToglH1.EQ. 1) Type *, 'in Stable Area'
Type *, ''
Type *, ''
If (ToglA2.EQ. 1) Type *, 'Finger 2-Joint Zero Torque Limits
# Exceeded'
If (ToglE2.EQ. 1) Type *, 'in Stable Area'
Type *, ''
If (ToglB2.EQ. 1) Type *, 'Finger 2-Joint One Torque Limits
# Exceeded'
If (ToglF2.EQ. 1) Type *, 'in Stable Area'
Type *, ''
If (ToglC2.EQ. 1) Type *, 'Finger 2-Joint Two Torque Limits
# Exceeded'
If (ToglG2.EQ. 1) Type *, 'in Stable Area'
Type *, ''
If (ToglD2.EQ. 1) Type *, 'Finger2-Joint Three Torque Limits
# Exceeded'
If (ToglH2.EQ. 1) Type *, 'in Stable Area'
Type *, ''
Type *, ''

```

```

If (Tog!ZZ .EQ. 1) Type *, 'Safe And Stable Areas Exist'
If (Tog!ZZ .EQ. 0) Type *, 'Safe And Stable Area Does Not Exist'
Type *, ' '
Type *, ' '
Type *, ' '

```

```

CCCCCCCCCCCCCCCCCCCCCCCCCCCCCCCCCCCC

```

```

C

```

```

C  Format For All Output Data Files

```

```

C

```

```

CCCCCCCCCCCCCCCCCCCCCCCCCCCCCCCCCCCC

```

```

220  Format({'',F11.6,'',F11.6,'',' ',' '))

```

```

225  Format({'',F11.6,'',F11.6,'',F11.6,'',F11.6,'',' ',' '))

```

```

230  Format({'',F11.6,'',F11.6,'',F11.6,'',' ',' '))

```

```

Write(13,240)

```

```

Write(14,240)

```

```

Write(15,240)

```

```

Write(16,240)

```

```

Write(17,240)

```

```

Write(18,240)

```

```

Write(19,240)

```

```

Write(20,240)

```

```

Write(21,240)

```

```

Write(22,240)

```

```

Write(23,240)

```

```

Write(24,240)

```

```

Write(26,240)

```

```

Write(27,240)

```

```

Write(28,240)

```

```

Write(29,240)

```

```

235  Format({' '))

```

```

240  Format({'1,1'})

```

```

CCCCCCCCCCCCCCCCCCCCCCCCCCCCCCCCCCCC

```

```

C

```

```

C  Close The Various Files That Were Opened

```

```

C

```

```

CCCCCCCCCCCCCCCCCCCCCCCCCCCCCCCCCCCC

```

```

Close(12,Status='Keep')

```

```

Close(13,Status='Keep')

```

```
Close(14,Status='Keep')
Close(15,Status='Keep')
Close(16,Status='Keep')
Close(17,Status='Keep')
Close(18,Status='Keep')
Close(19,Status='Keep')
Close(20,Status='Keep')
Close(21,Status='Keep')
Close(22,Status='Keep')
Close(23,Status='Keep')
Close(24,Status='Keep')
Close(25,Status='Keep')
Close(26,Status='Keep')
Close(27,Status='Keep')
Close(28,Status='Keep')
Close(29,Status='Keep')
Stop
End
```

Appendix H. *Manipulator Jacobian*

$$J_0 = \begin{vmatrix} a_{11} & a_{12} & a_{13} & a_{14} \\ a_{21} & a_{22} & a_{23} & a_{24} \\ a_{31} & a_{32} & a_{33} & a_{34} \\ a_{41} & a_{42} & a_{43} & a_{44} \\ a_{51} & a_{52} & a_{53} & a_{54} \\ a_{61} & a_{62} & a_{63} & a_{64} \end{vmatrix}$$

where

$$a_{11} = -(H_0 + l_1 C1 + l_2 C12 + l_3 C123) S0$$

$$a_{12} = -(l_1 S1 + l_2 S12 + l_3 S123) C0$$

$$a_{13} = -(l_2 S12 + l_3 S123) C0$$

$$a_{14} = -(l_3 S123) C0$$

$$a_{21} = (H_0 + l_1 C1 + l_2 C12 + l_3 C123) C0$$

$$a_{22} = -(l_1 S1 + l_2 S12 + l_3 S123) S0$$

$$a_{23} = -(l_2 S12 + l_3 S123) S0$$

$$a_{24} = -(l_3 C123)$$

$$a_{31} = 0$$

$$a_{32} = -(l_1 C1 + l_2 C12 + l_3 C123)$$

$$a_{33} = -(l_2 C12 + l_3 C123)$$

$$a_{34} = -(l_3 C123)$$

$$a_{41} = 0 \quad a_{42} = -S0 \quad a_{43} = -S0 \quad a_{44} = -S0$$

$$a_{51} = 0 \quad a_{52} = C0 \quad a_{53} = C0 \quad a_{54} = C0$$

$$a_{61} = 1 \quad a_{62} = 0 \quad a_{63} = 0 \quad a_{64} = 0$$

$$J_1 = \begin{vmatrix} b_{11} & b_{12} & b_{13} & b_{14} \\ b_{21} & b_{22} & b_{23} & b_{24} \\ b_{31} & b_{32} & b_{33} & b_{34} \\ b_{41} & b_{42} & b_{43} & b_{44} \\ b_{51} & b_{52} & b_{53} & b_{54} \\ b_{61} & b_{62} & b_{63} & b_{64} \end{vmatrix} \quad (\text{Note: } J_2 \text{ Same Form as } J_1)$$

where

$$a_{11} = -(l_1 C1 + l_2 C12 + l_3 C123 + L_0 \sin \phi_0) S0$$

$$a_{12} = -(l_1 S1 + l_2 S12 + l_3 S123) C0$$

$$a_{13} = -(l_2 S12 + l_3 S123) C0$$

$$a_{14} = -(l_3 S123) C0$$

$$a_{21} = (l_1 C1 + l_2 C12 + l_3 C123 + L_0 \sin \phi_0) C0$$

$$a_{22} = -(l_1 S1 + l_2 S12 + l_3 S123) S0$$

$$a_{23} = -(l_2 S12 + l_3 S123) S0$$

$$a_{24} = -(l_3 C123)$$

$$a_{31} = 0$$

$$a_{32} = -(l_1 C1 + l_2 C12 + l_3 C123)$$

$$a_{33} = -(l_2 C12 + l_3 C123)$$

$$a_{34} = -(l_3 C123)$$

$$a_{41} = 0 \quad a_{42} = -S0 \quad a_{43} = -S0 \quad a_{44} = -S0$$

$$a_{51} = 0 \quad a_{52} = C0 \quad a_{53} = C0 \quad a_{54} = C0$$

$$a_{61} = 1 \quad a_{62} = 0 \quad a_{63} = 0 \quad a_{64} = 0$$

Bibliography

1. Mark R. Cutkosky and Paul K. Wright. Modeling Manufacturing Grips and Correlations with the Design of Robotic Hands. In *Proc. of IEEE Int. Conf. of Robotics and Automation*, volume 3, pages 1533-1539, 1986.
2. David L. Brock. Enhancing the Dexterity of a Robot Hand Using Controlled Slip. In *Proc. of IEEE Int. Conf. on Robotics and Automation*, pages 249-251, 1988.
3. Capt Stephen Edwards. Use of Grasp Force Focus Positioning to Enhance the Torque Resistance Capability of Robotic Grasps. Master's thesis, Air Force Institute of Technology, December 1988. Dept. of Aero. and Astro. Eng.
4. Yoshihiko Nakamura. *Advanced Robotics: Redundancy and Optimization*. Addison-Wesley Publishing Company, 1991.
5. Zexiang Li, Ping Hsu, and Shankar Sastry. Grasping and Coordinated Manipulation by a Multifingered Hand. *The International Journal of Robotics Research*, volume 8(4), pages 33-50, 1989.
6. J. Salisbury. Kinematic and Force Analysis of Articulated Hands. Ph.D Thesis, Stanford University, 1982. Department of Mechanical Engineering.
7. J. Kerr. An Analysis of Multifingered Hands. Ph.D. Dissertation, Stanford University, 1985. Department of Mechanical Engineering.
8. H. Kobayashi. Geometric Considerations for a Multifingered Robot Hand. *International Journal of Robotics Research*, volume 4(1), 1985.
9. Mark R. Cutkosky. Grasping and Fine Manipulation for Automated Manufacturing. Ph.D Thesis, Carnegie-Mellon University, 1985. Department of Mechanical Engineering.
10. V. Nguyen. Constructing Stable Grasps in 3-D. In *Proc. of IEEE Int. Conf. of Robotics and Automation*, pages 234-245, 1987.
11. Zexiang Li and Shankar Sastry. Task Oriented Optimal Grasping by Multifingered Robot Hands. In *IEEE Journal of Robotics and Automation*, RA 2-14(1), pages 32-44, 1988.
12. R. S. Fearing. Implementing a Force Strategy for Object Re-Orientation. In *Proc. of IEEE Int. Conf. of Robotics and Automation*, pages 96-102, April 1986.
13. R. C. Brost. Automatic Grasp Planning in the Presence of Uncertainty. *The International Journal of Robotics Research*, volume 7(1), February 1986.

14. Arlene Cole, John Hauser, and Shankar Sastry. Kinematics and Control of Multifingered Hands with Rolling Contact. In *Proc. of IEEE Int. Conf. of Robotics and Automation*, pages 228-233, 1988.
15. Arlene Cole, Ping Hsu, and Shankar Sastry. Dynamic Regrasping by Coordinated Control of Sliding for a Multifingered Hand. In *Proc. of IEEE Int. Conf. of Robotics and Automation*, pages 781-786, 1989.
16. Tsuneo Yoshikawa and Kiyoshi Nagai. Manipulating and Grasping Forces in Manipulation by Multifingered Robot Hands. In *IEEE Transactions on Robotics and Automation*, volume 7(1), pages 67-77, February 1991.
17. Sundar Narasimhan. Dexterous Robotic Hands: Kinematics and Control. Master's Thesis, Massachusetts Inst. of Tech., November 1988. Dept. of Elect. Eng. and Comp. Sci.
18. Dr. Michael M. Stanišić, Steven J. Remis, and Kamran Lodi. A C-Code Algorithm for: Stable Grasping with the Utah/MIT Dexterous Robot Hand. Final Report to Universal Energy Systems. Contract No. F49620-88-C-0053/SB5881-0378, 5 November 1991.
19. Mark W. Spong and M. Vidyasagar. Robot Dynamics and Control. John Wiley & Sons, 1989.
20. No author given. Hand Electronics Documentation Package. Technical report. Sarcos Incorporated, 274 South 1200 E. Salt Lake City, Utah 84102, March 1987.

Vita

Freddie D. Zayas was born in Holyoake, Massachusetts on March 1, 1962. Born into an Air Force Family, he has lived and travelled throughout the country and abroad. In 1976 he moved with his family to Tampa, Florida where they lived until he went on to college. He graduated from the University of Florida in 1985 with a degree in Mechanical Engineering and was commissioned in the spring of 1986 through the ROTC program.

As a lieutenant his first assignment was to the Medium Launch Vehicle Program Office at HQ Space Division, Los Angeles AFB, Ca. His duties involved spacecraft-to-launch vehicle integration and launch operations. After serving a full four years at Space Division, he entered the Air Force Institute of Technology in May 90.

Permanent address: Rt 1 Box 2:
Bell, Fla 32619